Back in control

Towards early identification of treatment resistance in schizophrenia

van der Pluijm, M.

Publication date
2023

Document Version
Final published version

Back in control

Towards early identification of treatment resistance in schizophrenia

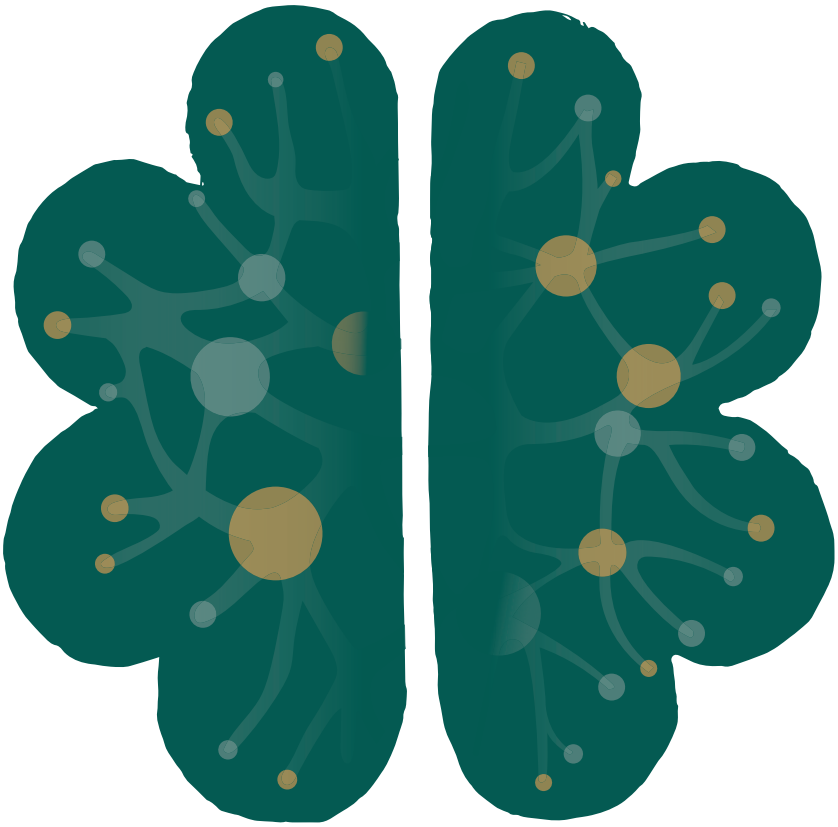

Marieke van der Pluijm

Back in control

Towards early identification of treatment resistance in schizophrenia

Marieke van der Pluijm

Colophon

Back in control: Towards early identification of treatment resistance in schizophrenia

Financial support for this research was provided by a Veni grant (91618075) from the Netherlands Organisation for Health Research and Development (ZonMw). In addition, parts of the research in this thesis are co-funded by Stichting J.M.C. Kapteinfonds, an NWO/Aspasia grant, the National Institute of Mental Health (R01 MH117323 and R01 MH114965), and VENI (016196153).

Cover	Thomas de Graaf & Proefschrift AIO
Layout	Proefschrift AIO
Printing	Proefschrift AIO

BACK IN CONTROL

Towards early identification of treatment resistance
in schizophrenia

ACADEMISCH PROEFSCHRIFT

ter verkrijging van de graad van doctor
aan de Universiteit van Amsterdam
op gezag van de Rector Magnificus
prof. dr. ir. P.P.C.C. Verbeek
ten overstaan van een door het College voor Promoties ingestelde commissie,
in het openbaar te verdedigen in de Agnietenkapel
op vrijdag 23 juni 2023, te 13.00 uur

door Marieke van der Pluijm
geboren te Langedijk

Promotiecommissie

Promotores:	prof. dr. J. Booij	AMC-UvA
	prof. dr. L. de Haan	AMC-UvA
Copromotores:	dr. E.M. van de Giessen	AMC-UvA
Overige leden:	prof. dr. G.A. van Wingen	AMC-UvA
	prof. dr. H.M. Geurts	Universiteit van Amsterdam
	prof. dr. B.U. Forstmann	Universiteit van Amsterdam
	prof. dr. N.E.M. van Haren	Erasmus Universiteit Rotterdam
	prof. dr. I.E.C. Sommer	Rijksuniversiteit Groningen
	dr. W.A.M. Vingerhoets	Maastricht University

Faculteit der Geneeskunde

Table of contents

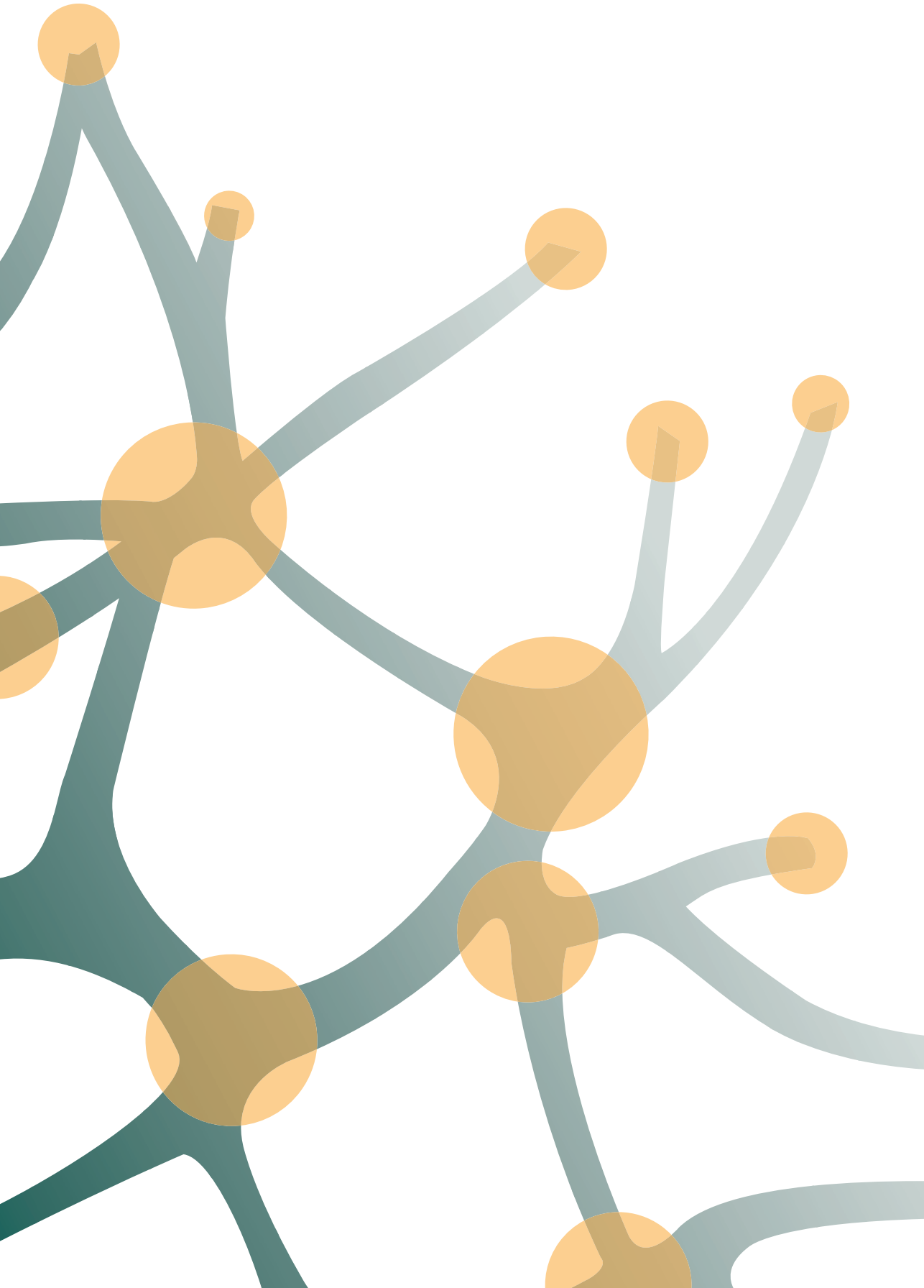

Chapter | 1

General introduction

Schizophrenia is a severe psychiatric disorder with a lifetime prevalence rate of approximately 0.75% (1). The disorder is characterized by the presence of positive symptoms (e.g., hallucinations and delusions), negative symptoms (e.g., apathy and avolition), and cognitive symptoms (2). A DSM-5 diagnosis of schizophrenia requires at least two symptoms (at least one from the positive symptom cluster) to be present over six months (3). Schizophrenia is associated with a high disease burden, due to the early age of onset, typically in late adolescence (4), combined with the persisting or fluctuating symptoms that a considerable part of the patient group experiences despite adequate treatment (2). As a result, schizophrenia is known as a relatively poor outcome disorder, including a severe decline in social and occupational functioning, although there is a substantial subgroup of patients with a better prognosis (5). The clinical presentation is highly heterogeneous and secondary to a complex neuropathology that, unfortunately, remains incompletely understood.

Neurobiology of schizophrenia

Dopamine hypothesis

Several theories exist regarding the underlying neurobiology of schizophrenia. The dopamine hypothesis is the most established and proposes that a combination of environmental and genetic factors leads to striatal hyperdopaminergic functioning (6). Striatal hyperdopaminergia is thought to disrupt salience attribution, leading to the positive symptoms. There is especially strong evidence for increased presynaptic striatal dopaminergic functioning (6). Multiple positron emission tomography (PET) studies, using [^{18}F]F-DOPA as a radiotracer, showed increased striatal dopaminergic synthesis capacity in schizophrenia compared to controls (7). In addition, patients with schizophrenia show larger radiotracer displacement after an amphetamine challenge (which induces a large increase in extracellular dopamine), indicating higher striatal dopamine release than healthy controls (8). The dopamine hypothesis implicates that hypodopaminergic functioning in frontal areas relates to the negative and cognitive symptoms of schizophrenia (6). However, especially for the cognitive and negative symptoms, the dopaminergic abnormalities alone are insufficient to explain schizophrenia pathology completely, and other neurotransmitter systems are increasingly recognized in theories about the underlying mechanisms of schizophrenia pathology (9,10).

Glutamate hypothesis

The second most recognized neurotransmitter systems in the neuropathology of schizophrenia are the glutamate and γ-aminobutyric acid (GABA) systems (9-11). Glutamate is the most abundant excitatory neurotransmitter in the brain and plays a crucial role in several processes, including learning, memory, and other cognitive processes. GABA is the primary inhibitory neurotransmitter in the brain and is especially involved in regulating brain activity. The excitatory glutamate and inhibitory GABA are considered to be interdependent and a balance between these two systems is essential for maintaining physiological homeostasis in the brain (12). Abnormal levels of glutamate and GABA have been observed in specific brain regions of patients with schizophrenia, and are thought to be implicated in the development and persistence of the disorder (13-15). The glutamate hypothesis proposes that hypofunctioning of N-methyl-D-aspartate (NMDA) receptors on GABAergic interneurons constitutes the main deficit underlying schizophrenia (16,17). Hypofunctioning of the NMDA receptor causes a reduction in GABAergic neuronal firing. As a consequence, there is insufficient inhibition of glutamatergic neurons, resulting in an excessive glutamate release. The dopamine and glutamate hypotheses are not mutually exclusive. Combined, they propose that presynaptic striatal hyperdopaminergia in schizophrenia might result from hyperactivation of glutamate neurons due to NMDA receptor dysfunction on GABA interneurons (9).

Treatment-resistant schizophrenia

First-line pharmacological treatment for schizophrenia consists of conventional antipsychotic medication. Although slight variations exist, all antipsychotics essentially have the same mechanism by blocking striatal dopamine D_2 receptors and thereby opposing the striatal hyperdopaminergic signal (6). Molecular imaging studies of antipsychotics showed substantial striatal D_2 receptor blockade with clinically effective doses that is needed for treatment response (6). In general, this is effective at treating the positive symptoms of the disorder and reduces the risk of relapse. However, the effect on negative and cognitive symptoms is limited (18). Additionally, approximately 30% of schizophrenia patients are treatment-resistant and do not sufficiently respond to these medications (19). Someone is considered treatment-resistant when they experience persistent moderate to severe positive symptoms, despite at least two different first-line antipsychotics with an adequate dose and duration (20,21). Clozapine is the only antipsychotic with proven effectiveness in treatment-resistant patients (22). Nevertheless, clozapine is underutilized because psychiatrists are reluctant to start clozapine, given the risk of serious adverse effects, including agranulocytosis, hyperglycemia, and seizures (23). Risks for agranulocytosis can be monitored by performing regular white blood cell counts and measuring clozapine levels in plasma. Nonetheless, delay in effective treatment for treatment-resistant patients can mount up to four years (24). This results in lower quality of life, hospitalizations, more severe comorbidities, and larger suicide risk (25). In adittion, a delay in effective treatment results in a poorer prognosis (26,27). Elucidating the

underlying neurobiology of treatment-resistant schizophrenia may aid in better treatment selection and result in markers for earlier identification of treatment-resistant patients.

Neurobiology of treatment-resistant schizophrenia

Dopamine

Patients with treatment-resistant schizophrenia show little or no response to antipsychotics, even with high levels of dopamine receptor blockade (28). This implies that there are dopaminergic differences between treatment-resistant patients and responders. Indeed, no increased striatal dopaminergic synthesis is detected in treatment-resistant patients, on the contrary, dopamine function seems comparable to healthy controls (29-31). This may explain why first-line antipsychotics are ineffective in treatment-resistant patients, as an important component of antipsychotic function depends on blocking striatal dopamine receptors to oppose elevated extracellular dopamine levels, and higher levels of striatal dopamine lead to better treatment response of positive symptoms (32). It appears that, although the dopamine hypothesis accounts for most of the patients, patients with treatment resistance do not show striatal hyperdopaminergia.

Glutamate

The pathophysiology of treatment-resistant schizophrenia might be more reliant upon non-dopaminergic metabolites, such as glutamate and GABA. Glutamate and GABA can be examined *in vivo* using proton magnetic resonance spectroscopy (MRS). MRS is a widely used scanning technique that is utilized to estimate concentrations of a variety of metabolites and to obtain information on the biochemical composition of the brain (33). Several MRS studies have shown elevated anterior cingulate cortex glutamate levels in treatment-resistant patients compared to responders (34-37). Since the glutamate hypothesis proposes that elevated glutamate in schizophrenia is secondary to NMDA receptor hypofunctioning, the regulation of GABA release might in turn be dysregulated (38,39).

Markers for treatment-resistant schizophrenia

Drawing upon the neuropathology in treatment-resistant schizophrenia, both dopamine functioning and glutamate/GABA levels could be potential biomarkers for treatment resistance. Such a marker could lead to earlier identification of treatment-resistant schizophrenia, reduce delays in effective treatment, and improve outcomes. One study has shown the predictive value of glutamate levels in the anterior cingulate cortex for treatment-resistant schizophrenia (40), and another for GABA (38). Nevertheless, there are inconsistent results regarding glutamate and GABA functioning in treatment-resistant schizophrenia (13,39,41). Striatal dopaminergic synthesis capacity appears to be a more consistent marker for treatment-resistant schizophrenia and has been shown to identify treatment-resistant

patients from responders with good accuracy (42). However, the gold standard for assessing striatal dopaminergic synthesis capacity, [^{18}F]F-DOPA PET imaging, is not feasible for routine screening to identify treatment-resistant patients since it is costly, time-consuming and, requires intravenous administration of a radiotracer.

Neuromelanin MRI

Neuromelanin-sensitive magnetic resonance imaging (NM-MRI) has been developed recently to non-invasively measure nigrostriatal dopamine functioning (43). Neuromelanin is a by-product of dopamine synthesis and accumulates as neuromelanin-iron complexes in the dopaminergic neurons of the substantia nigra (44). These dopaminergic neurons form the nigrostriatal pathway that projects to the dorsal striatum (45). The paramagnetic neuromelanin-iron complexes lead to T1 reduction and, in combination with reduced magnetization-transfer effects, result in high signal intensity in the substantia nigra using NM-MRI (46). NM-MRI signal correlates with regional neuromelanin concentration in post-mortem substantia nigra tissue and to PET measures of dopamine release in the dorsal striatum *in vivo* (47). NM-MRI signal in the substantia nigra is increased in schizophrenia compared to healthy controls (48), but has not yet been investigated in treatment-resistant schizophrenia.

Aims and outline of this thesis

The overall aim of this thesis is to explore markers for earlier identification of treatment-resistant schizophrenia. The main focus of the thesis is on developing and implementing the novel NM-MRI technique as a clinical marker for treatment-resistant schizophrenia. Earlier identification of treatment-resistant patients could aid caregivers in getting "back in control" of treatment decision making instead of being limited to a trial-and-error approach. Consequently, this could lead to earlier adequate treatment and help treatment-resistant patients to feel "back in control" again.

Part I: Development of NM-MRI

The first part of this thesis discusses the advancements in imaging the dopamine system using MRI, in particular NM-MRI (**chapter 2**). Furthermore, we validate NM-MRI as a reliable marker (**chapter 3**) and assess acceleration of NM-MRI to facilitate clinical applicability (**chapter 4**).

Part II: Substantia nigra in schizophrenia

The second part addresses the role of the substantia nigra in schizophrenia pathology, by integrating post-mortem and imaging findings (**chapter 5**). In addition, we explore the relation between NM-MRI of the substantia nigra and [^{18}F]F-DOPA PET in schizophrenia (**chapter 6**).

Part III: Markers for treatment-resistant schizophrenia

The last section concentrates on potential markers for treatment-resistant schizophrenia. First, we assess the potential of NM-MRI as a marker for treatment resistance (**chapter 7**). Second, we investigate whether plasma dopa-decarboxylase activity can be used as a marker for treatment-resistant schizophrenia (**chapter 8**). Third, we use MRS to examine glutamate and GABA levels in treatment-resistant patients (**chapter 9**). Lastly, we highlight the significance of early detection of treatment-resistant schizophrenia and propose the concept of duration of treatment resistance to facilitate future studies (**chapter 10**).

Finally, the main findings of these studies will be summarized and discussed in the context of existing literature.

References

1. Moreno-Kustner B, Martin C, Pastor L. Prevalence of psychotic disorders and its association with methodological issues. A systematic review and meta-analyses. PLoS One. 2018;13(4):e0195687.
2. McCutcheon RA, Reis Marques T, Howes OD. Schizophrenia-An Overview. JAMA Psychiatry. 2020;77(2):201-10.
3. Diagnostic and statistical manual of mental disorders: DSM-5™, 5th ed. Arlington, VA, US: American Psychiatric Publishing, Inc.; 2013. xliv, 947-xliv, p.
4. Gogtay N, Vyas NS, Testa R, Wood SJ, Pantelis C. Age of onset of schizophrenia: perspectives from structural neuroimaging studies. Schizophr Bull. 2011;37(3):504-13.
5. Harrow M, Grossman LS, Jobe TH, Herbener ES. Do patients with schizophrenia ever show periods of recovery? A 15-year multi-follow-up study. Schizophr Bull. 2005;31(3):723-34.
6. Howes OD, Kapur S. The dopamine hypothesis of schizophrenia: version III--the final common pathway. Schizophr Bull. 2009;35(3):549-62.
7. Fusar-Poli P, Meyer-Lindenberg A. Striatal presynaptic dopamine in schizophrenia, part II: meta-analysis of [(18)F/(11)C]-DOPA PET studies. Schizophr Bull. 2013;39(1):33-42.
8. Laruelle M, Abi-Dargham A, Gil R, Kegeles L, Innis R. Increased dopamine transmission in schizophrenia: relationship to illness phases. Biological Psychiatry. 1999;46(1):56-72.
9. Howes O, McCutcheon R, Stone J. Glutamate and dopamine in schizophrenia: an update for the 21st century. J Psychopharmacol. 2015;29(2):97-115.
10. Coyle JT. Glutamate and schizophrenia: beyond the dopamine hypothesis. Cell Mol Neurobiol. 2006;26(4-6):365-84.
11. Coyle JT. The GABA-glutamate connection in schizophrenia: which is the proximate cause? Biochem Pharmacol. 2004;68(8):1507-14.
12. Hampe CS, Mitoma H, Manto M. GABA and Glutamate: Their Transmitter Role in the CNS and Pancreatic Islets. In: Janko S, editor. GABA And Glutamate. Rijeka: IntechOpen; 2017. p. Ch. 5.
13. Egerton A, Modinos G, Ferrera D, McGuire P. Neuroimaging studies of GABA in schizophrenia: a systematic review with meta-analysis. Transl Psychiatry. 2017;7(6):e1147.
14. Merritt K, Egerton A, Kempton MJ, Taylor MJ, McGuire PK. Nature of Glutamate Alterations in Schizophrenia: A Meta-analysis of Proton Magnetic Resonance Spectroscopy Studies. JAMA Psychiatry. 2016;73(7):665-74.
15. Kumar V, Vajawat B, Rao NP. Frontal GABA in schizophrenia: A meta-analysis of (1)H-MRS studies. World J Biol Psychiatry. 2020:1-13.
16. Moghaddam B, Javitt D. From revolution to evolution: the glutamate hypothesis of schizophrenia and its implication for treatment. Neuropsychopharmacology. 2012;37(1):4-15.
17. Uno Y, Coyle JT. Glutamate hypothesis in schizophrenia. Psychiatry Clin Neurosci. 2019;73(5):204-15.
18. Leucht S, Tardy M, Komossa K, Heres S, Kissling W, Salanti G, et al. Antipsychotic drugs versus placebo for relapse prevention in schizophrenia: a systematic review and meta-analysis. The Lancet. 2012;379(9831):2063-71.
19. Elkis H, Buckley PF. Treatment-Resistant Schizophrenia. Psychiatr Clin North Am. 2016;39(2):239-65.
20. Andreasen CN, Carpenter J WT, Kane JM, Lasser MA, Marder SR, Weinberger, DR. Remission in Schizophrenia: Proposed Criteria and Rationale for Consensus. American Journal of Psychiatry. 2005;162(3):441-9.
21. Suzuki T, Remington G, Mulsant BH, Uchida H, Rajji TK, Graff-Guerrero A, et al. Defining treatment-resistant schizophrenia and response to antipsychotics: a review and recommendation. Psychiatry Res. 2012;197(1-2):1-6.
22. Lewis SW, Barnes TR, Davies L, Murray RM, Dunn G, Hayhurst KP, et al. Randomized controlled trial of effect of prescription of clozapine versus other second-generation antipsychotic drugs in resistant schizophrenia. Schizophr Bull. 2006;32(4):715-23.
23. Warnez S, Alessi-Severini S. Clozapine: a review of clinical practice guidelines and prescribing trends. BMC Psychiatry. 2014;14(1):102.
24. Howes OD, Vergunst F, Gee S, McGuire P, Kapur S, Taylor D. Adherence to treatment guidelines in clinical practice: study of antipsychotic treatment prior to clozapine initiation. Br J Psychiatry. 2012;201(6):481-5.
25. Kennedy JL, Altar CA, Taylor DL, Degtiar I, Hornberger JC. The social and economic burden of treatment-resistant schizophrenia: a systematic literature review. Int Clin Psychopharmacol. 2014;29(2):63-76.

26. Black K, Peters L, Rui Q, Milliken H, Whitehorn D, Kopala LC. Duration of untreated psychosis predicts treatment outcome in an early psychosis program. Schizophrenia Research. 2001;47(2):215-22.
27. Yoshimura B, Yada Y, So R, Takaki M, Yamada N. The critical treatment window of clozapine in treatment-resistant schizophrenia: Secondary analysis of an observational study. Psychiatry Res. 2017;250:65-70.
28. Kapur S, Zipursky R, Jones C, Remington G, Houle S. Relationship Between Dopamine D2 Occupancy, Clinical Response, and Side Effects: A Double-Blind PET Study of First-Episode Schizophrenia. American Journal of Psychiatry. 2000;157(4):514-20.
29. Demjaha A, Egerton A, Murray RM, Kapur S, Howes OD, Stone JM, et al. Antipsychotic treatment resistance in schizophrenia associated with elevated glutamate levels but normal dopamine function. Biol Psychiatry. 2014;75(5):e11-3.
30. Jauhar S, Veronese M, Nour MM, Rogdaki M, Hathway P, Turkheimer FE, et al. Determinants of treatment response in first-episode psychosis: an (18)F-DOPA PET study. Mol Psychiatry. 2019;24(10):1502-12.
31. Kim E, Howes OD, Veronese M, Beck K, Seo S, Park JW, et al. Presynaptic Dopamine Capacity in Patients with Treatment-Resistant Schizophrenia Taking Clozapine: An [(18)F]DOPA PET Study. Neuropsychopharmacology. 2017;42(4):941-50.
32. Abi-Dargham A, Rodenhiser J, Printz D, Zea-Ponce Y, Gil R, Kegeles LS, et al. Increased baseline occupancy of D2 receptors by dopamine in schizophrenia. Proceedings of the National Academy of Sciences. 2000;97(14):8104-9.
33. Faghihi R, Zeinali-Rafsanjani B, Mosleh-Shirazi MA, Saeedi-Moghadam M, Lotfi M, Jalli R, et al. Magnetic Resonance Spectroscopy and its Clinical Applications: A Review. J Med Imaging Radiat Sci. 2017;48(3):233-53.
34. Egerton A, Brugger S, Raffin M, Barker GJ, Lythgoe DJ, McGuire PK, et al. Anterior cingulate glutamate levels related to clinical status following treatment in first-episode schizophrenia. Neuropsychopharmacology. 2012;37(11):2515-21.
35. Egerton A, Murphy A, Donocik J, Anton A, Barker GJ, Collier T, et al. Dopamine and Glutamate in Antipsychotic-Responsive Compared With Antipsychotic-Nonresponsive Psychosis: A Multicenter Positron Emission Tomography and Magnetic Resonance Spectroscopy Study (STRATA). Schizophr Bull. 2021;47(2):505-16.
36. Iwata Y, Nakajima S, Plitman E, Caravaggio F, Kim J, Shah P, et al. Glutamatergic Neurometabolite Levels in Patients With Ultra-Treatment-Resistant Schizophrenia: A Cross-Sectional 3T Proton Magnetic Resonance Spectroscopy Study. Biol Psychiatry. 2019;85(7):596-605.
37. Mouchlianitis E, Bloomfield MAP, Law V, Beck K, Selvaraj S, Rasquinha N, et al. Treatment-Resistant Schizophrenia Patients Show Elevated Anterior Cingulate Cortex Glutamate Compared to Treatment-Responsive. Schizophrenia Bulletin. 2016;42(3):744-52.
38. Bojesen KB, Ebdrup BH, Jessen K, Sigvard A, Tangmose K, Edden RAE, et al. Treatment response after 6 and 26 weeks is related to baseline glutamate and GABA levels in antipsychotic-naive patients with psychosis. Psychol Med. 2020;50(13):2182-93.
39. Ueno F, Nakajima S, Iwata Y, Honda S, Torres-Carmona E, Mar W, et al. Gamma-aminobutyric acid (GABA) levels in the midcingulate cortex and clozapine response in patients with treatment-resistant schizophrenia: A proton magnetic resonance spectroscopy ((1) H-MRS) study. Psychiatry Clin Neurosci. 2022;76(11):587-94.
40. Egerton A, Broberg BV, Van Haren N, Merritt K, Barker GJ, Lythgoe DJ, et al. Response to initial antipsychotic treatment in first episode psychosis is related to anterior cingulate glutamate levels: a multicentre (1)H-MRS study (OPTiMiSE). Mol Psychiatry. 2018;23(11):2145-55.
41. Kumar V, Manchegowda S, Jacob A, Rao NP. Glutamate metabolites in treatment resistant schizophrenia: A meta-analysis and systematic review of (1)H-MRS studies. Psychiatry Res Neuroimaging. 2020;300:111080.
42. Veronese M, Santangelo B, Jauhar S, D'Ambrosio E, Demjaha A, Salimbeni H, et al. A potential biomarker for treatment stratification in psychosis: evaluation of an [(18)F] FDOPA PET imaging approach. Neuropsychopharmacology. 2021;46(6):1122-32.
43. Shibata E, Sasaki M, Tohyama K, Otsuka K, Endoh J, Terayama Y, et al. Use of neuromelanin-sensitive MRI to distinguish schizophrenic and depressive patients and healthy individuals based on signal alterations in the substantia nigra and locus ceruleus. Biol Psychiatry. 2008;64(5):401-6.
44. Zucca FA, Vanna R, Cupaioli FA, Bellei C, De Palma A, Di Silvestre D, et al. Neuromelanin organelles are specialized autolysosomes that accumulate undegraded proteins and lipids in aging human brain and are likely involved in Parkinson's disease. NPJ Parkinsons Dis. 2018;4:17.

45. McCutcheon RA, Abi-Dargham A, Howes OD. Schizophrenia, Dopamine and the Striatum: From Biology to Symptoms. Trends Neurosci. 2019;42(3):205-20.
46. Trujillo P, Summers PE, Ferrari E, Zucca FA, Sturini M, Mainardi LT, et al. Contrast mechanisms associated with neuromelanin-MRI. Magn Reson Med. 2017;78(5):1790-800.
47. Cassidy CM, Zucca FA, Girgis RR, Baker SC, Weinstein JJ, Sharp ME, et al. Neuromelanin-sensitive MRI as a noninvasive proxy measure of dopamine function in the human brain. Proc Natl Acad Sci U S A. 2019;116(11):5108-17.
48. Ueno F, Iwata Y, Nakajima S, Caravaggio F, Rubio JM, Horga G, et al. Neuromelanin accumulation in patients with schizophrenia: A systematic review and meta-analysis. Neurosci Biobehav Rev. 2022;132:1205-13.

PART I

DEVELOPMENT OF NEUROMELANIN-MRI

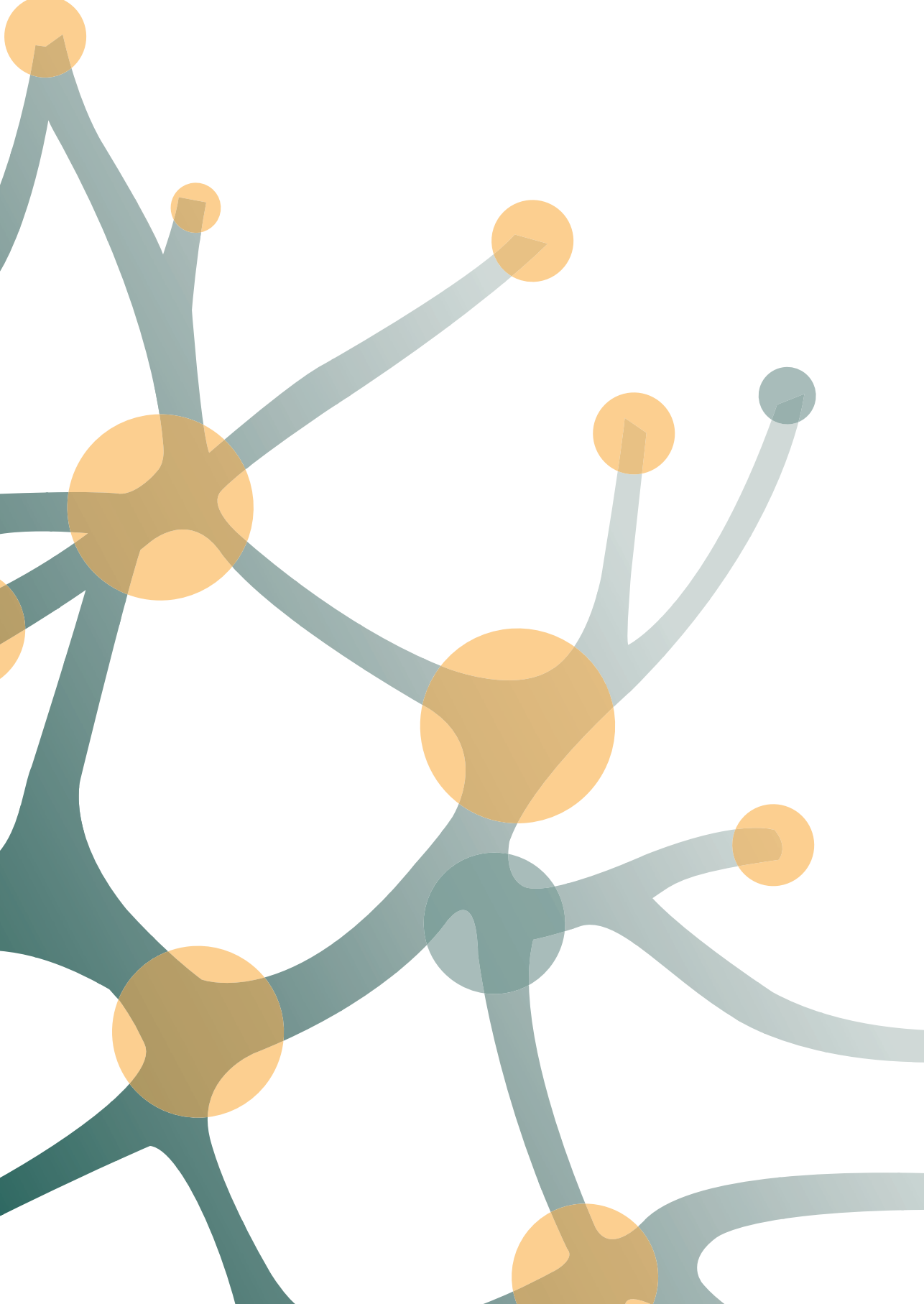

Chapter | 2

Imaging of the dopamine system with focus on pharmacological MRI and neuromelanin imaging

Liesbeth Reneman, Marieke van der Pluijm,
Anouk Schrantee, Elsmarieke van de Giessen

European Journal of Radiology, 2021; 140:109752
DOI: 10.1016/j.ejrad.2021.109752

Abstract

The dopamine system in the brain is involved in a variety of neurologic and psychiatric disorders, such as Parkinson's disease, attention-deficit/hyperactivity disorder and psychosis. Different aspects of the dopamine system can be visualized and measured with positron emission tomography (PET) and single photon emission computed tomography (SPECT), including dopamine receptors, dopamine transporters, and dopamine release. New developments in MR imaging also provide proxy measures of the dopamine system in the brain, offering alternatives with the advantages MR imaging, i.e. no radiation, lower costs, usually less invasive and time consuming. This review will give an overview of these developments with a focus on the most developed techniques: pharmacological MRI (phMRI) and neuromelanin sensitive MRI (NM-MRI). PhMRI is a collective term for functional MRI techniques that administer a pharmacological challenge to assess its effects on brain hemodynamics. By doing so, it indirectly assesses brain neurotransmitter function such as dopamine function. NM-MRI is an upcoming MRI technique that enables in vivo visualization and semi-quantification of neuromelanin in the substantia nigra. Neuromelanin is located in the cell bodies of dopaminergic neurons of the nigrostriatal pathway and can be used as a proxy measure for long term dopamine function or degeneration of dopaminergic neurons. Both techniques are still primarily used in clinical research, but there is promise for clinical application, in particular for NM-MRI in dopaminergic neurodegenerative diseases like Parkinson's disease.

Introduction

Visualization of the dopamine system in the brain is of interest due to its role in a variety of neurologic and psychiatric disorders, such as Parkinson's disease (PD), attention-deficit/hyperactivity disorder (ADHD) and psychosis. Apart from its role in pathology, dopamine is crucial for physiologic brain functions, e.g. motor control, reward and cognitive functions such as working memory. There is a wide variety of radioligands available to image different aspects of the dopamine system using positron emission tomography (PET) and single photon emission computed tomography (SPECT). It is possible to obtain measurements of dopamine production, storage, and reuptake capacity and of different types of dopamine receptors (D_1, D_2 and D_3). These imaging techniques are frequently used in research setting and have provided great insight in brain function. It is clear now that an optimal balance between dopamine levels and dopamine receptors is necessary in different regions and that either too much (such as during stress or after amphetamine stimulation) or too little (such as in aging and neurodegeneration) leads to impaired cognitive function (1). For example, we now know that the hallucinations and delusions in psychosis are related to increased dopamine production in the striatum (2). This explains why blocking dopamine D_2 receptors and decreasing dopamine signal transduction with antipsychotics reduces these symptoms.

In the clinical setting, imaging of the dopamine system is primarily applied in diseases with dopaminergic neurodegeneration, such as PD, progressive supranuclear palsy, multiple system atrophy and Lewy body dementia. The most common clinical indications are 1) to distinguish neurodegenerative parkinsonian disorders (usually PD) from non-neurodegenerative parkinsonian disorders (e.g. essential tremor, vascular parkinsonism or medication induced parkinsonism) and 2) to distinguish Lewy body disease dementia from Alzheimer's disease. In the case of PD, more than 30 percent of the dopaminergic neurons in the nigrostriatal pathway have been lost at onset of symptoms (3) and this can be visualized. The most commonly used radioligands are [^{123}I]FP-CIT (also known as DaTscan) for SPECT and [^{18}F]FDOPA for PET, although other radioligands may also be applied. [^{123}I]FP-CIT binds to the dopamine transporter and [^{18}F]FDOPA is taken up by dopa decarboxylase, an enzyme involved in the production of dopamine. Both techniques visualize the presynaptic dopaminergic neurons in the striatum and provide a sensitive measure of dopaminergic cell loss in neurodegeneration.

Whereas PET and SPECT are very useful for these different measures of the dopamine system, their disadvantages are that they are costly, lead to radiation exposure and are usually more time consuming than magnetic resonance imaging (MRI). Over the last decade, new techniques have been developed that provide both direct and indirect measures of the dopamine system. For example, invasive techniques like fast-scan cyclic voltammetry have been applied in the human brain to assess dopamine fluctuations in patients that underwent DBS surgery (4). But also novel MRI techniques have emerged that enable us to visualize

the dopamine system. One technique that is promising, but still in the stage of preclinical research, is the use of neurotransmitter-responsive nanosensors that can be imaged using T2-weighted MRI (5). Other MRI methods have advanced to the clinical research stage and they provide a great opportunity for studying the dopamine system in different populations such as children and for performing longitudinal studies with multiple measures, with great potential for clinical applications. The most developed and promising techniques today are pharmacological MRI (phMRI) and neuromelanin sensitive MRI (NM-MRI). In this paper we will review the present state of these imaging techniques and newest developments after giving a short background of the dopamine system in the brain.

Dopamine system

The dopamine system in the brain consists of several pathways of which three are most prominent (Fig. 1). The first is the nigrostriatal pathway. This pathway consists of dopaminergic neurons in the substantia nigra in the midbrain, whose axons project to the striatum. It is involved in motor function and associative learning amongst others. The second pathway is the mesolimbic pathway, consisting of dopaminergic neurons projecting from the ventral tegmental area to the ventral striatum, including the nucleus accumbens. This pathway is essential in reward processing and aversion. As both the nigrostriatal and mesolimbic pathways project to the striatum, this is the most dopamine rich region of the brain. Subsequently, it is the most common target of many dopaminergic imaging techniques. The third pathway is the mesocortical pathway. The dopaminergic neurons of this pathway also originate in the ventral tegmental area, but project to the cortex, mostly to the prefrontal cortex. This pathway is involved in executive and cognitive functioning.

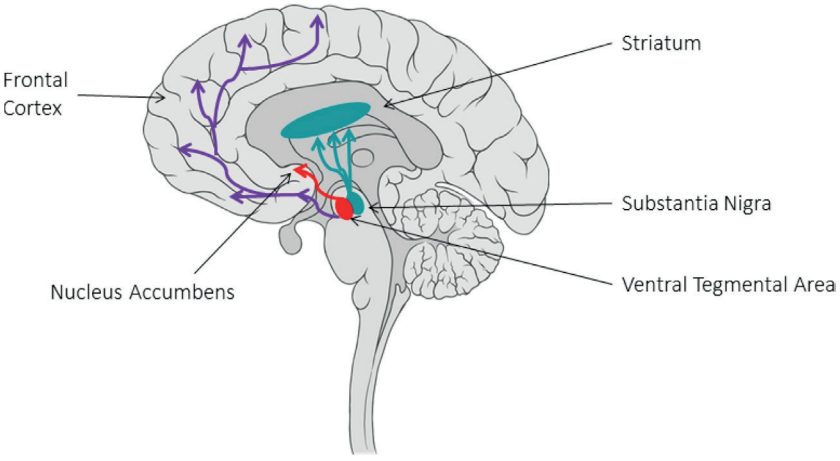

Fig. 1. Schematic representation of the major dopaminergic pathways in the brain: the nigrostriatal pathway (blue), the mesolimbic pathway (red) and the mesocortical pathway (purple).

These different pathways have a different constitution of the dopamine system. Signal transduction in the dorsal striatum (nigrostriatal pathway) is largely conducted by dopamine D_1 and D_2 receptors, whereas in the ventral striatum (mesolimbic pathway) also D_3 receptors are abundant. In the (pre)frontal cortex (mesocortical pathway) the primary receptor for signal transduction is the D_1 receptor, although there is also a relatively low number of D_2 receptors. Likewise, dopamine reuptake is facilitated by dopamine transporters in the striatum, but by norepinephrine transporters in the cortex. Whereas dopamine degradation is performed by monoamine oxidase (MAO) in the striatum, but by catechol-O-methyltransferase (COMT) in the cortex. Knowledge of these regional differences can aid in the interpretation of imaging outcomes. Moreover, these differences are important for targeted treatment, e.g. with drugs targeting specific types of receptors or transporters.

Pharmacological MRI (phMRI)

PhMRI is a collective term for functional MRI techniques that administer a pharmacological challenge to assess its effects on brain hemodynamics, and by doing so indirectly assess brain neurotransmitter function (6). A schematic example of the technique is shown in Fig. 2. The choice of the pharmacological challenge determines the neurotransmitter system that is visualized. For example, to obtain a readout of the function of the dopamine system, agonists or antagonists of dopamine receptors and transporters are used, such as apomorphine, amphetamine or methylphenidate. The technique is based on the principle that the pharmacological challenge binds to its targeted receptor subtype, whose activation evokes changes in neurovascular coupling that result in hemodynamic changes. This hemodynamic response consists of an increase in local cerebral blood flow (CBF), blood volume (CBV) and oxygenation (7). In this review we will focus specifically on *challenge phMRI* (during rest) rather than *task phMRI* (during the execution of a sensorimotor or cognitive task), as measuring the hemodynamic response to the drug during rest reflects a more direct measure of the dopamine response.

Two main MRI methods that have been used to assess changes in hemodynamic response in response to a pharmacological challenge in humans are Blood Oxygen Level-Dependent (BOLD) imaging and Arterial Spin Labeling (ASL). BOLD MRI makes use of the difference in magnetic susceptibility between oxygenated and deoxygenated blood, detectable by T2*-weighted sequences (8). Neuronal activation increases local blood flow and thus the inflow of oxygenated blood, which far exceeds the consumed oxygen. As oxygenated blood has a higher T2* this results in a net increase in the BOLD signal. ASL on the other hand, utilizes blood as an endogenous contrast agent. Blood passing into the brain is labeled at the main feeding arteries by applying an inversion pulse, after which the labeled blood travels to the brain and creates small decreases in longitudinal magnetization. The perfusion contrast is then generated by subtracting two acquired images, one with label and one without. The

advantage of ASL over BOLD is that it is quantitative and that it is a more direct technique because it measures CBF, whereas the BOLD signal is determined by changes in CBF, CBV and oxygen consumption. Moreover, as a result of the subtraction it is not sensitive to signal drift, which is a problem in BOLD imaging as the low frequencies of the drift often coincide with the low frequency of the signal changes following the pharmacological challenge (9). However, ASL suffers from a lower signal to noise ratio (SNR) and less spatial specificity (larger voxels) compared to BOLD imaging. A third MRI method that has been used is CBV imaging, but this uses an exogenous intravascular contrast agent that sensitizes images to relative CBV and is therefore only used in animal phMRI.

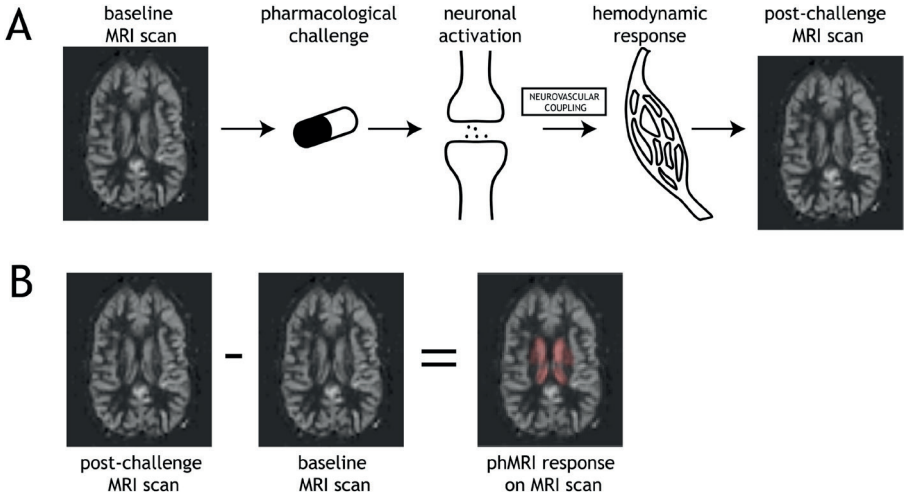

Fig. 2. Schematic of phMRI experiment. A) A baseline MRI scan (e.g. perfusion scan) is performed after which a pharmacological challenge is administered. Through its binding to target receptors, this challenge can elicit neuronal activation and, subsequently, through neurovascular coupling, also a hemodynamic response, which can be captured by a post-challenge MRI scan. B) Possible changes can be estimated using statistical analyses comparing the pre- and post-challenge MRI and the resulting parametric maps can be overlaid on the MRI image.

Initial phMRI studies in animals used pharmacological challenges that primarily targeted the dopamine system, and demonstrated that administration of e.g. amphetamine increased the BOLD signal in the striatum and cortex (10). Many of these studies focused on the validation of phMRI compared to conventional techniques such as autoradiography, microdialysis and PET and SPECT (10-12), and found that they were well correlated. For instance, phMRI faithfully reproduced DA denervation (-42 % with PET vs. -45% with phMRI) (10) and a strong correlation was found between the amplitude of the phMRI response in the SN and the number of dopaminergic neurons on the side ipsilateral to neurotoxic (MPTP) injection (12). Subsequent studies in rodents and non-human primates used unilateral lesioning with dopamine neurotoxins (including MPTP (1-methyl-4-phenyl-1,2,3,6-tetrahydropyridine) a model for PD (13)) to demonstrate that the phMRI response to a dopamine challenge was

restricted to the intact side, blunting the response on the lesioned side. Inducing remodeling of the dopamine system using repeated amphetamine exposure further demonstrated the sensitivity of phMRI to more subtle dopamine alterations (14). Together, these studies demonstrated the possibility of phMRI to detect damage or dysfunction of the dopamine system and opened up possibilities for use in humans. In subsequent validation studies in humans, phMRI with a dopamine challenge was able to demonstrate a blunted dopamine response in regular amphetamine users compared to controls, similar to [^{123}I]IBZM SPECT (15,16). Test-retest reliability has not been demonstrated for dopaminergic challenges, but was demonstrated for phMRI with a ketamine challenge. Reliable responses were observed at low doses, but the researchers stress the need for correct modeling of the data, including possible confounding effects, such as physiological variation and head motion, to increase reproducibility (17).

One of the strengths of phMRI is that it can be used to study numerous aspects of the dopamine system, as different receptor subtypes can be visualized with different challenges. Indeed, a large number of pharmaceuticals are available, which means that phMRI, compared to PET which requires specific radiolabels, is ideally suited for drug discovery. However, it is important to understand what aspects of the dopamine system the phMRI signal reflects (18). Being a functional technique, the signal is likely more representative of mRNA levels (19), extrasynaptic dopamine concentration or cyclicAMP levels (11), than that it reflects measures such as receptor density for example. In that sense, it also does not have the same sensitivity as PET and SPECT to assess receptor densities, as it is a non-invasive proxy measure. The obtained response after a dopamine challenge is also not dopamine specific per se, because the activated receptors will initiate a cascade on neuronal events downstream from the initial drug-to-target binding, which can also elicit a neuronal response. Although a disadvantage when one's goal is to identify receptor subtypes, it also implies that the phMRI response gives a more complete characterization the brain's response to the drug, and provide potential leads for experienced side effects. Notably, most medications are not "clean", i.e. they affect multiple neurotransmitter systems and multiple receptor subtypes, which precludes a neurotransmitter-specific phMRI response.

PhMRI offers many opportunities for drug discovery and clinical research studies, but also comes with some unique challenges, particularly in the field of data analysis and interpretation. For a more complete overview of these challenges and possible solutions, which is outside the scope of this review, see Jenkins et al. (6). Most phMRI studies employ intravenous administration of the challenge, because this eliminates the issue of individual differences in absorption levels. However, the brain's response to pharmaceuticals is mostly slow and does not always return to baseline within the scanning session. Therefore, it is difficult to separate the neuronal phMRI response from other slow-varying frequency signals, including scanner drift. Modelling the phMRI response also requires prior knowledge on the expected

waveform, e.g. obtained from pharmacokinetic and pharmacodynamic (PK/PD) modelling, or will have to rely on data driven approaches. This complicates the interpretation of the signal as there are numerous confounding variables that play a role. For example, the administered challenges could induce systemic or cerebral vascular effects that are not due to binding of the drug to the target receptor in the brain (20). Vasoactive drugs can induce changes in blood pressure, pCO_2, and vasodilation or constriction that are measured as hemodynamic responses in the brain. Possible solutions are to obtain baseline measures of such vascular characteristics (e.g. CBF from ASL), to monitor these during the scan (e.g. pCO_2, heart rate, respiration) or to correct for them by sophisticated post-processing techniques.

PhMRI has potential applications in the field of drug discovery and treatment prediction and monitoring. For drug discovery studies it is important to make use of standardized methods in order to define phMRI signatures for medications with proven clinical efficacy. In this way, phMRI responses to novel compounds can be compared to reference medications and as such be evaluated in terms of expected efficacy and side effects. Moreover, it could identify converging mechanisms of action across drug classes. This has been effectively demonstrated in rodent models for antipsychotics, antidepressants and anxiolytics, in which complex whole-brain phMRI responses were condensed into sensible multivariate metrics (21). This approach has the potential to be translated to human clinical trials as well, but is partially hampered by issues of MR acquisition and post-processing standardization, as well as patient group heterogeneity. Currently, phMRI is also used in clinical research studies, with a focus on longitudinal designs and vulnerable patient populations. For example, we have used phMRI as a technique to assess persistent effects of the ADHD medication methylphenidate on brain development and dopamine function in children and adults with ADHD (22). Using a slightly different approach, studies in PD have investigated hemodynamic responses in patients on and off their levodopa medication (23,24). And a recent study has demonstrated a method to evaluate the severity of dopamine denervation in PD (25). PhMRI is not yet clinically used for diagnosis and progression of PD, or other neuropsychiatric diseases in which the DA system is involved; possibly because the underlying mechanisms of phMRI signals are not fully understood, and/or unfamiliarity with the technique. Advancement in image acquisition and analysis techniques (e.g., AI for noise reduction) and the addition of pharmacokinetic-pharmacodynamic (PK-PD) modelling could further advance DA phMRI into the clinic. Indeed, a very recent phMRI study was able to stage PD disease using PK-PD modelling (25).

Neuromelanin sensitive MRI (NM-MRI)

NM-MRI is an upcoming MRI technique that enables in vivo visualization of the substantia nigra pars compacta (SN). It has gained increasing interest due to the role of the SN in a variety dopaminergic disorders, including schizophrenia, cocaine addiction, Huntington's

and Parkinson's disease (PD) (26-28). The SN in the mesencephalon is the location from where dopaminergic neurons project to the striatum forming the nigrostriatal pathway. Visualization of this relatively small brainstem area with use of MRI has been challenging for a long time. The structure is visible on T1, T2 and T2*/susceptibility weighted sequences, but usually with rather low contrast. Loss of hyperintensity of nigrosome-1, a substructure posterolateral in the SN, on susceptibility weighted imaging (swallow tail sign), has been indicated as a marker for PD and Lewy body disease, although it needs a targeted 3D susceptibility weighted imaging sequence and is not widely applied in clinical use. These conventional MRI techniques do not permit semi-quantitative measures, accurate delineation or volume measures of the SN. Therefore, NM-MRI has been introduced as a promising and non-invasive method to indirectly assess dopaminergic functioning in the SN (29).

Neuromelanin is a black pigmented by-product of catecholamine synthesis. The most common catecholamines are dopamine, noradrenaline and adrenaline. This black pigment is predominantly found in the SN pars compacta, hence its name, and in the smaller locus coeruleus, the major noradrenergic nucleus of the brain. Accumulation of neuromelanin in the SN pars compacta is mainly driven by excess cytosolic dopamine that has not been taken up into synaptic vesicles (30). After iron dependent oxidation of the cytosolic dopamine and reaction with proteins and lipids in midbrain dopamine neurons neuromelanin-iron complexes are deposited inside autophagic organelles (31,32). The accumulation of these neuromelanin complexes in the SN show a strong inverted U-shaped age effect (33). Neuromelanin production is initiated at approximately three years of age, and its accumulation steeply increases until the age of 20. Around the 3rd and 4th decade of age there is typically no significant change in neuromelanin levels, and after the age of 47 neuromelanin levels in the SN decline (33).

The paramagnetic neuromelanin-iron complexes lead to T1 reduction, which is thought to be the primary mechanism underlying image contrast in NM-MRI (34). Indeed, the first proposed NM-MRI scan was an interleaved multi-slice turbo-spin echo (TSE) T1-weighted sequence (29). Studies directly comparing post-mortem TSE NM-MRI with histological findings have confirmed NM-MRI signal intensity to be closely related to the quantity and location of the neuromelanin-containing dopaminergic neurons in the SN (35,36). Next to T1 reduction by the neuromelanin-iron complexes, the contrast in NM-MRI is due to magnetization transfer (MT) effect. This is probably partly related to higher macromolecular content in the adjacent white matter than in the grey matter of the substantia nigra (34,37-39) Therefore, an (off-resonance) MT-pulse in often added to the TSE sequence, to suppress the contribution of macromolecules to the signal, therewith increasing contrast (34,40).

Along with the development of the TSE NM-MRI, a Gradient Recalled Echo (GRE) NM-MRI sequence has been introduced, which also includes an MT pulse (41) (Fig. 3). The GRE NM-MRI is validated and compared with the TSE sequence and shows a higher sensitivity for imaging

the SN (42). In addition, reliability studies yield excellent reproducibility for the GRE NM-MRI (43-46) and most importantly the sequence correlates with regional NM concentration (47), even in the absence of neurodegeneration (44). Through these promising results the GRE NM-MRI has gained more recognition. There is still quite some variation in sequence parameters between centers and further optimization of the sequence is ongoing, including optimizing slice thickness, resolution, repetition time, flip angle, and acceleration of scan duration, next to optimization of analysis methods (42,44,45,48,49). Based on the most recent results approximately a 4–7-minute scan duration is needed for a 3D GRE NM-MRI acquisition (37) and 3–6 min for reliable 2D GRE NM-MRI data (45). However, this may need customization of the standard MT pulse provided by the major MRI system vendors.

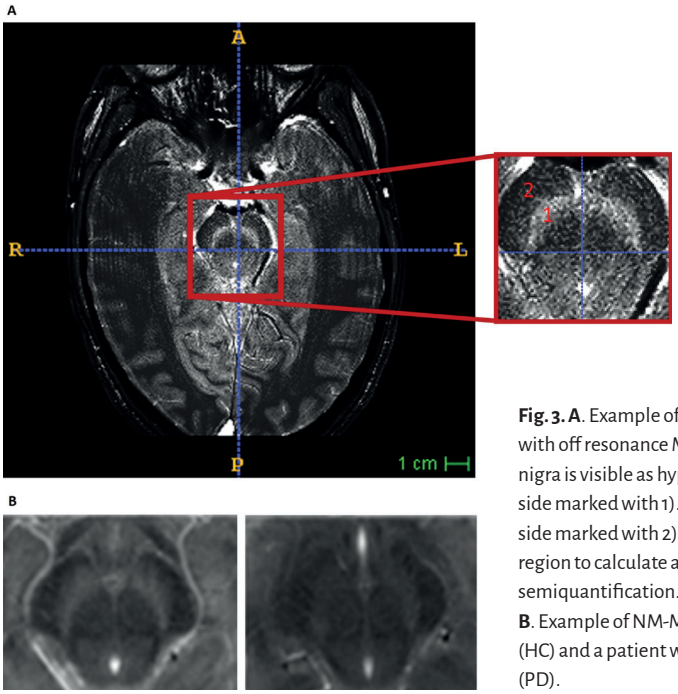

Fig. 3. A. Example of NM-MRI GRE sequence with off resonance MT pulse. The substantia nigra is visible as hyperintense area (right side marked with 1). The crus cerebri (right side marked with 2) is often used as reference region to calculate a contrast ratio for semiquantification.
B. Example of NM-MRI in a healthy control (HC) and a patient with Parkinson's disease (PD).

In order to evaluate which dopamine functions are best reflected in NM-MRI, there are several comparisons with different dopaminergic PET and SPECT imaging methods. NM-MRI signal in the SN correlates positively with the availability of dopamine D_2 receptors in the SN as measured with PET (50), which may suggest a local feedback mechanism of autoreceptors on the dopaminergic cells (i.e. in case of more dopamine, increased cytosolic dopamine leads to more neuromelanin deposit, and increased synaptic dopamine leads to higher expression of dopamine D_2 autoreceptors providing feedback to reduce dopamine production). There is no association between NM-MRI signal and dopamine transporter availability or dopamine synthesis capacity in the SN in young adults though (50). However, when comparing NM-MRI with dopaminergic functions in the synaptic

terminals of the nigrostriatal pathway, there is a positive correlation between NM-MRI signal in the SN and amphetamine induced dopamine release in the striatum (44). This indicates that NM-MRI could be used as an indirect marker for dopamine synthesis in the nigrostriatal pathway. Furthermore, there are several positive correlations between SN NM-MRI measures and striatal dopamine transporter availability in PD (51-55), supporting its role as a marker for dopaminergic neurodegeneration.

Considering its potential as noninvasive proxy for dopamine functioning, NM-MRI has been applied in multiple patient studies. The majority of studies focused on PD and showed a reliable decrease of SN volume and NM-MRI signal in the SN of patients with PD (51,54-67), for an example see Fig. 3B. These results are in line with the reduction of neuromelanin concentration in the SN in PD, due to the degeneration of dopaminergic neurons (68). Since clinical diagnosis of PD is challenging in a subset of patients (around 20%), in particular at early disease stage (69), NM-MRI may contribute to diagnostics. A recent meta-analysis evaluated the diagnostic utility of NM-MRI to differentiate PD from healthy controls and yielded a high pooled sensitivity (82%) and specificity (82 %) for distinguishing PD patients from healthy controls (70). There was high heterogeneity between the 10 studies included in this meta-analysis though, both in sample characteristics (early and advanced PD patients), NM-MRI sequence and NM-MRI analysis methods (volume and contrast measurements). In clinical practice it would be more important to distinguish PD from non-neurodegenerative parkinsonism rather than from healthy controls. NM-MRI indeed shows high diagnostic performance for differentiating essential tremor from PD with sensitivity ranging between 67–91% and specificity ranging between 80–93% (60-71). Combination of NM-MRI with quantitative susceptibility mapping (QSM) may even further improve diagnostic accuracy (51,72,73). As mentioned previously, NM-MRI also shows moderate to strong correlations with dopamine transporter (DAT) SPECT and PET imaging, the current standard for diagnostic imaging in parkinsonism (51-55). NM-MRI does not reach the high sensitivity and specificity of DAT SPECT though, which is up to 98 and 100% respectively (74). Longitudinal imaging in PD demonstrates further signal and SN volume reductions over time, as expected due to progressive degeneration (75). Despite these promising results, NM-MRI needs further development and standardization before it can be used as a diagnostic tool or for monitoring of disease progression in PD.

Other disorders with dopaminergic neurodegeneration also show decreased NM-MRI signal in the SN. The decrease in NM-MRI contrast in atypical parkinsonisms (multiple system atrophy, progressive supranuclear palsy and corticobasal degeneration) and in idiopathic rapid eye movement sleep behaviour disorder is similar as in PD (51,76-79). Moreover, in Huntington's Disease a decrease in NM-MRI signal compared to healthy controls has also been observed (80). Discriminating PD from atypical parkinsonism is difficult although advanced analysis shows potential (81).

Apart from the potential of NM-MRI in neurodegenerative disorders, NM-MRI could be an interesting tool to assess underlying dopaminergic pathology in psychiatric disorders such as ADHD, schizophrenia and addiction. The first study using NM-MRI in a psychiatric patient population showed increased NM-MRI signal in schizophrenia patients compared to depressive patients and healthy controls (27). This finding of increased NM-MRI signal in schizophrenia compared to controls has been replicated (82), although one study only reports an increase in the VTA and not SN (83). Moreover increased NM-MRI signal in the SN correlates positively with positive symptoms, i.e. hallucinations and delusions (44). This all fits previous findings with PET imaging that dopamine synthesis in the nigrostriatal pathway is increased in schizophrenia and related to positive symptoms (2). A recent study also provides a first indication NM-MRI signal is increased in the SN in cocaine addiction (28). Hence, NM-MRI appears to be a potential biomarker for dopamine dysfunction in psychiatric disorders. It should be taken into account that NM-MRI is not able to measure short-term dynamic changes in dopamine function (as can be assessed with SPECT/PET imaging and phMRI), but is rather a reflection of long-term dopamine function due to the nature of neuromelanin as a deposit in the dopaminergic cells.

Taken together, NM-MRI of the SN appears to be a promising tool as a proxy for dopaminergic functioning in the SN. Considering its noninvasive quality and short scan duration it may develop as a relatively easily accessible research tool for neuropsychiatric disorders and has the potential to aid diagnostics of dopaminergic neurodegeneration.

Conclusion

New developments in MR imaging provide highly promising proxy measures of the dopamine system in the brain. These measures will not replace dopaminergic PET and SPECT imaging, which are more direct measures of the different components of the dopamine system (e.g. receptors, transporters, dopamine release). However, they offer alternatives with the advantages of MR imaging, i.e. no radiation, lower costs, usually less invasive and time consuming and higher spatial resolution. The most developed MRI techniques are phMRI and NM-MRI. They both have specific characteristics which make them feasible for different purposes (see Fig. 4). PhMRI requires a pharmacological challenge and is a dynamic measure of dopamine function. NM-MRI on the other hand is rather a reflection of long-term dopamine function. Whereas phMRI visualizes the whole brain, NM-MRI visualizes the SN and only provides information about the nigrostriatal pathway. These characteristics make phMRI a useful technique to study reactivity of the dopamine system, which is important for drug development and for understanding the pathophysiology of dopamine related disorders related. phMRI opens up new possibilities to do so in a longitudinal setting with multiple measures and in specific patient populations like children. Applications in clinical practice are not expected in short term though. NM-MRI on the other hand has promise as marker for (chronic) dopamine

function of the nigrostriatal pathway and as marker of dopaminergic neurodegeneration. The first application is primarily useful in research on dopamine related disorders. The latter has the potential for clinical application in the diagnostic process of Parkinson's disease and neurodegenerative parkinsonisms. Optimization and standardization of imaging and analysis methods is still necessary though. NM-MRI will not reach the high accuracy of clinically applied DAT SPECT. However, it is a more accessible and lower cost imaging method that due to its short scan duration (3–10 min) could be added to conventional MRI scan protocols. Further development of these MR techniques for the dopaminergic system will prove what their value will be for research and clinical practice.

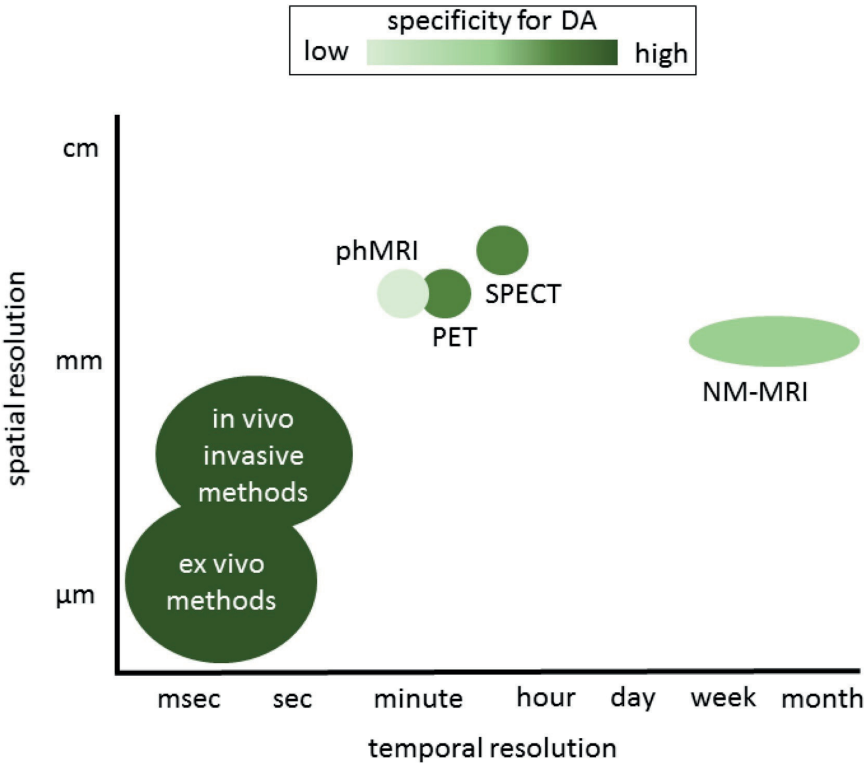

Fig. 4. Schematic scale of dopamine imaging techniques. Non-invasive techniques like phMRI and NM-MRI have lower spatial and temporal resolution, as well as specificity for DA, than invasive in-vivo and ex-vivo methods (e.g. microdialysis, voltammetry, autoradiography), which can only be applied in animal research though. Although phMRI and NM-MRI are less specific for DA (receptors) than certain PET and SPECT tracers, they do not use ionizing radiation and have comparable or better spatial resolution. The temporal resolution of NM-MRI is lower due to the nature of neuromelanin as a deposit that accumulates over time, however, advantages of NM-MRI over the other techniques are short scan duration and lower costs.

References

1. Goldman-Rakic PS, Muly EC, Williams GV. D1 receptors in prefrontal cells and circuits, Brain Res. Rev. 31 (2000) 295–301. https://doi.org/10.1016/S0165-0173(99)00045-4.
2. Weinstein JJ, Chohan MO, Slifstein M, Kegeles LS, Moore H, Abi-Dargham A. Pathway-Specific Dopamine Abnormalities in Schizophrenia, Biol. Psychiatry. 81 (2017) 31–42. https://doi.org/10.1016/j.biopsych.2016.03.2104.
3. Cheng HC, Ulane CM, Burke RE, Clinical progression in Parkinson disease and the neurobiology of axons, Ann. Neurol. 67 (2010) 715–725. https://doi.org/10.1002/ana.21995.
4. Kishida KT, Sandberg SG, Lohrenz T, Comair YG, Sáez I, Phillips PEM, Montague PR. Sub-Second Dopamine Detection in Human Striatum, PLoS One. 6 (2011) e23291. https://doi.org/10.1371/journal.pone.0023291.
5. Hsieh H, Okada S, Wei H, García-Álvarez I, Barandov A, Alvarado SR, et al. Neurotransmitter-Responsive Nanosensors for T2-Weighted Magnetic Resonance Imaging, J. Am. Chem. Soc. 141 (2019) 15751–15754. https://doi.org/10.1021/jacs.9b08744.
6. Jenkins BG. Pharmacologic magnetic resonance imaging (phMRI): Imaging drug action in the brain, Neuroimage. 62 (2012) 1072–1085.
7. Buxton RB, Uludağ K, Dubowitz DJ, Liu TT, Modeling the hemodynamic response to brain activation, in: Neuroimage, Neuroimage, 2004. https://doi.org/10.1016/j.neuroimage.2004.07.013.
8. Ogawa S, Tank DW, Menon R, Ellermann JM, Kim SG, Merkle H, Ugurbil K. Intrinsic signal changes accompanying sensory stimulation: Functional brain mapping with magnetic resonance imaging, Proc. Natl. Acad. Sci. U. S. A. 89 (1992) 5951–5955. https://doi.org/10.1073/pnas.89.13.5951.
9. Wang DJJ, Chen Y, Fernández-Seara MA, Detre JA. Potentials and challenges for arterial spin labeling in pharmacological magnetic resonance imaging, J Pharmacol Exp Ther. 337 (2011) 359–366.
10. Chen YC, Galpern WR, Brownell L, Matthews RT, Bogdanov M, Isacson O, et al. Detection of dopaminergic neurotransmitter activity using pharmacologic MRI: correlation with PET, microdialysis, and behavioral data., Magn. Reson. Med. 38 (1997) 389–98.
11. Ren J, Xu H, Choi JK, Jenkins BG, Chen YI. Dopaminergic response to graded dopamine concentration elicited by four amphetamine doses., Synapse. 63 (2009) 764–72. https://doi.org/10.1002/syn.20659.
12. Zhang Z, Andersen AH, Ai Y, Loveland A, Hardy PA, Gerhardt GA, Gash DM. Assessing nigrostriatal dysfunctions by pharmacological MRI in parkinsonian rhesus macaques., Neuroimage. 33 (2006) 636–43. https://doi.org/10.1016/j.neuroimage.2006.07.004.
13. Jenkins BG, Sanchez-Pernaute R, Brownell ALL, Chen YCCI, Isacson O. Mapping dopamine function in primates using pharmacologic magnetic resonance imaging., J. Neurosci. 24 (2004) 9553–60. https://doi.org/10.1523/JNEUROSCI.1558-04.2004.
14. Schrantee A, Tremoleda JL, Wylezinska-Arridge M, Bouet V, Hesseling P, Meerhoff GF, et al. Repeated dexamphetamine treatment alters the dopaminergic system and increases the phMRI response to methylphenidate, PLoS One. 12 (2017). https://doi.org/10.1371/journal.pone.0172776.
15. Schouw MLJ, De Ruiter MB, Kaag AM, van den Brink W, Lindauer RJL, Reneman L. Dopaminergic dysfunction in abstinent dexamphetamine users: results from a pharmacological fMRI study using a reward anticipation task and a methylphenidate challenge., Drug Alcohol Depend. 130 (2013) 52–60.
16. Schrantee A, Václavů L, Heijtel DFR, Caan MWA, Gsell W, Lucassen PJ, et al. Dopaminergic system dysfunction in recreational dexamphetamine users., Neuropsychopharmacology. 40 (2015) 1172–1180.
17. De Simoni S, Schwarz AJ, O'Daly OF, Marquand AF, Brittain C, Gonzales C, et al. Test-retest reliability of the BOLD pharmacological MRI response to ketamine in healthy volunteers., Neuroimage. 64 (2013) 75–90. https://doi.org/10.1016/j.neuroimage.2012.09.037.
18. Mervin LH, Mitricheva E, Logothetis NK, Bifone, Bender A, Noori HR, Neurochemical underpinning of hemodynamic response to neuropsychiatric drugs: A meta- and cluster analysis of preclinical studies, J. Cereb. Blood Flow Metab. (2020). https://doi.org/10.1177/0271678X20916003.
19. Choi JK, Mandeville JB, Chen YI, Grundt P, Sarkar SK, Newman AH, Jenkins BG. Imaging brain regional and cortical laminar effects of selective D3 agonists and antagonists.,

Psychopharmacology (Berl). 212 (2010) 59–72. https://doi.org/10.1007/s00213-010-1924-6.

20. McMillan R, Forsyth A, Campbell D, Malpas G, Maxwell E, Dukart J, Hipp JF, Muthukumaraswamy S. Temporal dynamics of the pharmacological MRI response to subanaesthetic ketamine in healthy volunteers: A simultaneous EEG/fMRI study., J. Psychopharmacol. 33 (2019) 219–229. https://doi.org/10.1177/0269881118822263.
21. Bruns A, Mueggler T, Künnecke B, Risterucci C, Prinssen EP, Wettstein JG, von Kienlin M. "Domain gauges": A reference system for multivariate profiling of brain fMRI activation patterns induced by psychoactive drugs in rats, Neuroimage. 112 (2015) 70–85. https://doi.org/10.1016/j.neuroimage.2015.02.032.
22. Schrantee A, Tamminga HGH, Bouziane C, Bottelier MA, Bron EE, Mutsaert, et al. Age-dependent effects of methylphenidate on the human dopaminergic system in young vs adult patients with attention-deficit/hyperactivity disorder, JAMA Psychiatry. 73 (2016) 955.
23. Buhmann C, Glauche V, Stürenburg HJ, Oechsner M, Weiller C, Büchel C. Pharmacologically modulated fMRI - Cortical responsiveness to levodopa in drug-naive hemiparkinsonian patients, Brain. 126 (2003) 451–461. https://doi.org/10.1093/brain/awg033.
24. Chen Y, Pressman P, Simuni T, Parrish TB, Gitelman DR. Effects of acute levodopa challenge on resting cerebral blood flow in Parkinson's disease patients assessed using pseudo-continuous arterial spin labeling, PeerJ. 2015 (2015). https://doi.org/10.7717/peerj.1381.
25. Black KJ, Acevedo HK, Koller JM. Dopamine Buffering Capacity Imaging: A Pharmacodynamic fMRI Method for Staging Parkinson Disease., Front. Neurol. 11 (2020) 370. https://doi.org/10.3389/fneur.2020.00370.
26. Sulzer D, Cassidy C, Horga G, Kang UJ, Fahn S, Casella L, et al. Neuromelanin detection by magnetic resonance imaging (MRI) and its promise as a biomarker for Parkinson's disease, Npj Park. Dis. 4 (2018). https://doi.org/10.1038/s41531-018-0047-3.
27. Shibata E, Sasaki M, Tohyama K, Otsuka K, Endoh J, Terayama Y, Sakai A. Use of Neuromelanin-Sensitive MRI to Distinguish Schizophrenic and Depressive Patients and Healthy Individuals Based on Signal Alterations in the Substantia Nigra and Locus Ceruleus, Biol. Psychiatry. 64 (2008) 401–406. https://doi.org/10.1016/j.biopsych.2008.03.021.
28. Cassidy CM, Carpenter KM, Konova AB, Cheung V, Grassetti A, Zecca L, et al. Evidence for Dopamine Abnormalities in the Substantia Nigra in Cocaine Addiction Revealed by Neuromelanin-Sensitive MRI, Am. J. Psychiatry. 177 (2020) 1038–1047. https://doi.org/10.1176/appi.ajp.2020.20010090.
29. Sasaki M, Shibata E, Tohyama K, Takahashi J, Otsuka K, Tsuchiya K, et al. Neuromelanin magnetic resonance imaging of locus ceruleus and substantia nigra in Parkinson's disease, Neuroreport. 17 (2006) 1215–1218. https://doi.org/10.1097/01.wnr.0000227984.84927.a7.
30. Sulzer D, Bogulavsky J, Larsen KE, Behr G, Karatekin E, Kleinman MH, et al. Neuromelanin biosynthesis is driven by excess cytosolic catecholamines not accumulated by synaptic vesicles, Proc. Natl. Acad. Sci. 97 (2000) 11869–11874. https://doi.org/10.1073/pnas.97.22.11869.
31. Zucca FA, Basso E, Cupaioli FA, Ferrari E, Sulzer D, Casella L, Zecca L. Neuromelanin of the human substantia Nigra: An update, Neurotox. Res. 25 (2014) 13–23. https://doi.org/10.1007/s12640-013-9435-y.
32. Sulzer D, Bogulavsky J, Larsen KE, Behr G, Karatekin, Kleinman MH, et al. Neuromelanin biosynthesis is driven by excess cytosolic catecholamines not accumulated by synaptic vesicles, Proc. Natl. Acad. Sci. 97 (2000) 11869–11874. https://doi.org/10.1073/pnas.97.22.11869.
33. Xing Y, Sapuan A, Dineen RA, Auer DP. Life span pigmentation changes of the substantia nigra detected by neuromelanin-sensitive MRI, Mov. Disord. 33 (2018) 1792–1799. https://doi.org/10.1002/mds.27502.
34. Trujillo P, Summers PE, Ferrari E, Zucca FA,Sturini M, Mainardi LT, et al. Contrast mechanisms associated with neuromelanin-MRI, Magn. Reson. Med. 78 (2017) 1790–1800. https://doi.org/10.1002/mrm.26584.
35. Blazejewska AL, Schwarz ST,Pitiot A, Stephenson MC, Lowe J, Bajaj N, et al. Visualization of nigrosome 1 and its loss in PD: Pathoanatomical correlation and in vivo 7 T MRI, Neurology. 81 (2013) 534–540. https://doi.org/10.1212/WNL.0b013e31829e6fd2.
36. Keren NI, Taheri S, Vazey EN, Morgan PS, Granholm ACE, Aston-Jones GS, Eckert MA, et al. Histologic validation of locus coeruleus MRI contrast in post-mortem tissue, Neuroimage. 113 (2015) 235–245. https://doi.org/10.1016/j.neuroimage.2015.03.020.
37. Liu Y, Li J, He N, Chen Y, Jin Z, Yan F, Haacke EM. Optimizing neuromelanin contrast in the

substantia nigra and locus coeruleus using a magnetization transfer contrast prepared 3D gradient recalled echo sequence, Neuroimage. 218 (2020) 116935. https://doi.org/10.1016/j.neuroimage.2020.116935.

38. Priovoulos N, van Boxel SCJ, Jacobs HIL, Poser BA, Uludag K, Verhey FRJ, Ivanov D. Unraveling the contributions to the neuromelanin-MRI contrast, Brain Struct. Funct. 225 (2020) 2757–2774. https://doi.org/10.1007/s00429-020-02153-z.
39. Trujillo P, Smith AK, Summers PE, Mainardi LM, Cerutti S, Smith SA, Costa A, High-resolution quantitative imaging of the substantia nigra, Proc. Annu. Int. Conf. IEEE Eng. Med. Biol. Soc. EMBS. 2015-Novem (2015) 5428–5431. https://doi.org/10.1109/EMBC.2015.7319619.
40. Langley J, Huddleston DE, Chen X, Sedlacik J, Zachariah N, Hu X. A multicontrast approach for comprehensive imaging of substantia nigra., Neuroimage. 112 (2015) 7–13. https://doi.org/10.1016/j.neuroimage.2015.02.045.
41. Nakane T, Nihashi T, Kawai H, Naganawa S. Visualization of neuromelanin in the substantia nigra and locus ceruleus at 1.5T using a 3D-gradient echo sequence with magnetization transfer contrast, Magn. Reson. Med. Sci. 7 (2008) 205–210. https://doi.org/10.2463/mrms.7.205.
42. Chen X, Huddleston DE, Langley J, Ahn S, Barnum CJ, Factor SA, Levey AI, Hu X, Simultaneous imaging of locus coeruleus and substantia nigra with a quantitative neuromelanin MRI approach, Magn. Reson. Imaging. 32 (2014) 1301–1306. https://doi.org/10.1016/j.mri.2014.07.003.
43. Langley J, Huddleston DE, Liu CJ, Hu X. Reproducibility of locus coeruleus and substantia nigra imaging with neuromelanin sensitive MRI, Magn. Reson. Mater. Physics, Biol. Med. 30 (2017) 121–125. https://doi.org/10.1007/s10334-016-0590-z.
44. Cassidy CM, Zucca FA, Girgis RR, Baker SC, Weinstein JJ, Sharp ME, et al. Neuromelanin-sensitive MRI as a noninvasive proxy measure of dopamine function in the human brain, Proc. Natl. Acad. Sci. U. S. A. 116 (2019) 5108–5117. https://doi.org/10.1073/pnas.1807983116.
45. K. Wengler, X. He, A. Abi-Dargham, G. Horga, Reproducibility assessment of neuromelanin-sensitive magnetic resonance imaging protocols for region-of-interest and voxelwise analyses, Neuroimage. 208 (2020) 116457. https://doi.org/10.1016/j.neuroimage.2019.116457.
46. van der Pluijm M, Cassidy C, Zandstra M, Wallert E, de Bruin K, Booij J, et al. Reliability and Reproducibility of Neuromelanin-Sensitive Imaging of the Substantia Nigra: A Comparison of Three Different Sequences, J. Magn. Reson. Imaging. (2020). https://doi.org/10.1002/jmri.27384.
47. Kitao S, Matsusue E, Fujii S, Miyoshi F, Kaminou T, Kato S, et al. Correlation between pathology and neuromelanin MR imaging in Parkinson's disease and dementia with Lewy bodies, Neuroradiology. 55 (2013) 947–953. https://doi.org/10.1007/s00234-013-1199-9.
48. Le Berre A, Kamagata K, Otsuka Y, Andica C, Hatano T, Saccenti L, et al. Convolutional neural network-based segmentation can help in assessing the substantia nigra in neuromelanin MRI, Neuroradiology. 61 (2019) 1387–1395. https://doi.org/10.1007/s00234-019-02279-w.
49. Liu XL, Yang LQ, Liu FT, Wu PY, Zhang Y, Zhuang H, et al. Short-echo-time magnitude image derived from quantitative susceptibility mapping could resemble neuromelanin-sensitive MRI image in substantia nigra, BMC Neurol. 20 (2020) 1–8. https://doi.org/10.1186/s12883-020-01828-8.
50. Ito H, Kawaguchi H, Kodaka F, Takuwa H, Ikoma Y, Shimada H, et al. Normative data of dopaminergic neurotransmission functions in substantia nigra measured with MRI and PET: Neuromelanin, dopamine synthesis, dopamine transporters, and dopamine D2 receptors, Neuroimage. 158 (2017) 12–17. https://doi.org/10.1016/j.neuroimage.2017.06.066.
51. Isaias IU, Trujillo P, Summers P, Marotta G, Mainardi L, Pezzoli G, et al. Neuromelanin imaging and dopaminergic loss in parkinson's disease, Front. Aging Neurosci. 8 (2016) 1–12. https://doi.org/10.3389/fnagi.2016.00196.
52. Kuya K, Shinohara Y, Miyoshi F, Fujii S, Tanabe Y, Ogawa T. Correlation between neuromelanin-sensitive MR imaging and (123)I-FP-CIT SPECT in patients with parkinsonism., Neuroradiology. 58 (2016) 351–356. https://doi.org/10.1007/s00234-016-1644-7.
53. Okuzumi A, Hatano T, Kamagata K, Hori M, Mori A, Oji Y, Taniguchi D, et al. Neuromelanin or DaT-SPECT: which is the better marker for discriminating advanced Parkinson's disease?, Eur. J. Neurol. 26 (2019) 1408–1416. https://doi.org/10.1111/ene.14009.
54. Martín-Bastida A, Lao-Kaim NP, Roussakis AA, Searle GE, Xing Y, Gunn RN, et al. Relationship between neuromelanin and dopamine terminals within the Parkinson's nigrostriatal system, Brain. 142 (2019) 2023–2036. https://doi.org/10.1093/brain/awz120.

55. Kawaguchi H, Shimada H, Kodaka F, Suzuki M, shinotoh H, Hirano S, et al. Principal component analysis of multimodal neuromelanin MRI and dopamine transporter PET data provides a specific metric for the nigral dopaminergic neuronal density, PLoS One. 11 (2016) 1–13. https://doi.org/10.1371/journal.pone.0151191.

56. Ariz M, Abad RC, Castellanos G, Martinez M, Munoz-Barrutia A, Fernandez-Seara MA, et al. Dynamic atlas-based segmentation and quantification of neuromelanin-rich brainstem structures in Parkinson disease, IEEE Trans. Med. Imaging. 38 (2019) 813–823. https://doi.org/10.1109/TMI.2018.2872852.

57. Castellanos G, Fernández-Seara MA, Lorenzo-Betancor O, Ortega-Cubero S,Puigvert M, Uranga J, et al. Automated Neuromelanin Imaging as a Diagnostic Biomarker for Parkinson's Disease, Mov. Disord. 30 (2015) 945–952. https://doi.org/10.1002/mds.26201.

58. Moon WJ, Park JY, Yun WS, Jeon JY, Moon YS, Kim H, et al. A comparison of substantia nigra T1 hyperintensity in parkinson's disease dementia, alzheimer's disease and age-matched controls: Volumetric analysis of neuromelanin imaging, Korean J. Radiol. 17 (2016) 633–640. https://doi.org/10.3348/kjr.2016.17.5.633.

59. Ohtsuka C, Sasaki M, Konno K, Koide M, Kato K, Takahashi J, et al. Changes in substantia nigra and locus coeruleus in patients with early-stage Parkinson's disease using neuromelanin-sensitive MR imaging, Neurosci. Lett. 541 (2013) 93–98. https://doi.org/10.1016/j.neulet.2013.02.012.

60. Reimão S, Pita Lobo P, Neutel D, Correia Guedes L, Coelho M, Rosa MM, et al. Substantia nigra neuromelanin magnetic resonance imaging in de novo Parkinson's disease patients, Eur. J. Neurol. 22 (2015) 540–546. https://doi.org/10.1111/ene.12613.

61. Schwarz ST, Xing Y, Tomar P, Bajaj N, Auer DP. In Vivo assessment of brainstem depigmentation in Parkinson disease: Potential as a severity marker for multicenter studies, Radiology. 283 (2017) 789–798. https://doi.org/10.1148/radiol.2016160662.

62. Schwarz ST, Rittman T, Gontu V, Morgan PS, Bajaj N, Auer DP, T1-Weighted MRI shows stage-dependent substantia nigra signal loss in Parkinson's disease, Mov. Disord. 26 (2011) 1633–1638. https://doi.org/10.1002/mds.23722.

63. Fabbri M, Reimão S, Carvalho M, Nunes RG, Abreu D, Guedes LC, et al. Substantia Nigra Neuromelanin as an Imaging Biomarker of Disease Progression in Parkinson's Disease, J. Parkinsons. Dis. 7 (2017) 491–501. https://doi.org/10.3233/JPD-171135.

64. T. Hatano T, A. Okuzumi A, K. Kamagata K, K. Daida K, D. Taniguchi D, M. Hori M, et al. Neuromelanin MRI is useful for monitoring motor complications in Parkinson's and PARK2 disease, J. Neural Transm. 124 (2017) 407–415. https://doi.org/10.1007/s00702-017-1688-9.

65. Kashihara K, Shinya T, Higaki F. Neuromelanin magnetic resonance imaging of nigral volume loss in patients with Parkinson's disease, J. Clin. Neurosci. 18 (2011) 1093–1096. https://doi.org/10.1016/j.jocn.2010.08.043.

66. Matsuura K, Maeda M, Yata K, Ichiba Y, Yamaguchi T, Kanamaru K, Tomimoto H. Neuromelanin magnetic resonance imaging in Parkinson's disease and multiple system atrophy, Eur. Neurol. 70 (2013) 70–77. https://doi.org/10.1159/000350291.

67. Miyoshi F, Ogawa T, Kitao SI, Kitayama M, Shinohara Y, Takasugi M, et al. Evaluation of Parkinson disease and Alzheimer disease with the use of neuromelanin MR imaging and123I-metaiodobenzylguanidine scintigraphy, Am. J. Neuroradiol. 34 (2013) 2113–2118. https://doi.org/10.3174/ajnr.A3567.

68. Braak H, Del Tredici K, Rüb U, De Vos RAI, Jansen Steur ENH, Braak E, Staging of brain pathology related to sporadic Parkinson's disease, Neurobiol. Aging. 24 (2003) 197–211. https://doi.org/10.1016/S0197-4580(02)00065-9.

69. Rizzo G, Copetti M, Arcuti S, Martino D, Fontana A, Logroscino G. Accuracy of clinical diagnosis of Parkinson disease, Neurology. 86 (2016) 566–576. https://doi.org/10.1212/WNL.0000000000002350.

70. Wang X, Zhang Y, Zhu C, Li G, Kang J, Chen F, Yang L, The diagnostic value of SNpc using NM-MRI in Parkinson's disease: meta-analysis, Neurol. Sci. 40 (2019) 2479–2489. https://doi.org/10.1007/s10072-019-04014-y.

71. Jin L, Wang J, Wang C, Lian D, Zhou Y, Zhang Y, et al. Combined Visualization of Nigrosome-1 and Neuromelanin in the Substantia Nigra Using 3T MRI for the Differential Diagnosis of Essential Tremor and de novo Parkinson's Disease, Front. Neurol. 10 (2019) 1–8. https://doi.org/10.3389/fneur.2019.00100.

72. Kuya K, Ogawa T, Shinohara Y, Ishibashi M, Fujii S, Mukuda N, Tanabe Y. Evaluation of Parkinson's disease by neuromelanin-sensitive magnetic resonance imaging and 123I-FP-CIT SPECT, Acta Radiol. 59 (2018) 593–598. https://doi.org/10.1177/0284185117722812.

73. Takahashi H, Watanabe Y, Tanaka H, Mihara M, Mochizuki H, Liu T, et al. Quantifying changes in nigrosomes using quantitative susceptibility mapping and neuromelanin imaging for the diagnosis of early-stage Parkinson's disease, Br. J. Radiol. 91 (2018). https://doi.org/10.1259/bjr.20180037.

74. Suwijn SR, van Boheemen CJM, de Haan RJ, Tissingh G, Booij J, de Bie RMA. The diagnostic accuracy of dopamine transporter SPECT imaging to detect nigrostriatal cell loss in patients with Parkinson's disease or clinically uncertain parkinsonism: A systematic review, EJNMMI Res. 5 (2015) 1–8. https://doi.org/10.1186/s13550-015-0087-1.

75. Matsuura K, Maeda M, ichi Tabei K, Umino M, Kajikawa H, Satoh M, et al. A longitudinal study of neuromelanin-sensitive magnetic resonance imaging in Parkinson's disease, Neurosci. Lett. 633 (2016) 112–117. https://doi.org/10.1016/j.neulet.2016.09.011.

76. Kashihara K, Shinya T, Higaki F, Reduction of neuromelanin-positive nigral volume in patients with MSA, PSP and CBD, Intern. Med. 50 (2011) 1683–1687. https://doi.org/10.2169/internalmedicine.50.5101.

77. Ohtsuka C, Sasaki M, Konno K, Kato K, Takahashi J, Yamashita F, et al. Differentiation of early-stage parkinsonisms using neuromelanin-sensitive magnetic resonance imaging, Park. Relat. Disord. 20 (2014) 755–760. https://doi.org/10.1016/j.parkreldis.2014.04.005.

78. Pyatigorskaya N, Gaurav, Arnaldi D, Leu-Semenescu S, Yahia-Cherif L, Valabregue R, et al. Magnetic Resonance Imaging Biomarkers to Assess Substantia Nigra Damage in Idiopathic Rapid Eye Movement Sleep Behavior Disorder, Sleep. 40 (2017). https://doi.org/10.1093/sleep/zsx149.

79. Knudsen K, Fedorova TD, Hansen AK, Sommerauer M, Otto M, Svendsen KB, et al. In-vivo staging of pathology in REM sleep behaviour disorder: a multimodality imaging case-control study, Lancet Neurol. 17 (2018) 618–628. https://doi.org/10.1016/S1474-4422(18)30162-5.

80. Leitão R, Guerreiro C, Nunes RG, Gonçalves N, Galati G, Rosário M, et al. Neuromelanin Magnetic Resonance Imaging of the Substantia Nigra in Huntington's Disease, J. Huntingtons. Dis. 9 (2020) 143–148. https://doi.org/10.3233/JHD-190388.

81. Shinde S, Prasad S, Saboo Y, Kaushick R, Saini J, Pal PK, Ingalhalikar M. Predictive markers for Parkinson's disease using deep neural nets on neuromelanin sensitive MRI, NeuroImage Clin. 22 (2019) 101748. https://doi.org/10.1016/j.nicl.2019.101748.

82. Watanabe Y, Tanaka H, Tsukabe A, Kunitomi Y, Nishizawa M, Hashimoto R, et al. Neuromelanin magnetic resonance imaging reveals increased dopaminergic neuron activity in the substantia nigra of patients with schizophrenia, PLoS One. 9 (2014) 1–6. https://doi.org/10.1371/journal.pone.0104619.

83. Yamashita F, Sasaki M, Fukumoto K, Otsuka K, Uwano I, Kameda H, et al. Detection of changes in the ventral tegmental area of patients with schizophrenia using neuromelanin-sensitive MRI, Neuroreport. 27 (2016) 289–294. https://doi.org/10.1097/WNR.0000000000000530.

Author Contributions

EvdG and LR conceived and conceptualized the study. AS, EvdG, MvdP and LR wrote the original draft of the manuscript. All the authors critically reviewed the manuscript for intellectual content. All authors approved the final version of the manuscript for publication.

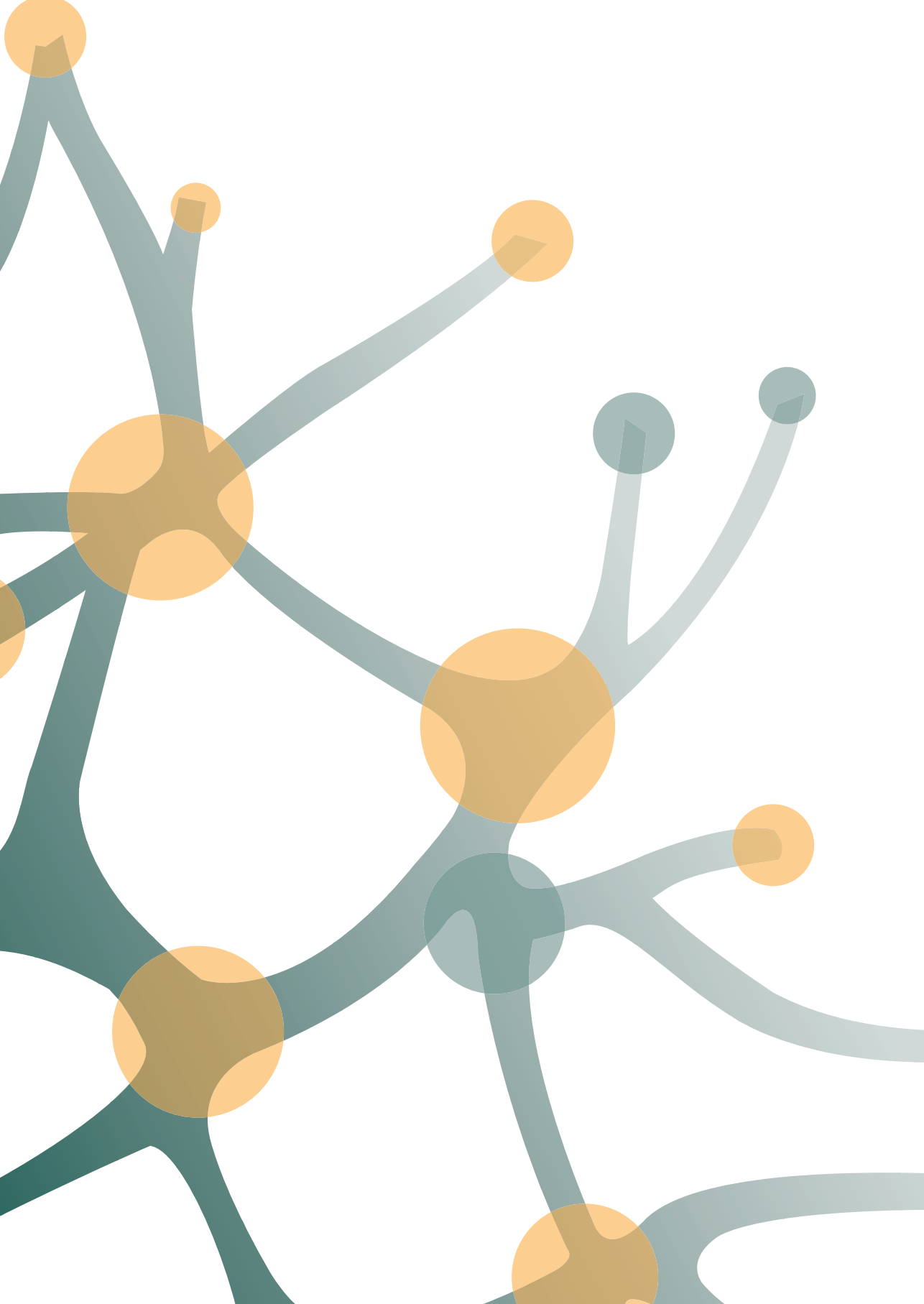

Chapter | 3

Reliability and reproducibility of neuromelanin-sensitive imaging of the substantia nigra: a comparison of three different sequences

Marieke van der Pluijm, Clifford Cassidy, Melissa Zandstra, Elon Wallert, Kora de Bruin, Jan Booij, Lieuwe de Haan, Guillermo Horga, Elsmarieke van de Giessen

Journal of Magnetic Resonance Imaging, 2020; 53:712-721
DOI: 10.1002/jmri.27384

Abstract

Background: Neuromelanin-sensitive MRI (NM-MRI) of the substantia nigra provides a noninvasive way to acquire an indirect measure of dopamine functioning. Despite the potential of NM-MRI as a candidate biomarker for dopaminergic pathology, studies about its reproducibility are sparse.

Purpose: To assess the test–retest reproducibility of three commonly used NM-MRI sequences and evaluate three analysis methods.

Study Type: Prospective study.

Population: A total of 11 healthy participants age between 20–27 years.

Field Strength/Sequence: 3.0T; NM-MRI gradient recalled echo (GRE) with magnetization transfer (MT) pulse; NM-MRI turbo spin echo (TSE) with MT pulse; NM-MRI TSE without MT pulse.

Assessment: Participants were scanned twice with a 3-week interval. Manual analysis, threshold analysis, and voxelwise analysis were performed for volume and contrast ratio (CR) measurements.

Statistical Tests: Intraclass correlation coefficients (ICCs) were calculated for test–retest and inter- and intrarater variability.

Results: The GRE sequence achieved the highest contrast and lowest variability (4.9–5.7%) and showed substantial to almost perfect test–retest ICC (0.72–0.90) for CR measurements. For volume measurements, the manual analysis showed a higher variability (10.7–17.9%) and scored lower test–retest ICCs (–0.13–0.73) than the other analysis methods. The threshold analysis showed higher test–retest ICC (0.77) than the manual analysis for the volume measurements.

Data Conclusion: NM-MRI is a highly reproducible measure, especially when using the GRE sequence and CR measurements. Volume measurements appear to be more sensitive to inter/intrarater variability and variability in placement and orientation of the NM-MRI slab. The threshold analysis appears to be the best alternative for volume analysis.

Introduction

In vivo visualization of the dopamine system is of interest due to its role in a variety of psychiatric and neurodegenerative disorders, including Parkinson's disease (PD) (1) and psychosis (2). The substantia nigra (SN) in the mesencephalon is the location from where dopaminergic neurons project to the striatum, forming the nigrostriatal pathway (3). A novel neuromelanin-sensitive magnetic resonance imaging sequence (NM-MRI) provides a noninvasive way to acquire an indirect measure of dopamine functioning in the SN (4). NM-MRI has been successfully used to examine changes in the SN in PD and schizophrenia (2,5,6) and seems promising as a biomarker in these disorders. Considering the non-invasive nature of NM-MRI, it has the potential to be applied in clinical practice.

Neuromelanin (NM) is synthesized from cytosolic dopamine and dihydroxyphenylalanine derivatives that have not been taken up into synaptic vesicles (7,8). After iron dependent oxidation of the cytosolic dopamine NM-iron complexes are stacked inside autophagic organelles that fuse with lysosomes, and lipid and protein components forming the final autolysosomal NM-containing organelles (7,9). These NM-containing organelles accumulate over age in the SN (10), or rather show an inverted U-shaped age effect (11). The paramagnetic NM-iron complexes lead to T1 reduction, which contributes to the NM-MRI contrast (4).

NM sensitive T1-weighted turbo spin echo (TSE) is the most frequently used NM-MRI sequence and multiple studies have shown a reliable decrease of NM-MRI signal in the SN of patients with PD (5,12-27). The TSE sequence can be performed with or without a magnetization transfer (MT) pulse. An off resonance MT pulse suppresses the contribution of macromolecules to the signal and can thereby increase contrast (4,24,28,29). A smaller number of patient studies have been performed with an NM sensitive gradient echo pulse (GRE) sequence with an MT pulse (6,30).

Despite the promise of NM-MRI as a biomarker, studies on the reproducibility and reliability of the different sequences have been sparse. Reproducibility provides vital information for study designs, since outcome measures with lower reliability have diminished power. One study has shown a lower sensitivity for imaging the SN with a TSE sequence compared to a GRE sequence (31), but reproducibility was not compared. Reproducibility studies have been performed for the GRE sequence and yielded excellent results for volume measurements (32) and contrast ratio measurements (6,32,33) while using the TSE sequence, a study has shown moderate reproducibility in the noradrenaline-rich locus coeruleus (34). A study directly comparing the GRE and TSE NM-MRI sequences in terms of their reproducibility in SN imaging would be useful.

In addition to differences in image acquisition, there are also differences in the analysis of NM-MRI data. Most studies have used an average contrast ratio based on a manual approach in which the SN and a reference region are manually traced on one or more axial slices in each NM-MRI scan. While this has shown differences between groups (15,19,20,24,35), it does not assess the entire SN. Furthermore, this method is sensitive to inter/intra-rater variability resulting from variability in the placement and orientation of the NM-MRI imaging slab within and across studies. An intensity threshold method avoids the inter/intra-rater variability and when applied to scans normalized to Montreal Neurological Institute (MNI) space it can give an estimate of the entire SN, independent of slab placement (32). More recently, Cassidy et al validated a voxelwise approach (6). This method is semi-automated using an average mask of the normalized dataset instead of a subject specific mask. This approach captures the voxel anatomical information in the scan and can be implemented for various measurements including mapping the (sub)regional variation of the SN.

In order to further develop NM-MRI for research and clinical applications, it is important to determine optimal acquisition and analysis methods. Therefore, the aim of this study was to compare the test-retest reproducibility of three NM-MRI sequences in SN imaging; 1) the GRE sequence with MT pulse, 2) the TSE sequence with MT pulse, and 3) the TSE sequence without MT pulse and, also, to assess and compare the reliability of three analysis techniques; i) manual analysis, ii) threshold analysis, and iii) voxelwise analysis.

Materials and Methods

Participants

This study was approved by the local Medical Ethics Committee. All participants gave written informed consent prior to the first scan after the nature of the procedure had been fully explained. Eleven healthy participants (mean (SD) age: 24.82 (2.04), range: 20-27 years, seven male and four female) were included in the study. Prior to inclusion, all participants were screened by means of an interview and excluded if they had a history of neurological or psychiatric disorders, used any medication (with the exception of contraceptives), or had any MRI contraindications.

Image Acquisition

All MR data were acquired at a single center using a 3 Tesla Ingenia MRI system (Philips, Best, The Netherlands) with a 32-channel SENSE head coil. All participants participated in two identical NM-MRI scanning sessions, with a 3-week interval (mean [SD] days: 20.9 [1.4], range: 18-24 days).

For slice placement and registration, transversal high-resolution structural T1-weighted volumetric images, with full head coverage were acquired (echo time [TE]/ repetition time

[TR]) = 4.1/9.0 msec; 189 slices; field of view [FOV] = 284 x 284 x 170 mm; voxel size: 0.9 x 0.9 x 0.9 mm, flip angle [FA]=8°). On these, the NM-MRI sections were placed perpendicular to the fourth ventricle floor with coverage from the posterior commissure to halfway through the pons.

The following three NM-MRI scans were acquired; 1) GRE MT off-resonance pulse (GRE MT on) (TE/TR = 3.9/260 msec, FA = 40°, 8 slices, slice thickness = 2.5 mm, in-plane resolution = 0.39 x 0.39 mm^2, FOV = 162 x 199 mm, number of signal averages [NSA] = 2, magnetization transfer frequency offset = 1200 Hz and duration = 15.6 msec, based on (6,33)); 2) TSE with MT off resonance pulse (TSE MT on) (TE/TR = 10/641 msec, FA = 90°, 8 slices, slice thickness = 2.5 mm, in-plane resolution = 0.40x0.40 mm^2, FOV = 180x180 mm, NSA = 2, magnetization transfer frequency offset = 1200 Hz and duration = 15.6 msec, based on (24)); 3) TSE without MT pulse (TSE MT off) (TE/TR = 10/500 msec, FA = 90°, 8 slices, slice thickness = 2.5 mm, in-plane resolution = 0.40 x 0.40 mm^2, FOV = 180 x 180 mm, NSA = 2, based on (20)).

Manual Segmentation

ITK-Snap (v. 3.6.0, www.itksnap.org) (36) was used to manually segment the SN. In addition, the crus cerebri (CC) and red nucleus (RN) were segmented and served as reference areas (6,20,33). Segmentation was performed by three independent raters (M.Z., K.B., E.W.) and the raters segmented both the test and retest scans twice. The interval between segmentation 1 and segmentation 2 was a minimum of 3 weeks and a maximum of 6 weeks. To ensure raters had the same segmentation approach, a segmentation protocol was used and all attended a training session. No raters had experience with the NM-MRI segmentations prior to this study. For every sequence two contrast ratios (CR), $CR_{SN\text{-}RN}$ and $CR_{SN\text{-}CC}$, were determined. These were calculated as: $CR_{SN\text{-}RN} = (S_{SN} - S_{RN})/S_{RN}$ and $CR_{SN\text{-}CC} = (S_{SN} - S_{CC})/S_{CC}$, where S_{SN}, S_{RN}, and S_{CC} represent the mean signal intensities of the SN, RN, and CC, respectively. For each participant the two slices with the highest voxel intensity were segmented. Segmentation of the CC consisted of six default circles (three on each side of the SN), each with a diameter of 8 mm.

Standardized Analyses

For the standardized analyses, we preprocessed the NM-MRI scans using Statistical Parametric Mapping's (SPM 12; Wellcome Trust, London, UK). We first co-registered the NM-MRI retest scans to the NM-MRI test scans and subsequently coregistered both to the T1-weighted test scans. Tissue segmentation was performed using the T1-weighted test scan. All scans were normalized into MNI standard brain space using DARTEL routines with a gray and white matter template generated from all T1-weighted test scans and spatially smoothed with a 1-mm full-width at half-maximum Gaussian kernel. For post-hoc analysis, the preprocessing was performed without spatial smoothing to assess the effect of spatial smoothing. All images were visually inspected following each preprocessing step.

Semi-automated Thresholding Segmentation

For each sequence a large area around the (left and right) SN was manually traced on the standardized average image with ITK-Snap. This was done carefully to avoid contamination from CSF space. This mask was overlaid on the individual NM-MRI scans in MNI space and voxels with signal intensity S_V >3 standard deviations from S_{CC} were considered part of the SN. All high-intensity voxels generated by the thresholding method were visually inspected to ensure no outlying/aberrant voxels were included in the mask.

Voxelwise Analysis

We used FSL (FMRIB Software Library, v. 5.0.10, Oxford University, UK) to create one standardized average for each of the three sequences based on the 22 standardized NM-MRI scans (test and retest). Template population masks for both the SN and CC were created for each sequence by manual tracing with ITK-Snap on the standardized average image (Fig. 1b). For each scan and voxel in the SN mask a CR_V was calculated as $CR_V = (S_V - S_{CC})/S_{CC}$. Voxels with a CR_V smaller than 0 or greater than 3 standard deviations from the mean were excluded.

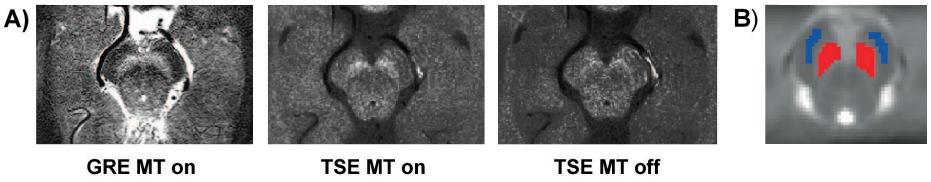

Figure 1. NM-MRI of the substantia nigra. (a) An individual example of the three NM-MRI sequences. (b) Manual segmentation of subsantia nigra (SN) and crus cerebri (CC) mask on a standardized image in MNI space. The mask of the SN is shown in red and the mask of the CC in blue. GRE: gradient recalled echo; MT: magnetization transfer pulse; TSE: turbo spin echo.

Statistical Analysis

To assess reliability in test-retest, intra-rater, and inter-rater reliability the intraclass correlation coefficient (ICC) was used (37). For the manual analysis the ICC estimates and their 95% confident intervals (CIs) were calculated using SPSS 26.0 (IBM Corporation, Armonk, NY, USA) and the ICC for the thresholding and voxelwise analyses were calculated using MatLab (MathWorks Inc., R2016a, Natick, MA). The test-retest ICC was based on a single measures and consistency two-way mixed-effects and the ICC for the intra-rater and inter-rater agreement was based on a single measures and absolute agreement two-way mixed-effects model. Standard thresholds were used for interpretability of ICC values: “almost perfect” for ICC 0.81-1.00, “substantial” for ICC 0.61-0.80, “moderate” for ICC between 0.41-0.60, “fair” for ICC 0.21-0.40, “slight” 0.00-0.20, and “poor” for ICC <0.00 (37).

Test-retest variability was assessed as a measure of agreement and was calculated using the following equation $\mathrm{VAR} = \frac{|\text{test-retest}|}{(\text{test+retest})/2} \cdot 100\%$ and performed for the manual analysis on both

contrast ratios ($CR_{SN\text{-}RN}$ and $CR_{SN\text{-}CC}$) and SN volumes for all three sequences and raters. Furthermore, Bland-Altman plots for test and retest were constructed as an additional measure of agreement for the manual analysis. For the semi-automated thresholding segmentation additionally the Dice Similarity Coefficient (DSC) was calculated to determine reproducibility between the mean test and retest volume measurements. The DSC was calculated with MatLab and defined as DSC = (2*volume (Test Retest)) / (volume(Test) + volume(Retest)), where represents the intersection operator.

Results

Manual Segmentation

In all subjects the SN was consistently detected as an area of hyperintensity (Fig, 1a). Tables 1 and 2 show the test-retest variability, test-retest reliability, intra-rater reliability and inter-rater reliability based on the manual segmentation protocol for the CR and volume measurements, respectively. For CR, variability was lowest for the GRE MT on sequence with $CR_{SN\text{-}CC}$ analysis. Test-retest ICC was substantial to almost perfect (0.60-0.86) for all three sequences with $CR_{SN\text{-}CC}$ analysis. Also, intra-rater ICC was substantial to almost perfect (0.75-0.97) for all three sequences with $CR_{SN\text{-}CC}$ analysis, whereas the inter-rater ICC was substantial (0.63-0.81). Since the $CR_{SN\text{-}CC}$ yielded better reproducibility than the $CR_{SN\text{-}RN}$, further analysis focused solely on the $CR_{SN\text{-}CC}$ (CR_{SN}). For volume measurements, the TSE MT on sequence yielded the lowest variability (10.74-11.47%) and highest ICCs with a slight to substantial test-retest ICC (0.11-0.73) and intra- and inter-rater ICC varying from slight to almost perfect (0.34-0.87). Bland Altman plots of the CR_{SN}, depicted in Fig. 2, give a graphical representation of the agreement for the CR_{SN} and volume between the test and the retest for all three sequences.

Table 1. Reproducibility and reliability based on the manual segmented CRSN of NM-MRI sequences

	GRE MT on		TSE MT on		TSE MT off	
	CR_{SN-RN}	CR_{SN-CC}	CR_{SN-RN}	CR_{SN-CC}	CR_{SN-RN}	CR_{SN-CC}
Mean CR% (SD)						
Rater 1 (test)	21.59 (2.26)	21.64 (2.13)	21.35 (2.32)	13.51 (2.20)	16.49 (2.96)	9.04 (2.20)
Rater 1 (re-test)	22.89 (2.69)	21.42 (2.15)	20.90 (2.57)	12.96 (2.07	16.27 (3.54)	9.14 (2.13)
Rater 2 (test)	20.86 (3.21)	22.48 (2.18)	19.63 (3.45)	13.19 (2.25)	16.29 (3.42)	9.07 (2.21)
Rater 2 (re-test)	23.14 (2.80)	21.75 (2.35)	21.13 (2.15)	12.87 (1.76)	16.76 (2.68)	8.98 (2.28)
Rater 3 (test)	21.59 (2.86)	19.72 (1.93)	20.37 (3.05)	12.14 (1.98)	16.54 (2.42)	7.73 (1.72)
Rater 3 (re-test)	22.28 (2.81)	20.37 (2.10)	20.63 (1.91)	11.78 (2.01)	16.69 (2.29)	7.94 (1.88)
Raters combined (test)	21.35 (2.74)	21.28 (2.33)	20.45 (2.97)	12.95 (2.16)	16.44 (2.87)	8.61 (2.09)
Raters combined (re-test)	22.77 (2.71)	21.18 (2.22)	20.89 (2.17)	12.54 (1.97)	16.58 (2.80)	8.69 (2.11)
Test-retest Variability (SD)						
Rater 1	7.47 (5.94)	4.92 (2.58)	7.35 (5.55)	9.92 (7.38)	12.83 (9.09)	8.70 (9.23)
Rater 2	13.51 (9.72)	5.98 (4.25)	11.25 (11.30)	7.41 (5.30)	14.87 (12.38)	15.68 (15.57)
Rater 3	7.86 (6.81)	5.73 (4.23)	8.65 (9.25)	10.29 (9.18)	8.84 (5.42)	16.55 (9.39)
Test-retest ICC (95% CI)						
Rater 1	0.74 (0.28 – 0.91)	0.84 (0.51 – 0.95)	0.70 (0.21 – 0.91)	0.76 (0.32 – 0.93)	0.73 (0.27 – 0.92)	0.86 (0.55 – 0.96)
Rater 2	0.58 (0.05 – 0.87)	0.79 (0.40 – 0.94)	0.61 (0.05 – 0.88)	0.85 (0.54 – 0.96)	0.54 (-0.05 – 0.85)	0.60 (0.04 – 0.88)
Rater 3	0.69 (0.19 – 0.91)	0.79 (0.39 – 0.94)	0.55 (-0.04 – 0.84)	0.67 (0.15 – 0.90)	0.75 (0.320– 0.93)	0.66 (0.13 – 0.89)
Rater ICC (95% CI)						
Intra-rater ICC (R1)	0.94 (0.86 – 0.98)	0.92 (0.80 – 0.97)	0.80 (0.58 – 0.91)	0.97 (0.92 – 0.99)	0.86 (0.70 – 0.94)	0.85 (0.68 – 0.94)
Intra-rater ICC (R2)	0.85 (0.68 – 0.94)	0.88 (0.56 – 0.96)	0.75 (0.46 – 0.89)	0.75 (0.49 – 0.89)	0.81 (0.58 – 0.92)	0.87 (0.66 – 0.95)
Intra-rater ICC (R3)	0.93 (0.83 – 0.97)	0.93 (0.83 – 0.97)	0.55 (0.17 – 0.78)	0.90 (0.79 – 0.96)	0.86 (0.69 – 0.94)	0.92 (0.72 – 0.97)
Inter-rater ICC	0.75 (0.57 – 0.88)	0.63 (0.22 – 0.84)	0.65 (0.44 – 0.82)	0.81 (0.45 – 0.93)	0.62 (0.39 – 0.81)	0.79 (0.44 – 0.92)

Given are the test-retest variability for each rater and ICC values with 95% confidence interval.
SN=Substantia Nigra, CR=Contrast ratio, CR%= Contrast ratio * 100, SD= standard deviation, R1=rater 1, R2=rater 2, R3 = rater 3, ICC = Intraclass Correlation Coefficient, 95% CI= 95 percent confidence interval, GRE=Gradient Recalled Echo, MT=Magnetization Transfer pulse, TSE=Turbo Spin Echo

Table 2. Reproducibility and reliability based on the manual segmented SN volumes of the NM-MRI sequences

	GRE MT on	TSE MT on	TSE MT off
Mean Volume mm³ (SD)			
Rater 1 (test)	355.52 (54.53)	337.93 (64.73)	328.15 (69.43)
Rater 1 (re-test)	373.91 (56.48)	362.99 (67.62)	306.11 (48.99)
Rater 2 (test)	333.87 (35.48)	343.10 (55.18)	302.84 (42.80)
Rater 2 (re-test)	308.35 (36.73)	340.14 (45.73)	304.31 (37.37)
Rater 3 (test)	365.56 (52.83)	386.50 (42.14)	378.63 (36.38)
Rater 3 (re-test)	391.11 (40.90)	414.67 (40.96)	380.67 (47.00)
Raters combined (test)	351.65 (48.73)	355.85 (57.49)	336.54 (59.30)
Raters combined (re-test)	357.79 (57.03)	372.50 (60.08)	330.36 (56.41)
Test-retest Variability (SD)			
Rater 1	14.31% (13.08)	10.74% (10.16)	13.03% (12.76)
Rater 2	13.04% (10.68)	10.99% (7.84)	17.88% (9.82)
Rater 3	14.47% (12.05)	11.47% (9.84)	12.76% (7.83)
Test-retest ICC (95% CI)			
Rater 1	0.13 (-0.48 – 0.66)	0.73 (0.26 – 0.92)	0.43 (-0.19 – 0.81)
Rater 2	0.05 (-0.54 – 0.61)	0.57 (-0.11 – 0.86)	-0.13 (-0.66 – 0.48)
Rater 3	-0.10 (-0.64 – 0.51)	0.11 (-0.50 – 0.65)	-0.01 (-0.59 – 0.57)
Rater ICC (95% CI)			
Intra-rater ICC (R1)	0.84 (0.67 – 0.93)	0.87 (0.71 – 0.94)	0.64 (0.32 – 0.83)
Intra-rater ICC (R2)	0.33 (-0.9 – 0.65)	0.35 (-0.9 – 0.67)	0.53 (0.17 – 0.77)
Intra-rater ICC (R3)	0.82 (0.30 – 0.94)	0.72 (0.45 – 0.87)	0.58 (0.12 – 0.81)
Inter-rater ICC	0.11 (-0.07 – 0.36)	0.34 (0.07 – 0.61)	0.21 (-0.01 – 0.47)

Given are the test-retest variability for each rater and ICC values with 95% confidence interval.
R1 = rater 1, R2 = rater 2, R3 = rater 3, SD= standard deviation, ICC = Intraclass Correlation Coefficient, 95% CI = 95% confidence interval, GRE=Gradient Recalled Echo, MT=Magnetization Transfer pulse, TSE=Turbo Spin Echo

Semi-automated Thresholding Segmentation

The semi-automated thresholding segmented SN volumes were reproducible with a substantial ICC reliability (0.67-0.77, see Table 3). In addition the semi-automated thresholding segmented SN volume showed significant overlap between the two scans (Table 3), especially for the GRE MT on (0.91). The post-hoc non-smoothed preprocessed data yielded lower reliability compared to the smoothed preprocessed data (Table 3).

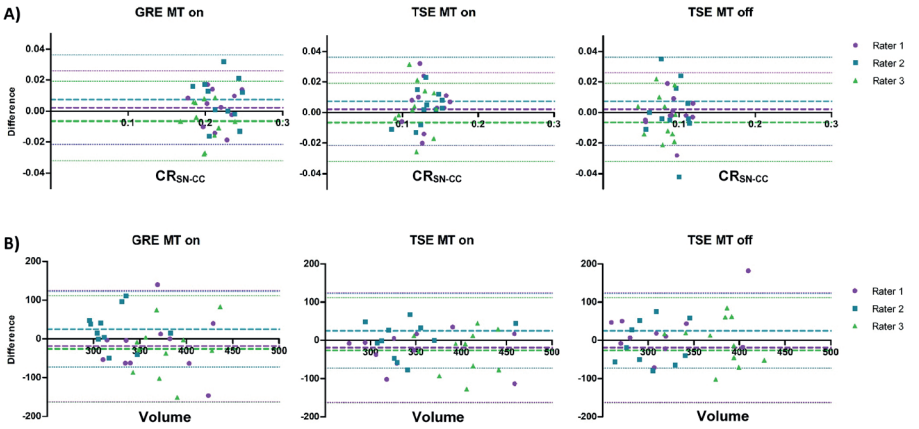

Fig. 2. Bland–Altman plots representing the difference between the test and the retest of (a) manual segmented contrast ratios and (b) manual segmented volumes. With the representation of the mean difference (dashed lines) and the limits of agreement (dotted lines), from –1.96 SD to +1.96 SD; in purple Rater 1, in blue Rater 2, in green Rater 3. GRE: gradient recalled echo; MT: magnetization transfer pulse; TSE: turbo spin echo.

Table 3. Mean Test–Retest reliability of the semiautomated analyses

	GRE MT on	**TSE MT on**	**TSE MT off**
Threshold analysis			
ICC Volume (95% CI)	0.77 (0.31-0.94)	0.71 (0.18-0.92)	0.67 (0.12-0.91)
DSC Volume (SD)	0.91 (0.03)	0.71 (0.07)	0.68 (0.13)
Voxelwise analysis			
ICC CR_V (95% CI)	0.72 (0.25-0.92)	0.52 (-0.05-0.84)	0.37 (-0.25-0.78)
ICC CR_{SN} (95% CI)	0.90 (0.66-0.97)	0.79 (0.36-0.94)	0.66 (0.09-0.90)
Analysis without spatial smoothing			
	GRE MT on	**TSE MT on**	**TSE MT off**
Threshold analysis			
ICC Volume (95% CI)	0.78 (0.26-0.94)	0.64 (0.07-0.90)	0.65 (0.08-0.90)
DSC Volume (SD)	0.86 (0.03)	0.72 (0.08)	0.51 (0.18)
Voxelwise analysis			
ICC CR_V (95% CI)	0.63 (-0.00-0.87)	0.38 (-0.21-0.79)	0.26 (-0.34-0.71)
ICC CR_{SN} (95% CI)	0.83 (-0.45-0.95)	0.61 (0.01-0.89)	0.64 (0.06-0.90)

The contrast ratios from the voxelwise analysis and the volumes from the semiautomated thresholding segmentation
ICC: intraclass correlation coefficient; ICC CRv: average ICC of voxels in substantia nigra ROI for contrast ratio; ICC CRsn: ICC for average contrast ratio in the substantia nigra ROI; DSC: Dice similarity coefficient; GRE: gradient recalled echo; MT: magnetization transfer pulse; TSE: turbo spin echo.

Voxelwise analysis

The standardized mask did not fit the retest scan of one participant, due to suboptimal imaging slab placement (top part of SN was missing), therefore this participant was excluded from the automatic analysis.

CR for each voxel in the standardized average was calculated for test and retest (Fig, 3). Two-way mixed, single score ICC and consistency values between test and retest per voxel were calculated, creating a map of ICC values in the SN (Fig, 3). The mean ICC across voxels for each sequence was calculated with the available data in at least 10 participants (Table 3). The results yielded a substantial ICC (0.72) for the GRE sequence, moderate ICC (0.52) for the TSE MT on and fair ICC (0.37) for the TSE MT off. In addition, the ICC for the average CR_{SN} in the whole ICC mask was calculated for each sequence (Table 3). ICC values of the average CR in the SN were almost perfect for the GRE sequence (0.90), substantial for TSE MT on (0.79), and the TSE MT off (0.66). The post hoc non-smoothed preprocessed data yielded lower reliability compared to the smoothed preprocessed data (Table 3).

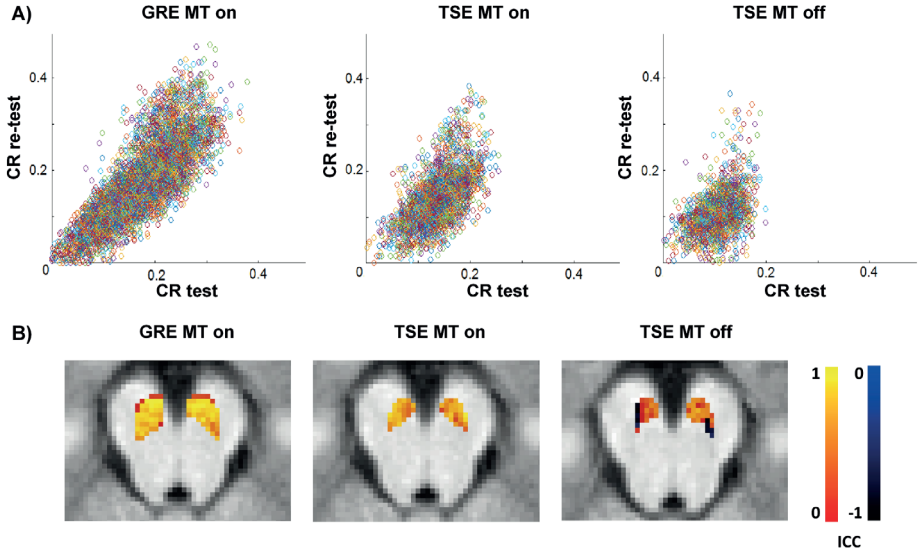

Figure 3. Contrast ratios **A)** and ICC values **B)** per voxel between test and retest measurement in the substantia nigra for the three different NM-sequences. CR: contrast ratio; GRE: gradient recalled echo; MT: magnetization transfer pulse; TSE: turbo spin echo.

Discussion

This study compared NM-MRI sequences with regard to their reproducibility and evaluated different analysis methods in young healthy controls. Overall, the GRE MT on sequence achieved the best reproducibility and reliability, for all analysis methods (manual, threshold,

and voxelwise). For CR measurements, the CC was a more stable reference region than the RN and the test-retest, intra- and inter rater ICCs ranged from substantial to almost excellent. The SN volume measurements were more variable, with poor to slight test-retest variability and slight to almost perfect inter- and intra-rater ICCs for the manual segmention and a substantial ICC for the threshold analysis.

The better performance of the GRE MT on sequence is an important result, as most NM-MRI studies have been performed with TSE sequences (5,12-27). Our results for the GRE MT on sequence are in line with previous reliability studies. Langley et al found a lower ICC (0.81) for the CR_{SN} for the threshold analysis, even though in our study the two MRI scans were separated by a 3-week interval instead of a single session day (32). This difference might be due to variation in analysis design. For example, this study used SPM with DARTEL routines for normalization to MNI space, whereas Langley et al used FSL (32). However, they found a higher ICC (0.94) for the volume measurements using a semi-automated thresholding method, although they yielded a lower DSC (0.80) for the volume measurement. The ICC is more clinically relevant though than the DSC, however, since it measures the reproducibility of CR and volume measurements instead of the reproducibility of the volume location and center. The current study replicated the analysis design of Cassidy et al and, indeed, their results (an ICC of 0.95 for the CR_{SN}) are more comparable to ours (0.90), while they had only an hour interval between test and retest acquisitions (6). The voxelwise analysis also showed similar results, with a mean ICC CR_v of 0.72 compared to a median ICC of 0.64. This result suggests that a longer period between test and retest (3 weeks instead of an hour) does not result in increased variability. A recent study compared different acquisition parameters for GRE MT on sequences and different voxelwise analysis toolboxes (33) with higher ICCs than ours, which is most likely related to further optimized slab placement and co-registration methods. These comparisons emphasize the influence of analysis and acquisition design.

In this study a single measures and absolute agreement two-way mixed-effects model was chosen for the intra-rater and inter-rater reliability, since the purpose was to compare the absolute score from the raters on the same measurement (scan). For the test-retest ICC, single measures and consistency 2-way mixed-effects was used. This ICC does not penalize systematic variability across test and retest (eg, if the retest is consistently higher than the test measurements). The consistency ICC has been used in previous reliability studies of the GRE MT on NM-MRI (6,33). We observed, however, hardly any differences between the absolute agreement and consistency ICC values.

A previous study has also compared different NM-MRI sequences and showed a higher CR for the GRE sequence compared to a TSE sequence (31). Our study replicated this finding and additionally indicated that a higher contrast goes together with better reproducibility. Adding the MT pulse increased the contrast for the TSE sequences and also resulted in an

overall better reproducibility. This supports previous work that has shown that contrast in NM-MRI is associated with MT effects (next to T1 reduction by neuromelanin), which is probably partly related to higher macromolecular content in the adjacent white matter than in the gray matter of the SN (4,28,38).

It is reassuring to see that different analysis methods achieved substantial to almost perfect reliability for the CR. The method with the highest ICC was the analysis in which all scans were normalized to standard space, before calculating the CR for the whole SN mask. The choice of analysis method may be based on a number of considerations. Manual segmentation might be considered with a small sample size. Since it does not require a normalization step, there is no introduction of normalization errors and the low complexity could increase clinical applicability. In addition, manual segmentation might be more suitable for comparing two anatomically different groups (eg, due to atrophy), since this could complicate the registration/normalization process and defining the template mask. However, manual segmentation is labor-intensive and susceptible to rater differences and imaging slab placement, especially for the volume measurements. This is an important finding, since numerous studies on PD have used the manual approach for volume measurements (5,14,19,21,22,24).For the manual volume measurements, the test-retest ICCs were mainly poor to slight and considerably lower than the intra-rater ICCs, which ranged from slight to excellent. For the CR measurements, however, test-retest ICCs were fair to good, while intra-rater ICCs were all excellent. This may indicate that the manual volume measurements were more susceptible to differences in imaging slab placement between test and retest sessions. The thresholding method could be a better alternative for volume measurements and could also be applied without the normalization step. It is less susceptible to rater differences than the manual volume analysis, since is detects the most intense voxels in a large region of interest (ROI) around the SN, but variability from imaging slab placement (in particular, angle) would remain. The normalization step does seem to reduce the test-retest variability, and thus reduce variability from imaging slab placement, with a substantial ICC for the threshold method applied in this study. Moreover, a semi-automated approach would be less time- and labor-consuming, especially for research studies with a large sample size. The voxelwise method has the potential to explore the (sub)regional variation of the SN, yielding a substantial combined CR_V mean ICC, although some individual voxels, in particular those close to the borders of the ROI, showed somewhat lower reliability.

Limitations

In the current study all imaging slabs were placed by one person (M.P.) according to a commonly used method to reduce variation However, we still had to exclude one subject for the voxelwise analysis due to suboptimal placement. Correct placement of the NM-MRI is challenging and susceptible to differences in acquisition in and between studies. This would suggest that using a detailed volume placement protocol, such as that described recently

(33), is advisable to increase the reproducibility of the NM measurements. Furthermore, the current raters were inexperienced with NM-MRI segmentation. We tried to overcome this by employing a segmentation protocol and a training session. However, reliability might increase with more experience.

Another limitation might be that MRI scan parameters such as TR and TE differed between sequences and that adjustments might affect the reproducibility. The sequences that we applied were based on previously published sequences. Unpublished data from our lab has demonstrated that increasing the TR (to 633 msec) for the GRE MT on sequence leads to higher CR, which might improve reliability. This is in line with data by Wengler et al who showed higher CR at a higher TR (33), although in that study, other parameters such as slice thickness, were also adjusted simultaneously. In addition, a recent study by Liu et al showed that optimizing the FA increased the contrast-to-noise, which could also affect the reproducibility (39). They found a different optimal FA for imaging the LC than for the SN. This means that optimization of NM-MRI for SN measurements may not be the same as for LC measurements. Since the LC is also an important structure that can be visualized with NM-MRI, separate (or simultaneous) studies assessing the reproducibility and optimization of NM-MRI of the LC are necessary (31,34,40). Further optimization of the sequences by adjusting different MRI acquisition parameters is therefore of interest. Combining such an optimization study with post mortem research is meaningful to evaluate the correlation with regional NM concentration and to evaluate the reliability for quantification of neuronal loss, for instance in PD.

Due to the inclusion of only relatively young and healthy subjects, the results of this study might not be generalizable to other populations. In addition, when using a clinical sample, such as PD patients, the reproducibility of the SN may be decreased, since the NM signal in PD patients is lower, leading to lower contrast and clinical symptoms may introduce (movement) artifacts in NM-MRI images.

Conclusion

NM-MRI CR is a highly reproducible measure, especially when using the GRE MT on sequence. Different analysis methods can be applied for CR analyses; however, for volume analyses the manual method is unreliable, whereas a thresholding method shows good results. Future research with the GRE MT on sequence is encouraged to further optimize NM-MRI as a noninvasive measurement of neuromelanin in the SN as a proxy biomarker for functioning of the dopamine system in different neuropathology.

References

1. Sulzer D, Cassidy C, Horga G, et al. Neuromelanin detection by magnetic resonance imaging (MRI) and its promise as a biomarker for Parkinson's disease. npj Park. Dis. 2018;4 doi: 10.1038/s41531-018-0047-3.
2. Shibata E, Sasaki M, Tohyama K, et al. Use of Neuromelanin-Sensitive MRI to Distinguish Schizophrenic and Depressive Patients and Healthy Individuals Based on Signal Alterations in the Substantia Nigra and Locus Ceruleus. Biol. Psychiatry 2008;64:401–406 doi: 10.1016/j.biopsych.2008.03.021.
3. Lee J, Park S. Working memory impairments in schizophrenia: a meta-analysis. J. Abnorm. Psychol. 2005;114:599–611 doi: 10.1037/0021-843X.114.4.599.
4. Trujillo P, Summers PE, Ferrari E, et al. Contrast mechanisms associated with neuromelanin-MRI. Magn. Reson. Med. 2017;78:1790–1800 doi: 10.1002/mrm.26584.
5. Matsuura K, Maeda M, Yata K, et al. Neuromelanin magnetic resonance imaging in Parkinson's disease and multiple system atrophy. Eur. Neurol. 2013;70:70–77 doi: 10.1159/000350291.
6. Cassidy CM, Zucca FA, Girgis RR, et al. Neuromelanin-sensitive MRI as a noninvasive proxy measure of dopamine function in the human brain. Proc. Natl. Acad. Sci. U. S. A. 2019;116:5108–5117 doi: 10.1073/pnas.1807983116.
7. Sulzer D, Bogulavsky J, Larsen KE, et al. Neuromelanin biosynthesis is driven by excess cytosolic catecholamines not accumulated by synaptic vesicles. Proc. Natl. Acad. Sci. 2000;97:11869–11874 doi: 10.1073/pnas.97.22.11869.
8. Biesemeier A, Eibl O, Eswara S, et al. Elemental mapping of Neuromelanin organelles of human Substantia Nigra: correlative ultrastructural and chemical analysis by analytical transmission electron microscopy and nano-secondary ion mass spectrometry. J. Neurochem. 2016:339–353 doi: 10.1111/jnc.13648.
9. Zucca FA, Basso E, Cupaioli FA, et al. Neuromelanin of the human substantia Nigra: An update. Neurotox. Res. 2014;25:13–23 doi: 10.1007/s12640-013-9435-y.
10. Zecca L, Stroppolo A, Gatti A, et al. The role of iron and molecules in the neuronal vulnerability of locus coeruleus and substantia nigra during aging. Proc. Natl. Acad. Sci. U. S. A. 2004;101:9843–9848 doi: 10.1073/pnas.0403495101.
11. Xing Y, Sapuan A, Dineen RA, Auer DP. Life span pigmentation changes of the substantia nigra detected by neuromelanin-sensitive MRI. Mov. Disord. 2018;33:1792–1799 doi: 10.1002/mds.27502.
12. Moon WJ, Park JY, Yun WS, et al. A comparison of substantia nigra T1 hyperintensity in parkinson's disease dementia, alzheimer's disease and age-matched controls: Volumetric analysis of neuromelanin imaging. Korean J. Radiol. 2016;17:633–640 doi: 10.3348/kjr.2016.17.5.633.
13. Hatano T, Okuzumi A, Kamagata K, et al. Neuromelanin MRI is useful for monitoring motor complications in Parkinson's and PARK2 disease. J. Neural Transm. 2017;124:407–415 doi: 10.1007/s00702-017-1688-9.
14. Kashihara K, Shinya T, Higaki F. Neuromelanin magnetic resonance imaging of nigral volume loss in patients with Parkinson's disease. J. Clin. Neurosci. 2011;18:1093–1096 doi: 10.1016/j.jocn.2010.08.043.
15. Martín-Bastida A, Lao-Kaim NP, Roussakis AA, et al. Relationship between neuromelanin and dopamine terminals within the Parkinson's nigrostriatal system. Brain 2019;142:2023–2036 doi: 10.1093/brain/awz120.
16. Miyoshi F, Ogawa T, Kitao SI, et al. Evaluation of Parkinson disease and Alzheimer disease with the use of neuromelanin MR imaging and123I-metaiodobenzylguanidine scintigraphy. Am. J. Neuroradiol. 2013;34:2113–2118 doi: 10.3174/ajnr.A3567.
17. Reimão S, Pita Lobo P, Neutel D, et al. Substantia nigra neuromelanin magnetic resonance imaging in de novo Parkinson's disease patients. Eur. J. Neurol. 2015;22:540–546 doi: 10.1111/ene.12613.
18. Isaias IU, Trujillo P, Summers P, et al. Neuromelanin imaging and dopaminergic loss in parkinson's disease. Front. Aging Neurosci. 2016;8:1–12 doi: 10.3389/fnagi.2016.00196.
19. Kawaguchi H, Shimada H, Kodaka F, et al. Principal component analysis of multimodal neuromelanin MRI and dopamine transporter PET data provides a specific metric for the nigral dopaminergic neuronal density. PLoS One 2016;11:1–13 doi: 10.1371/journal.pone.0151191.

20. Sasaki M, Shibata E, Tohyama K, et al. Neuromelanin magnetic resonance imaging of locus ceruleus and substantia nigra in Parkinson's disease. Neuroreport 2006;17:1215–1218 doi: 10.1097/01.wnr.0000227984.84927.a7.

21. Pyatigorskaya N, Gaurav R, Arnaldi D, et al. Magnetic Resonance Imaging Biomarkers to Assess Substantia Nigra Damage in Idiopathic Rapid Eye Movement Sleep Behavior Disorder. Sleep 2017;40 doi: 10.1093/sleep/zsx149.

22. Pyatigorskaya N, Magnin B, Mongin M, et al. Comparative study of MRI biomarkers in the substantia nigra to discriminate idiopathic Parkinson disease. Am. J. Neuroradiol. 2018;39:1460–1467 doi: 10.3174/ajnr.A5702.

23. Schwarz ST, Xing Y, Tomar P, Bajaj N, Auer DP. In Vivo assessment of brainstem depigmentation in Parkinson disease: Potential as a severity marker for multicenter studies. Radiology 2017;283:789–798 doi: 10.1148/radiol.2016160662.

24. Schwarz ST, Rittman T, Gontu V, Morgan PS, Bajaj N, Auer DP. T1-Weighted MRI shows stage-dependent substantia nigra signal loss in Parkinson's disease. Mov. Disord. 2011;26:1633–1638 doi: 10.1002/mds.23722.

25. Ariz M, Abad RC, Castellanos G, et al. Dynamic atlas-based segmentation and quantification of neuromelanin-rich brainstem structures in Parkinson disease. IEEE Trans. Med. Imaging 2019;38:813–823 doi: 10.1109/TMI.2018.2872852.

26. Fabbri M, Reimão S, Carvalho M, et al. Substantia Nigra Neuromelanin as an Imaging Biomarker of Disease Progression in Parkinson's Disease. J. Parkinsons. Dis. 2017;7:491–501 doi: 10.3233/JPD-171135.

27. Ohtsuka C, Sasaki M, Konno K, et al. Changes in substantia nigra and locus coeruleus in patients with early-stage Parkinson's disease using neuromelanin-sensitive MR imaging. Neurosci. Lett. 2013;541:93–98 doi: 10.1016/j.neulet.2013.02.012.

28. Langley J, Huddleston DE, Chen X, Sedlacik J, Zachariah N, Hu X. A multicontrast approach for comprehensive imaging of substantia nigra. Neuroimage 2015;112:7–13 doi: 10.1016/j.neuroimage.2015.02.045.

29. Huddleston DE, Langley J, Dusek P, et al. Imaging Parkinsonian Pathology in Substantia Nigra with MRI. Curr. Radiol. Rep. 2018;6 doi: 10.1007/s40134-018-0272-x.

30. Huddleston DE, Langley J, Sedlacik J, Boelmans K, Factor SA, Hu XP. In vivo detection of lateral–ventral tier nigral degeneration in Parkinson's disease. Hum. Brain Mapp. 2017;38:2627–2634 doi: 10.1002/hbm.23547.

31. Chen X, Huddleston DE, Langley J, et al. Simultaneous imaging of locus coeruleus and substantia nigra with a quantitative neuromelanin MRI approach. Magn. Reson. Imaging 2014;32:1301–1306 doi: 10.1016/j.mri.2014.07.003.

32. Langley J, Huddleston DE, Liu CJ, Hu X. Reproducibility of locus coeruleus and substantia nigra imaging with neuromelanin sensitive MRI. Magn. Reson. Mater. Physics, Biol. Med. 2017;30:121–125 doi: 10.1007/s10334-016-0590-z.

33. Wengler K, He X, Abi-Dargham A, Horga G. Reproducibility Assessment of Neuromelanin-Sensitive Magnetic Resonance Imaging Protocols for Region-of-Interest and Voxelwise Analyses. Neuroimage 2019:1–37 doi: 10.1101/781815.

34. Tona KD, Keuken MC, de Rover M, et al. In vivo visualization of the locus coeruleus in humans: quantifying the test–retest reliability. Brain Struct. Funct. 2017;222:4203–4217 doi: 10.1007/s00429-017-1464-5.

35. Ohtsuka C, Sasaki M, Konno K, et al. Differentiation of early-stage parkinsonisms using neuromelanin-sensitive magnetic resonance imaging. Park. Relat. Disord. 2014;20:755–760 doi: 10.1016/j.parkreldis.2014.04.005.

36. Yushkevich PA, Piven J, Hazlett HC, et al. User-guided 3D active contour segmentation of anatomical structures: Significantly improved efficiency and reliability. Neuroimage 2006;31:1116–1128 doi: 10.1016/j.neuroimage.2006.01.015.

37. Landis R., Koch G. An Application of Hierarchical Kappa-type Statistics in the Assessment of Majority Agreement among Multiple Observers Author (s): J . Richard Landis and Gary G . Koch Published by : International Biometric Society Stable URL : https://www.jstor.org/stab. Biometrics 1977;33:363–374.

38. Trujillo P, Smith AK, Summers PE, et al. High-resolution quantitative imaging of the substantia nigra. Proc. Annu. Int. Conf. IEEE Eng. Med. Biol. Soc. EMBS 2015;2015-Novem:5428–5431 doi: 10.1109/EMBC.2015.7319619.

39. Liu Y, Li J, He N, et al. Optimizing neuromelanin contrast in the substantia nigra and locus coeruleus using a magnetization transfer contrast prepared 3D gradient recalled echo sequence. Neuroimage 2020;218:116935 doi: 10.1016/j.neuroimage.2020.116935.

40. Betts MJ, Cardenas-Blanco A, Kanowski M, Jessen F, Düzel E. In vivo MRI assessment of the human locus coeruleus along its rostrocaudal extent in young and older adults. Neuroimage 2017;163:150–159 doi: 10.1016/j.neuroimage.2017.09.042.

Author Contributions

EvdG conceived and designed the study. MvdP performed the data collection with the support of MZ. MvdP, MZ, EW and KB, analysed the data with the support of CC, GH and EvdG. MvdP wrote the original draft of the manuscript. All the authors critically reviewed the manuscript for intellectual content. All authors approved the final version of the manuscript for publication. EvdG supervised the project.

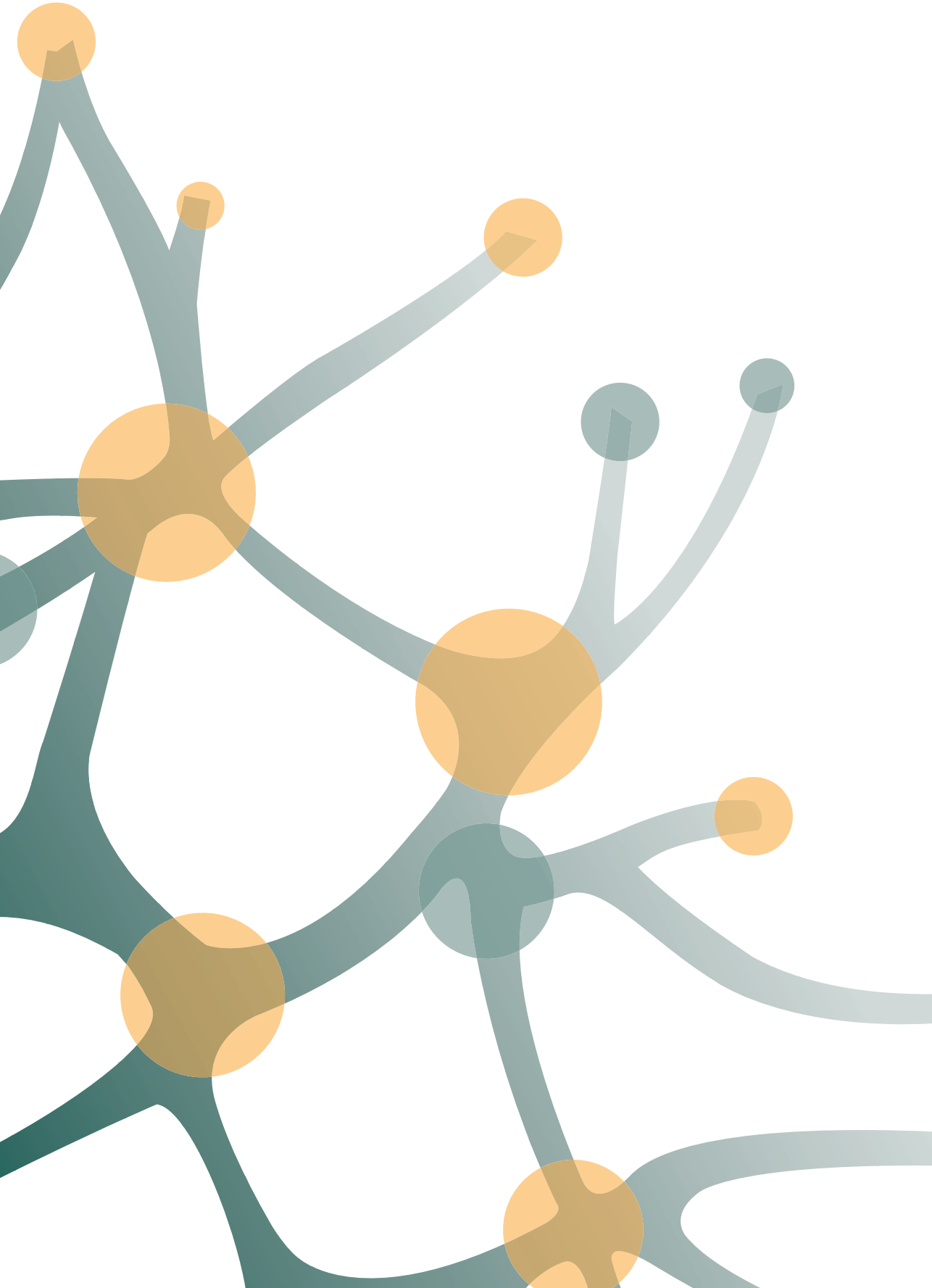

Chapter | 4

Acceleration of neuromelanin-sensitive MRI sequences in the substantia nigra using standard MRI options

Marieke van der Pluijm, Elon D. Wallert, Bram F. Coolen, Kaithlyn T. Tjong Tjin Joe, Lieuwe de Haan, Jan Booij, Elsmarieke van de Giessen

Neuroradiology, 2023; 65:307-312
DOI: 10.1007/s00234-022-03058-w

Abstract

Purpose: Neuromelanin MRI (NM-MRI) is applied as a proxy measurement of dopaminergic functioning of the substantia nigra pars compacta (SN). To increase its clinical applicability, a fast and easily applicable NM-MRI sequence is needed. This study therefore compared accelerated NM-MRI sequences using standard available MRI options with a validated 2D gradient recalled echo NM-MRI sequence with off-resonance magnetization transfer (MT) pulse (2D-MToffRes).

Methods: We used different combinations of compressed sense (CS) acceleration, repetition times (TR), and MT pulse to accelerate the validated 2D-MToffRes. In addition, we compared a recently introduced 3D sequence with the 2D-MToffRes.

Results: Our results show that the 2D sequences perform best with good to excellent reliability. Only excellent intraclass correlation coefficients were found for the CS factor 2 sequences.

Conclusion: We conclude that there are several reliable approaches to accelerate NM-MRI, in particular by using CS.

Introduction

Neuromelanin MRI (NM-MRI) is becoming a key instrument for in-vivo visualization of dopaminergic functioning of the substantia nigra pars compacta (SN) and has potential for clinical application in disorders characterized by dopaminergic alterations such as Parkinson's disease and schizophrenia (1). Several NM-MRI sequences have been investigated, but most commonly used is the 2D gradient recalled echo NM-MRI sequence with off-resonance MT pulse (2D-MToffRes), as its contrast ratio (CR) has been validated with postmortem regional NM concentration and already successfully applied in clinical research (2). An important drawback of the sequence is its scan duration of over 10 min. Customization of the standard MT pulse can reduce scan duration to 4–7 min; however, this is not readily applicable in clinical practice (3). Instead, for a clinical protocol, it is essential to accelerate the scan using standard available MRI options. Most recently, a 3D sequence using on-resonance MT pulse with a scan duration of approximately 4 min has been introduced (4). Advantages of 3D scanning are the potentially higher resolution for small structures such as the SN and a better contrast to noise ratio. This sequence has not been validated or compared to other sequences, yet. The aim of the current study is therefore to assess the performance in terms of CR in the SN of several accelerated NM-MRI sequences using standard available MRI options, including compressed sense (CS) and 3D scanning, and compare these with the validated 2D-MToffRes. Sequences with good to excellent reliability are considered useful alternatives.

Methods

Participants

This study was approved by the Medical Ethics Committee of the Amsterdam Medical Centre. All participants gave written informed consent prior to the scan after the procedure had been fully explained. Nine healthy participants (aged 26.2 ± 3.3 years; 5 males) were included in de CS protocol and 10 healthy participants (aged 26.3 ± 6.1 years; 2 males) in the 3D protocol. All participants were aged between 18 and 40 years. Prior to inclusion, participants were screened by means of an interview and excluded if they had a neurological or psychiatric disorder or had any MRI contraindication.

Image acquisition

All MR data were acquired using a 3 Tesla Ingenia MRI system (Philips, Best, The Netherlands) with a 32 channel SENSE head coil. For slice placement and registration, high-resolution structural T1-weighted volumetric images were acquired (TE/TR = 4.1/9.0 ms; 189 slices; FOV = 284 × 284 × 170 mm; voxel size = 0.9 × 0.9 × 0.9 mm, FA = 8°). Two protocols with different NM-MRI sequences were acquired (Table 1). In the CS protocol, we used CS factors 2 and 3 and adjusted repetition time (TR) to assure most efficient scanning (i.e., using only one slice package instead of three in the original 2D MToffRes). In the 3D protocol, we acquired 3D

sequences with different FA and one 2D sequence without MT pulse preparation. For all NM-MRI scans, the axial slice orientation was the anterior commissure to posterior commissure line. To calculate the CR in the SN, we applied both manual and standardized analysis methods with crus cerebri (CC) as reference region.

Manual analysis

The SN was manually segmented on the three consecutive slices and six consecutive slices, for the 2D and 3D respectively, with the highest voxel intensity using ITK-Snap (v. 3.6.0). The CC was segmented as reference region and consisted of six default circles three on each side of the SN. Segmentation was performed by K.T.T.J., who was trained and performed over a 100 segmentations of the SN on NM-MRI prior to this research. The CR ($[S_{SN} - S_{CC}]/S_{CC}$) was calculated as described previously (2, 5), where SSN and SCC illustrate the mean signal intensities of the SN and CC, respectively. In addition, we calculated the contrast to noise ratio ($CNR = [S_{SN} - S_{CC}]/SD_{CC}$) as a measure for image quality with the standard deviation of the CC (SD_{CC}) representing the noise (6).

Standardized analysis

In addition, the NM-MRI scans were analyzed using a pipeline from a previous study (3). All NM-MRI data were normalized to MNI standard space and spatially smoothed with a 1-mm full-width-at-half-maximum Gaussian kernel using ANTS software. Template masks of the SN and CC were created by manual tracing with ITK-Snap on a standardized average image of all 2D-MToffRes scans. The CR was calculated at each voxel in the SN mask using the CC as reference region. The mean CR per participant was acquired by averaging the CR values of all voxels in the SN mask that had a non-negative value.

Statistical analyses

Statistical analyses were performed in SPSS (7). Sequences were compared with the validated original 2D-MToffRes using the intraclass correlation coefficients (ICC) from a mixed consistency model and Pearson correlation coefficients. ICC values > 0.75 are considered good and > 0.90 excellent (8).

Table 1. Scan parameters

Parameter	TE (msec)	TR (msec)	FA°	Slices	Slice gap	Spatial resolution (mm)	FOV (mm)	NSA	Accel. factor	MT offset (Hz)	MT dur. (msec)	Acq. time (min)
CS-protocol												
2D-MToffRes	3.9	260	40	8	0.25	0.39 x 0.39 x 2.5	162 x 199	2	-	1200	15.6	13:20
2D-noMTRes	3.9	260	40	8	0.25	0.39 x 0.39 x 2.5	162 x 199	2	-	-	-	04:26
2D-CS2	3.9	260	40	8	0.25	0.39 x 0.39 x 2.5	162 x 199	2	CS = 2	1200	15.6	06:42
2D-CS3	3.9	260	40	8	0.25	0.39 x 0.39 x 2.5	162 x 199	2	CS = 3	1200	15.6	04:28
2D-TRad	3.9	633	40	8	0.25	0.39 x 0.39 x 2.5	162 x 199	2	-	1200	15.6	10:47
2D-TRad-CS2	3.9	633	40	8	0.25	0.39 x 0.39 x 2.5	162 x 199	2	CS = 2	1200	15.6	05:25
2D-TRad-CS3	3.9	633	40	8	0.25	0.39 x 0.39 x 2.5	162 x 199	2	CS = 3	1200	15.6	03:36
3D-protocol												
2D-MToffRes	3.9	260	40	8	0.25	0.39 x 0.39 x 2.5	162 x 199	2	-	1200	15.6	13:20
2D-MTonRes	3.9	260	40	8	0.25	0.39 x 0.39 x 2.5	162 x 199	2	-	0	8.5	08:54
3D-FA12	7.5	62	12	48	-	0.67 x 0.67 x 1.34	256 x 192	1	S = 2	0	8.5	04:03
3D-FA15	7.5	62	15	48	-	0.67 x 0.67 x 1.34	256 x 192	1	S = 2	0	8.5	04:03
3D-FA25	7.5	62	25	48	-	0.67 x 0.67 x 1.34	256 x 192	1	S = 2	0	8.5	04:03

The CS protocol consisted of; 1) the original 2D NM-MRI with off resonance MT-pulse (2D-MToffRes); 2) the original 2D NM-MRI without MT-pulse (2D-MTno); 3/4) the 2D-MToffRes with CS factor 2 and 3 (2D-CS2 and 2D-CS3, respectively); 5/6/7) the 2D-MToffRes with an adjusted TR of 633 msec (2D-TRad) and with CS factor 2 and 3 (2D-TRad-CS2 and 2D-TRad-CS3, respectively). The 3D protocol consisted of; 1) the 2D-MToffRes; 2) the original 2D NM-MRI with on resonance MT-pulse (2D-MTonRes); 3/4/5) a 3D NM-MRI scan with on resonance MT-pulse and a flip angle of 12, 15 and 25 (3D-FA12, 3D-FA15 and 3D-FA25, respectively). TE = echo time, TR = repetition time, FA = flip angle, FOV = field of view, NSA = number of signal averages, Accel. factor = acceleration factor, MT = magnetization transfer, Acq. time = acquisition time, CS = compressed sense, S = sense

Results

An overview of the NM-MRI scans are depicted in Fig. 1. The scans demonstrated a CNR between 2.18 and 4.47, with the highest CNR for the 2D sequence with a TR of 633 ms and 3D sequences. CR was lowest for the 3D sequence with a FA of 25 and highest for the 2D sequence with a TR of 633 ms (Table 2). Only excellent ICCs were found for the sequences with CS factor 2, with a TR of 260 ms and 633 ms (Table 2). The manual analysis performed worse than the standardi

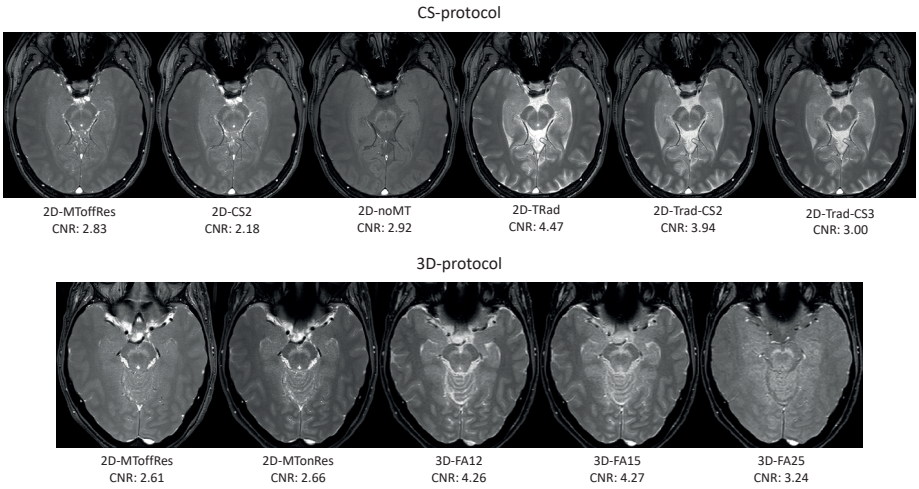

Figure 1. Overview of the NM-MRI scans. An example of the NM-MRI sequences of one participant of the CS protocol and one participant of the 3D protocol, with the mean contrast to noise ratio (CNR) of all participants per scan. MT, magnetization transfer; Res, resonance; CS, compressed sense; TRad, repetition time adjusted; FA, flip angle

Table 2. Mean contrast ratio and reliability of the different sequences

	Manual analysis						Standardized analysis					
	Mean	**SD**	**R**	**p-value**	**ICC**	**p-value**	**Mean**	**SD**	**R**	**p-value**	**ICC**	**p-value**
CS-protocol												
2D-MToffRes	21.81	1.83					16.60	1.82				
2D-noMT	20.93	1.55	0.79	0.06	0.79	0.02	16.72	1.31	0.83	0.04	0.79	0.02
2D-CS2	20.37	1.51	0.55	0.12	0.54	0.05	15.01	1.96	0.91	0.00	0.91	0.00
2D-TRad	27.29	2.93	0.91	0.00	0.82	0.00	20.05	2.27	0.86	0.00	0.84	0.00
2D-TRad-CS2	26.21	3.11	0.87	0.00	0.76	0.01	19.09	2.02	0.93	0.00	0.93	<0.001
2D-TRad-CS3	26.21	3.18	0.89	0.00	0.79	0.01	19.30	1.74	0.87	0.01	0.86	0.00
3D-protocol												
2D-MToffRes	19.33	2.06					14.94	1.42				
2D-MTonRes	24.51	2.37	0.91	0.00	0.90	0.00	18.71	2.28	0.88	0.00	0.69	0.01
3D-FA12	24.78	3.97	0.80	0.01	0.66	0.01	17.24	5.15	0.80	0.01	0.41	0.11
3D-FA15	22.56	3.58	0.87	0.00	0.75	0.00	13.23	3.25	0.77	0.01	0.56	0.04
3D-FA25	15.95	1.91	0.84	0.00	0.84	<0.001	9.64	2.27	0.66	0.04	0.60	0.03

TRad = repetition time adjusted, FA = flip angle, MT = magnetization transfer, Res = resonance, CS = compressed sense, SD=standard deviation, R = Pearson's correlation coefficient, ICC = Intraclass Correlation Coefficient

Discussion

This study demonstrates that several directly applicable strategies to accelerate NM-MRI show good to excellent reliability compared to the validated 2D-MToffRes sequence. The 2D sequence with a TR of 633 ms and 3D sequences demonstrate the highest CNR, as expected for the 3D sequences (4). However, in terms of reliability, the 3D sequences perform worse than the 2D sequences. The 2D sequences with CS most reliably correspond to the validated 2D-MToffRes, especially using the standardized analysis protocol. The sequences with CS factor 2 show excellent ICCs, which is unaffected by increasing TR.

We used CS to accelerate the sequences as CS does not affect the MT and T1-shortening effects, but instead undersamples k-space to reduce scan time (9). The paramagnetic neuromelanin-iron complexes in combination with the high water content of neuromelanin compared to the surrounding tissues lead to the T1-shortening and MT effects which are thought to underlie the contrast (10). We assessed the CS sequences also with adjusted TR. Using a TR of 260 ms on our scanner resulted in separating the slices in 3 packages. This was less time efficient, because of the incorporated waiting time due to specific absorption rate limits. Adjusting the TR to 633 ms made it possible to fit all slices in one package, decreasing scan duration. In addition, more slices in one package increases the multi-slice MT effect and thereby the CR (11). Higher CR could result in easier manual tracing of the SN and may thereby explain the better performance of the manual analysis (5). It should be noted though that the 3D sequences with higher CR and CNR show lower ICCs. This underlines that higher CR and CNR are not necessarily more reliable and stresses the importance of comparing optimized sequences to a validated sequence or post mortem data.

The 3D sequences show a relatively high CNR and moderate to good ICCs using the manual analysis; however, they fail to reach good ICCs using the standardized analysis. The manual analysis is biased though by intra-rater differences and the circularity of acquiring the CR in a mask based on the highest contrast (5). Therefore, the results of the standardized analysis are an important indication that the 3D sequences are less reliable for semi-quantification than the 2D sequences. This finding is in line with the results of a meta-analysis on findings in Parkinson's disease, showing that studies using 2D sequences report a slightly better diagnostic performance than studies using a 3D sequence (12). We should mention though that the standardized analysis is validated for the 2D sequences and might be less accurate for the 3D sequences (3). Advantages of the 3D sequences are the short scan duration and high resolution. They may be useful for anatomical localization of the SN. However, for semi-quantitative purposes, the 2D sequences with CS appear to be most reliable.

We also adjusted the MT effects by changing the MT pulse to the on-resonance MT pulse and by omitting the MT pulse. The on-resonance MT pulse is more time efficient than the off-resonance

MT sequence which requires a longer TR to avoid too high specific absorption rates. Adjusting the MT pulse did not appear to markedly affect the reliability. It should be noted that the 2D sequence without MT pulse was scanned in one package and thereby the increased multi-slice MT effect could have compensated the effect of the off-resonance MT pulse.

Interestingly, our results show some difference in CR for the validated 2D-MToffRes sequence between the two protocols. It should be noted that the CS protocol and 3D protocol consisted of different participant samples and, albeit scanned on the same scanner, the protocols were scanned more than a year apart during which two scanner software updates occurred. The difference is not likely related to reproducibility issues since several NM-MRI 2D sequences have demonstrated a good to excellent reproducibility (3,13), including the validated 2D-MToffRes sequence used in this study with a test–retest variability below 6% (5).

Finally, it will be essential to further validate the accelerated sequences in patient samples. Our samples consisted of small and homogenous groups (e.g., similar age), making the statistical results more prone to limited variation in data points. To conclude, there are several reliable approaches to accelerate NM-MRI. CS or similar acceleration techniques appear to be most suitable for semi-quantitative purposes.

References

1. Reneman L, van der Pluijm M, Schrantee A, van de Giessen E. Imaging of the dopamine system with focus on pharmacological MRI and neuromelanin imaging. Eur J Radiol. 2021;140, 109752.
2. Cassidy CM, Zucca FA, Girgis RR et al. Neuromelanin-sensitive MRI as a noninvasive proxy measure of dopamine function in the human brain. Proc Natl Acad Sci U S A. 2019;116, 5108-5117.
3. Wengler K, He X, Abi-Dargham A, Horga G. Reproducibility assessment of neuromelanin-sensitive magnetic resonance imaging protocols for region-of-interest and voxelwise analyses. Neuroimage. 2020; 208, 116457.
4. Liu Y, Li J, He N, Chen Y, Jin Z, Yan F. Optimizing neuromelanin contrast in the substantia nigra and locus coeruleus using a magnetization transfer contrast prepared 3D gradient recalled echo sequence. Neuroimage. 2020;218, 116935.
5. van der Pluijm M, Cassidy C, Zandstra M et al. Reliability and Reproducibility of Neuromelanin-Sensitive Imaging of the Substantia Nigra: A Comparison of Three Different Sequences. J Magn Reson Imaging. 2020;53, 712-721.
6. Chen X, Huddleston DE, Langley J et al. Simultaneous imaging of locus coeruleus and substantia nigra with a quantitative neuromelanin MRI approach. Magn Reson Imaging. 2014;32(10), 1301-1306.
7. IBM Corp. Released 2021. IBM SPSS Statistics for Mac, Version 28.0. Armonk, NY: IBM Corp.
8. Koo TK, Li MY. A Guideline of Selecting and Reporting Intraclass Correlation Coefficients for Reliability Research. J Chiropr Med. 2016;15, 155-163.
9. Lustig M, Donoho D, Pauly, JM. Sparse MRI: The application of compressed sensing for rapid MR imaging. Magn Reson Med. 2007;58(6), 1182-1195.
10. Trujillo P, Summers PE, Ferrari E et al. Contrast mechanisms associated with neuromelanin-MRI. Magn Reson Med, 78, 1790-1800. doi:10.1002/mrm.26584
11. Chang Y, Bae SJ, Lee YJ et al (2007) Incidental magnetization transfer effects in multislice brain MRI at 3.0T. J Magn Reson Imaging. 2017;25(4), 862-865
12. Cho SJ, Bae YJ, Kim, JM et al. Diagnostic performance of neuromelanin-sensitive magnetic resonance imaging for patients with Parkinson's disease and factor analysis for its heterogeneity: a systematic review and meta-analysis. Eur Radiol. 2021;31(3),
13. Langley J, Huddleston DE, Liu CJ, Hu X. Reproducibility of locus coeruleus and substantia nigra imaging with neuromelanin sensitive MRI. MAGMA. 2017;30(2), 121-125.

Author Contributions

EvdG and MvdP conceived and designed the study. MvdP performed the data collection with support of EW. MvdP, EW, KTTJ analysed the data with the support of BC and EvdG. MvdP wrote the original draft of the manuscript. All the authors critically reviewed the manuscript for intellectual content. All authors approved the final version of the manuscript for publication. EvdG supervised the project.

Supplementary material

Manual analysis

The SN was manually segmented on the three slices and six slices, for the 2D and 3D respectively, with the highest voxel intensity using ITK-Snap (v. 3.6.0). The crus cerebri (CC) was segmented as reference region and consisted of six default circles three on each side of the SN). Subsequently, the contrast ratio ($CR=[S_{SN}-S_{CC}]/S_{CC}$) was calculated as described previously (1), where S_{SN} and S_{CC} illustrates the mean signal intensities of the SN and CC, respectively.

Standardized analysis

In addition, the NM-MRI scans were analysed using a pipeline from a previous study (2). All NM-MRI data were normalized to MNI standard space and spatially smoothed with a 1-mm full-width-at-half-maximum Gaussian kernel using ANTS software. Template masks of the SN and CC were created by manual tracing with ITK-Snap on a standardized average image of all 2D gradient recalled echo NM-MRI sequence with off-resonance MT-pulse (2D-MToffRes) scans. The CR was calculated at each voxel in the SN mask using the CC as reference region. The mean CR per participant was acquired by averaging the CR-values of all voxels in the SN mask that had a non-negative value.

References

1. van der Pluijm M, Cassidy C, Zandstra M, et al. Reliability and Reproducibility of Neuromelanin-Sensitive Imaging of the Substantia Nigra: A Comparison of Three Different Sequences. J Magn Reson Imaging. 2020;53, 712-721. doi:10.1002/jmri.27384
2. Wengler K, He X, Abi-Dargham A, Horga G. Reproducibility assessment of neuromelanin-sensitive magnetic resonance imaging protocols for region-of-interest and voxelwise analyses. Neuroimage. 2020;208, 116457.

PART II

SUBSTANTIA NIGRA IN SCHIZOPHRENIA

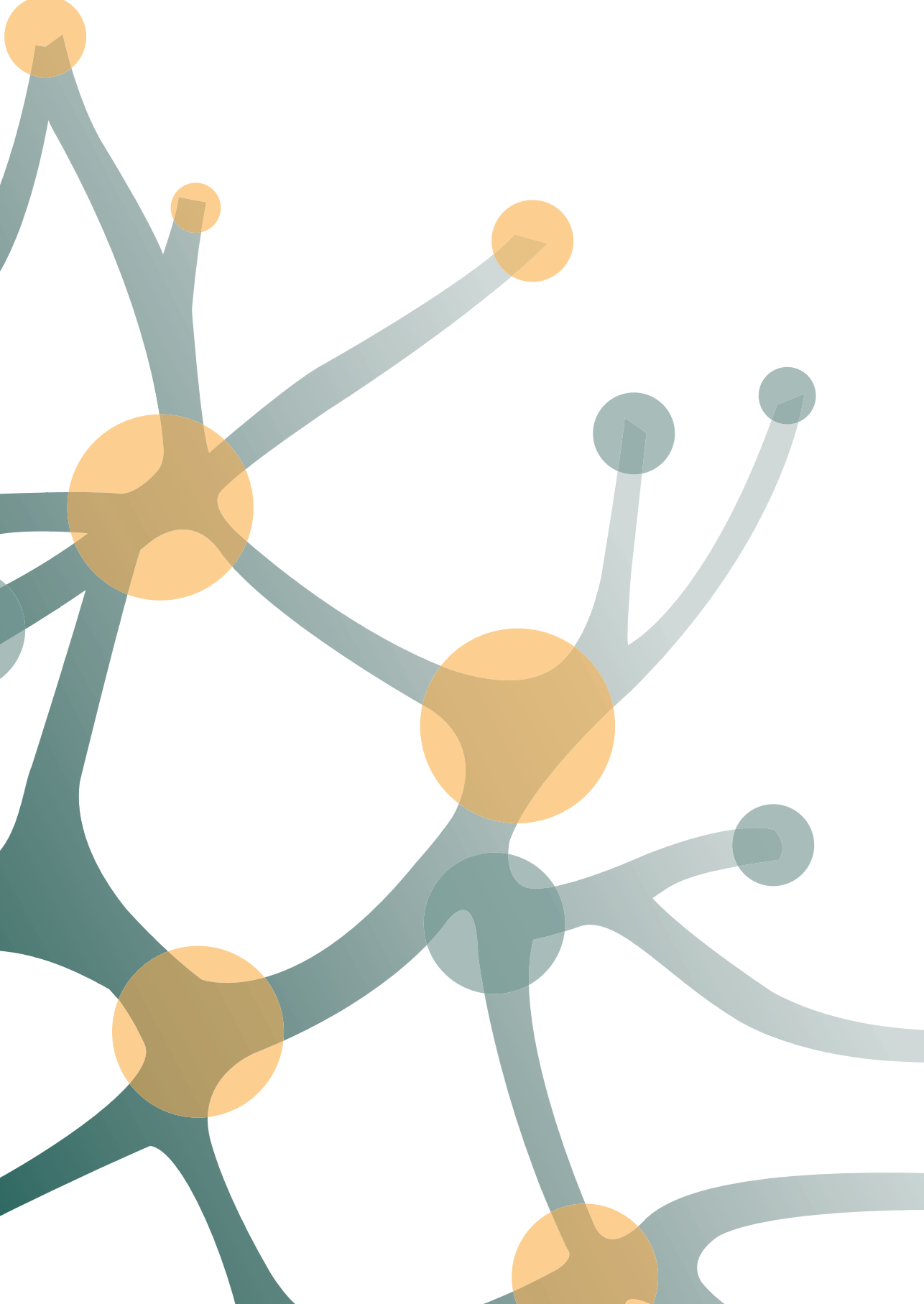

Chapter | 5

The substantia nigra in the pathology of schizophrenia: a review on post-mortem and molecular imaging findings

Carmen F.M. van Hooijdonk*, Marieke van der Pluijm*,
Iris Bosch, Therese A.M.J. van Amelsvoort,
Jan Booij, Lieuwe de Haan, Jean-Paul Selten,
Elsmarieke van de Giessen
**equal contribution*

European Neuropsychopharmacology, 2023; 68:57-77
DOI: 10.1016/j.euroneuro.2022.12.008

Abstract

Dysregulation of striatal dopamine is considered to be an important driver of pathophysiological processes in schizophrenia. Despite being one of the main origins of dopaminergic input to the striatum, the (dys)functioning of the substantia nigra (SN) has been relatively understudied in schizophrenia. Hence, this paper aims to review different molecular aspects of nigral functioning in patients with schizophrenia compared to healthy controls by integrating post-mortem and molecular imaging studies. We found evidence for hyperdopaminergic functioning in the SN of patients with schizophrenia (i.e. increased AADC activity in antipsychotic-free/-naïve patients and elevated neuromelanin accumulation). Reduced GABAergic inhibition (i.e. decreased density of GABAergic synapses, lower VGAT mRNA levels and lower mRNA levels for $GABA_A$ receptor subunits), excessive glutamatergic excitation (i.e. increased NR1 and Glur5 mRNA levels and a reduced number of astrocytes), and several other disturbances implicating the SN (i.e. immune functioning and copper concentrations) could potentially underlie this nigral hyperactivity and associated striatal hyperdopaminergic functioning in schizophrenia. These results highlight the importance of the SN in schizophrenia pathology and suggest that some aspects of molecular functioning in the SN could potentially be used as treatment targets or biomarkers.

Introduction

Schizophrenia is a severe mental disorder characterized by positive symptoms including hallucinations and delusions, negative symptoms such as social withdrawal and avolition, and cognitive symptoms including deficits in executive functioning and working memory (1). A complex pathology is thought to underlie schizophrenia. The dopamine hypothesis proposes a framework that links the interaction between multiple risk factors (e.g. drug use, genes, and stress) and frontotemporal dysfunction to a final common pathway of dopamine dysregulation, more specifically striatal hyperdopaminergia. Striatal hyperdopaminergia is thought to alter the appraisal of stimuli, subsequently leading to the development of psychotic symptoms. Converging evidence showed that the striatal hyperdopaminergia is primarily located presynaptically (for descriptions of versions I, II, and III of the dopamine hypothesis see respectively (2-4)). Dopaminergic neurons primarily originate from two midbrain structures: the substantia nigra pars compacta (SNc) and the ventral tegmental area (VTA). Projections from the SNc to the dorsal striatum form the nigrostriatal dopaminergic pathway, while projections from the VTA to the nucleus accumbens/ventromedial striatum form the mesolimbic pathway and from the VTA to cortical regions (in particular the frontal cortex) the mesocortical pathway. The mesocortical pathway and frontal hypodopaminergia have been implicated in the cognitive symptoms of schizophrenia (3). Originally, dysfunction of the mesolimbic pathway was thought to underlie the striatal hyperdopaminergia and the psychotic symptoms, but insights from neuroimaging studies suggest that dopaminergic dysfunction in schizophrenia is greatest within the nigrostriatal pathway (as reviewed in (5)). Several studies have identified the associative striatum as the main region of increased striatal dopaminergic functioning in psychosis (6-8). The associative striatum receives dopaminergic innervation from primarily the ventral tier of the SNc (9) and it has been hypothesized that the increase in striatal dopamine functioning might be related to upstream alterations in the substantia nigra (SN). Despite the importance of dopamine dysregulation in the pathology of schizophrenia, and the SN as the main origin of dopaminergic neurons of the nigrostriatal pathway, this midbrain structure has been relatively understudied in patients with schizophrenia.

Dopaminergic abnormalities on their own do not explain all facets of schizophrenia pathology. Other neurotransmitters, such as glutamate and γ-aminobutyric acid (GABA) are likely to be involved. This suggestion is based on the observation that blocking of N-methyl-D-aspartate (NMDA) receptors on GABAergic interneurons in the cortex by antagonists, such as phencyclidine (PCP) and ketamine, results in schizophrenia-like symptoms in healthy individuals and worsens these symptoms in patients (for review see (10,11). Alterations in GABAergic and glutamatergic functioning have been widely studied in schizophrenia (as reviewed in (12,13)) and the glutamate hypothesis suggests hypo-functioning of NMDA receptors on GABAergic interneurons in the cortex, which leads to excessive glutamate

release (14). The dopamine and glutamate hypotheses are not mutually exclusive. In fact, the glutamate hypothesis can function as an extension of the dopamine hypothesis, and combined they propose that presynaptic striatal hyperdopaminergia in patients with schizophrenia might be secondary to alterations in glutamatergic functioning (15). Most of the studies on GABAergic and glutamatergic functioning in schizophrenia did not investigate the SN, even though the SN pars reticulata (SNr) is mainly involved in GABAergic signalling (16). This suggests that nigral glutamatergic and GABAergic functioning might also be relevant for schizophrenia pathology.

Hence, we aim to review the molecular alterations that occur in the SN of patients with schizophrenia, investigate how these changes may contribute to schizophrenia pathology and identify knowledge gaps. We investigated these aims by reviewing post-mortem and molecular imaging studies (i.e. by use of Positron Emission Tomography [PET], Single Photon Emission Computed Tomography [SPECT], proton Magnetic Resonance Spectroscopy [^{1}H-MRS], or neuromelanin-sensitive Magnetic Resonance Imaging [NM-MRI]) that investigated different molecular aspects of nigral functioning in patients with schizophrenia compared to controls. We first focus on the dopaminergic signalling pathway within the SN. Next, we discuss the nigral glutamatergic and GABAergic signalling pathways. We then overview other molecular alterations in the SN that might be relevant for schizophrenia pathology. Finally, we integrate the different topics, place our findings in the context of what has been found by animal studies, and identify avenues for future research.

Dopaminergic alterations in the substantia nigra of patients with schizophrenia

Within dopaminergic synapses, tyrosine hydroxylase (TH) converts tyrosine into l-3,4-dihydroxyphenylalanine (L-DOPA) and is the rate-limiting enzyme for dopamine production (17) (Fig. 1). Multiple post-mortem studies reported elevated TH protein levels in the SN (18-20) and increased TH messenger RNA (mRNA) levels in the SNc (21) of patients with schizophrenia compared to controls (Table 1). However, other studies found no differences in TH protein levels in the SN (22) or TH mRNA levels in the SN (22,23) or midbrain (which includes the SN and ventral tegmental area [VTA]) (24). In addition, decreased TH protein levels in the SN/VTA (24) and lower TH mRNA levels in the SN of patients with schizophrenia relative to controls have also been reported ((25); same cohort as (22), but using a more sensitive quantitative polymerase chain reaction [qPCR] platform). The opposing study outcomes might be explained by differences in exposure to antipsychotic medication, illness duration, cohort size, and sampling area (i.e. SN versus SN/VTA). Rodent studies, however, suggest that antipsychotic medication does either not change (24) or reduces TH levels (26).

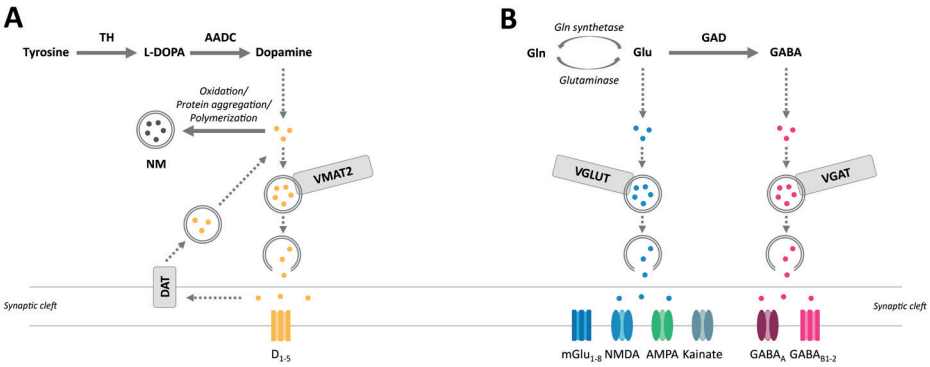

Figure 1. Systematic overview of the dopaminergic, glutamatergic and GABAergic signalling pathways.

A. Schematic overview of the dopaminergic signalling pathway: TH converts tyrosine into L-DOPA, which is then converted into dopamine by AADC. VMAT-2 transports and stores dopamine in synaptic vesicles before dopamine is released into the synaptic cleft. Excess cytosolic dopamine is packaged as NM complexes inside autophagic organelles after a process of iron-dependent oxidation, protein aggregation, and polymerization. Exocytosis of the synaptic vesicles containing dopamine induces dopamine release into the synaptic cleft. After dopamine release, dopamine binds to dopamine metabotropic receptors ($D_{1\text{-}5}$). The presynaptic DAT is responsible for the reuptake of dopamine from the synaptic cleft into the presynaptic terminal.

B. Schematic overview of the glutamatergic/GABAergic signalling pathway: Gln is converted to Glu and Glu to Gln by Glutaminase and Gln synthetase, respectively. GAD synthesizes GABA from Glu. The VGLUT and VGAT transport and store Glu and GABA, respectively, in synaptic vesicles before release in the synaptic cleft. After release, Glu binds to ionotropic receptors (NMDA, AMPA, and kainate) and metabotropic receptors ($mGlu_{1\text{-}8}$). GABA binds to the ionotropic receptor ($GABA_A$) and metabotropic receptor ($GABA_B$).

Abbreviations: AADC, aromatic acid decarboxylase; AMPA, α-amino-3-hydroxy-5-methyl-4-isoxazolepropionic acid receptor; DAT, dopamine transporter; $D_{1\text{-}5}$, dopaminergic (metabotropic) receptors; GABA, γ-aminobutyric acid; $GABA_A$, ionotropic GABA receptor; $GABA_B$, metabotropic receptor; GAD, glutamic acid decarboxylase; Gln, glutamine; Glu, glutamate; kainate, kainate receptor, L-DOPA, l-3,4-dihydroxyphenylalanine; $mGlu_{1\text{-}8}$, metabotropic glutamate receptors; NM, neuromelanin; NMDA, N-methyl-D-aspartate receptor; TH, tyrosine hydroxylase; VGAT, vesicular GABA transporter; VGLUT, vesicular Glu transporter; VMAT-2, vesicular monoamine transporter 2.

Additionally, in the largest cohort of 27 patients, Purves-Tyson et al found no correlation between (1) measures of antipsychotic drug treatment or illness duration and (2) TH mRNA or protein levels in the SN, supporting that these factors did not change the molecular parameters (22). TH activity might be differently regulated in different subregions of the midbrain, as Perez-Costas et al found decreased and unaltered TH protein levels in the rostro-caudal and mid-caudal parts of the SN/VTA in patients with schizophrenia compared to controls, respectively (24). Even though these findings underline the importance of regional differences in TH activity in the midbrain, this analysis only included eight patients and six controls. The current data does, therefore, not support a clear increase or decrease of TH protein- and mRNA levels in the SN and underlines the need for larger well-powered studies that consider regional differences within the SN/VTA.

Table 1. Studies examing different molecular aspects of nigral functioning in patients with schiozphrenia

Source	Method(s): constituent(s)	ROI	Sample size, No. (F:M)	Age, mean (SD), y	Antipsychotic mediation status, No.	Illness duration, mean (SD), y	Main result(s)
Allen et al. (2012)	[^{18}F]-FDOPA PET: dopamine synthesis	SN/VTA	5 (2:3) UHR-t 16 (7:9) UHR-nt 14 (4:10) HC	UHR-t: 26.32 (4.22) UHR-nt: 25.51 (5.81) HC: 25.40 (3.60)	AP naïve (5 UHR-t, 14 UHR-nt) AP free (2 UHR-nt)	NA	↑↑ Dopamine synthesis in UHR-t vs UHR-nt = Dopamine synthesis in UHR-t vs HC
Arakawa et al. (2009)	[^{11}C]-PE2I PET: DAT binding	SN	8 (2:6) SCZ 12 (2:10) HC	SCZ: 36.50 (9.50) HC: 33.20 (12.00)	AP naïve (2 SCZ) AP free[1] (6 SCZ)	SCZ: 32.10 (42.80)[2]	= DAT binding in SCZ vs HC
Artiges et al. (2017)	[^{11}C]-PE2I PET: DAT binding	Left and right SN/VTA	21 (0:21) SCZ 30 (0:30) HC	SCZ: 34.19 (10.23) HC: 30.17 (9.65)	AP naïve (1 SCZ) On AP (20 SCZ)	SCZ: 13.57 (9.25)	↑↑ Left and right DAT binding in SCZ vs HC
Cassidy et al. (2019)	NM-MRI: NM	SN	33 (10:23) SCZ 30 (12:18) HC	SCZ: 33.90 (2.20)[5] HC: 34.00 (2.20)[5]	AP naïve[5] (17 SCZ) AP free[5] (16 SCZ)	NR	= NM in SCZ vs HC
Elkashef et al. (2000)	[^{18}F]-FDOPA PET: dopamine synthesis	SN/VTA	10 (2:8) SCZ on medication 9 (2:7) SCZ off medication 13 (5:8) HC	SCZ on medication: 39.30 (8.70) SCZ off medication: 33.30 (7.90) HC: 34.70 (10.75)	AP free[8] (9 SCZ) On AP (10 SCZ)	SCZ on medication: 19.60 (7.80) SCZ off medication: 15.00 (8.40)	= Dopamine synthesis in SCZ on medication vs SCZ off medication vs HC
Graff-Guerrero et al. (2009)	[^{11}C]-(+)-PHNO PET: $D_{2/3}$ receptor availability	SN	13 (4:9) SCZ 13 (4:9) HC	SCZ: 25.85 (5.90) HC: 26.85 (6.40)	AP naïve (10 SCZ) AP free[16] (3 SCZ)	NR	= $D_{2/3}$ receptor availability in SCZ vs HC
Howes et al. (2013)	Immunohisto-chemistry: TH; [^{18}F]-FDOPA PET: AADC activity	SN	Post-mortem cohort 12 (5:7) SCZ 13 (4:9) HC In vivo cohort 29 (3:26) SCZ 29 (7:22) HC	Post-mortem cohort SCZ: 60.10 (2.30)[5] HC: 51.90 (2.80)[5] In vivo cohort SCZ: 33.70 (10.60)[5] HC: 29.30 (7.50)[5]	Post-mortem cohort On AP (12 SCZ) In vivo cohort AP naïve (5 SCZ) AP free[9] (8 SCZ) On AP (16 SCZ)	NR	↑↑ TH staining in SCZ vs HC ↑↑ AADC activity in SCZ vs HC
Ichinose et al. (1994)	RT-PCR: TH mRNA, AADC activity	SN	8 (2:6) SCZ 12 (6:6) HC	SCZ: 67.00 (6.00)[5] HC: 71.00 (3.00)[5]	NR	NR	= TH mRNA in SCZ vs HC = AADC activity in SCZ vs HC

Table 1. *(continued)*

Source	Method(s): constituent(s)	ROI	Sample size, No. (F:M)	Age, mean (SD), y	Antipsychotic mediation status, No.	Illness duration, mean (SD), y	Main result(s)
Jauhar et al. (2017)	[^{18}F]-FDOPA PET: AADC activity	SN	16 (2:14) SCZ 22 (8:14) HC	SCZ: 26.31 (4.40) HC: 24.45 (4.54)	AP naïve (11 SCZ) AP free[10] (3 SCZ) On AP (2 SCZ)	SCZ: 24[2,3,4]	= AADC activity in SCZ vs HC
Joo et al. (2018)	[^{18}F]-fallypride PET: $D_{2/3}$ receptor availability	Left and right SN	16 (10:6) SCZ 17 (9:8) HC	SCZ: 36.90 (11.40) HC: 32.30 (9.50)	On AP (16 SCZ)	SCZ: 6.50 (3.70)	↓↓ Left and right $D_{2/3}$ receptor availability in SCZ vs HC
Kegeles et al. (2010b)	[^{18}F]-fallypride PET: $D_{2/3}$ receptor availability	SN	21 (7:14) SCZ 22 (5:17) HC	SCZ: 31.00 (12.00) HC: 26.00 (6.00)	AP naïve (5 SCZ) AP free[16] (16 SCZ)	NR	= $D_{2/3}$ receptor availability in SCZ vs HC
Kessler et al. (2009)	[^{18}F]-fallypride PET: $D_{2/3}$ receptor availability	Left and right SN/ VTA	11 (5:6) SCZ 11 (6:5) HC	SCZ: 30.50 (8.00) HC: 31.60 (9.20)	AP naïve (4 SCZ) AP free[7] (7 SCZ)	NR	↑↑ Left and right $D_{2/3}$ receptor availability in SCZ vs HC
Kumakura et al. (2007)	[^{18}F]-FDOPA PET: AADC activity	Midbrain	8 (0:8) SCZ 15 (0:15) HC	SCZ: 37.30 (6.30) HC: 37.30 (6.40)	AP naïve (3 SCZ) AP free[1] (5 SCZ)	NR	↑↑ AADC activity in SCZ vs HC
Mabry et al. (2019)	Immunohisto-chemistry: VGLUT1, VGLUT2, and GAD67; Electron microscopy: density of glutamatergic and GABAergic synapses	SN	Immunohistochem-istry cohort 6 (2:4) SCZ 5 (2:3) HC Electron microscopy cohort 11 (3:8) SCZ 8 (2:6) HC	Immunohistochem-istry cohort SCZ: 53.80 (13.70) HC: 51.20 (11.40) Electron microscopy cohort SCZ: 50.60 (10.60) HC: 43.40 (15.30)	Immunohistochem-istry cohort AP free[1] (3 SCZ) On AP (2 SCZ) NR (1 SCZ) Electron miscroscopy cohort On AP (11 SCZ)	NR	= VGLUT1 and VGLUT2 levels in SCZ vs HC = GAD67 in SCZ vs HC = Density of glutamatergic synapses in SCZ vs HC ↓ Density of GABAergic synapses in SCZ vs HC

Table 1. *(continued)*

Source	Method(s): constituent(s)	ROI	Sample size, No. (F:M)	Age, mean (SD), y	Antipsychotic mediation status, No.	Illness duration, mean (SD), y	Main result(s)
Mueller et al. (2004)	In situ hybridization: TH, NR1, NR2A-D, NR3A, GluR1-7, and KA1-2 mRNA, and PSD-93, PSD-95, NF-L, SAP102, and Yotiao protein expression	SNc	17 (9:8) SCZ 7 (5:2) HC	SCZ: 73.88 (NR) HC: 76.00 (NR)	AP free[11] (5 SCZ) On AP (12 SCZ)	NR	Mueller et al. (2004)
Owen et al. (1984)	[^{3}H]-spiperone PET: $D_{2/3}$ receptor availability	SN	10 (5:5) SCZ AP free 9 (5:4) SCZ On AP 9 (4:5) HC	SCZ AP free: 71.20 (11.90) SCZ On AP: 63.70 (16.80) HC: 73.40 (12.70)	AP free[12] (10 SCZ) On AP (9 SCZ)	NR	Owen et al. (1984)
Perez-Costas et al. (2012)	In situ hybridization: TH mRNA; Western blot: TH protein expression	SN/VTA	6 (2:4) SCZ 5 (2:3) HC	SCZ: 54.33 (14.73) HC: 54.80 (9.28)	On AP (6 SCZ)	NR	Perez-Costas et al. (2012)
Purves-Tyson et al. (2017)	Western blot: TH and DAT protein levels; RT-PCR: TH, DAT, AADC, VMAT-2, and D_2/D_3 receptor (i.e. DRD2S, DRD2L, DRD2Longer, DRD3 full-length, and DRD3 non-functional) mRNA	SN	mRNA cohort 28 (9:19) SCZ 29 (9:20) HC Protein cohort 26 (10:16) SCZ 27 (8:19) HC	mRNA cohort SCZ: 51.40 (26-67)[13] HC: 51.20 (22-69)[13] Protein cohort SCZ: 52.29 (26-67)[13] HC: 52.21 (22-69)[13]	mRNA cohort On AP (28 SCZ) Protein cohort On AP (26 SCZ)	mRNA cohort SCZ: 28.31 (12.72) Protein cohort SCZ: 29.12 (13.02)	Purves-Tyson et al. (2017)

Table 1. *(continued)*

Source	Method(s): constituent(s)	ROI	Sample size, No. (F:M)	Age, mean (SD), y	Antipsychotic mediation status, No.	Illness duration, mean (SD), y	Main result(s)
Purves-Tyson et al. (2020)	RT-PCR: ICAM1, CD163, FN1, C1qA, C3, and C4 mRNA; Western blotting: CD163, C3, and C4 protein expression; DAB immunohisto-chemistry: CD163+ denisty	SN	mRNA cohort 15 (4:11) SCZ LIS 13 (5:8) SCZ HIS 28 (8:20) HC Protein cohort 13 (4:9) SCZ LIS 12 (5:7) SCZ HIS 26 (7:19) HC	mRNA cohort SCZ LIS: 48.27 (30-64)[13] SCZ HIS: 54.92 (26-67)[13] HC: 50.54 (22-67)[13] Protein cohort SCZ LIS: 49.31 (30-64)[13] SCZ HIS: 56.17 (26-67)[13] HC: 51.19 (22-67)[13]	mRNA cohort On AP (15 SCZ LIS and 13 SCZ HIS) Protein cohort On AP (13 SCZ LIS and 12 SCZ HIS)	mRNA cohort SCZ LIS: 26.43 (11.65) SCZ HIS: 31.62 (13.93) Protein cohort SCZ LIS: 25.92 (11.30) SCZ HIS: 32.33 (14.29)	↑↑ ICAM1, CD163, C1qA, C3, and C4 mRNA in SCZ HIS vs SCZ LIS/HC ↑↑ CD163 protein expression in SCZ HIS vs HC ↑ CD163 protein expression in SCZ HIS vs SCZ LIS ↑↑ FN1 mRNA in SCZ HIS vs HC ↑ CD163+ denisty in SCZ HIS vs HC = C3 protein expression in SCZ HIS vs SCZ LIS/HC ↑↑ C4 protein expression in SCZ LIS vs SCZ HIS ↑ C4 protein expression in SCZ LIS vs HC
Purves-Tyson et al. (2021a)	Fluidigm qPCR: TH, GAD1, VGAT, GABRA1-3, GABRA-5, and DAT mRNA; Western blotting: GAD65/67 and GABRA3 protein levels	SN	mRNA cohort 28 (9:19) SCZ 28 (8:20) SCZ Protein cohort 26 (10:16) SCZ 28 (9:19) HC	mRNA cohort SCZ: 51.36 (26-67)[13] HC: 50.54 (22-67)[13] Protein cohort SCZ: 52.29 (26-67)[13] HC: 52.21 (22-69)[13]	mRNA cohort On AP (28 SCZ) Protein cohort On AP (26 SCZ)	mRNA cohort SCZ: 28.31 (12.72) Protein cohort SCZ: 29.12 (13.02)	↓ TH mRNA in SCZ vs HC ↓↓ GAD1 and VGAT mRNA in SCZ vs HC ↓↓ DAT mRNA in SCZ vs HC ↓↓ GABRA1-3 mRNA in SCZ vs HC ↓ GABRA5 mRNA in SCZ vs HC ↓ GAD65/67 protein levels in SCZ vs HC = GABRA3 protein levels in SCZ vs HC

Table 1. *(continued)*

Source	Method(s): constituent(s)	ROI	Sample size, No. (F:M)	Age, mean (SD), y	Antipsychotic mediation status, No.	Illness duration, mean (SD), y	Main result(s)
Purves-Tyson et al. (2021b)	qPCR: IL1β, IL6, IL8, IL18, TNF-α, IL6ST, IL1A, IL17RA, and SERPINA3 mRNA; Immunohisto-chemistry: AIF1, CD68, GFAP, HLA, and TPSO	SN	28 (9:19) SCZ 29 (9:20) HC	SCZ: 51.40 (26-67)[13] HC: 51.20 (22-69)[13]	On AP (28 SCZ)	SCZ: 28.31 (12.72)	↑↑ IL1β, IL6, IL17RA, and SERPINA3 mRNA in SCZ vs HC ↑ TNF-α and IL6ST mRNA in SCZ vs HC = IL8, IL18, and IL1A mRNA in SCZ vs HC = AIF1, CD68, HLA, TSPO mRNA in SCZ vs HC ↑↑ GFAP mRNA in SCZ vs HC
Reid et al. (2013)	1H-MRS: Glx/Cr, Glx/NAA	SN	35 (9:26) SCZ[14] 22 (9:13) HC	SCZ: 37.90 (12.00) HC: 37.90 (12.4)	On AP (35 SCZ)	SCZ: 17.20 (11.20)	= Glx/Cr in SCZ vs HC ↑ Glx/NAA in SCZ vs HC
Rice et al. (2016)	Immunohisto-chemistry: number of dopaminergic neurons, total neurons, and their ratio	SN/VTA	6 (2:4) SCZ 7 (1:6) HC	SCZ: 53.80 (15.04) HC: 53.43 (10.92)	On AP (6 SCZ)	NR	= Number of dopaminergic neurons, total neurons, and their ratio in SCZ vs HC
Sasaki et al. (2010)	NM-MRI: NM	SNc	23 (8:15) SCZ 23 (13:10) HC	SCZ: 44.90 (13.60) HC: 47.00 (16.90)	On AP (23 SCZ)	SCZ: 19.40 (10.90)	= NM in SCZ vs HC
Schoonover et al. (2017)	Western blotting: TH, VGLUT1, VGLUT2, and GAD67 protein levels	Caudal SN	13 (3:10) SCZ 12 (3:9) HC	SCZ: 42.20 (13.10) HC: 50.40 (15.70)	AP free[1] (4 SCZ) On AP (9 SCZ)	SCZ: 18.60 (9.80)	↑↑ TH and GAD67 protein levels in SCZ vs HC = VGLUT1 and VGLUT2 levels in SCZ vs HC

Table 1. *(continued)*

Source	Method(s): constituent(s)	ROI	Sample size, No. (F:M)	Age, mean (SD), y	Antipsychotic mediation status, No.	Illness duration, mean (SD), y	Main result(s)
Schoonover et al. (2020)	Western blotting: ATP7A N and C terminus, ATP7B, extracellular and transmembrane CTR1, and dysbindin 1A and 1B/C protein levels; ICP-MS: copper content	SN	Western blot cohort 15 (4:11) SCZ 11 (2:9) HC Tissue copper content cohort 14 (3:11) SCZ 14 (3:10) HC	Western blot cohort SCZ: 42.10 (12.20) HC: 50.90 (16.30) Tissue copper content cohort SCZ: 41.20 (13.00) HC: 39.40 (10.80)	Western blot cohort AP free[1] (4 SCZ) On AP (11 SCZ) Tissue copper content cohort AP free (4 SCZ) On AP (10 SCZ)	Western blot cohort SCZ: 18.60 (9.30) Tissue copper content cohort SCZ: 19.10 (9.30)	↑ ATP7A C terminus protein levels in SCZ vs HC. ↓↓ Transmembrane CTR1 protein levels in SCZ vs HC ↓ Dysbindin 1B/C protein levels in SCZ vs HC = ATP7A N terminus, ATP7B, extracellular CTR1, and dysbindin 1A protein levels in SCZ vs HC ↓↓ Copper content in SCZ vs HC
Shibata et al. (2008)	NM-MRI: NM	SNc	20 (7:13) SCZ 34 (17:17) HC	SCZ: 44.60 (12.40) HC: 43.80 (11.20)	On AP (20 SCZ)	SCZ: 18.30 (11.70)	↑ NM in SCZ vs HC
Slifstein et al. (2015)	[^{11}C]-FLB457 PET + amphetamine challenge: dopamine release	SN/VTA	20 (10:10) SCZ[14] 21 (11:10) HC	SCZ: 33.10 (10.20) HC: 32.60 (8.10)	AP naïve (6 SCZ) AP free[7] (14 SCZ)	SCZ: 13.20 (11.30)	= Dopamine release in SCZ vs HC
Spokes et al. (1980a)	Radiochemical method: GAD activity	SN	42 (20:22) SCZ 52 (22:30) HC	SCZ: 59.80 (18.10) HC: 64.40 (21.60)	On AP (42 SCZ)	NR	= GAD activity in SCZ vs HC
Suridjan et al. (2013)	[^{11}C]-(+)-PHNO PET: $D_{2/3}$ receptor availability	SN	13 (3:10) SCZ 12 (5:7) HC	SCZ: 23.38 (4.60) HC: 26.10 (3.80)	AP naïve (13 SCZ)	NR	= $D_{2/3}$ receptor availability in SCZ vs HC

Table 1. *(continued)*

Source	Method(s): constituent(s)	ROI	Sample size, No. (F:M)	Age, mean (SD), y	Antipsychotic mediation status, No.	Illness duration, mean (SD), y	Main result(s)
Toru et al. (1988)	$^{14}CO_2$-trapping method: TH protein levels; Spectroflurometry: Glutamate and GABA protein levels	SN	14 (5:9) SCZ 10 (3:7) HC	SCZ: 57.90 (3.50)[5] HC: 66.70 (2.70)	AP naïve (1 SCZ) AP free (6 SCZ) On AP (7 SCZ)	NR	↑↑ TH protein levels in SCZ vs HC = Glutamate and GABA protein levels in SCZ vs HC
Tuppurainen et al. (2006)	[^{123}I]-epidepride SPECT	Midbrain	6 (4:2) SCZ 7 (3:4) HC	SCZ: 33.00 (14.00) HC: 31.00 (9.00)	AP naïve (6 SCZ)	SCZ: 11.00[2] (1.00 -36.00)[13]	↓ $D_{2/3}$ receptor availability in SCZ vs HC
Tseng et al. (2018)	[^{11}C]-(+)-PHNO PET + psychosocial stress challenge: dopamine release	SN	9 (3:6) SCZ[15] 25 (12:13) HC	SCZ: 24.11 (5.33) HC: 25.12 (4.45)	AP naïve (9 SCZ)	NR	↑↑ Dopamine release in SCZ vs HC
Watanabe et al. (2014)	NM-MRI: NM	SNc	52 (25:27) SCZ 52 (25:27) HC	SCZ: 35.10 (13.30) HC: 34.60 (13.70)	NR	SCZ: 10.40 (10.90)	↑↑ NM in SCZ vs HC
Williams et al. (2014)	Histochemistry: nuclear length, nucleolar volume, nuclear area, and somal cross-sectional area of dopaminergic neurons and oligodendrocyte density; Immunohisto-chemistry: astrocyte denisty	SN	12 (5:7) SCZ 13 (4:9) HC	SCZ: 60.10 (2.30) HC: 51.90 (2.80)	NR	NR	↑ Nuclear length, nucleolar volume, and nuclear area of dopaminergic neurons in SCZ vs HC = Somal cross-sectional area of dopaminergic neurons in SCZ vs HC ↓ Astrocyte denisty in SCZ vs HC

Table 1. *(continued)*

Source	Method(s): constituent(s)	ROI	Sample size, No. (F:M)	Age, mean (SD), y	Antipsychotic mediation status, No.	Illness duration, mean (SD), y	Main result(s)
Yamashita et al. (2016)	NM-MRI: NM	SNc	14 (3:11) SCZ 22 (8:14) HC	SCZ: 37.00 (27-63)[13] HC: 40.00 (25-59)[13]	On AP (14 SCZ)	SCZ: 9.50 (3.00 -32.00)[13]	= NM in SCZ vs HC
Zubieta et al. (2001)	(+)-α-[^{11}C]DTBZ PET: VMAT-2 binding	Ventral brainstem	12 (4:8) SCZ 15 (6:9) HC	SCZ: 36.00 (11.00) HC: 38.00 (11.00)	On AP (12 SCZ)	NR	↑ VMAT-2 binding in SCZ vs HC

Abbreviations: AADC, Aromatic L-amino acid decarboxylase; AIF1, allograft inflammatory factor 1; AP, antipsychotic medication; CD68, cluster of differentiation 68; Cr, creatine; CT1, copper transporter-1; DAB, 3,3 diaminobenzidine; DAT, dopamine transporter; DRD2, dopamine receptor D2; DRD3, dopamine receptor D3; FN1, fibronectin 1; GABA, γ-aminobutyric acid; GAD, glutamate decarboylase; GABRA, GABAA receptor alpha subunit; GFAP, glial fibrillary acidic protein; Glx, glutamate and glutamine; HC, (healthy) controls; HIS, high inflammatory status; HLA, human leukocyte antigen; ICAM1, intracellular adhesion molecule 1; ICP-MS, inductively-coupled plasma mass spectrometry; IL6ST, IL6 signal transducer; LIS, low inflammatory status; mRNA, messenger ribonucleic acid; NA, not applicable; NAA, N-acetyl-aspartate; NM, neuromelanin; NM-MRI, neuromelanin-sensitive magnetic resonance imaging; NR, not reported; PET, positron emission tomography; qPCR, quantitative polymerase chain reaction; ROI, region of interest; RT-PCR, reverse transcription polymerase chain reaction; SCZ, patient with schizophrenia; SERPINA3, serpin family A member 3; SN, substantia nigra; SNc, substantia nigra pars compacta; SN/VTA, a midbrain region including the SN and ventral tegmental area; SPECT, single-photon emission computerized tomography; TH, tyrosine hydroxylase; TNF-α, tumor necrosis factor α; TSPO, translocator protein; UHR-nt, ultra-high-risk individuals who did not develop a psychotic disorder; UHR-t, ultra-high-risk individuals who developed a psychotic disorder; VGAT, vesicular GABA transporter; VGLUT, vesicular glutamate transporter; VMAT-2, a. vesicular monoamine transporter 2; 1H-MRS, proton magnetic resonance spectroscopy; ↑↑, significantly increased with $p<0.01$; ↑, significantly increased with $p\leq0.05$; ↓↓, significantly decreased with $p<0.01$; ↓, significantly decreased with $p\leq0.05$; =, no significant difference.

1 For at least six months. 2 Illness duration is expressed in months instead of years. 3 The median is reported instead of the mean. 4 Interquartile range is reported instead of the standard deviation. 5 Standard error is reported instead of the standard deviation. 6 Lifetime exposure was less than six weeks and patients did not use antipsychotic medication in the past three weeks. 7 For at least three weeks. 8 For at least thirty-three days. 9 For at least three months. 10 For at least six weeks in case of oral medication and for at least six months in case of depot medication. 11 For at least six weeks. 12 For at least one year. 13 The range is reported instead of the standard deviation. 14 The patient sample also consisted of patients diagnosed with schizoaffective disorder. 15 The patient sample also consisted of patients diagnosed with schizophreniform disorder. 16 For at least two weeks.

After the conversion of tyrosine to L-DOPA, L-DOPA is subsequently converted into dopamine by aromatic L-amino acid decarboxylase (AADC). *Ex vivo* post-mortem studies have found unaltered AADC mRNA levels in the SN of patients with schizophrenia (22,23), although there was a trend for lower AADC mRNA levels in patients in one of the studies (22). Aditionally, two *in vivo* [^{18}F]-FDOPA PET imaging studies reported no significant differences in [^{18}F]-FDOPA uptake in the SN (27) or SN/VTA (28) between patients with schizophrenia and healthy controls (HC). The study of Elkashef et al may have been less sensitive to detect group differences due to the lower scanner resolution of earlier generation PET scanners (28). In contrast, two other studies showed elevated [^{18}F]-FDOPA uptake in the SN (18) and midbrain of patients with schizophrenia (29). These inconsistencies might be explained by differences in antipsychotic medication usage. Although five weeks of antipsychotic treatment did not alter nigral [^{18}F]-FDOPA uptake in the study of Jauhar et al (30), a decrease of [^{18}F]-FDOPA uptake in the caudate nucleus, putamen, thalamus, and cortex following at least twenty days of treatment with haloperidol has been reported (31). Furthermore, Howes et al performed a post-hoc analysis and found an increase in nigral [^{18}F]-FDOPA uptake in antipsychotic-free patients compared to HC (18). No differences were found for antipsychotic-treated patients, suggesting a medication effect that downregulates AADC levels, and consequently [^{18}F]-FDOPA uptake. Additionally, Allen et al found a significant increase of [^{18}F]-FDOPA uptake in the SN/VTA of antipsychotic-naïve or -free people at ultra-high risk (UHR) for psychosis who subsequently made the transition to psychosis relative to UHR individuals who did not (32). Furthermore, a trend was found for an elevation in the SN/VTA [^{18}F]-FDOPA uptake in antipsychotic-naïve transitioned UHR subjects compared to HC. Taking the *ex vivo* and *in vivo* data together, there seems to be increased AADC activity in the SN in schizophrenia, but only in antipsychotic-free or -naïve patients, whereas antipsychotics seem to reduce AADC activity.

After dopamine synthesis, the vesicular monoamine transporter 2 (VMAT-2) is responsible for transporting and storing dopamine (and other monoamines) from the cytoplasm into secretory vesicles (as reviewed in (33)). One post-mortem study found a significant decrease in VMAT-2 mRNA levels in the SN of patients with schizophrenia compared to controls (22). This might suggest the presence of a compensatory mechanism to reduce dopaminergic signal transduction (i.e. less dopamine is stored and subsequently released). However, VMAT-2 binding, as assessed by (+)-α-[^{11}C]DTBZ PET, was elevated in the ventral brainstem (which includes the SN/VTA and the raphe nuclei) of patients with schizophrenia in comparison with HC (34). Importantly, these findings should be taken with caution due to the relatively poor resolution of the PET camera and the possibility that ventral (+)-α-[^{11}C]DTBZ uptake in the brainstem predominantly reflects serotonergic instead of dopaminergic projections. Despite the observation that nigral VMAT-2 mRNA levels were not correlated with antipsychotic medication usage or illness duration (22), additional studies are required to understand potential changes in VMAT-2 in the SN in schizophrenia.

Excess cytosolic dopamine, which is not accumulated into synaptic vesicles, subsequently gets packaged as neuromelanin complexes inside autophagic organelles after a process of iron-dependent oxidation, protein aggregation, and polymerization (35). Therefore, neuromelanin is thought to be an indirect marker of dopamine synthesis (36). *In vivo* studies reported both significant elevations (37,38) and no alterations in NM-MRI signal in the SNc of patients with schizophrenia relative to age-matched HC (36,39,40). The findings of increased NM-MRI signal in the SN of patients are in line with the finding of reduced nigral VMAT-2 mRNA levels (22). A decrease in nigral VMAT-2 gene expression might contribute to lower levels of VMAT-2 protein and this might result in less efficient vesicular packing of dopamine. This would cause more build-up of dopamine in the cytosol and consequently more formation of neuromelanin complexes. It is noteworthy that Watanabe et al included roughly twenty more patients and controls (N=52 patients, N=52 controls) than the other studies (38) (Table 1). Therefore, limited sample sizes in the other studies might have hampered finding group differences in nigral NM-MRI signal. Furthermore, illness severity might contribute to the findings, as neuromelanin levels in the SN have been found to correlate positively with psychotic symptom severity and are significantly greater in patients with high psychosis severity (positive subscale scores > 19 on the positive and negative syndrome scale [PANSS]) (39). Alternatively, chronic exposure to antipsychotic treatment might decrease dopaminergic signalling, which could correct for differences in neuromelanin. In addition, as neuromelanin in the SN is known to accumulate during ageing (41), differences in NM-MRI signal in the SN between older patients and controls might be masked by the age-related accumulation of neuromelanin. Taken together, preliminary evidence suggests increased neuromelanin accumulation in the SN of patients with schizophrenia, although the effect of age, antipsychotic medication, and illness duration and severity should be re-examined in large longitudinal studies.

Following vesicular packaging, dopamine release can be induced by an action potential that causes exocytosis of synaptic vesicles (42). In the SN, Tseng et al reported a significant increase in psychosocial stress-induced dopamine release in antipsychotic-naïve patients with schizophrenia (N=9) compared to HC and a positive correlation between psychosocial stress-induced [^{11}C]-(+)-PHNO displacement in the SN and whole striatum across all subjects (43). In contrast, Slifstein et al reported a trend towards lower amphetamine-induced dopamine release capacity in the midbrain (SN/VTA) of antipsychotic-naïve (N=6) and antipsychotic-free (N=14) patients with schizophrenia relative to HC using [^{11}C]-FLB457 PET (44). A possible explanation for this inconsistency is the use of different PET tracers. Whereas [^{11}C]-FLB457 is a very high-affinity antagonist tracer for the dopamine D_2 receptor, [^{11}C]-(+)-PHNO is a dopamine D_3 receptor preferring PET agonist tracer. Agonist tracers appear to be more sensitive to detecting dopamine release compared to antagonist tracers (45). Furthermore, psychosocial and psychostimulant challenges are proposed to affect endogenous dopamine release differently due to distinctive activation pathways (43). Stress induces dopamine release

endogenously by upregulating cell firing, whereas amphetamine elicits dopamine release pharmacologically by interfering with dopamine signalling (46). In addition, previous exposure to antipsychotic medication might have downregulated dopamine release capacity in the second study, as antipsychotic medication does not only block postsynaptic striatal dopamine $D_{2/3}$ receptors, but also presynaptic $D_{2/3}$ autoreceptors in the midbrain, which are known to be involved in regulating dopamine release (47). mRNA levels of the dopamine D2 receptor splice variant DRD2S are decreased in the SN of post-mortem schizophrenia compared to controls (22) and the D2S splice variant plays a role in presynaptic autoreceptor functioning. This might suggest that there is reduced local autoinhibition via $D_{2/3}$ autoreceptors, and thus less inhibition of somatodendritic dopamine release (i.e. increased nigral dopamine release). Overall, the small number of studies in combination with small sample sizes limits the interpretation of the data and provides no definitve evidence yet for increased or decreased dopamine release in the SN.

After exocytosis, the presynaptic dopamine transporter (DAT) is responsible for the reuptake of dopamine from the synaptic cleft into the presynaptic terminal (48). Post-mortem studies of patients with chronic schizophrenia reported a significant decrease in DAT mRNA in the SN compared to controls ((25); same cohort as (22)), but no change in DAT protein levels (22). The lack of alteration in DAT protein levels may suggest that alterations in DAT mRNA do not influence protein levels in the midbrain or that protein functioning may be changed causing DAT transcription to be altered via feedback mechanisms. Otherwise, DAT utilisation and breakdown may be decreased or translation of DAT protein may be increased, both resulting in no change in DAT protein levels and a decrease in DAT mRNA (22). Two *in vivo* [^{11}C]PE2I PET studies reported greater DAT binding in the SN/VTA of patients with schizophrenia compared to HC (49), as well as, no significant differences in the SN (50). The aforementioned studies included mostly antipsychotic-treated patients. However, it has been shown that antipsychotic medication does not affect DAT binding (49,51,52). Furthermore, DAT binding seems not to be correlated with the duration of illness or age of onset (49). Taken together, these studies suggest that DAT protein levels in the SN are unaltered or may be increased. Although no alterations in DAT binding have been reported in the striatum of patients with schizophrenia (53), increased DAT functioning in the SN could theoretically serve as a compensatory mechanism to reduce hyperactive functioning of the dopaminergic system in schizophrenia by reducing extracellular dopamine levels. Further studies are required to investigate this hypothesis and understand potential changes in nigral DAT functioning in schizophrenia.

Dopamine that is released into the synaptic cleft can bind to dopamine receptors. In the SN, dopamine receptors primarily belong to the dopamine D_2 and D_3 subtypes (54,55). The nigral D_2 receptors are mainly functioning as inhibitory autoreceptors that regulate the release of dopamine (56,57). Purves-Tyson et al reported significantly lower mRNA levels of one dopamine

D_2 receptor splice variant (i.e. DRD2S) in the SN of post-mortem schizophrenia compared to controls, while other splice variants displayed a trend towards reduced expression (i.e. DRD2L and DRD2Longer) (22). mRNA levels of dopamine D_3 receptor splice variants (i.e. DRD3 full-length and DRD3 non-functional) remained unaltered. Different splice variants have been associated with different functions, with D2S playing a role in presynaptic autoreceptor functioning and D2L mainly acting at postsynaptic sites (58,59). Another post-mortem study showed an increased [^{3}H]spiperone binding, which is a measure of dopamine D_2 receptor availability, in the SN of neuroleptic-free and -treated patients compared to controls (60). *In vivo* [^{11}C]-(+)-PHNO PET, [^{18}F]-fallypride PET, and [^{123}I]-epidepride SPECT studies report increased (61), decreased (62,63), and unaltered (43,64-66) dopamine $D_{2/3}$ receptor availabilities in the SN or midbrain of patients with schizophrenia relative to HC. A meta-analysis that combined most of these studies reported no change in dopamine $D_{2/3}$ receptor availability in the SN of patients with schizophrenia (67). This is in line with the results of a meta-analysis that reported no significant differences in $D_{2/3}$ receptor availability in the striatum between HC and patients with schizophrenia (53). Although the vast majority of studies investigated antipsychotic-naïve and -free patients (43,64-66), some studies did include patients that were treated with antipsychotic medication during the measurements or when passing away (22,60,62). As antipsychotic medication binds to dopamine $D_{2/3}$ receptors, PET and SPECT tracers compete with antipsychotic medication, as well as, endogenous dopamine for binding to the dopamine $D_{2/3}$ receptors and therefore antipsychotic medication potentially affects the results. However, no differences in nigral dopamine $D_{2/3}$ receptor availabilities have been found between antipsychotic-naïve and -free (65), or antipsychotic-free and -treated patients (60). Furthermore, Purves-Tyson et al reported no significant correlations between mRNA levels of different dopamine receptors and antipsychotic use (22). In sum, the results of individual studies do not perfectly align (potentially also due to small sample sizes). Meta-analytic evidence, however, suggests no alterations in the availability of nigral dopamine $D_{2/3}$ receptors. Unfortunately, PET and SPECT imaging cannot distinguish between D_2 and D_3 receptor binding (68) and, therefore, *in vivo* alterations of specific receptor types cannot be excluded. This remains a topic for future research.

Finally, cytoarchitecture describes the density, morphology, and distribution of cells of the central nervous system (69). Changes in cytoarchitecture of dopaminergic cells in the SN could, therefore, theoretically influence the functioning of the nigrostriatal pathway. One post-mortem study reported significant increases in nuclear length, nucleolar volume, and nuclear area of nigral dopaminergic neurons in schizophrenia (70). However, no alterations were found with regard to the somal cross-sectional area. Another study did not find significant alterations in the total number of dopaminergic neurons, total neurons, or their ratio in the SN/VTA of patients with schizophrenia compared to controls (71). Knowledge regarding nigral neuroarchitecture in schizophrenia and how alterations affect pathology is limited and could be of interest to future research.

Glutamatergic alterations in the substantia nigra of patients with schizophrenia

Yamaguchi et al found expression of vesicular glutamate transporter (VGLUT) 2 mRNA in the SNc of rats and therefore suggested that there are neurons within the SNc that can participate in glutamatergic neurotransmission (72). Another animal study showed that there are glutamatergic afferents to neurons in the SNc, which mainly originate in the pedunculopontine and subthalamic nuclei (73). This glutamatergic input may affect the nigrostriatal pathway by excitatory effects on the dopaminergic neurons and thus could potentially play a role in schizophrenia pathology.

A post-mortem study found that the density of glutamatergic synapses in the central area of the SN, i.e. the area with dopaminergic projections to the associative striatum, was not significantly altered in antipsychotic-treated patients with schizophrenia compared to controls (74). Within the glutamatergic synapse, VGLUT1-3 store glutamate from the cytoplasm into synaptic vesicles (75). Two post-mortem studies found no differences in nigral VGLUT1 and VGLUT2 levels between patients with schizophrenia and controls (19,74). Likewise, VGLUT1 and VGLUT2 levels were similar in the medial, central, and lateral parts of the SN in patients with schizophrenia compared to controls (74). Importantly, the sample sizes of both studies were small and most patients were not antipsychotic-naïve. As antipsychotic medication reduces the concentration of striatal glutamate (76), this might have prevented the researchers from finding group differences. In addition, Schoonover et al found higher VGLUT2 levels in the SN of antipsychotic-free patients compared to controls, whereas no significant differences were reported between antipsychotic-treated and -free patients (19). Interestingly, Mabry et al found VGLUT1 levels to be significantly negatively correlated to glutamic acid decarboxylase (GAD) 67 levels in the central area of the SN of controls, whereas this correlation was positive in patients with schizophrenia (74). Similar patterns were found in the medial and lateral regions of the SN. As GAD67 synthesizes GABA from glutamate, this finding suggests a deviation in the modulation of glutamate concentrations by GAD67 in schizophrenia. In sum, VGLUT1 levels seem not to be altered in patients with schizophrenia, although VGLUT2 levels might be increased in antipsychotic-free patients.

After the release of glutamate into the synaptic cleft, glutamate can bind to ionotropic NMDA, kainate, and α-amino-3-hydroxy-5-methyl-4-isoxazolepropionic acid (AMPA) receptors, as well as metabotropic glutamate receptors ($mGlu_{1\text{-}8}$) (77). A post-mortem study investigated the expression of NMDA (i.e. NR1, NR2A-D, and NR3A), AMPA (i.e. GluR1-4), and kainate receptor subunits (i.e. GluR5-7 and KA1-2) in the SNc of patients with schizophrenia and controls (21). Only NR1 and GluR5 mRNA levels were significantly increased in the SN of antipsychotic-treated and -free patients. Furthermore, the expression of several NMDA receptor-associated proteins (i.e. PSD-93, PSD-95, NF-L, SAP102, and Yotiao) in the SNc did

not differ between both groups. Altogether, increased nigral NR1 mRNA levels in patients with schizophrenia might lead to the upregulation of NR1 subunits available for the formation of functional NMDA receptors (21). This could subsequently result in elevated expression of NMDA receptors since NR1 is the obligatory subunit to form NMDA receptors (78). Even though hypofunctioning of NMDA receptors in the cortex is widely implicated in the glutamate hypothesis of schizophrenia (12), future research needs to examine whether elevated nigral NR1 mRNA expression could result in increased expression of the NMDA receptor in the SN. In addition to NR1 abnormalities, Mueller et al reported nigral GluR5 alterations in schizophrenia (21). A modification in GluR5 expression may change kainate receptor functioning, as GluR5 homomers and GluR5/6 containing receptors both desensitize faster and recover slower from desensitization than homomeric GluR6 receptors (79). So far, only one study, with a limited sample size, indicates increased NR1 and GluR5 mRNA levels in the SNc of patients with schizophrenia. No evidence exists for dysregulation of other glutamate receptors in the SN in schizophrenia. To our knowledge, no PET studies on glutamate receptors have been performed although radiotracers for mGluR5 (e.g. [^{18}F]FPEB) and mGluR1 (e.g. [^{18}F]FIMX) have been developed. It would be of interest to confirm the post-mortem findings *in vivo*.

In vivo studies using proton magnetic resonance spectroscopy (^{1}H-MRS) have been conducted to investigate concentrations in the brain of glutamate, glutamine, and their combination Glx (as it is difficult to distinguish the signal of glutamate from glutamine at 3T or lower magnetic field strengths). ^{1}H-MRS is a non-invasive neuroimaging technique that can be used to measure the concentrations of chemical components within tissues. Often the metabolite concentrations are reported as a ratio to creatine (Cr; a marker of energy metabolism) or N-acetyl-aspartate (NAA; a marker of neuronal integrity). Reid et al reported no significant alterations in Glx/Cr levels in the SN of antipsychotic-treated patients with schizophrenia or schizoaffective disorder compared to HC, although they found a trend towards increased Glx/NAA in the SN of patients ($p = .05$). An older post-mortem study by Toru et al reported no significant changes in nigral glutamate levels between patients with schizophrenia and controls (20). Glutamate levels in the SN are therefore most likely unaltered in schizophrenia, or possibly slightly increased. For a more definitive answer, future research should preferably investigate the glutamatergic system with high magnetic field (7T instead of 3T) MRI, use absolute quantification instead of a reference metabolite, and assess the potential effect of antipsychotics on glutamate levels.

Overall, although most aspects of glutamatergic functioning seem unaltered in the SN of patients, other aspects support increased glutamatergic neurotransmission (i.e. increased NR1 and Glur5 mRNA levels, possibly increased VGLUT2 levels in antipsychotic-free patients, and possibly slightly increased Glx levels). Since glutamate is an excitatory neurotransmitter, an increase in glutamatergic transmission on the dopaminergic neurons in the SN may increase the excitation of the nigrostriatal pathway and may contribute to nigrostriatal hyperdopaminergia.

GABAergic alterations in the substantia nigra of patients with schizophrenia

The large majority of inputs to dopaminergic neurons in the SNc are inhibitory GABAergic afferents, which project from the globus pallidus, neostriatum, and SNr (80). The inhibitory neurotransmitter GABA is therefore an important regulator of the nigrostriatal dopaminergic pathway.

One study investigated synaptic density and reported a significant decrease in the density of GABAergic synapses in the central area of the SN (projecting to the associative striatum) in antipsychotic-treated patients with schizophrenia compared to controls (74). This may be in line with Feinberg's excessive synaptic pruning hypothesis, which postulates that a critical step in the development of schizophrenia is an incorrectly programmed synaptic pruning process (81).

Most studies that investigated nigral GABAergic functioning have focused on measuring GAD, which synthesizes GABA from glutamate (82). The first post-mortem study in antipsychotic-treated patients with schizophrenia found no alterations in nigral GAD levels compared to controls (83). Another post-mortem study reported a moderate, albeit not significant increase in GAD67 levels, an isoform of GAD, in the SN of antipsychotic-treated patients with schizophrenia compared to controls (74). In addition, a sub-analysis in which the SN was subdivided into medial, central, and lateral sections also revealed no significant group differences (74). These findings are in concordance with the study by Toru et al, which reported no changes in nigral GABA protein levels between patients with schizophrenia and controls (20). In contrast, Schoonover et al did report a significant increase in GAD67 protein levels in the caudal SN of antipsychotic-treated patients with schizophrenia compared to controls (19). This was not demonstrated for antipsychotic-free patients. Subsequently, it was proposed that GAD67 levels of antipsychotic-treated patients may be increased due to medication usage, potentially as a compensatory response to inhibit dopaminergic functioning (74). This is in line with an animal study that showed that the antipsychotic drug olanzapine, but not haloperidol or sertindole, increased GAD67 mRNA in the SNr of rats (84). Furthermore, chronic treatment with haloperidol, but not olanzapine or sertindole, resulted in increased $GABA_A$ receptor binding in the SNr of rats (84). A more recently published study, however, reported reduced GAD mRNA and protein levels in the SN of antipsychotic-treated patients with schizophrenia compared to controls (25). These findings suggests that although antipsychotic treatment might increase GAD levels, this may not be the case for all antipsychotics. As GAD protein levels were found to positively correlate with illness duration in patients with schizophrenia (25), longer illness durations may further increase GAD67 levels in patients, although this might also be related to longer antipsychotic exposure.

Within the GABAergic neurons, the vesicular GABA transporter (VGAT) is responsible for the vesicular storage and exocytosis of GABA (85). Purves-Tyson et al reported significantly decreased VGAT mRNA in the SN of patients with schizophrenia compared to controls (25). This finding may indicate less storage capacity for GABA and, therefore, possibly less GABA release and GABAergic inhibition in the midbrain of patients. After exocytosis, GABA can bind to the ionotropic receptor ($GABA_A$) and metabotropic receptor ($GABA_B$). One post-mortem study found significantly decreased mRNA levels of $GABA_A$ receptor alpha subunits 1-3 (GABRA1-3) and 5 (GABRA5) in the SN of patients with schizophrenia compared to controls (25). In contrast, no significant group differences were observed with regard to GABRA3 protein levels.

Taken together, these findings suggest reduced GABAergic neurotransmission in the SN in schizophrenia, with lower density of GABAergic synapses and lower VGAT mRNA levels. Also mRNA levels for $GABA_A$ receptor subunits are lower although it is not clear yet whether this also leads to reduced receptor expression. Antipsychotic treatment may partly revert the reduced GABAergic neurotransmission by increasing GAD levels, although this may not be the case for all antipsychotics. All these data are based on post-mortem findings and in vivo research of the GABAergic system with PET imaging and MRS may further support these findings and might give more insight in the effect of antipsychotics and illness duration. Reduced cortical GABAergic neurotransmission in schizophrenia patients is indeed found in a study using [^{11}C]flumazenil PET combined with blocking the GABA membrane transporter GAT1, although there was no data reported on the SN (86). This study is in line with the suggestion of reduced GABAergic transmission in the SN, where due to lower density of GABAergic synapses, less storage and subsequent release of GABA, there might be less inhibition of the nigrostriatal dopaminergic pathway contributing to hyperdopaminergia.

Neuroinflammatory processes contribute to abnormalities in nigral functioning

Previous research has reported elevated expression of cytokines and other mediators of inflammation in the periphery and brains of patients with schizophrenia ((87,88); as reviewed in (89)). These findings suggest a role of inflammation in schizophrenia (as reviewed in (90)). As inflammatory mediators, such as chemokines and cytokines, influence the maintenance, development, and functional properties of dopaminergic neurons in the midbrain (91,92), inflammatory processes in the SN might affect the nigral dopaminergic and other signalling pathways. One post-mortem study found increased mRNA levels of pro-inflammatory cytokines (i.e. IL1β, IL6, TNF-α, IL6ST, and IL17RA) and an acute-phase protein (i.e. serpin family A member 3 [SERPINA3]) in the SN of patients with schizophrenia (93). In a subsequent analysis, mRNA levels of the pro-inflammatory cytokines (expect IL1A) and SERPINA3 were found to be elevated in patients with a high inflammatory biotype (i.e. high expression of inflammatory transcripts in the midbrain) compared to patients with a low inflammatory biotype (i.e. low expression of inflammatory transcripts in the midbrain) and controls.

Multiple cells within the brain can produce cytokines, such as microglia, astrocytes, and other glial cells. The glial hypothesis of schizophrenia has become a prominent theory of cognitive impairment and proposes that initial perturbations in glial cells (particularly astrocytes) can result in anomalies in neurotransmitters and neurons, which are involved in the pathogenesis of schizophrenia (94). Purves-Tyson et al reported no alterations in mRNA levels of multiple microglial markers in the SN (93) (i.e. allograft inflammatory factor 1 [AIF1], cluster of differentiation 68 [CD68], human leukocyte antigen [HLA], and translocator protein [TSPO]). However, CD68 and TSPO mRNA were elevated in patients with a high compared to a low inflammatory biotype and compared to controls. Another post-mortem study found that the density of astrocytes was significantly decreased in the SN of antipsychotic-treated patients with schizophrenia compared to both patients with major depressive disorder and controls (70). Since astrocytes eliminate excessive extracellular glutamate from the synaptic cleft, decreased astrocyte density is suggested to result in relatively higher synaptic levels of glutamate, which may contribute to the hyperexcitability of dopaminergic synapses. In contrast, Purves-Tyson et al found higher glial fibrillary acidic protein (GFAP) mRNA levels, which is used to index astrocyte activity, in the SN of patients with schizophrenia compared to controls (93). Patients with a high inflammatory biotype had significantly higher GFAP mRNA levels compared to patients with a low inflammatory biotype and controls. These results may indicate a compensatory mechanism to counteract the decreased astrocyte density in a subgroup of patients.

During neuroinflammatory conditions, CD163+ macrophages enter the brain tissue. Multiple lines of research suggest that macrophages also infiltrate the brain in schizophrenia (95,96). Specifically, Purves-Tyson et al found increased macrophage density (i.e. CD163+ cell density), as well as, higher levels of macrophage markers (i.e. intracellular adhesion molecule 1 [ICAM1] mRNA, CD163 mRNA and protein expression, and fibronectin 1 mRNA) in the SN of patients with schizophrenia and a high inflammatory biotype compared to controls (97). This increase in macrophage markers appears to be related to an increase in complement synthesis, as elevated nigral C1qA, C3, and C4 complement mRNA levels were also found in patients with a high inflammatory status compared to controls (97). This is of relevance since microglia regulate synaptic pruning via the complement pathway and as previously described in the section on GABAergic alterations, there is reduced GABAergic synaptic density which may be a result of aberrant synaptic pruning (81). However, no corresponding increases in C3 and C4 complement protein levels were found (97). In conclusion, as schizophrenia is a heterogeneous disease, alterations in nigral immune-related transcripts, complement synthesis, and markers of microglia and macrophages might be present in subgroups of patients and tend to be elevated particularly in patients with a high inflammatory biotype. Future research is needed to unravel the link between these alterations and the well-known dysregulation of dopaminergic neurotransmission in schizophrenia. The finding that astrocyte density is decreased in the SN in schizophrenia may result in higher synaptic levels of glutamate, and might thereby directly affect the nigrostriatal pathway through increased excitation.

Disrupted copper homeostasis in the substantia nigra

The copper hypothesis of schizophrenia is a relatively old theory that proposes that excess tissue copper can cause schizophrenia. Although elevated copper in the blood of patients has been reported in many studies (as reviewed in (98)), the hypothesis has never been convincingly refuted nor demonstrated. As copper can affect the production, as well as, the breakdown of dopamine, copper might also be relevant for the signalling pathways within the SN. Endothelial cells at the blood-brain barrier take up copper from the bloodstream via the copper transporter-1 (CTR1) (99). Subsequently, copper is released into the brain parenchyma via the copper transporter ATP7A (99). One post-mortem study compared dysbindin (i.e. dysbindin isoforms 1A and 1B/C), a protein which controls copper transport, and copper transport protein (i.e. ATP7A, ATP7B, and CTR1) expression and copper content in the copper-rich SN between patients with schizophrenia and controls (100). ATP7A C terminus protein levels were increased, transmembrane CTR1 and dysbindin 1B/C protein levels were decreased, and ATP7A N terminus and extracellular CTR1, dysbindin 1A and ATP7B protein levels were unaltered in the SN of patients with schizophrenia compared to controls. Additional post-hoc analyses revealed significantly lower N terminus ATP7A protein levels in unmedicated patients compared to controls and medicated patients, whereas C terminus ATP7A protein levels were increased in medicated patients compared to controls. Finally, a reduced amount of nigral copper was observed in patients with schizophrenia compared to controls. Medicated patients demonstrated significantly lower levels of copper than controls. This was not the case for unmedicated patients. Although we cannot rule out the possibility that antipsychotic medication modulates copper homeostasis, there may be a copper-deficient state within the SN of patients. So far, it remains poorly understood how disrupted copper homeostasis might be related to the pathology of schizophrenia. Some researchers have hypothesized that the blood-brain barrier is leaky in schizophrenia (101). This potentially results in the uncontrolled leaking of copper into the brain, which incorrectly triggers a signal of excess copper. Subsequently, CTR1 prevents additional copper transport (100). Copper-decreasing experimental manipulation, through for example administering the copper chelator cuprizone, has been shown to result in increased dopamine levels (via inhibition of dopamine-β-hydroxylase [DBH]), decreased oligodendrocytic protein expression, and demyelination in animals (102,103). Further research is needed to validate these findings in humans and to clarify the association between a copper-deficient state and schizophrenia.

Summary of molecular alterations in the substantia nigra

The available literature suggests that molecular alterations occur in the SN of patients with schizophrenia. These changes entail alterations in dopaminergic, glutamatergic, and GABAergic functioning, as well as, the functioning of the immune system and copper homeostasis (Fig. 2). Overall, there is some evidence for hyperdopaminergia in the SN of patients (i.e. increased

AADC activity in antipsychotic-free/-naïve patients and elevated neuromelanin accumulation). These findings are in line with the well-established finding of striatal hyperdopaminergia in schizophrenia (i.e. increased dopamine synthesis capacity and dopamine release in the striatum) and show that the hyperdopaminergia is not only present in the striatum. Within the SN, the hyperdopaminergia might be compensated by reduced functioning of VMAT-2, which subsequently could limit the release of dopamine. In addition, the hyperdopaminergia could theoretically be compensated by increased functioning of DAT. However, the current literature does not support such a compensatory mechanism. Hyperdopaminergia in the SN of patients with schizophrenia might be secondary to alterations in other molecular aspects of the SN. Reduced GABAergic function in the SN (i.e. lower density of GABAergic synapses, lower VGAT mRNA levels and lower mRNA levels for $GABA_A$ receptor subunits) may contribute to the nigrostriatal hyperdopaminergia by providing reduced inhibition. Due to antipsychotic use, nigral GAD levels, and potentially other aspects of GABAergic functioning in the SN, might change to increase the inhibition of dopaminergic neurons and thereby compensate for the hyperdopaminergic state. Accordingly, evidence has emerged that the tail of the VTA may act as a GABAergic brake to inhibit dopaminergic neurons of the SNc (104). Therefore, GABAergic dysregulation in the VTA might also contribute to the presynaptic hyperdopaminergia in the SN. Increased glutamatergic excitation of the SN may also contribute to nigrostriatal hyperdopaminergia. The increased glutamatergic neurotransmission may be due to increased NR1 and Glur5 mRNA levels, increased VGLUT2 levels in antipsychotic-free patients (which might be indicative of elevated glutamate release), and reduced density of astrocytes (since astrocytes remove extracellular glutamate this might result in prolonged neurotransmission). As increased GFAP mRNA levels have also been reported in schizophrenia, this might be a compensatory mechanism to counteract the decreased astrocyte density. Finally, nigrostriatal hyperdopaminergia could also be related to alterations in the immune system and copper functioning, through the influence of inflammatory mediators on the functioning of dopaminergic neurons in the midbrain (91,92) or due to a possible inability to break down monoamines in a copper-dependent way, respectively.

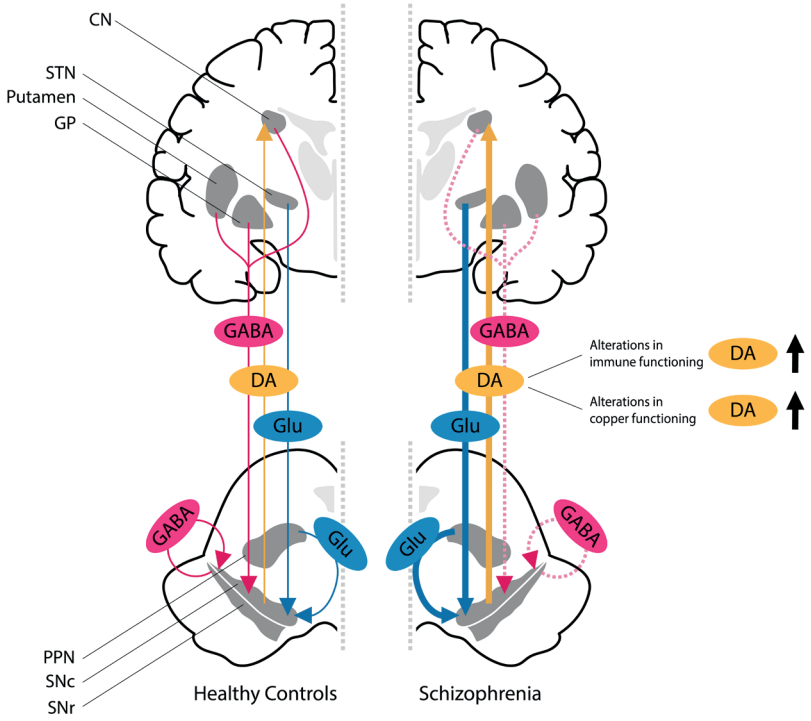

Figure. 2 Substantia nigra pathology in schizophrenia. Hyperdopaminergia in the SN of patients with schizophrenia is most likely a manifestation of a hyperactive dopaminergic nigrostriatal pathway compared to HC. The nigrostriatal pathway projects from the SNc to the associative striatum. GABAergic projections from the neostriatum, GP, and SNr to the SNc might provide reduced inhibition in patients with schizophrenia compared to HC and thereby contribute to the nigrostriatal hyperdopaminergia. In addition, the nigrostriatal hyperdopaminergia could also be a result of increased glutamatergic excitation of the SNc compared to HC via glutamatergic projections that originate in the PPN and STN. Finally, molecular changes with regard to immune and copper functioning within the SN could also contribute to the nigrostriatal hyperdopaminergia.
Abbreviations: DA, dopamine; CN, caudate nucleus; GABA, γ-aminobutyric acid; Glu, glutamate; GP, globus pallidus; PPN, pedunculopontine nucleus; SNc, substantia nigra pars compacta; SNr, substantia nigra pars reticulata; STN, subthalamic nucleus

Additional insights into the striatonigrostriatal circuit in schizophrenia

This review focused on human studies. Due to practical reasons, it is challenging and often impossible to study the interactions between the different regions of the striatonigrostriatal (SNS) circuit in the living brain of humans. Animal circuit studies, however, can provide additional insight into the functions of the SNS circuit. Haber et al showed in primates that the SNS projection from the ventromedial, central, and dorsolateral striatal subregions contain three SN components: 1) a dorsal region of nigrostriatal projecting cells, 2) a central group of both nigrostriatal projecting cells and their reciprocal striatonigral terminal fields, and 3) a ventral region that contains a striatonigral projection but not its reciprocal nigrostriatal

projection (9). Information can travel through the SNS circuit in multiple ways: 1) via direct/reciprocal connections and 2) via indirect/nonreciprocal connections. Midbrain projections from the shell of the striatum target both the ventromedial SNc and the VTA. Projections from the VTA back to the shell of the striatum form the reciprocal SNS loop. Midbrain projections from the medial SN feedforward to the core of the striatum and form the first part of the nonreciprocal connections (also referred to as spiral). Subsequently, the spiral continues through the SNS circuit with pathways originating in the core of the striatum and projecting more dorsally. In this way, ventral striatal regions affect dorsal striatal regions via these spiralling SNS projections (9). In addition, Lerner et al implied that, besides a ventral-to-dorsal route, there might also be a lateral-to-medial information flow through the circuit (105). Haber et al proposed the following model of the synaptic interactions of the SNS projections in the reciprocal and non-reciprocal loops (9). The reciprocal component of the SNS circuit terminates directly on an SNc dopaminergic cell. Activation of this component results in inhibition. The nonreciprocal component, in contrast, terminates indirectly on an SNc dopaminergic cell, i.e. via a GABAergic interneuron, and activation of this component results in disinhibition and facilitation of the dopaminergic cell burst firing. Consequently, each part of the spiral sends an inhibitory feedback response, but also facilitates the transfer of information to the next step of the spiral via disinhibition. The model of Haber et al is supported by rodent studies which demonstrate that stimulation of the striatum can result in an elevation of dopamine firing via inhibition of GABAergic interneurons (106-109). This is in line with the human data summarized in this review and stresses that an imbalance between inhibition and disinhibition of the SNS circuit might be important in the pathology of schizophrenia. Indeed, the GABAergic projections from the striatum to SNc as depicted in Fig. 2 might reflect the reciprocal component of the SNS circuit (9,105), which seems to be downregulated in patients with schizophrenia. The GABAergic interneuron of the nonreciprocal component might correspond to the GABAergic connection between the SNr and SNc as depicted in Fig. 2. These interneurons are innervated by GABAergic projections from the striatum (perhaps as part of the nonreciprocal component) and the globus pallidus, as well as by glutamatergic projections from the subthalamic nucleus (110). Possibly, the function of these non-reciprocal GABAergic interneurons is also reduced in schizophrenia, due to the reduced density of GABAergic synapses and consequently reduced storage and exocytosis of GABA, as described in the human studies reviewed above. Reduction of the GABAergic inhibition of the dopaminergic neurons in schizophrenia likely results in the disinhibition of dopaminergic striatonigral projections to the striatum. Several animal models have been developed in an attempt to understand the neurobiological basis of schizophrenia, but to our knowledge, the SNS circuit has not yet been examined within this context. Future studies that address animal models for schizophrenia which focus on the SNS circuit would be necessary to translate the findings on reciprocal and nonreciprocal SNS connections and the role of glutamatergic and GABAergic inputs to the SN to patients with schizophrenia.

Limitations and future directions

Importantly, some limitations of the included studies and suggestions for future studies can be delineated. First of all, only a limited number of findings (primarily the dopaminergic findings) have been replicated, whereas the findings on GABAergic, glutamatergic, as well as, other molecular aspects of the SN, are based on a limited number of studies. In addition, some molecular aspects of the SN, such as nigral VGLUT3 levels, have never been investigated in patients with schizophrenia or only in underpowered cohorts. Additional research is therefore urgently needed to validate and expand the previous findings. Secondly, this review has discussed numerous post-mortem studies. The patient samples in these studies have often been treated with antipsychotic medication for extended periods. Therefore, the effect of antipsychotic medication on post-mortem findings can often not be excluded. Although post-mortem studies are essential to guide theories on schizophrenia pathology, support for these findings at an earlier disease stage and without chronic antipsychotic use *in vivo* is crucial. Furthermore, multimodal imaging techniques, such as combined PET and ^{1}H-MRS, or other techniques, such as fMRI and pharmacological MRI, could be used to study how alterations in multiple neurotransmitters systems relate to each other in the same individual, as well as, how changes in neurotransmitter systems are related to functional abnormalities in the prefrontal-striatal-nigro circuit (111,112). Thirdly, although imaging techniques such as PET and SPECT have enabled researchers to study dopaminergic functioning in the SN *in vivo*, the spatial resolution of these techniques is limited, especially for small brain structures such as the SN. Fortunately, new developments in MR imaging, such as NM-MRI and pharmacological MRI, offer new opportunities to indirectly investigate the dopaminergic system, without radiation burden, with fewer costs, and within a shorter time frame. Additionally, since schizophrenia is a heterogeneous disease, it might be possible that the reported abnormalities in the SN are only present in a subgroup of patients. Previous research has suggested neurobiological differences between patients with schizophrenia that respond well (i.e. responders) compared to patients that do not respond adequately to antipsychotic treatment (i.e. non-responders) (113). In line with this hypothesis, two subtypes of schizophrenia have been proposed: a hyperdopaminergic type A and a normodopaminergic type B, which are characterized by elevated striatal dopamine synthesis and normal presynaptic dopaminergic functioning in the striatum, respectively (114). Conflicting findings might therefore be explained by different distributions of schizophrenia subtypes across studies. Neurobiological heterogeneity could also explain why some antipsychotic-naïve patients with schizophrenia have parkinsonism (115,116). Those findings suggest the presence of a third subtype of schizophrenia with a hypoactive dopaminergic nigrostriatal pathway. In addition, as summarized in this review, there might also be schizophrenia subtypes with altered immune and/or copper functioning. Future research is needed to disentangle differences between multiple subgroups of patients. This might eventually contribute to the development of subgroup-specific treatment. Box 1 summarises limitations of current findings and future directions for research identified by this review.

Conclusions

This paper provides a comprehensive overview of molecular abnormalities in the SN of patients with schizophrenia, by addressing post-mortem and molecular imaging studies. Overall, there is some evidence for hyperdopaminergia in the SN of patients with schizophrenia. Reduced GABAergic inhibition, excessive glutamatergic excitation, as well as, alterations in other molecular aspects of the SN, such as immune functioning and copper homeostasis, could potentially underlie this nigrostriatal hyperdopaminergia. Importantly, these findings should be replicated and further investigated, as many studies consisted of small cohorts and may have been influenced by factors such as antipsychotic use and heterogeneity of patient cohorts. If replicated, some aspects of molecular functioning in the SN (e.g. neuromelanin concentrations) might provide important implications for future clinical practice as potential biomarkers or treatment targets.

References

1. McCutcheon RA, Krystal JH, Howes OD. Dopamine and glutamate in schizophrenia: biology, symptoms and treatment. World Psychiatry. 2020;19(1):15-33.
2. Snyder SH. The dopamine hypothesis of schizophrenia: focus on the dopamine receptor. American Journal of Psychiatry. 1976;133(2):197-202.
3. Davis LK, Kahn RS, Ko G, Davidson M. Dopamine in schizophrenia: a review and reconceptualization. The American journal of psychiatry. 1991;148(11):1474-86.
4. Howes OD, Kapur S. The dopamine hypothesis of schizophrenia: Version III - The final common pathway. Schizophrenia Bulletin. 2009;35(3):549-62.
5. McCutcheon RA, Abi-Dargham A, Howes OD. Schizophrenia, Dopamine and the Striatum: From Biology to Symptoms. Trends in Neurosciences. 2019;42(3):205-20.
6. Kegeles LS, Abi-Dargham A, Frankle WG, Gil R, Cooper TB, Slifstein M, et al. Increased synaptic dopamine function in associative regions of the striatum in schizophrenia. Archives of General Psychiatry. 2010;67(3):231-9.
7. Mizrahi R, Addington J, Rusjan PM, Suridjan I, Ng A, Boileau I, et al. Increased stress-induced dopamine release in psychosis. Biological Psychiatry. 2012;71(6):561-7.
8. McCutcheon R, Beck K, Jauhar S, Howes OD. Defining the Locus of Dopaminergic Dysfunction in Schizophrenia: A Meta-analysis and Test of the Mesolimbic Hypothesis. Schizophrenia bulletin. 2018;44(6):1301-11.
9. Haber SN, Fudge JL, McFarland NR. Striatonigrostriatal pathways in primates form an ascending spiral from the shell to the dorsolateral striatum. Journal of Neuroscience. 2000;20(6):2369-82.
10. Krystal JH, D'Souza DC, Mathalon D, Perry E, Belger A, Hoffman R. NMDA receptor antagonist effects, cortical glutamatergic function, and schizophrenia: toward a paradigm shift in medication development. Psychopharmacology (Berl). 2003;169(3-4):215-33.
11. Javitt DC. Glutamate and schizophrenia: phencyclidine, N-methyl-D-aspartate receptors, and dopamine-glutamate interactions. Int Rev Neurobiol. 2007;78:69-108.
12. Egerton A, Grace AA, Stone J, Bossong MG, Sand M, McGuire P. Glutamate in schizophrenia: Neurodevelopmental perspectives and drug development. Schizophrenia research. 2020;223:59-70.
13. Egerton A, Modinos G, Ferrera D, McGuire P. Neuroimaging studies of GABA in schizophrenia: a systematic review with meta-analysis. Transl Psychiatry. 2017;7(6):e1147.
14. Moghaddam B, Javitt D. From revolution to evolution: The glutamate hypothesis of schizophrenia and its implication for treatment. Neuropsychopharmacology. 2012;37(1):4-15.
15. Howes O, McCutcheon R, Stone J. Glutamate and dopamine in schizophrenia: An update for the 21st century. Journal of psychopharmacology. 2015;29(2):97–115.
16. Perez-Costas E, Melendez-Ferro M, Roberts RC. Basal ganglia pathology in schizophrenia: Dopamine connections and anomalies. John Wiley & Sons, Ltd; 2010. p. 287-302.
17. Tekin I, Roskoski R, Carkaci-Salli N, Vrana KE. Complex molecular regulation of tyrosine hydroxylase. Journal of Neural Transmission. 2014;121(12):1451-81.
18. Howes OD, Williams M, Ibrahim K, Leung G, Egerton A, McGuire PK, et al. Midbrain dopamine function in schizophrenia and depression: A post-mortem and positron emission tomographic imaging study. Brain. 2013;136(11):3242-51.
19. Schoonover KE, McCollum LA, Roberts RC. Protein Markers of Neurotransmitter Synthesis and Release in Postmortem Schizophrenia Substantia Nigra. Neuropsychopharmacology. 2017;42(2):540-50.
20. Toru M, Watanabe S, Shibuya H, Nishikawa T, Noda K, Mitsushio H, et al. Neurotransmitters, receptors and neuropeptides in post-mortem brains of chronic schizophrenic patients. Acta psychiatrica Scandinavica. 1988;78(2):121-37.
21. Mueller HT, Haroutunian V, Davis KL, Meador-Woodruff JH. Expression of the ionotropic glutamate receptor subunits and NMDA receptor-associated intracellular proteins in the substantia nigra in schizophrenia. Molecular Brain Research. 2004;121(1-2):60-9.

22. Purves-Tyson TD, Owens SJ, Rothmond DA, Halliday GM, Double KL, Stevens J, et al. Putative presynaptic dopamine dysregulation in schizophrenia is supported by molecular evidence from post-mortem human midbrain. Translational Psychiatry. 2017;7(1):1003-12.
23. Ichinose H, Ohye T, Fujita K, Pantucek F, Lange K, Riederer P, et al. Quantification of mRNA of tyrosine hydroxylase and aromatic L-amino acid decarboxylase in the substantia nigra in Parkinson's disease and schizophrenia. Journal of Neural Transmission - Parkinsons Disease and Dementia Section. 1994;8(1-2):149-58.
24. Perez-Costas E, Melendez-Ferro M, Rice MW, Conley RR, Roberts RC. Dopamine pathology in schizophrenia: Analysis of total and phosphorylated tyrosine hydroxylase in the substantia nigra. Frontiers in Psychiatry. 2012;3(31):1-14.
25. Purves-Tyson TD, Brown AM, Weissleder C, Rothmond DA, Shannon Weickert C. Reductions in midbrain GABAergic and dopamine neuron markers are linked in schizophrenia. Molecular brain. 2021;14(1):96-.
26. Tejedor-Real P, Faucon Biguet N, Dumas S, Mallet J. Tyrosine hydroxylase mRNA and protein are down-regulated by chronic clozapine in both the mesocorticolimbic and the nigrostriatal systems. Journal of Neuroscience Research. 2003;72(1):105-15.
27. Jauhar S, Nour MM, Veronese M, Rogdaki M, Bonoldi I, Azis M, et al. A test of the transdiagnostic dopamine hypothesis of psychosis using positron emission tomographic imaging in bipolar affective disorder and schizophrenia. JAMA Psychiatry. 2017;74(12):1206-13.
28. Elkashef AM, Doudet D, Bryant T, Cohen RM, Li SH, Wyatt RJ. 6-^{18}F-DOPA PET study in patients with schizophrenia. Psychiatry Research - Neuroimaging. 2000;100(1):1-11.
29. Kumakura Y, Cumming P, Vernaleken I, Buchholz HG, Siessmeier T, Heinz A, et al. Elevated [^{18}F] fluorodopamine turnover in brain of patients with schizophrenia: An [^{18}F]fluorodopa/ positron emission tomography study. Journal of Neuroscience. 2007;27(30):8080-7.
30. Jauhar S, Veronese M, Nour MM, Rogdaki M, Hathway P, Natesan S, et al. The Effects of Antipsychotic Treatment on Presynaptic Dopamine Synthesis Capacity in First-Episode Psychosis: A Positron Emission Tomography Study. Biological psychiatry. 2019;85(1):79-87.
31. Gründer G, Vernaleken I, Müller MJ, Davids E, Heydari N, Buchholz HG, et al. Subchronic haloperidol downregulates dopamine synthesis capacity in the brain of schizophrenic patients in vivo. Neuropsychopharmacology. 2003;28(4):787-94.
32. Allen P, Luigjes J, Howes OD, Egerton A, Hirao K, Valli I, et al. Transition to psychosis associated with prefrontal and subcortical dysfunction in ultra high-risk individuals. Schizophrenia bulletin. 2012;38(6):1268-76.
33. Henry JP, Scherman D. Radioligands of the vesicular monoamine transporter and their use as markers of monoamine storage vesicles. Biochemical pharmacology. 1989;38(15):2395-404.
34. Zubieta JK, Taylor SF, Huguelet P, Koeppe RA, Kilbourn MR, Frey KA. Vesicular monoamine transporter concentrations in bipolar disorder type I, schizophrenia, and healthy subjects. Biological psychiatry. 2001;49(2):110-6.
35. Sulzer D, Bogulavsky J, Larsen KE, Behr G, Greene LA, Karatekin E, et al. Neuromelanin biosynthesis is driven by excess cytosolic catecholamines not accumulated by synaptic vesicles. Proceedings of the National Academy of Sciences. 2000;97(22):11869-74.
36. Sasaki M, Shibata E, Ohtsuka K, Endoh J, Kudo K, Narumi S, et al. Visual discrimination among patients with depression and schizophrenia and healthy individuals using semiquantitative color-coded fast spin-echo T1-weighted magnetic resonance imaging. Neuroradiology. 2010;52(2):83-9.
37. Shibata E, Sasaki M, Tohyama K, Otsuka K, Endoh J, Terayama Y, et al. Use of Neuromelanin-Sensitive MRI to Distinguish Schizophrenic and Depressive Patients and Healthy Individuals Based on Signal Alterations in the Substantia Nigra and Locus Ceruleus. Biological Psychiatry. 2008;64(5):401-6.
38. Watanabe Y, Tanaka H, Tsukabe A, Kunitomi Y, Nishizawa M, Hashimoto R, et al. Neuromelanin magnetic resonance imaging reveals increased dopaminergic neuron activity in the substantia nigra of patients with schizophrenia. PloS one. 2014;9(8):e104619-e.
39. Cassidy CM, Zucca FA, Girgis RR, Baker SC, Weinstein JJ, Sharp ME, et al. Neuromelanin-sensitive MRI as a noninvasive proxy measure of dopamine function in the human brain. Proceedings of the National Academy of Sciences. 2019;116(11):5108-17.

40. Yamashita F, Sasaki M, Fukumoto K, Otsuka K, Uwano I, Kameda H, et al. Detection of changes in the ventral tegmental area of patients with schizophrenia using neuromelanin-sensitive MRI. Neuroreport. 2016;27(5):289-94.
41. Zucca FA, Basso E, Cupaioli FA, Ferrari E, Sulzer D, Casella L, et al. Neuromelanin of the human substantia Nigra: An update. Neurotoxicity Research. 2014;25(1):13-23.
42. Kelly RB, Deutsch JW, Carlson SS, Wagner JA. Biochemistry of neurotransmitter release. Annual Review of Neuroscience. 1979;2(1):399-446.
43. Tseng HH, Watts JJ, Kiang M, Suridjan I, Wilson AA, Houle S, et al. Nigral Stress-Induced Dopamine Release in Clinical High Risk and Antipsychotic-Naïve Schizophrenia. Schizophrenia Bulletin. 2018;44(3):542-51.
44. Slifstein M, Van De Giessen E, Van Snellenberg J, Thompson JL, Narendran R, Gil R, et al. Deficits in prefrontal cortical and extrastriatal dopamine release in schizophrenia a positron emission tomographic functional magnetic resonance imaging study. JAMA Psychiatry. 2015;72(4):316-24.
45. Shalgunov V, van Waarde A, Booij J, Michel MC, Dierckx R, Elsinga PH. Hunting for the high-affinity state of G-protein-coupled receptors with agonist tracers: Theoretical and practical considerations for positron emission tomography imaging. Med Res Rev. 2019;39(3):1014-52.
46. Hernaus D, Collip D, Kasanova Z, Winz O, Heinzel A, Van Amelsvoort T, et al. No evidence for attenuated stress-induced extrastriatal dopamine signaling in psychotic disorder. Translational Psychiatry. 2015;5(4):1-10.
47. Mercuri NB, Saiardi A, Bonci A, Picetti R, Calabresi P, Bernardi G, et al. Loss of autoreceptor function in dopaminergic neurons from dopamine D2 receptor deficient mice. Neuroscience. 1997;79(2):323-7.
48. Mortensen OV, Amara SG. Dynamic regulation of the dopamine transporter. European Journal of Pharmacology. 2003;479(1-3):159-70.
49. Artiges E, Leroy C, Dubol M, Prat M, Pepin A, Mabondo A, et al. Striatal and extrastriatal dopamine transporter availability in schizophrenia and its clinical correlates: A voxel-based and high-resolution PET study. Schizophrenia Bulletin. 2017;43(5):1134-42.
50. Arakawa R, Ichimiya T, Ito H, Takano A, Okumura M, Takahashi H, et al. Increase in thalamic binding of [^{11}C]PE2I in patients with schizophrenia: A positron emission tomography study of dopamine transporter. Journal of Psychiatric Research. 2009;43(15):1219-23.
51. Laruelle M, Abi-Dargham A, Van Dyck C, Gil R, D'Souza DC, Krystal J, et al. Dopamine and serotonin transporters in patients with schizophrenia: An imaging study with [123I]β-CIT. Biological Psychiatry. 2000;47(5):371-9.
52. Tatsumi M, Jansen K, Blakely RD, Richelson E. Pharmacological profile of neuroleptics at human monoamine transporters. European Journal of Pharmacology. 1999;368(2-3):277-83.
53. Brugger SP, Angelescu I, Abi-Dargham A, Mizrahi R, Shahrezaei V, Howes OD. Heterogeneity of Striatal Dopamine Function in Schizophrenia: Meta-analysis of Variance. Biological psychiatry. 2020;87(3):215-24.
54. Gurevich EV, Joyce JN. Distribution of dopamine D3 receptor expressing neurons in the human forebrain comparison with D2 receptor expressing neurons. Neuropsychopharmacology. 1999;20(1):60-80.
55. Murray AM, Ryoo HL, Gurevich E, Joyce JN. Localization of dopamine D3 receptors to mesolimbic and D2 receptors to mesostriatal regions of human forebrain. Proceedings of the National Academy of Sciences. 1994;91(23):11271-5.
56. Ford CP. The role of D2-autoreceptors in regulating dopamine neuron activity and transmission. Neuroscience. 2014;282:13-22.
57. Meador-Woodruff JH, Damask SP, Watson SJ. Differential expression of autoreceptors in the ascending dopamine systems of the human brain. Proceedings of the National Academy of Sciences. 1994;91(17):8297-301.
58. Lindgren N, Usiello A, Goiny M, Haycock J, Erbs E, Greengard P, et al. Distinct roles of dopamine D2L and D2S receptor isoforms in the regulation of protein phosphorylation at presynaptic and postsynaptic sites. Proceedings of the National Academy of Sciences. 2003;100(7):4305-9.
59. Usiello A, Baik JH, Rougé-Pont F, Picetti R, Dierich A, LeMeur M, et al. Distinct functions of the two isoforms of dopamine D2 receptors. Nature. 2000;408(6809):199-203.
60. Owen R, Owen F, Poulter M, Crow TJ. Dopamine D2 receptors in substantia nigra in schizophrenia. Brain Research. 1984;299(1):152-4.
61. Kessler RM, Woodward ND, Riccardi P, Li R, Ansari MS, Anderson S, et al. Dopamine D2 Receptor Levels in Striatum, Thalamus, Substantia Nigra, Limbic Regions, and Cortex in Schizophrenic

Subjects. Biological Psychiatry. 2009;65(12):1024-31.

62. Joo YH, Kim JH, Son YD, Kim HK, Shin YJ, Lee SY, et al. The relationship between excitement symptom severity and extrastriatal dopamine D2/3 receptor availability in patients with schizophrenia: a high-resolution PET study with [^{18}F]fallypride. European Archives of Psychiatry and Clinical Neuroscience. 2018;268(6):529-40.
63. Tuppurainen H, Kuikka JT, Laakso MP, Viinamäki H, Husso M, Tiihonen J. Midbrain dopamine D2/3 receptor binding in schizophrenia. European Archives of Psychiatry and Clinical Neuroscience. 2006;256(6):382-7.
64. Graff-Guerrero A, Mizrahi R, Agid O, Marcon H, Barsoum P, Rusjan P, et al. The dopamine D2 receptors in high-affinity state and D 3 receptors in schizophrenia: A clinical [^{11}C]-(+)-PHNO PET study. Neuropsychopharmacology. 2009;34(4):1078-86.
65. Kegeles LS, Slifstein M, Xu X, Urban N, Thompson JL, Moadel T, et al. Striatal and extrastriatal dopamine D2/D3 receptors in schizophrenia evaluated with [^{18}F]fallypride positron emission tomography. Biological Psychiatry. 2010;68(7):634-41.
66. Suridjan I, Rusjan P, Addington J, Wilson AA, Houle S, Mizrahi R. Dopamine D2 and D3 binding in people at clinical high risk for schizophrenia, antipsychotic-naive patients and healthy controls while performing a cognitive tasks. Journal of Psychiatry and Neuroscience. 2013;38(2):98-106.
67. Kambeitz J, Abi-Dargham A, Kapur S, Howes OD. Alterations in cortical and extrastriatal subcortical dopamine function in schizophrenia: systematic review and meta-analysis of imaging studies. The British journal of psychiatry : the journal of mental science. 2014;204(6):420-9.
68. Booij J, van Amelsvoort T. Imaging as tool to investigate psychoses and antipsychotics. Handb Exp Pharmacol. 2012(212):299-337.
69. Amunts K, Zilles K. Architectonic Mapping of the Human Brain beyond Brodmann. Neuron. 2015;88(6):1086-107.
70. Williams MR, Galvin K, O'Sullivan B, MacDonald CD, Ching EWK, Turkheimer F, et al. Neuropathological changes in the substantia nigra in schizophrenia but not depression. European archives of psychiatry and clinical neuroscience. 2014;264(4):285-96.
71. Rice MW, Roberts RC, Melendez-Ferro M, Perez-Costas E. Mapping dopaminergic deficiencies in the substantia nigra/ventral tegmental area in schizophrenia. Brain Structure and Function. 2016;221(1):185-201.
72. Yamaguchi T, Wang H-L, Morales M. Glutamate neurons in the substantia nigra compacta and retrorubral field. The European journal of neuroscience. 2013;38(11):3602-10.
73. Pearlstein E, Gouty-Colomer L-A, Michel FJ, Cloarec R, Hammond C. Glutamatergic synaptic currents of nigral dopaminergic neurons follow a postnatal developmental sequence. 2015. p. 210-.
74. Mabry SJ, McCollum LA, Farmer CB, Bloom ES, Roberts RC. Evidence for altered excitatory and inhibitory tone in the post-mortem substantia nigra in schizophrenia. World Journal of Biological Psychiatry. 2019;0(0):1-18.
75. Vigneault É, Poirel O, Riad M, Prud'homme J, Dumas S, Turecki G, et al. Distribution of vesicular glutamate transporters in the human brain. Frontiers in Neuroanatomy. 2015;9(23).
76. de la Fuente-Sandoval C, León-Ortiz P, Azcárraga M, Stephano S, Favila R, Díaz-Galvis L, et al. Glutamate levels in the associative striatum before and after 4 weeks of antipsychotic treatment in first-episode psychosis: a longitudinal proton magnetic resonance spectroscopy study. JAMA psychiatry. 2013;70(10):1057-66.
77. Pin JP, Duvoisin R. The metabotropic glutamate receptors: Structure and functions. Neuropharmacology. 1995;34(1):1-26.
78. Rubio MD, Drummond JB, Meador-Woodruff JH. Glutamate receptor abnormalities in schizophrenia: Implications for innovative treatments. Biomolecules and Therapeutics. 2012;20(1):1-18.
79. Bleakman D. Kainate receptor pharmacology and physiology. Cellular and molecular life sciences : CMLS. 1999;56(7-8):558-66.
80. Tepper JM, Lee CR. GABAergic control of substantia nigra dopaminergic neurons. Progress in Brain Research. 2007;160(06):189-208.
81. Germann M, Brederoo SG, Sommer IEC. Abnormal synaptic pruning during adolescence underlying the development of psychotic disorders. Current opinion in psychiatry. 2021;34(3):222-7.
82. Erlander MG, Tillakaratne NJK, Feldblum S, Patel N, Tobin AJ. Two genes encode distinct glutamate decarboxylases. Neuron. 1991;7(1):91-100.
83. Spokes EG. Neurochemical alterations in Huntington's chorea: a study of post-mortem brain tissue. Brain: a journal of neurology. 1980;103(1):179-210.
84. Sakai K, Gao XM, Hashimoto T, Tamminga

CA. Traditional and new antipsychotic drugs differentially alter neurotransmission markers in basal ganglia-thalamocortical neural pathways. Synapse. 2001;39(2):152-60.

85. Juge N, Omote H, Moriyama Y. Vesicular GABA transporter (VGAT) transports β-alanine. J Neurochem. 2013;127(4):482-6.
86. Frankle WG, Cho RY, Prasad KM, Mason NS, Paris J, Himes ML, et al. In vivo measurement of GABA transmission in healthy subjects and schizophrenia patients. Am J Psychiatry. 2015;172(11):1148-59.
87. Fillman SG, Cloonan N, Catts VS, Miller LC, Wong J, McCrossin T, et al. Increased inflammatory markers identified in the dorsolateral prefrontal cortex of individuals with schizophrenia. Mol Psychiatry. 2013;18(2):206-14.
88. Fillman SG, Sinclair D, Fung SJ, Webster MJ, Shannon Weickert C. Markers of inflammation and stress distinguish subsets of individuals with schizophrenia and bipolar disorder. Transl Psychiatry. 2014;4(2):e365.
89. Miller BJ, Buckley P, Seabolt W, Mellor A, Kirkpatrick B. Meta-analysis of cytokine alterations in schizophrenia: clinical status and antipsychotic effects. Biol Psychiatry. 2011;70(7):663-71.
90. Khandaker GM, Cousins L, Deakin J, Lennox BR, Yolken R, Jones PB. Inflammation and immunity in schizophrenia: implications for pathophysiology and treatment. Lancet Psychiatry. 2015;2(3):258-70.
91. Felger JC, Miller AH. Cytokine effects on the basal ganglia and dopamine function: the subcortical source of inflammatory malaise. Front Neuroendocrinol. 2012;33(3):315-27.
92. Zalcman S, Green-Johnson JM, Murray L, Nance DM, Dyck D, Anisman H, et al. Cytokine-specific central monoamine alterations induced by interleukin-1, -2 and -6. Brain Res. 1994;643(1-2):40-9.
93. Purves-Tyson TD, Weber-Stadlbauer U, Richetto J, Rothmond DA, Labouesse MA, Polesel M, et al. Increased levels of midbrain immune-related transcripts in schizophrenia and in murine offspring after maternal immune activation. Molecular psychiatry. 2021;26(3):849-63.
94. Chang C-Y, Luo D-Z, Pei J-C, Kuo M-C, Hsieh Y-C, Lai W-S. Not Just a Bystander: The Emerging Role of Astrocytes and Research Tools in Studying Cognitive Dysfunctions in Schizophrenia. International journal of molecular sciences. 2021;22(10).
95. Cai Z, Li S, Zhang W, Pracitto R, Wu X, Baum E, et al. Synthesis and Preclinical Evaluation of an ^{18}F-Labeled Synaptic Vesicle Glycoprotein 2A PET Imaging Probe: [^{18}F]SynVesT-2. ACS Chemical Neuroscience. 2020;11(4):592-603.
96. Hwang Y, Kim J, Shin JY, Kim JI, Seo JS, Webster MJ, et al. Gene expression profiling by mRNA sequencing reveals increased expression of immune/inflammation-related genes in the hippocampus of individuals with schizophrenia. Transl Psychiatry. 2013;3(10):e321.
97. Purves-Tyson TD, Robinson K, Brown AM, Boerrigter D, Cai HQ, Weissleder C, et al. Increased Macrophages and C1qA, C3, C4 Transcripts in the Midbrain of People With Schizophrenia. Frontiers in Immunology. 2020;11.
98. Bowman MB, Lewis MS. The copper hypothesis of schizophrenia: a review. Neuroscience & Biobehavioral Reviews. 1982;6(3):321-8.
99. Scheiber IF, Mercer JF, Dringen R. Copper accumulation by cultured astrocytes. Neurochem Int. 2010;56(3):451-60.
100. Schoonover KE, Queern SL, Lapi SE, Roberts RC. Impaired copper transport in schizophrenia results in a copper-deficient brain state: A new side to the dysbindin story. The world journal of biological psychiatry : the official journal of the World Federation of Societies of Biological Psychiatry. 2020;21(1):13-28.
101. Axelsson R, Martensson E, Alling C. Impairment of the blood-brain barrier as an aetiological factor in paranoid psychosis. Br J Psychiatry. 1982;141:273-81.
102. Chang H, Liu J, Zhang Y, Wang F, Wu Y, Zhang L, et al. Increased central dopaminergic activity might be involved in the behavioral abnormality of cuprizone exposure mice. Behav Brain Res. 2017;331:143-50.
103. Gregg JR, Herring NR, Naydenov AV, Hanlin RP, Konradi C. Downregulation of oligodendrocyte transcripts is associated with impaired prefrontal cortex function in rats. Schizophr Res. 2009;113(2-3):277-87.
104. Faivre F, Sánchez-Catalán MJ, Dovero S, Bido S, Joshi A, Bezard E, et al. Ablation of the tail of the ventral tegmental area compensates symptoms in an experimental model of Parkinson's disease. Neurobiol Dis. 2020;139:104818.
105. Lerner TN, Shilyansky C, Davidson TJ, Evans KE, Beier KT, Zalocusky KA, et al. Intact-Brain Analyses Reveal Distinct Information Carried by SNc Dopamine Subcircuits. Cell. 2015;162(3):635-47.
106. Grace AA, Bunney BS. Paradoxical GABA excitation of nigral dopaminergic cells: indirect

mediation through reticulata inhibitory neurons. Eur J Pharmacol. 1979;59(3-4):211-8.

107. Ikeda H, Saigusa T, Kamei J, Koshikawa N, Cools AR. Spiraling dopaminergic circuitry from the ventral striatum to dorsal striatum is an effective feed-forward loop. Neuroscience. 2013;241:126-34.

108. Johnson SW, North RA. Two types of neurone in the rat ventral tegmental area and their synaptic inputs. J Physiol. 1992;450:455-68.

109. Mailly P, Charpier S, Menetrey A, Deniau JM. Three-dimensional organization of the recurrent axon collateral network of the substantia nigra pars reticulata neurons in the rat. J Neurosci. 2003;23(12):5247-57.

110. Zhou FM, Lee CR. Intrinsic and integrative properties of substantia nigra pars reticulata neurons. Neuroscience. 2011;198:69-94.

111. Fisher PM, Hariri AR. Linking variability in brain chemistry and circuit function through multimodal human neuroimaging. Genes, Brain and Behavior. 2012;11(6):633-42.

112. Schultz CC, Fusar-Poli P, Wagner G, Koch K, Schachtzabel C, Gruber O, et al. Multimodal functional and structural imaging investigations in psychosis research. European Archives of Psychiatry and Clinical Neuroscience. 2012;262(2):97-106.

113. Howes OD, Thase ME, Pillinger T. Treatment resistance in psychiatry: state of the art and new directions. Mol Psychiatry. 2022;27(1):58-72.

114. Howes OD, Kapur S. A neurobiological hypothesis for the classification of schizophrenia: type A (hyperdopaminergic) and type B (normodopaminergic). Br J Psychiatry. 2014;205(1):1-3.

115. Caligiuri MP, Lohr JB, Jeste DV. Parkinsonism in neuroleptic-naive schizophrenic patients. Am J Psychiatry. 1993;150(9):1343-8.

116. Peralta V, Cuesta MJ. Neuromotor abnormalities in neuroleptic-naive psychotic patients: antecedents, clinical correlates, and prediction of treatment response. Compr Psychiatry. 2011;52(2):139-45.

Author Contributions

EvdG and MvdP conceived and designed the study. CvH, EvdG, IB, and MvdP designed the search strategy. CvH and IB did the literature search, selected the studies, and extracted the relevant information with support from EvdG and MvdP. CvH and IB synthesized the data and wrote the manuscript with support from MvdP and EvdG. All the authors critically reviewed the manuscript for intellectual content. All authors approved the final version of the manuscript for publication. EvdG supervised the project.

Chapter | 6

Striatal dopamine synthesis capacity and neuromelanin in the substantia nigra: a cross-sectional multimodal imaging study in schizophrenia and healthy controls

Carmen F.M. van Hooijdonk, Marieke van der Pluijm, Charlotte Smith, Maqsood Yaqub, Floris H. P. van Velden, Guillermo Horga, Kenneth Wengler, Monja Hoven, Ruth J. van Holst, Lieuwe de Haan, Jean-Paul Selten, Therese A.M.J. van Amelsvoort, Jan Booij, Elsmarieke van de Giessen

Submitted

Abstract

[^{18}F]F-DOPA PET is an established *in-vivo* method for investigating striatal dopamine synthesis capacity (DSC) and has demonstrated abnormalities in striatal DSC in schizophrenia. Neuromelanin-sensitive MRI (NM-MRI) is a promising, more accessible, tool that indirectly assesses dopaminergic functioning in the substantia nigra (SN). However, how [^{18}F]F-DOPA PET and NM-MRI, as measures of nigrostriatal dopaminergic functioning, interrelate is still unknown. We hypothesize that NM-MRI signal in the SN is positively correlated with striatal DSC in patients with a schizophrenia spectrum disorder (SSD) and healthy controls (HC). We acquired NM-MRI and dynamic [^{18}F]F-DOPA PET scans in 12 patients with SSD and 16 HC. In both groups, we assessed the correlation between nigral NM-MRI signal and DSC in the whole, associative, limbic, and sensorimotor striatum using voxelwise analyses within the SN. In HC, we found subsets of voxels within the SN where NM-MRI signal correlated negatively with DSC in the whole and limbic striatum. There were no significant associations between NM-MRI and DSC in the associative or sensorimotor striatum in HC and no significant associations in patients. These results show that NM-MRI signal and striatal DSC are negatively related in HC, but not in patients. Our results indicate that [^{18}F]F-DOPA PET and NM-MRI reflect different aspects of dopaminergic functioning. The negative correlation in HC might be explained by vesicular monoamine transporter-2 functioning. A lack of a correlation in patients might be due to the small sample size, effects of symptom severity or antipsychotic medication.

Introduction

[^{18}F]F-DOPA positron emission tomography (PET) is a well-established method for investigating striatal dopamine synthesis capacity (DSC). Originally, [^{18}F]F-DOPA PET was preferentially used to evaluate the integrity of the nigrostriatal dopaminergic pathway in patients with Parkinson's disease, but subsequently, it has been used to investigate other neuropsychiatric disorders. For example, [^{18}F]F-DOPA PET studies have repeatedly demonstrated elevated striatal DSC (i.e. indicating striatal hyperdopaminergia), specifically in the associative striatum of patients with schizophrenia (as reviewed by (1,2)) . PET imaging leads to (limited) radiation exposure to the patient and can be time-consuming and expensive. Therefore, new imaging methods have been developed to assess the dopaminergic system.

One promising and more accessible tool that indirectly assesses dopaminergic functioning in the substantia nigra (SN) is neuromelanin-sensitive MRI (NM-MRI)(3). Neuromelanin is a black, insoluble pigment, that primarily accumulates in the dopaminergic neurons of the SN pars compacta (SNc) (4). As a result of paramagnetic properties and magnetization transfer effects, neuromelanin-iron complexes cause T1-shortening (5). This creates a notable contrast in NM-MRI signal between the SN and the surrounding brain tissue. Multiple NM-MRI studies have demonstrated elevated neuromelanin concentration in the SN of patients with schizophrenia compared to healthy controls (HC)(as reviewed in Wieland, Fromm (6)). As the deposition of neuromelanin depends on the amount of excess cytosolic dopamine that has not been transferred into synaptic vesicles (4,7), we hypothesized that higher concentrations of neuromelanin might be related to higher rates of striatal DSC.

The findings of elevated striatal DSC and elevated neuromelanin concentration in the SN of patients with schizophrenia also suggest that these measures might relate positively to each other. This is supported by the observation that NM-MRI signal in the SN is positively associated with amphetamine-induced dopamine release (i.e. another indicator of striatal hyperdopaminergia) in the whole striatum, as assessed with [^{11}C]raclopride PET, across patients with schizophrenia and HC (3). It is unknown though whether striatal DSC and NM-MRI signal in the SN are interrelated. Therefore, we investigated the association between NM-MRI signal in the SN and DSC in the whole, associative, limbic, and sensorimotor striatum in HC and patients with a schizophrenia spectrum disorder. In addition, we explored the association between nigral DSC and NM-MRI signal in the SN of patients and HC. Herewith, we aimed to improve our understanding of how these measures of nigrostriatal dopaminergic functioning relate to each other and whether NM-MRI can be used to address striatal DSC abnormalities in neuropsychiatric disorders. We hypothesized that NM-MRI signal in the SN is positively correlated with striatal DSC in both groups. We assessed the relation between NM-MRI signal and striatal DSC in both groups separately since meta-analytic evidence shows that both measures are altered in patients with schizophrenia compared to controls (1,2,6),

and more importantly, striatal DSC seems to fluctuate with psychotic symptom severity and medication status in patients, (8-11), whereas there are indications that this is not the case for NM-MRI (unpublished data).

Methods

This study combines data from two patient and two HC cohorts, collected in the context of three Dutch studies approved by the Medical Ethical Committee (MEC) of Leiden, The Hague, and Delft (NL72218.058.20), the MEC of the Amsterdam UMC, University of Amsterdam (NL63410.018.17), and the MEC of East Netherlands (NL72675.091.20). All participants gave written informed consent after a full explanation of the study procedure and before the start of the study.

Participants

For this study, early psychosis patients who recently experienced an episode of psychosis were recruited via two Dutch mental health institutes (i.e. Rivierduinen Institute for Mental Health Care in Leiden and the specialized Early Psychosis Clinic of the Amsterdam UMC in Amsterdam). All of these patients were currently undergoing treatment at a mental health institute and were diagnosed with a schizophrenia spectrum disorder (i.e. schizophrenia, schizoaffective disorder, schizophreniform disorder, brief psychotic disorder, other specified schizophrenia spectrum and other psychotic disorder, or unspecified schizophrenia spectrum and other psychotic disorder) by a registered psychiatrist. Diagnoses were confirmed with the semi-structured Comprehensive Assessment of Symptoms and History (CASH) interview (12). In addition, a cohort consisting of HC matched for age, gender, smoking status, and educational level was recruited via social media and poster advertisements. Patients and HC were both aged between 18-50 years. Exclusion criteria for patients included: 1) onset of first psychotic episode longer than five years ago; and 2) previous antipsychotic use longer than one year. Additional exclusion criteria for both groups were: 1) current or history of a substance use disorder other than nicotine, alcohol, or cannabis, as assessed with the Composite International Diagnostic Interview (CIDI) (13) or the Mini International Neuropsychiatric Interview (MINI) (14); 2) use of substances other than nicotine, alcohol, or cannabis (i.e. illicit drugs or psychotropic medication that influence the dopaminergic system) in the month (in case of HC) or the three months (in case of patients) before study participation. For patients, the use of benzodiazepines, hypnotics and antidepressants in amounts within the therapeutic range was allowed; 3) positive urine drug screening on the day of the PET or MRI scan. Participants were tested on use of cannabis, amphetamine, XTC, cocaine, and opiates. Only recent cannabis use was allowed; 4) neurological disorder (e.g. epilepsy) or evidence of brain damage; 5) contra-indications for MRI or PET (e.g. ferromagnetic implants, pacemaker, or pregnancy); 6) participation in a scientific examination where radiation was used in the year before study participation; and 7) inability to provide informed consent.

Lastly, HC with a current psychiatric disorder or history of any psychiatric disorder were excluded, as assessed with the MINI (14).

Design and procedures

Participants were assessed on 1 to 3 testing days, depending on the availability of the research facilities. The study procedure consisted of three parts: 1) screening for in- and exclusion criteria and completing measures on general demographic information (e.g. age and gender), positive and negative symptoms severity by use of the Positive and Negative Syndrome Scale (PANSS; patients only) (15), depressive symptom severity by use of the Beck Depression Inventory (BDI-II) (16, 17), and medication use; 2) MRI scan including the NM-MRI; and 3) [^{18}F]F-DOPA PET scan. Additionally, a urine drug screening was completed on each day that an MRI and/or PET scan was scheduled to examine pregnancy (females only) and drug use. All patients used antipsychotic medication during the study (Results S1). Chlorpromazine (CPZ) equivalent doses (100 mg/day) were calculated for antipsychotic medication by use of the defined daily dose (DDD) method (18) (Methods S1). In addition, we calculated antipsychotic dose-years, which is a cumulative measure of antipsychotic usage (19) (Methods S1).

MRI procedures

NM-MRI acquisition

All participants were instructed to refrain from alcohol and cannabis 24 h before the MRI scan. All magnetic resonance (MR) images were acquired on a 3T MR scanner (Phillips, Ingenia Elition X, Best, The Netherlands) with a 32-channel head coil at the Amsterdam UMC, the Netherlands. Structural whole-brain T1-weighted volumetric images were acquired for NM-MRI slice placement by use of a transversal high-resolution 3D sequence (repetition time [TR] = 9.0 ms; echo time [TE] = 4.1 ms; 189 slices; field of view [FOV] = 284 × 284 × 170 mm; voxel size= 0.9 × 0.9 × 0.9 mm; flip angle [FA] = 8°) or MPRAGE sequence (TR = 7.0 ms; TE = 3.2 ms; 180 slices; FOV = 256 x 240 x 180 mm; voxel size= 1 x 1 x 1 mm; FA = 9°). On the T1-weighted images, the NM-MRI slices were orientated perpendicular to the fourth ventricle floor. For logistic reasons, the NM-MRI slices were orientated along the anterior commissure-posterior commissure line for a few scans (six of the 42 scans). Both placement protocols provided coverage of the SN. NM-MRI was acquired with a T1-weighted 2D gradient echo sequence with magnetization transfer (MT) pulse (TR = 260 ms; TE = 3.9 ms; 8 slices; FOV = 162 x 199 mm; slice thickness = 2.5 mm; number of signal averages = 2; FA = 40°; MT frequency offset = 1200 Hz; MT duration = 15.6 ms).

NM-MRI pre-processing

The NM-MRI scans were pre-processed with a Matlab (MathWorks, Natrick, MA) pipeline from Wengler et al. (2020) (20). First, Advanced Normalization Tools (ANTs) registration (rigid) was used to coregister the NM-MRI images to the T1-weighted images. Second, ANTs brain extraction was used to perform the brain extraction of the T1-weighted images. Third,

ANTs registration (rigid + affine + deformable syn) was used to spatially normalize the brain-extracted T1-weighted images to Montreal Neurological Imaging (MNI) standard space. Fourth, the coregistered NM-MRI images were spatially normalized to MNI standard space using the warping parameters that were used for the normalization of the T1-weighted images. Fifth, smoothing was performed with Analysis of Functional NeuroImages (AFNI) to spatially smooth the normalized NM-MRI images with a 1-mm full-width-at-half-maximum (FWHM) Gaussian kernel. Visual inspection of all images occurred after each pre-processing step. Finally, the NM-MRI signal in the SN was calculated as a contrast-to-noise ratio (CNR) with the crus cerebri (CC) as the reference region, using SN and CC template masks. The template masks were generated by manually tracing the SN and CC on an average image of 28 spatially normalized NM-MRI images of a subgroup of the participating individuals (12 patients and 16 HC; these are the subjects included in the primary analyses; Figure 1). For each participant, the CNR at each voxel v in the SN was calculated as the percent NM-MRI signal difference between a given voxel in the SN mask (*IV*) and the mode of the signal intensity in the CC (*ICC*) with $CNR_V = \left\{\frac{[I_V\text{-mode}(I_{CC})]}{\text{mode}(I_{CC})}\right\} * 100$. The mode (*ICC*) was calculated from a kernel-smoothing-function fitted to a histogram of the distribution of all voxels in the CC mask. The mode rather than the median or mean was used, as this is more robust to outliers (3).

PET procedures

PET acquisition

All participants were asked to refrain from alcohol and cannabis 24 h before PET imaging. In addition, participants were asked to refrain from eating and drinking (except water) six hours before PET imaging and to refrain from smoking three hours before PET imaging. For logistic reasons, six of the HC refrained from eating, drinking, and smoking two hours before the PET scan. One hour before the PET scan, all participants received 150 mg carbidopa (a peripheral aromatic acid decarboxylase inhibitor) and 400 mg entacapone (a peripheral catechol-O-methyltransferase inhibitor) to block peripheral metabolization of [^{18}F]F-DOPA and reduce the formation of radiolabelled metabolites (21,22). Before PET acquisition, a low-dose computed tomography (CT) scan of the brain was acquired for attenuation correction purposes. Subsequently, approximately 185 MBq [^{18}F]F-DOPA was administered as a single intravenous bolus injection. Immediately thereafter a 90-minute dynamic PET acquisition started. PET data were acquired on a Siemens PET/CT system (Biograph mCT FlowTrue-V-128) (FOV = 256 x 256 mm; slice thickness = 2 mm; pixel spacing = 1.59 x 1.59 mm) and binned in 25 frames (5 x 1, 3 x 2, 3 x 3, and 14 x 5 minute[s]). Head straps and a headrest were used to minimize head and neck movement during PET imaging.

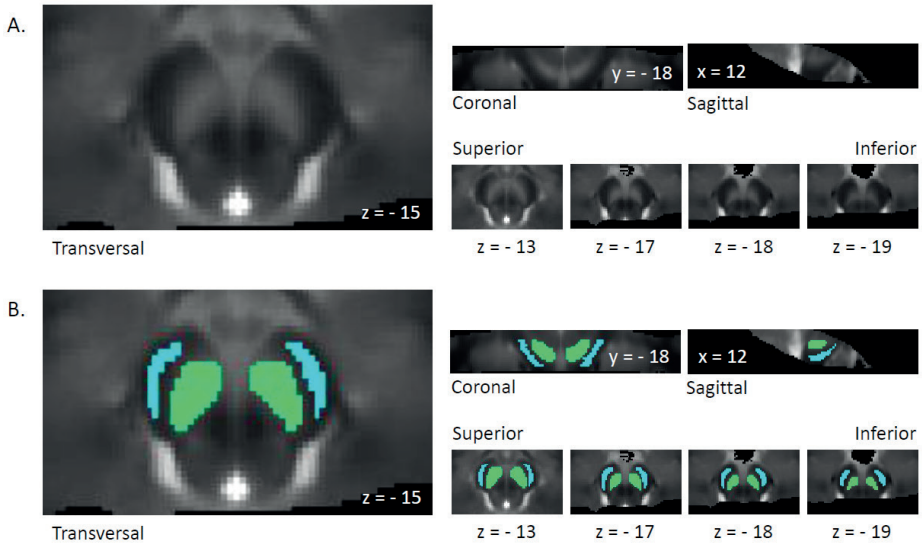

Figure 1. Template masks of the substantia nigra and the crus cerebri. A. Average image of spatially normalized NM-MRI images from 28 participants. The SN is visible as a hyperintense area. B. Template masks of the SN (in green) and CC (in blue) in MNI space were created by manually tracing the regions on the average NM-MRI image. The template masks were used for calculating the contrast-to-noise ratio in all subjects. Abbreviations: CC, crus cerebri; MNI, Montreal Neurological Imaging; NM-MRI, neuromelanin-sensitive magnetic resonance imaging; SN, substantia nigra.

PET pre-processing

PET data were reconstructed with an iterative reconstruction algorithm (5 iterations, 21 subsets) that corrects for the time of flight (TOF) and point spread function (PSF), followed by a 2 mm FWHM Gaussian smoothing filter. First, the PET images were visually inspected for movement with Vinci (v4.66; Max Planck Institute for Neurological Research, Cologne, Germany) (23,24). Participants who moved more than 7.5 mm during the data acquisition were excluded from further analyses, as attenuation correction might no longer be reliable. Second, the structural T1-weighted and PET images were co-registered, by use of Vinci, to a single PET frame acquired 7 minutes post-injection. This was done to correct for minor head movements and was based on mutual information (25). Third, the structural T1-weighted images were segmented into white matter (WM), grey matter (GM), and cerebral spinal fluid (CSF) by use of PVElab (v2.3; Neurobiology Research Unit, Copenhagen, Denmark) (26,27) and Statistical Parametric Mapping (SPM) 12 (Wellcome Centre for Human Neuroimaging, London, UK). Partial volume correction was part of the reconstruction procedure and therefore not performed by PVElab. Fourth, the volumes of interest (i.e. striatum and cerebellum) were generated based on Hammers' maximum probability atlas (28). Fifth, Patlak graphical analysis (29), which is implemented in PPET (30), was used to calculate the influx constant k_i^{cer} (min^{-1}; from here on labelled as k_i^{cer}) as a measure of DSC with the GM of the cerebellum as reference region since GM tracts of the cerebellum have negligible dopamine content

and the cerebellum has previously been validated as reference region (31). Finally, linear fitting was conducted on the PET images acquired between 25 and 90 minutes to acquire a whole-brain parametric image (Figure 2A). The k_i^{cer} of the GM striatum was extracted from this whole-brain parametric image.

The striatal functional subdivisions (i.e. associative, limbic, and sensorimotor striatum), defined in the Oxford-GSK-Imanova brain atlas (32), and a standard MNI brain template were extracted from FSLeyes v0.3 in FSL (v6.0; Analysis Group, Oxford, United Kingdom) (33,34). The MNI template was warped with a non-linear affine transformation to the subject's MRI using Vinci. Thereafter, the same transformation matrix was applied to the striatal subdivisions to warp the striatal subdivisions from MNI to subject space. Subsequently, the GM k_i^{cer} for voxels with at least a 90% probability of belonging to the striatal subdivision was extracted from the whole-brain parametric image. To investigate the influence of mask threshold, we repeated the procedure for voxels with at least a 60% probability of belonging to the striatal subdivision (Methods S2).

To calculate the k_i^{cer} in the SN, we used the MNI template and our SN template mask. We warped the SN mask from standard to subject space by applying the same transformation matrix as used for warping the striatal subdivisions. Afterwards, the k_i^{cer} in the GM and WM combined were extracted from the whole-brain parametric image for voxels within the SN mask with at least a 50% probability of belonging to GM or WM. We extracted the k_i^{cer} in GM and WM, as the segmentation of the brainstem can reliably separate CSF from GM and WM, but is less accurate in distinguishing GM and WM.

NM-MRI and PET analyses

All analyses were conducted in MATLAB. In line with previous work, our primary analysis consisted of voxelwise analyses (3,35). We chose voxelwise analyses to reduce statistical circularity in defining the SN region via signal-intensity thresholding and to account for regional heterogeneity of dopamine neurons across tiers without well-defined anatomical boundaries. Age was used as a covariate in all analyses, as neuromelanin accumulation is known to be age-related (36). For the primary analysis, we examined the association between striatal DSC and nigral NM-MRI signal in both groups separately using a voxelwise robust linear regression that predicted CNR at every voxel within the SN based on mean k_i^{cer} values (for whole, associative, limbic, and sensorimotor striatum regions of interest [ROIs]) and age. Missing CNR values due to incomplete coverage of the SN and extreme CNR values were excluded (i.e. smaller and greater than the 1st and 99th percentile, respectively; patients: CNR < 4.35 and CNR > 26.52; HC: CNR < 2.46 and CNR > 26.46). On average, 30 voxels (SD = 24 for patients; SD = 44 for HC) or 2% of the SN voxels were excluded per patient or HC. Subsequently, significance testing was determined by use of a permutation test in which mean k_i^{cer} values of the striatal ROI were randomly shuffled, 10,000 times, with respect to

the individual maps of the NM-MRI signal in the SN. This resulted in a null distribution of the number of SN voxels that exceeded a threshold of $p < 0.050$. The permutation test corrects for multiple comparisons by deciding whether the effect's spatial extent k is larger compared to chance (corrected $p < 0.050$). In case of significant results, we subsequently performed post-hoc partial Spearman's rank-order correlation coefficient tests to address the strength of the correlation (i.e. Spearman's rho). In addition, we calculated the 95%-confidence interval of Spearman's rho by use of the Fisher z-transformation. The associations between the mean CNR values from the significant voxels (thresholded at $p < 0.050$) and mean k_i^{cer} values in the striatal ROI were assessed with age as covariate. We did this with mean CNR values uncorrected and corrected for voxel selection (i.e. obtained by a leave-one-subject-out analysis to get an unbiased effect size). In the leave-one-out analysis significant voxels for each HC were identified in a voxelwise analysis including the complete HC sample except the left-out subject. The significant voxels were subsequently used to extract the mean CNR for the left-out subject. For completeness, we also conducted a ROI analysis where we correlated the mean k_i^{cer} values in the different striatal ROIs with the average NM-MRI signal across non-negative values within the whole SN mask. In addition, we explored the association between nigral DSC and NM-MRI signal in the SN with a similar voxel-based method.

Group differences concerning NM-MRI signal were also assessed with a voxelwise analysis with age as covariate. Additionally, demographical, clinical, and other imaging characteristics (e.g. age, gender, depressive symptom severity, k_i^{cer} values) were examined by use of a parametric independent t-test, Mann-Whitney U test, and Fisher's exact test, depending on the type of variable and its distribution. Finally, Spearman's rank-order correlation coefficient tests were used to address correlations between imaging measures and clinical variables. Correlations with NM-MRI signal were corrected for age. Statistical significance was evaluated with a two-tailed alpha of 0.05.

Results

Eighteen patients with a schizophrenia spectrum disorder and 24 HC completed the study. For various reasons, we were unable to use the data of 14 participants (N = 6 patients, N = 8 HC; Results S2). The main reasons for exclusion were movement during PET imaging and poor neuromelanin data quality. The final sample included 12 patients and 16 HC. Average head movement during the PET scan was comparable in these groups (patients: 2.39 mm, SD = 1.20; HC: 2.10 mm, SD = 1.20; Methods S3). Table 1 shows the demographical and clinical characteristics of both groups. There were no between-group differences in sex, age, current nicotine use, ethnicity, educational level, or injected [^{18}F]F-DOPA dose. However, patients had significantly higher BDI scores compared to HC ($U = 6.000$, $p < 0.001$). The voxelwise analysis to address group differences in CNR signal in the SN revealed no voxels with significant differences between groups (robust linear regression controlling for age, CNR patients >

CNR HC corrected p = 0.377, CNR HC > CNR patients corrected p = 0.760, permutation test). Additionally, we found no significant group differences for mean k_i^{cer} values in the whole, associative, or limbic striatum, or the SN. Patients exhibited lower mean k_i^{cer} values in the sensorimotor striatum than HC (U = 45.000; p = 0.018). This was no longer the case when using GM k_i^{cer} of voxels with at least a 60% instead of a 90% probability of belonging to the sensorimotor striatum (Results S3). Non-specific uptake of [^{18}F]-FDOPA in the cerebellum was not significantly different in patients and HC (Figure S1; Results S4).

Voxelwise and post-hoc analyses

We found a significant negative association in HC between mean k_i^{cer} values in the whole striatum and CNR in a subset of voxels in the SN (hereafter called SN-striatum voxels; 218 of 1,480 voxels at p < 0.050, robust linear regression controlling for age; corrected p = 0.033, permutation test; peak voxel MNI coordinates [x, y, z]: -5, -12, -9 mm; Figure 2C). Similarly, we found a subset of voxels in the SN of HC (hereafter called SN-limbic voxels) that demonstrated a significant negative association between CNR and mean k_i^{cer} values in the limbic striatum (333 of 1,480 voxels at p < 0.050, robust linear regression controlling for age; corrected p = 0.005, permutation test; peak voxel MNI coordinates [x, y, z]: -6, -19, -13 mm; Figure 2D). As previous research found a strong correlation between mean k_i^{cer} values in the whole striatum and its functional subdivisions for data from a 95-min acquisition and data from a 60-min acquisition (37), we performed a sensitivity analyses in which we repeated the voxelwise analysis for the whole and limbic striatum with four additional HC who were excluded due to movement. We applied linear fitting on the PET images of these four HC acquired between 25 min and the start of substantial (>7.5 mm) movement. Similarly to the previous findings, we found largely overlapping voxels within the SN where CNR significantly negatively correlated with k_i^{cer} values in the whole and limbic striatum (whole striatum: p = 0.021; limbic striatum: p = 0.015; Results S5). We performed an additional sensitivity analysis in which we repeated the voxelwise analysis for the whole and limbic striatum without the five HC who fasted for two instead of six hours. This resulted in a borderline significant negative association between mean k_i^{cer} values in the limbic striatum and CNR in a smaller (compared to the primary analysis) subset of voxels in the SN (p = 0.051; Results S6). The results for the whole striatum were no longer significant (p = 0.167).

Right page: Abbreviations: AST, associative striatum; BDI, Beck Depression Inventory; CNR, contrast-to-noise ratio; CPZ, chlorpromazine; F, female; LST, limbic striatum; M, male; MBq, megabecquerel; NA, not applicable; NM-MRI, neuromelanin-sensitive magnetic resonance imaging; PANSS, positive and negative symptom scale; PET, positron emission tomography; SD, standard deviation; SN, substantia nigra; SMST, sensorimotor striatum; WS, whole striatum. Significant results are bold.

[a]Group differences were assessed with Fisher's exact test. [b]Group differences were assessed with the Mann-Whitney U test. [c]Current nicotine use is defined as having used nicotine daily for at least one month in the past twelve months. [d]During the first scan. [e]Based on average for the whole SN mask (i.e. not the voxelwise analysis).

Table 1. Sample characteristics

	Patients	Healthy controls	p-value
Demographics and clinical characteristics	**N=12**	**N=16**	
Sex (F/M)	2/10	4/12	0.673a
Age in years, mean (SD)	20.8 (2.7)	24.5 (6.2)	0.129b
Current nicotine usec (Yes/No)	4/8	3/16	0.418a
Education, No.	-	-	0.125a
Secondary vocational education / Senior general secondary education / Pre-university education	9	6	-
Higher professional education / Bachelor's degree	3	9	-
University education (Master's degree)	0	1	-
Ethnicity, No. (White/Other)	10/2	15/1	0.560a
Injected [18F]F-DOPA dose in MBq, mean (SD)	180.6 (13.8)	179.1 (15.5)	0.963b
Number of days between PET and MRI, mean (range)	14.8 (0-33)	5.4 (0-71)	0.001b
PANSS at study enrollment	-	-	-
Positive score, mean (SD)	12.2 (5.0)	NA	NA
Negative score, mean (SD)	12.9 (6.2)	NA	NA
General score, mean (SD)	25.1 (8.7)	NA	NA
Total score, mean (SD)	50.2 (14.3)	NA	NA
BDI, mean (SD)	12.8 (8.0)	1.8 (2.1)	<0.001b
Current 100 mg CPZ-equivalent dose in mg, mean (SD)d	398.6 (222.0)	NA	NA
Total days on antipsychotic medication, mean (SD)d	122.1 (98.0)	NA	NA
CPZ dose-years, mean (SD) d	0.078 (0.088)	NA	NA
Diagnosis, No.	-	-	-
Schizophrenia	5	NA	NA
Schizoaffective disorder	2	NA	NA
Schizophreniform disorder	3	NA	NA
Unspecified schizophrenia spectrum	1	NA	NA
Other specified schizophrenia spectrum	1	NA	NA
NM-MRI and [18F]F-DOPA PET outcome parameters			
CNR, mean (SD)e	15.3 (1.0)	15.0 (1.6)	0.889b
kicer WS, mean (SD)	0.0159 (0.0024)	0.0164 (0.0011)	0.227b
kicer LST (0.9 threshold), mean (SD)	0.0173 (0.0021)	0.0179 (0.0012)	0.163b
kicer AST (0.9 threshold), mean (SD)	0.0189 (0.0026)	0.0194 (0.0014)	0.486b
kicer SMST (0.9 threshold), mean (SD)	0.0196 (0.0037)	0.0216 (0.0019)	0.018b
kicer SN, mean (SD)	0.0099 (0.0014)	0.0099 (0.0011)	0.329b

Caption: see left page

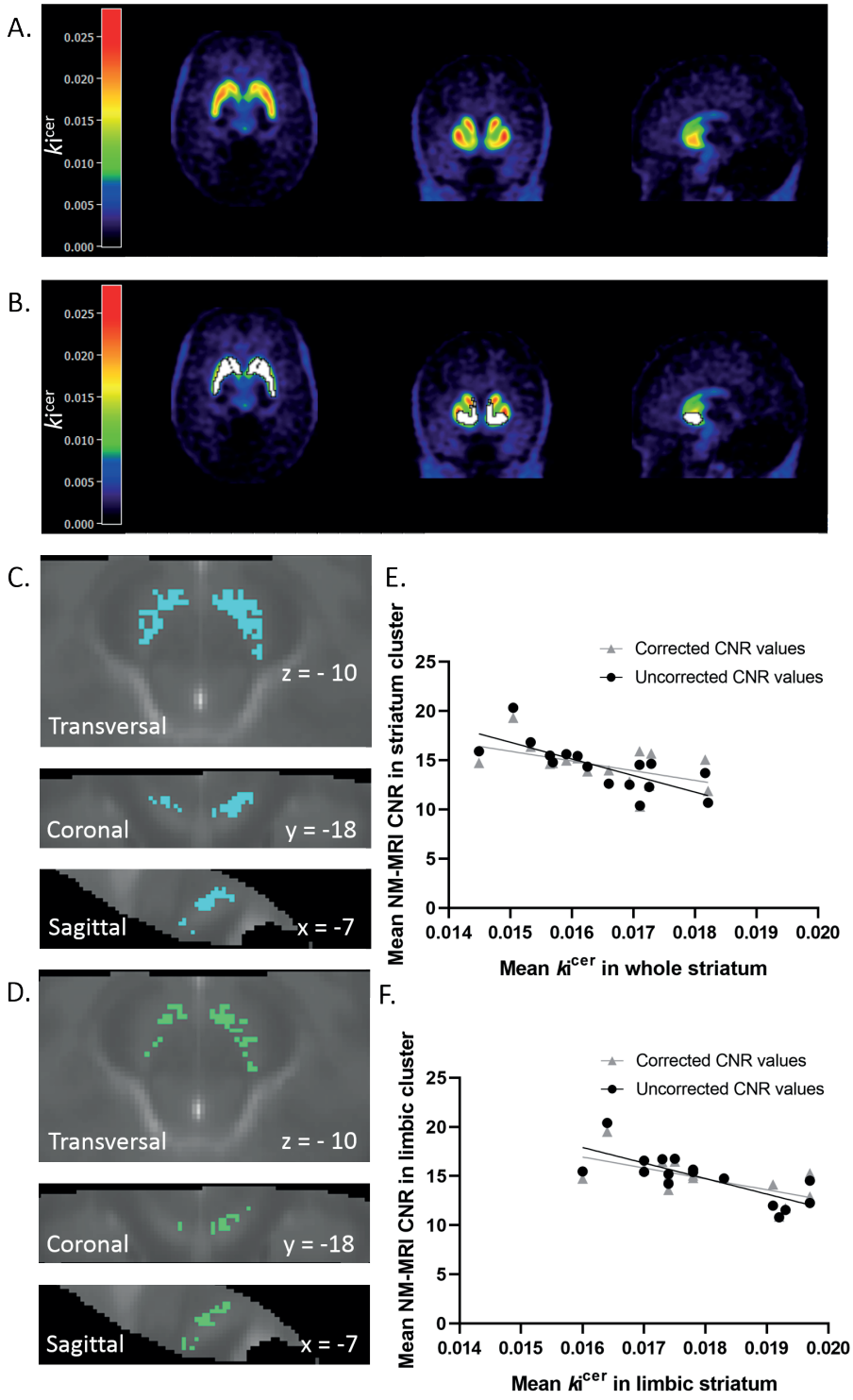
A.
B.
ki^{cer}
0.025
0.020
0.015
0.010
0.005
0.000
C.
Transversal
z = - 10
Coronal
y = -18
Sagittal
x = -7
D.
Transversal
z = - 10
Coronal
y = -18
Sagittal
x = -7
E.
Corrected CNR values
Uncorrected CNR values
Mean NM-MRI CNR in striatum cluster
Mean ki^{cer} in whole striatum
0.014
0.015
0.016
0.017
0.018
0.019
0.020
F.
Corrected CNR values
Uncorrected CNR values
Mean NM-MRI CNR in limbic cluster
Mean ki^{cer} in limbic striatum

There were no significant associations between CNR in the SN and mean k_i^{cer} values in the associative and sensorimotor striatum in HC and no significant associations between CNR in the SN and mean k_i^{cer} values in any of the striatal ROIs in patients (Results S7). Similar to the sensitivity analysis in HC, we repeated the voxelwise analysis in patients for the whole and limbic striatum with three additional patients who were excluded due to movement. This again resulted in non-significant findings (Results S5). In addition, the results of the striatal subdivisions did not change when using the mean k_i^{cer} values with a 60% instead of a 90% probability of belonging to the striatal subdivision (Results S8). Our exploratory analyses revealed no subsets of voxels within the SN where CNR correlated significantly with mean k_i^{cer} values in the SN in patients or HC (Results S9).

The post-hoc analyses revealed a significant negative correlation between the mean CNR in SN-striatum voxels and mean k_i^{cer} values in the whole striatum of HC (controlling for age; uncorrected for voxel selection, rho = -0.853, 95%-CI: (-0.560, -0.956), $p < 0.001$; corrected for voxel selection, rho = -0.445, 95%-CI: (-0.781, 0.091), $p = 0.097$; Figure 2E). In addition, we found a negative correlation between the mean CNR in SN-limbic voxels and mean k_i^{cer} values in the limbic striatum of HC (controlling for age; uncorrected for voxel selection, rho = -0.840, 95%-CI: (-0.529, -0.952), $p < 0.001$; corrected for voxel selection, rho = -0.616, 95%-CI: (-0.125, -0.865), $p = 0.015$; Figure 2F). For completeness, we also assessed the association between mean CNR within the whole SN mask and mean k_i^{cer} values in the different ROIs with age as covariate (Results S10). We found no significant associations.

Exploratory analyses

Within the patient group, we found no significant associations between 1) mean CNR in the SN or mean k_i^{cer} values in the whole, associative, limbic, and sensorimotor striatum or SN and 2) symptom scores (i.e. positive PANSS scores, negative PANSS scores, general PANSS scores, total PANSS scores, and BDI scores; Results S11). The association between age and mean CNR in the SN was trend significant (rho = -0.563; 95%-CI: (-0.872, 0.066), $p = 0.057$). In patients, antipsychotic medication usage (i.e. total number of days on medication, CPZ-equivalent dose, and CPZ dose-years at the moment of the first scan) also did not correlate with mean k_i^{cer} values in the different ROIs or mean CNR in the SN (Results S12). In HC, we found that

Figure 2. (Left page) Results of voxelwise analysis in the substantia nigra. Visualized in MNI space: A) Average kicer in voxels of the healthy controls (HC) without and B) with a mask of the limbic striatum (in white). C) Map of voxels (in blue) in which HC exhibit a negative correlation between NM-MRI contrast-to-noise ratio (CNR) and mean kicer values in the whole striatum (WS), i.e. SN-striatum voxels. D) Map of voxels (in green) in which HC exhibit a negative correlation between CNR and mean kicer values in the limbic striatum (LST), i.e. SN-limbic voxels. E) Scatterplot displaying the correlation between mean uncorrected and corrected CNR values in SN-striatum voxels and mean kicer value in the WS in HC (uncorrected rho=-0.853, 95%-confidence interval (CI): (-0.560,-0.956), p<0.001; corrected rho=-0.445, CI: (-0.781, 0.091), p=0.097). F) Scatterplot displaying the correlation between mean uncorrected and corrected for voxel selection CNR values in SN-limbic voxels and mean kicer value in the LST in HC (uncorrected rho=-0.840, CI: (-0.529,-0.952), p<0.001; corrected rho=-0.616, CI:(-0.125,-0.865), p=0.015).

the association between mean CNR in the SN and BDI scores reached trend-level significance while correcting for age (rho = -0.597; 95%-CI: (-0.894, 0.064), p = 0.069)(Results S13).

Discussion

We used NM-MRI and [^{18}F]F-DOPA PET imaging to investigate the association between NM-MRI signal in the SN and DSC in the striatum and SN of patients with a schizophrenia spectrum disorder and HC. Contrary to our expectations, we found voxels within the SN of HC where NM-MRI signal correlated negatively with DSC in the whole and/or limbic striatum. The negative associations in the limbic subdivision of the striatum of HC were largely confirmed in post-hoc and sensitivity analyses and not found in patients. Our exploratory analysis did not reveal any significant association between DSC in the SN and NM-MRI signal, which is in line with the findings of Ito et al, who also reported that NM-MRI signal in the SN of healthy individuals (N=11) was not associated with DSC in the SN (38).

Our finding of a negative correlation between NM-MRI and [^{18}F]F-DOPA measures in HC is surprising given that the accumulation of neuromelanin is mostly determined by the amount of excessive cytosolic dopamine (7) and that neuromelanin concentration in the SN positively correlates with amphetamine-induced dopamine release in the whole striatum across patients with schizophrenia and HC (3). The negative correlation in HC might be explained by functioning of the vesicular monoamine transporter-2 (VMAT-2), which transports cytosolic dopamine into synaptic vesicles. VMAT-2 levels were found to be positively associated with tyrosine hydroxylase levels (i.e. the rate-limiting enzyme for dopamine synthesis, which synthesizes L-DOPA from tyrosine) and negatively associated with neuromelanin pigment in the ventral SN of post-mortem human brains (39). It might therefore be that dopaminergic neurons in the midbrain of HC with greater amounts of dopamine synthesis have more vesicular storage capacity and consequently less neuromelanin deposition in the SN. This is in line with the finding of Sulzer et al. (2000) who found that neuromelanin synthesis is inhibited by adenoviral-mediated overexpression of VMAT-2. In addition, in rat striata, VMAT-2 functionally and physically interacts with the enzymes tyrosine and aromatic acid decarboxylase (AADC; which synthesizes dopamine from L-DOPA) (40), indicating that these components of the dopamine system are directly linked to each other (7). The negative association in HC suggests that NM-MRI and [^{18}F]F-DOPA PET reflect different components of the dopamine system. This is also supported by the fact that striatal [^{18}F]F-DOPA signal decreases with age (41), while NM-MRI signal increases with age until it reaches a decline at old age (36).

We most consistently found a negative association between NM-MRI and [^{18}F]F-DOPA measures in HC for the limbic striatum, as our post-hoc analysis demonstrated a negative association between DSC in the limbic striatum and NM-MRI signal uncorrected and corrected for voxel

selection, while the post-hoc analysis for the whole striatum only confirmed a significant negative association for the NM-MRI signal uncorrected for voxel section. The significant findings in the whole striatum might therefore be driven by the association present in the limbic striatum. The voxels in the SN where NM-MRI signal correlated negatively with DSC in the limbic striatum (Figure 2D) largely overlap with the medial SN, which is found to be connected to the ventral striatum (i.e. the anatomical subregion of the striatum previously classified as belonging to the limbic functional subdivision of the striatum) (42,43). In addition, the medial SN is anatomically adjacent to the ventral tegmental area (VTA) (44), which innervates the nucleus accumbens and ventromedial striatum (i.e. mesolimbic dopaminergic pathway). The reason why the association with the limbic striatum is strongest is still unclear, although it is also known that VMAT-2 levels are lower in the more lateral parts of the ventral SN than in the medial parts of the SN (39).

The lack of a correlation in patients might be explained by multiple factors. First, the results in the patient group might be explained by the small sample size. Second, striatal DSC might fluctuate more over time in patients compared to HC, as striatal DSC is associated with psychotic symptom severity in patients (8,9). We did not find significant associations between symptom severity and striatal DSC in our sample, which might be due to the relatively low symptom severity in our patients and the relatively small sample size. Illness severity, duration of illness, and antipsychotic medication usage might affect striatal DSC (10,11), whereas no changes in NM-MRI signal have been found after six months of antipsychotic treatment in patients with schizophrenia (44, unpublished data). This suggests that [^{18}F]-FDOPA PET might be a dynamic measure of DSC (i.e. state-like feature of schizophrenia), while as neuromelanin is a deposit, NM-MRI signal in the SN might reflect more chronic changes in dopamine synthesis (i.e. trait-like feature of schizophrenia). Third, in patients, the relationship between striatal DSC and VMAT-2 functioning might be dysfunctional. Although VMAT-2 function is unchanged in the striatum (46) and VMAT-2 binding in the ventral brainstem (which includes the SN/VTA) has been found to be elevated in patients with schizophrenia compared to HC (47), a post-mortem study found decreased VMAT-2 mRNA levels in the SN of patients with schizophrenia (48). This might indicate that in at least a subgroup of patients, increased DSC, which is suggested to be a core feature of the illness (1), might not always be accompanied by an increase in VMAT-2 functioning, which would consequently result in more cytosolic dopamine and thereby more deposition of neuromelanin. Finally, Kumakura et al. (2007) reported that besides elevated striatal [^{18}F]F-DOPA utilization (i.e. the net blood-brain clearance), patients with schizophrenia also exhibited reduced storage or retention of [^{18}F]-fluorodopamine within synaptic vesicles compared to HC (49). This would be in line with reduced VMAT-2 functioning in patients. Future studies should address [^{18}F]-FDOPA, VMAT-2, and NM-MRI measures in a large cohort of patients and HC to further elucidate the underlying relationships. In addition, it might be that the relation between striatal [^{18}F]-FDOPA and NM-MRI measures fluctuates over time, as seasonal effects on striatal DSC have

been reported in humans (50). Hence, establishing time-courses of [^{18}F]F-DOPA, VMAT-2, and NM-MRI measures across the lifespan, while taking into account factors such as illness duration, symptom severity, and antipsychotic medication usage, will provide more insight into temporal relationships between the different measures.

Previous studies reported elevated striatal DSC in patients with schizophrenia (as reviewed in Brugger, Angelescu (1)). In contrast, we found a significantly lower mean DSC in the sensorimotor striatum and no differences in the other striatal ROIs in patients compared to HC. These contrasting findings might be due to remission of psychosis in some patients, as lower DSC has been reported in the whole, associative, and sensorimotor striatum of patients in psychotic remission (51,52) (almost completely overlapping study samples). The group difference in the sensorimotor striatum did not remain significant when using GM k_i^{cer} of voxels with at least a 60% instead of a 90% probability of belonging to the sensorimotor striatum. This finding might therefore be an incidental finding. In addition, we found no significant group differences for NM-MRI signal in the SN. This might be due to the small sample size or heterogeneity, as schizophrenia is a heterogeneous disorder and the existence of multiple subgroups of patients with varying neurobiology has been suggested (53).

Strengths and limitations

A major strength of this study is that, to our knowledge, we are the first to combine NM-MRI and [^{18}F]F-DOPA PET in HC and patients with a schizophrenia spectrum disorder to assess their interrelationship. However, some limitations have to be taken into account. First, due to the difficulty in recruiting this study population and the complexity of the procedures, the sample size of our final sample is limited. To increase our sample size, we aggregated data from three studies with similar selection criteria that used the same NM-MRI and [^{18}F]F-DOPA scanning protocol, except for the length of the fasting time. As [^{18}F]F-DOPA competes with other substrates for transport across the blood-brain barrier, this might have influenced the [^{18}F]F-DOPA PET results. The sensitivity analysis, without five HC that fasted for two instead of six hours, remained borderline significant in the LST and was no longer significant for the whole striatum (Results S6), which is likely due to a lack of power. Second, [^{18}F]F-DOPA PET measures a combination of cellular processes (i.e. uptake and conversion of [^{18}F]-FDOPA, as well as, storage of [^{18}F]-fluorodopamine). Therefore, additional research needs to investigate which specific aspects of striatal dopamine synthesis are associated with NM-MRI signal in the SN. This might be done with compartmental modelling in combination with arterial blood sampling during data collection, or by use of other PET tracers, such as 6-[^{18}F]Fluoro-l-*m*-tyrosine (6-[^{18}F]FMT), which is not, unlike DOPA ligands, subject to transport into vesicles and post-release processes (54). Third, some participants were regular smokers and/or recreationally used drugs (mainly cannabis). We included these subjects, as a substantial

part of patients with a schizophrenia spectrum disorder uses nicotine and cannabis, and excluding these subject will therefore make recruitment even more difficult and result in a non-representative sample. We found no association between the number of cigarettes or cigars daily smoked by the tobacco users in our sample (4 patients; 2 HC; i.e. during the period when the subject used the most in the 12 months before study participation) and mean CNR in the SN or mean k_i^{cer} values in the whole, associative, limbic, and sensorimotor striatum or SN. Although acute effects of smoking on our imaging measures were likely to be small as the majority of subjects were nonsmokers and others were instructed to refrain from smoking two/three hours before the [^{18}F]F-DOPA PET scan, effects of smoking on striatal DSC are not yet completely understood and studies have reported higher (55), lower (56) and unchanged striatal DSC in smokers compared to nonsmokers (57). Further studies are needed to examine the short- and long-term effects of smoking on striatal DSC. Finally, we expect that previous recreational drug use had little effect on our outcome measures, as we selected participants with little to no drug use, who were not dependent on any substance (58).

Conclusion

NM-MRI and [^{18}F]F-DOPA PET are negatively related to each other in HC, but not significantly in patients with a schizophrenia spectrum disorder. These results indicate that [^{18}F]F-DOPA PET and NM-MRI are measures that reflect different aspects of dopaminergic functioning. We hypothesize that the negative correlation between neuromelanin and striatal DSC in HC might be explained by VMAT-2 functioning. A lack of a correlation in patients might be due to the small sample size or might be explained by effects of symptom severity or antipsychotic medication. In addition, striatal [^{18}F]F-DOPA PET might reflect a dynamic, state-like, aspect of dopaminergic functioning, while NM-MRI signal in the SN might reflect a chronic, trait-like, aspect of dopaminergic functioning. Future studies should assess the interrelationships between DSC, neuromelanin, VMAT-2, and related processes in larger homogeneous cohorts. As NM-MRI is more accessible than PET imaging, this might eventually enable clinicians and researchers to study specific aspects of the dopaminergic system of humans more efficiently and at lower costs.

References

1. Brugger SP, Angelescu I, Abi-Dargham A, Mizrahi R, Shahrezaei V, Howes OD. Heterogeneity of striatal dopamine function in schizophrenia: meta-analysis of variance. Biological psychiatry. 2020;87(3):215-24.
2. McCutcheon R, Beck K, Jauhar S, Howes OD. Defining the locus of dopaminergic dysfunction in schizophrenia: a meta-analysis and test of the mesolimbic hypothesis. Schizophrenia bulletin. 2018;44(6):1301-11.
3. Cassidy CM, Zucca FA, Girgis RR, Baker SC, Weinstein JJ, Sharp ME, et al. Neuromelanin-sensitive MRI as a noninvasive proxy measure of dopamine function in the human brain. Proceedings of the National Academy of Sciences. 2019;116(11):5108-17.
4. Zecca L, Bellei C, Costi P, Albertini A, Monzani E, Casella L, et al. New melanic pigments in the human brain that accumulate in aging and block environmental toxic metals. Proceedings of the National Academy of Sciences. 2008;105(45):17567-72.
5. Trujillo P, Summers PE, Ferrari E, Zucca FA, Sturini M, Mainardi LT, et al. Contrast mechanisms associated with neuromelanin-MRI. Magnetic resonance in medicine. 2017;78(5):1790-800.
6. Wieland L, Fromm S, Hetzer S, Schlagenhauf F, Kaminski J. Neuromelanin-Sensitive Magnetic Resonance Imaging in Schizophrenia: A Meta-Analysis of Case-Control Studies. Frontiers in psychiatry. 2021;12.
7. Sulzer D, Bogulavsky J, Larsen KE, Behr G, Karatekin E, Kleinman MH, et al. Neuromelanin biosynthesis is driven by excess cytosolic catecholamines not accumulated by synaptic vesicles. Proceedings of the National Academy of Sciences. 2000;97(22):11869-74.
8. Jauhar S, McCutcheon R, Borgan F, Veronese M, Nour M, Pepper F, et al. The relationship between cortical glutamate and striatal dopamine in first-episode psychosis: a cross-sectional multimodal PET and magnetic resonance spectroscopy imaging study. The Lancet Psychiatry. 2018;5(10):816-23.
9. Jauhar S, Nour MM, Veronese M, Rogdaki M, Bonoldi I, Azis M, et al. A test of the transdiagnostic dopamine hypothesis of psychosis using positron emission tomographic imaging in bipolar affective disorder and schizophrenia. JAMA psychiatry. 2017;74(12):1206-13.
10. Gründer G, Vernaleken I, Müller MJ, Davids E, Heydari N, Buchholz H-G, et al. Subchronic haloperidol downregulates dopamine synthesis capacity in the brain of schizophrenic patients in vivo. Neuropsychopharmacology. 2003;28(4):787-94.
11. Vernaleken I, Kumakura Y, Cumming P, Buchholz H-G, Siessmeier T, Stoeter P, et al. Modulation of [18F] fluorodopa (FDOPA) kinetics in the brain of healthy volunteers after acute haloperidol challenge. Neuroimage. 2006;30(4):1332-9.
12. Andreasen NC. Comprehensive Assessment of Symptoms and History (CASH): Department of Psychiatry, University of Iowa College of Medicine; 1987.
13. Ter Smitten M, Smeets R, Van den Brink W. Composite international diagnostic interview (CIDI), version 2.1, 12 months. Amsterdam: World Health Organization. 1998.
14. Sheehan DV, Lecrubier Y, Sheehan KH, Amorim P, Janavs J, Weiller E, et al. The Mini-International Neuropsychiatric Interview (MINI): the development and validation of a structured diagnostic psychiatric interview for DSM-IV and ICD-10. Journal of clinical psychiatry. 1998;59(20):22-33.
15. Kay SR, Fiszbein A, Opler LA. The positive and negative syndrome scale (PANSS) for schizophrenia. Schizophrenia bulletin. 1987;13(2):261-76.
16. Beck AT, Steer RA, Brown GK. Manual for the beck depression inventory-II. San Antonio, TX: Psychological Corporation. 1996;1(82):10.1037.
17. Van der Does A. De Nederlandse versie van de Beck depression inventory-Tweede Editie.[The Dutch version of the Beck depression inventory-]. Lisse, The Netherlands: Swets & Zeitlinger; 2002.
18. Leucht S, Samara M, Heres S, Davis JM. Dose equivalents for antipsychotic drugs: the DDD method. Schizophrenia bulletin. 2016;42(suppl_1):S90-S4.
19. Andreasen NC, Pressler M, Nopoulos P, Miller D, Ho B-C. Antipsychotic dose equivalents and dose-years: a standardized method for comparing exposure to different drugs. Biological psychiatry. 2010;67(3):255-62.
20. Hoffman JM, Melega WP, Hawk TC, Grafton

SC, Luxen A, Mahoney DK, et al. The effects of carbidopa administration on 6-[18F] fluoro-L-dopa kinetics in positron emission tomography. Journal of Nuclear Medicine. 1992;33(8):1472-7.

21. Sawle G, Burn D, Morrish P, Lammertsma A, Snow B, Luthra S, et al. The effect of entacapone (OR-611) on brain [18F]-6-L-fluorodopa metabolism: Implications for levodopa therapy of Parkinson's disease. Neurology. 1994;44(7):1292-.
22. Vollmar S, Cizek J, Sué M, Klein J, Jacobs A, Herholz K. VINCI-volume imaging in neurological research, co-registration and ROIs included. Forschung und wissenschaftliches Rechnen. 2003;2004(114):115-31.
23. Research MPIfM. VINCI 2020 Available from: http://vinci.sf.mpg.de/.
24. Čížek J, Herholz K, Vollmar S, Schrader R, Klein J, Heiss W-D. Fast and robust registration of PET and MR images of human brain. Neuroimage. 2004;22(1):434-42.
25. Quarantelli M, Berkouk K, Prinster A, Landeau B, Svarer C, Balkay L, et al. Integrated software for the analysis of brain PET/SPECT studies with partial-volume-effect correction. Journal of Nuclear Medicine. 2004;45(2):192-201.
26. Svarer C, Madsen K, Hasselbalch SG, Pinborg LH, Haugbøl S, Frøkjær VG, et al. MR-based automatic delineation of volumes of interest in human brain PET images using probability maps. Neuroimage. 2005;24(4):969-79.
27. Hammers A, Allom R, Koepp MJ, Free SL, Myers R, Lemieux L, et al. Three-dimensional maximum probability atlas of the human brain, with particular reference to the temporal lobe. Human brain mapping. 2003;19(4):224-47.
28. Patlak CS, Blasberg RG. Graphical evaluation of blood-to-brain transfer constants from multiple-time uptake data. Generalizations. Journal of Cerebral Blood Flow & Metabolism. 1985;5(4):584-90.
29. Boellaard R, Yaqub M, Lubberink M, Lammertsma A. PPET: a software tool for kinetic and parametric analyses of dynamic PET studies. NeuroImage. 2006(31):T62.
30. Hoshi H, Kuwabara H, Léger G, Cumming P, Guttman M, Gjedde A. 6-[18F] fluoro-L-dopa metabolism in living human brain: a comparison of six analytical methods. Journal of Cerebral Blood Flow & Metabolism. 1993;13(1):57-69.
31. Tziortzi AC, Haber SN, Searle GE, Tsoumpas C, Long CJ, Shotbolt P, et al. Connectivity-based functional analysis of dopamine release in the striatum using diffusion-weighted MRI and positron emission tomography. Cerebral cortex. 2014;24(5):1165-77.
32. Jenkinson M, Beckmann CF, Behrens TE, Woolrich MW. Smith sm. FSL neuroimage. 2012;62:782-90.
33. FSLeyes 2019 Available from: https://open.win.ox.ac.uk/pages/fsl/fsleyes/fsleyes/userdoc/.
34. Cassidy CM, Carpenter KM, Konova AB, Cheung V, Grassetti A, Zecca L, et al. Evidence for dopamine abnormalities in the substantia nigra in cocaine addiction revealed by neuromelanin-sensitive MRI. American Journal of Psychiatry. 2020;177(11):1038-47.
35. Xing Y, Sapuan A, Dineen RA, Auer DP. Life span pigmentation changes of the substantia nigra detected by neuromelanin-sensitive MRI. Movement Disorders. 2018;33(11):1792-9.
36. Veronese M, Santangelo B, Jauhar S, D'Ambrosio E, Demjaha A, Salimbeni H, et al. A potential biomarker for treatment stratification in psychosis: evaluation of an [18F] FDOPA PET imaging approach. Neuropsychopharmacology. 2021;46(6):1122-32.
37. Ito H, Kawaguchi H, Kodaka F, Takuwa H, Ikoma Y, Shimada H, et al. Normative data of dopaminergic neurotransmission functions in substantia nigra measured with MRI and PET: Neuromelanin, dopamine synthesis, dopamine transporters, and dopamine D2 receptors. Neuroimage. 2017;158:12-7.
38. Liang CL, Nelson O, Yazdani U, Pasbakhsh P, German DC. Inverse relationship between the contents of neuromelanin pigment and the vesicular monoamine transporter-2: human midbrain dopamine neurons. Journal of Comparative Neurology. 2004;473(1):97-106.
39. Cartier EA, Parra LA, Baust TB, Quiroz M, Salazar G, Faundez V, et al. A biochemical and functional protein complex involving dopamine synthesis and transport into synaptic vesicles. Journal of Biological Chemistry. 2010;285(3):1957-66.
40. Kumakura Y, Vernaleken I, Gründer G, Bartenstein P, Gjedde A, Cumming P. PET studies of net Blood—Brain clearance of FDOPA to human brain: age-dependent decline of [18F] Fluorodopamine storage capacity. Journal of Cerebral Blood Flow & Metabolism. 2005;25(7):807-19.
41. Zhang Y, Larcher KM-H, Misic B, Dagher A. Anatomical and functional organization of the human substantia nigra and its connections. Elife. 2017;6:e26653.
42. Martinez D, Slifstein M, Broft A, Mawlawi O, Hwang D-R, Huang Y, et al. Imaging human mesolimbic dopamine transmission with positron

emission tomography. Part II: amphetamine-induced dopamine release in the functional subdivisions of the striatum. Journal of Cerebral Blood Flow & Metabolism. 2003;23(3):285-300.

43. Peterson AC, Zhang S, Hu S, Chao HH, Li C-SR. The effects of age, from young to middle adulthood, and gender on resting state functional connectivity of the dopaminergic midbrain. Frontiers in Human Neuroscience. 2017;11:52.
44. van der Pluijm M, Wengler K, Reijers PN, Cassidy CM, Tjong Tjin Joe K, de Peuter OR, Horga G, Booij J, de Haan L, van de Giessen E, Neuromelanin MRI as candidate marker for treatment resistance in first episode schizophrenia patients.
45. Kumakura Y, Cumming P, Vernaleken I, Buchholz H-G, Siessmeier T, Heinz A, et al. Elevated [18F] fluorodopamine turnover in brain of patients with schizophrenia: an [18F] fluorodopa/positron emission tomography study. Journal of Neuroscience. 2007;27(30):8080-7.
46. Eisenberg DP, Kohn PD, Baller EB, Bronstein JA, Masdeu JC, Berman KF. Seasonal effects on human striatal presynaptic dopamine synthesis. Journal of Neuroscience. 2010;30(44):14691-4.
47. Avram M, Brandl F, Cabello J, Leucht C, Scherr M, Mustafa M, et al. Reduced striatal dopamine synthesis capacity in patients with schizophrenia during remission of positive symptoms. Brain. 2019;142(6):1813-26.
48. Brandl F, Knolle F, Avram M, Leucht C, Yakushev I, Priller J, et al. Negative symptoms, striatal dopamine and model-free reward decision-making in schizophrenia. Brain. 2022.
49. Howes OD, Kapur S. A neurobiological hypothesis for the classification of schizophrenia: type A (hyperdopaminergic) and type B (normodopaminergic). The British Journal of Psychiatry. 2014;205(1):1-3.
50. Endres CJ, Swaminathan S, DeJesus OT, Sievert M, Ruoho AE, Murali D, et al. Affinities of dopamine analogs for monoamine granular and plasma membrane transporters: implications for PET dopamine studies. Life sciences. 1997;60(26):2399-406.
51. Salokangas RK, Vilkman H, Ilonen T, Taiminen T, Bergman Jn, Haaparanta M, et al. High levels of dopamine activity in the basal ganglia of cigarette smokers. American Journal of Psychiatry. 2000;157(4):632-4.
52. Rademacher L, Prinz S, Winz O, Henkel K, Dietrich CA, Schmaljohann J, et al. Effects of smoking cessation on presynaptic dopamine function of addicted male smokers. Biological psychiatry. 2016;80(3):198-206.
53. Bloomfield MA, Pepper F, Egerton A, Demjaha A, Tomasi G, Mouchlianitis E, et al. Dopamine function in cigarette smokers: an [18F]-DOPA PET study. Neuropsychopharmacology. 2014;39(10):2397-404.
54. Bloomfield MA, Morgan CJ, Egerton A, Kapur S, Curran HV, Howes OD. Dopaminergic function in cannabis users and its relationship to cannabis-induced psychotic symptoms. Biological psychiatry. 2014;75(6):470-8.

Author Contributions

CvH, MvdP, MH, RvH, LdH, JPS, TvA, JB, and EvdG designed and planned the study. CvH, MvdP, and MH performed the data collection. CvH, CS, and MvdP analyzed the data under supervision of EvdG, FvV, GH, KW, and MY. CvH wrote the original draft of the manuscript. All authors reviewed and edited the manuscript. All authors have read and agreed to the published version of the manuscript.

Supplementary material

Table of contents:

Supplementary methods

Methods S1: Antipsychotic medication

To investigate the effect of antipsychotic medication on our outcome measures, we converted antipsychotic doses to 100 mg/day of chlorpromazine (CPZ) equivalents with the defined daily dose (DDD) method(1). We used the following conversion factors as provided in the Excel sheet of Leucht et al. (2018):

Antipsychotic (administration form)	Conversion factor
Risperidone (oral)	60
Olanzapine (oral	30
Olanzapine (depot)[1]	3.33
Quetiapine (oral)	0.75
Aripiprazol (oral)	20
Aripiprazol (depot)[1]	22.57
Clozapine (oral)	1
Haloperidol (oral)	37.5
Haloperidol (depot)[1]	90.90
Lurisadone (oral)	5
Clotiapine (oral)	3.75
Paliperidone (oral	50
Penfluridol (oral)	50
Amisulpride (oral)	0.75
Zuclopenthixol (oral)	10

[1]For depot drugs, the injected dose should be divided by the injection interval in days.

The current CPZ-equivalent dose was calculated by adding the CPZ-equivalent doses of all antipsychotic descriptions that were prescribed during the first scan. In addition, we also calculated the total number of days that patients had used antipsychotic medication at the time of the first scan. To obtain a cumulative measure of antipsychotic usage, we also calculated antipsychotic dose-years by use of Equation 1 (2). A dose-year is defined as the product of the CPZ-equivalent dose (or the dose equivalent to another standard antipsychotic, such as haloperidol) of a particular antipsychotic and the period on that dose expressed in years. This concept is equivalent to a pack-year, which is often used to quantify a person's exposure to tobacco.

$$DoseYears = \frac{(Dose) * (DaysOnDrugsDose)}{(CPZ-equivalent)(365.25)} \quad \text{(Equation 1)}$$

In Equation 1, Dose is equal to the dose of a given antipsychotic. For depot antipsychotics, the dose should be divided by the injection interval in days. DaysOnDrugsDose represents the number of days that a person has been using a particular dose of the antipsychotic. CPZ-equivalent is the amount of a particular antipsychotic equivalent to CPZ 100 mg. To account for leap years, 365.25 days/year were used.

Methods S2: Mask threshold of striatal subdivisions

In our analysis, we averaged ki^{cer} values across all grey matter (GM) voxels of the different functional subdivisions of the striatum. To ensure that only GM voxels within the subdivision were included in our analysis, we applied a conservative threshold, which allowed only GM voxels with at least a 90% chance of belonging to the subdivision to be included. To investigate the influence of mask threshold, we repeated the procedure with a more liberate threshold, which allowed GM voxels with at least a 60% chance of belonging to the subdivision to be included in the analysis. To ensure the validity of using a lower threshold, we investigated the Spearman's rank-order correlation between GM ki^{cer} values with a 60% and 90% probability of belonging to the striatal subdivision, across all participants of our final sample (12 patients; 16 controls). All of the correlations were significant: limbic striatum, rho = 0.993, 95%-confidence interval (CI): (0.98, 1.00), $p < 0.001$; associative striatum, rho = 0.959, 95%-CI: (0.90, 0.98), $p < 0.001$; sensorimotor striatum, rho = 0.951, 95%-CI: (0.88, 0.98), $p < 0.001$.

Methods S3: Quantification of head movement during [^{18}F]FDOPA PET

Head movement was quantified for each participant in our final sample. This was done by extracting the movement in the x-, y- and z-directions of the last PET frame relative to the reference frame from the coregistration step (see PET pre-processing section in the main article). We calculated the amount of head movement for each participant by using Equation 2.

$$Head\ movement\ (in\ mm) = \sqrt{(x^2 + y^2 + z^2)} \qquad \text{(Equation 2)}$$

In Equation 2, x is the movement in mm in the x-direction, y is the movement in mm in the y-direction, and z is the movement in the z-direction of the last PET frame relative to the reference frame.

Supplementary results

Results S1: Antipsychotic medication
All patients with a schizophrenia spectrum disorder used antipsychotic medication during the first scan. The different antipsychotic drugs that were used at that moment by patients in the final sample (N=12):

Antipsychotic drug(s)	Number of patients using these/this antipsychotic(s) during first scan
Haloperidol	2
Aripiprazole	2
Olanzapine	1
Quetiapine	5
Clozapine	1
Olanzapine & Aripiprazole	1

Results S2: Exclusion of participants

We excluded three patients with a schizophrenia spectrum disorder (SSD) and four healthy controls because of substantial head movement (>7.5 mm) during the [^{18}F]FDOPA PET scan. Three healthy controls and one patient with SSD were excluded due to poor neuromelanin data quality. In addition, we excluded one control due to the occurrence of significant illness after study participation, one patient with SSD due to the presence of structural brain damage, and one patient with SSD due to early termination of the [^{18}F]FDOPA PET scan.

Results S3: Group differences striatal subdivisions with a 0.6 threshold in patients with a schizophrenia spectrum disorder and healthy controls[1]

	Patients N=12	Healthy controls N=16	p-value
ki^{cer} LST (0.6 threshold), mean (SD)	0.0163 (0.0019)	0.0170 (0.0013)	0.163
ki^{cer} AST (0.6 threshold), mean (SD)	0.0170 (0.0024)	0.0177 (0.0012)	0.210
ki^{cer} SMST (0.6 threshold), mean (SD)	0.0188 (0.0036)	0.0202 (0.0021)	0.054

Abbreviations: AST, associative striatum; LST, limbic striatum; SMST, sensorimotor striatum.
[1]Group differences were assessed with the Mann-Whitney U test.

Results S4: Post-injection mean standardized uptake values of [^{18}F]FDOPA in grey matter cerebellum of patients with a schizophrenia spectrum disorder and healthy controls[1]

Timepoint post-injection	Patients N=12	Healthy controls N=16	p-value
1 min, mean SUV (SD)	1.20 (0.23)	1.15 (0.25)	0.616
2 min, mean SUV (SD)	1.48 (0.34)	1.44 (0.35)	0.738
3 min, mean SUV (SD)	1.61 (0.37)	1.59 (0.40)	0.900
4 min, mean SUV (SD)	1.72 (0.40)	1.73 (0.42)	0.947
5 min, mean SUV (SD)	1.80 (0.43)	1.82 (0.45)	0.916
7 min, mean SUV (SD)	1.88 (0.45)	1.92 (0.47)	0.827
9 min, mean SUV (SD)	1.94 (0.48)	2.02 (0.50)	0.693
11 min, mean SUV (SD)	1.98 (0.49)	2.06 (0.51)	0.649
14 min, mean SUV (SD)	1.97 (0.51)	2.09 (0.52)	0.519
17 min, mean SUV (SD)	1.94 (0.52)	2.07 (0.52)	0.509
20 min, mean SUV (SD)	1.89 (0.51)	2.04 (0.52)	0.459
25 min, mean SUV (SD)	1.80 (0.49)	1.96 (0.51)	0.409
30 min, mean SUV (SD)	1.68 (0.47)	1.85 (0.48)	0.363
35 min, mean SUV (SD)	1.58 (0.45)	1.74 (0.46)	0.360
40 min, mean SUV (SD)	1.46 (0.42)	1.62 (0.43)	0.350
45 min, mean SUV (SD)	1.35 (0.39)	1.51 (0.41)	0.312
50 min, mean SUV (SD)	1.25 (0.36)	1.41 (0.38)	0.254
55 min, mean SUV (SD)	1.16 (0.34)	1.32 (0.36)	0.251
60 min, mean SUV (SD)	1.09 (0.32)	1.23 (0.34)	0.259
65 min, mean SUV (SD)	1.02 (0.30)	1.17 (0.33)	0.244
70 min, mean SUV (SD)	0.96 (0.28)	1.10 (0.31)	0.244
75 min, mean SUV (SD)	0.92 (0.27)	1.04 (0.29)	0.287
80 min, mean SUV (SD)	0.87 (0.26)	0.98 (0.28)	0.289
85 min, mean SUV (SD)	0.83 (0.24)	0.93 (0.26)	0.328
90 min, mean SUV (SD)	0.79 (0.23)	0.89 (0.25)	0.306

Abbreviations: SD, standard deviation; SUV, standardized uptake value in cerebellar grey matter corrected for body weight.
Group differences for each time point were assessed with an independent t-test.

Results S5: Voxelwise analyses in the SN of patients with a schizophrenia spectrum disorder and healthy controls with additional subjects[1]
For this analysis, we added the data of subjects who moved >7.5 mm during the PET acquisition:

	Description of movement
Extra HC 1	Movement from frame 18 onwards (45 min). Linear fitting was conducted on the PET images acquired between 25 and 45 minutes.
Extra HC 2	Movement from frame 19 onwards (50 min). Linear fitting was conducted on the PET images acquired between 25 and 50 minutes.
Extra HC 3	Movement from frame 23 onwards (70 min). Linear fitting was conducted on the PET images acquired between 25 and 70 minutes.
Extra HC 4	Movement from frame 24 onwards (75 min). Linear fitting was conducted on the PET images acquired between 25 and 75 minutes.
Extra patient 1	Movement from frame 16 onwards (35 min). Linear fitting was conducted on the PET images acquired between 25 and 35 minutes.
Extra patient 2	Movement from frame 16 onwards (35 min). Linear fitting was conducted on the PET images acquired between 25 and 35 minutes.
Extra patient 3	Movement from frame 18 onwards (45 min). Linear fitting was conducted on the PET images acquired between 25 and 45 minutes.

Group	**Brain region for which mean kicer values are used in the analysis**	**Number of voxels in cluster with positive association**	**Positive corrected p-value**	**Number of voxels in cluster with negative association**	**Negative corrected p-value**
HC (N=20)	LST (0.9 threshold)	48/1480	0.587	275/1480	**0.015**
HC (N=20)	WS	18/1480	0.880	261/1480	**0.021**
Patients (N=15)	LST (0.9 threshold)	90/1480	0.290	35/1480	0.842
Patients (N=15)	WS	76/1480	0.428	34/1480	0.882

Significant results are bold. Abbreviations: HC, healthy controls; LST, limbic striatum; WS, whole striatum. Robust linear regression controlling for age. p-corrected < 0.05

Results S6: Voxelwise analysis of the relationship between NM-MRI signal in the SN and mean DSC in the striatum without healthy controls who fasted two instead of six hours[1]

Group	**Brain region for which mean kicer values are used in the analysis**	**Number of voxels in cluster with positive association**	**Positive corrected p-value**	**Number of voxels in cluster with negative association**	**Negative corrected p-value**
HC (N=11)	WS	10/1480	0.965	126/1480	0.167
HC (N=11)	LST (0.9 threshold)	6/1480	0.990	222/1480	0.051

Abbreviations: AST, associative striatum; HC, healthy controls; LST, limbic striatum; SMST, sensorimotor striatum; WS, whole striatum.[1]Robust linear regression controlling for age. p-corrected < 0.05.

Results S7: Voxelwise analysis of the relationship between NM-MRI signal in the SN and mean DSC in the striatum of patients with a schizophrenia spectrum disorder and healthy controls[1]

Group	Brain region for which mean ki^{cer} values are used in the analysis	Number of voxels in cluster with positive association	Positive corrected p-value	Number of voxels in cluster with negative association	Negative corrected p-value
Patients (N=12)	WS	40/1480	0.834	39/1480	0.814
Patients (N=12)	LST (0.9 threshold)	41/1480	0.792	49/1480	0.674
Patients (N=12)	AST (0.9 threshold)	47/1480	0.728	41/1480	0.784
Patients (N=12)	SMST (0.9 threshold)	38/1480	0.830	46/1480	0.702
HC (N=16)	WS	32/1480	0.760	218/1480	**0.033**
HC (N=16)	LST (0.9 threshold)	29/1480	0.780	333/1480	**0.005**
HC (N=16)	AST (0.9 threshold)	21/1480	0.877	78/1480	0.364
HC (N=16)	SMST (0.9 threshold)	109/1480	0.214	66/1480	0.437

Significant results are bold.Abbreviations: AST, associative striatum; HC, healthy controls; LST, limbic striatum; SMST, sensorimotor striatum; WS, whole striatum.
[1]Robust linear regression controlling for age. p-corrected < 0.05.

Results S8: Voxelwise analysis of the relationship between NM-MRI signal in the SN and mean DSC in the striatal subdivisions with a 0.6 threshold in patients with a schizophrenia spectrum disorder and healthy controls[1]

Group	Brain region for which mean ki^{cer} values are used in the analysis	Number of voxels in cluster with positive association	Positive corrected p-value	Number of voxels in cluster with negative association	Negative corrected p-value
Patients (N=12)	LST (0.6 threshold)	34/1480	0.866	46/1480	0.704
Patients (N=12)	AST (0.6 threshold)	39/1480	0.834	42/1480	0.774
Patients (N=12)	SMST (0.6 threshold)	47/1480	0.695	47/1480	0.685
HC (N=16)	LST (0.6 threshold)	36/1480	0.704	309/1480	**0.008**
HC (N=16)	AST (0.6 threshold)	15/1480	0.926	83/1480	0.330
HC (N=16)	SMST (0.6 threshold)	115/1480	0.186	80/1480	0.343

Significant results are bold.Abbreviations: AST, associative striatum; HC, healthy controls; LST, limbic striatum; SMST, sensorimotor striatum.
[1]Robust linear regression controlling for age. p-corrected < 0.05.

Results S9: Voxelwise analysis of the relationship between NM-MRI signal in the SN and mean DSC in the SN of patients with a schizophrenia spectrum disorder and healthy controls[1]

Group	Brain region for which mean ki^{cer} values are used in the analysis	Number of voxels in cluster with positive association	Positive corrected p-value	Number of voxels in cluster with negative association	Negative corrected p-value
Patients (N=12)	SN (0.5 threshold)	34/1480	0.833	58/1480	0.531
HC (N=16)	SN (0.5 threshold)	100/1480	0.259	26/1480	0.828

Abbreviations: HC, healthy controls; SN, substantia nigra.[1]Robust linear regression controlling for age. p-corrected < 0.05.

Results S10: Association between mean NM-MRI signal within the whole SN mask and mean ki^{cer} values in patients with a schizophrenia spectrum disorder and healthy controls[1]

	ROI	Statistics
Patients (N=12)	Mean ki^{cer} WS	rho = 0.110, 95%-CI[2]: (-0.50:0.64), p = 0.748
	Mean ki^{cer} LST (0.9 threshold)	rho = 0.077, 95%-CI: (-0.52:0.62), p = 0.822
	Mean ki^{cer} AST (0.9 threshold)	rho = 0.140, 95%-CI: (-0.47:0.66), p = 0.682
	Mean ki^{cer} SMST (0.9 threshold)	rho = 0.050, 95%-CI: (-0.54:0.61), p = 0.883
	Mean ki^{cer} LST (0.6 threshold)	rho = 0.059, 95%-CI: (-0.53:0.61), p = 0.863
	Mean ki^{cer} AST (0.6 threshold)	rho = -0.031, 95%-CI: (-0.59:0.55), p = 0.928
	Mean ki^{cer} SMST (0.6 threshold)	rho = 0.068, 95%-CI: (-0.53:0.62), p = 0.842
	Mean ki^{cer} SN	rho = -0.103, 95%-CI: (-0.64:0.50), p = 0.762
HC (N=16)	Mean ki^{cer} WS	rho = -0.424, 95%-CI: (-0.77:0.11), p = 0.116
	Mean ki^{cer} LST (0.9 threshold)	rho = -0.343, 95%-CI: (-0.72:0.20), p = 0.211
	Mean ki^{cer} AST (0.9 threshold)	rho = -0.436, 95%-CI: (-0.78:0.10), p = 0.104
	Mean ki^{cer} SMST (0.9 threshold)	rho = -0.070, 95%-CI: (-0.55:0,44), p = 0.804
	Mean ki^{cer} LST (0.6 threshold)	rho = -0.229, 95%-CI: (-0.65:0.31), p = 0.412
	Mean ki^{cer} AST (0.6 threshold)	rho = -0.332, 95%-CI: (-0.72:0.21), p = 0.226
	Mean ki^{cer} SMST (0.6 threshold)	rho = -0.050, 95%-CI: (-0.53:0.46), p = 0.858
	Mean ki^{cer} SN	rho = 0.153, 95%-CI: (-0.37:0.60), p = 0.587

Abbreviations: AST, associative striatum; HC, healthy controls; LST, limbic striatum; NM-MRI, neuromelanin-sensitive magnetic resonance imaging; ROI, region-of-interest; SMST, sensorimotor striatum; WS, whole striatum; 95%-CI,
95%-confidence interval.[1]We conducted Spearman's rank-order correlation coefficient tests with age as covariate.[2]95%-CI were calculated by use of Fisher z-transformation.

Results S11: Associations between imaging measures and clinical variables in patients with a schizophrenia spectrum disorder[1,2]

	Positive PANSS scores	Negative PANSS scores	General PANSS scores	Total PANSS scores	BDI scores	Age[3]
Mean NM-MRI signal in SN[4]	rho = 0.219 p = 0.518 95%-CI[5]: (-0.41:0.71)	rho = 0.231 p = 0.495 95%-CI: (-0.40:0.71)	rho = 0.346 p = 0.297 95%-CI: (-0.30:0.78)	rho = 0.349 p = 0.294 95%-CI: (-0.30:0.78)	rho = -0.267 p = 0.427 95%-CI: (-0.73:0.37)	rho = -0.563 p = 0.057 95%-CI: (-0.87:0.07)
Mean *ki*^{cer} WS	rho = 0.352 p = 0.262 95%-CI: (-0.30:0.78)	rho = 0.345 p = 0.272 95%-CI: (-0.30:0.77)	rho = 0.112 p = 0.729 95%-CI: (-0.50:0.65)	rho = 0.245 p = 0.442 95%-CI: (-0.39:0.72)	rho = 0.137 p = 0.671 95%-CI: (-0.48:0.66)	rho = -0.177 p = 0.582 95%-CI: (-0.68:0.45)
Mean *ki*^{cer} LST (0.9 threshold)	rho = 0.428 p = 0.166 95%-CI: (-0.22:0.81)	rho = 0.205 p = 0.523 95%-CI: (-0.42:0.70)	rho = 0.063 p = 0.845 95%-CI: (-0.53:0.62)	rho = 0.204 p = 0.525 95%-CI: (-0.42:0.70)	rho = 0.030 p = 0.926 95%-CI: (-0.55:0.59)	rho = -0.144 p = 0.656 95%-CI: (-0.66:0.47)
Mean *ki*^{cer} AST (0.9 threshold)	rho = 0.515 p = 0.087 95%-CI: (-0.13:0.85)	rho = 0.279 p = 0.380 95%-CI: (-0.36:0.74)	rho = 0.140 p = 0.664 95%-CI: (-0.47:0.66)	rho = 0.312 p = 0.323 95%-CI: (-0.33:0.76)	rho = 0.058 p = 0.858 95%-CI: (-0.53:0.61)	rho = -0.243 p = 0.447 95%-CI: (-0.72:0.39)
Mean *ki*^{cer} SMST (0.9 threshold)	rho = 0.279 p = 0.380 95%-CI: (-0.36:0.74)	rho = 0.085 p = 0.794 95%-CI: (-0.51:0.63)	rho = -0.056 p = 0.863 95%-CI: (-0.61:0.54)	rho = 0.063 p = 0.845 95%-CI: (-0.53:0.62)	rho = 0.217 p = 0.499 95%-CI: (-0.41:0.71)	rho = -0.032 p = 0.922 95%-CI: (-0.60:0.55)
Mean *ki*^{cer} SN	rho = 0.078 p = 0.811 95%-CI: (-0.52:0.62)	rho = -0.078 p = 0.811 95%-CI: (-0.62:0.52)	rho = -0.231 p = 0.470 95%-CI: (-0.71:0.40)	rho = -0.144 p = 0.656 95%-CI: (-0.66:0.47)	rho = -0.336 p = 0.285 95%-CI: (-0.77:0.31)	rho = -0.229 p = 0.475 95%-CI: (-0.71:0.40)

Abbreviations: AST, associative striatum; BDI, Beck Depression Inventory; LST, limbic striatum; NM-MRI, neuromelanin-sensitive magnetic resonance imaging; PANSS, positive and negative symptom scale; SN, substantia nigra; SMST, sensorimotor striatum; WS, whole striatum; 95%-CI, 95%-confidence interval.
[1]We conducted Spearman's rank-order correlation coefficient tests. [2]N=12. [3]Age during PET and MRI scans. [4]Correlation analyses with mean NM-MRI signal in the SN and clinical scores were corrected for age. [5]95%-CI were calculated by use of Fisher z-transformation.

Results S12: Associations between imaging measures and antipsychotic medication in patients with a schizophrenia spectrum disorder[1,2,3]

	Total number of days on medication	**CPZ-equivalent dose**	**CPZ dose-years**
Mean NM-MRI signal in SN[4]	rho = 0.165 p = 0.627 95%-CI[5]: (-0.46:0.68)	rho = -0.327 p = 0.326 95%-CI: (-0.77:0.32)	rho = 0.279 p = 0.406 95%-CI: (-0.36:0.74)
Mean ki^{cer} WS	rho = 0.035 p = 0.914 95%-CI: (-0.55:0.60)	rho = -0.392 p = 0.207 95%-CI: (-0.80:0.26)	rho = -0.147 p = 0.649 95%-CI: (-0.67:0.47)
Mean ki^{cer} LST (0.9 threshold)	rho = 0.109 p = 0.736 95%-CI: (-0.50:0.64)	rho = -0.257 p = 0.420 95%-CI: (-0.73:0.38)	rho = -0.119 p = 0.712 95%-CI: (-0.65:0.49)
Mean ki^{cer} AST (0.9 threshold)	rho = 0.067 p = 0.837 95%-CI: (-0.53:0.62)	rho = -0.086 p = 0.792 95%-CI: (-0.63:0.51)	rho = -0.081 p = 0.803 95%-CI: (-0.63:0.52)
Mean ki^{cer} SMST (0.9 threshold)	rho = -0.095 p = 0.770 95%-CI: (-0.64:0.51)	rho = -0.113 p = 0.727 95%-CI: (-0.65:0.49)	rho = -0.116 p = 0.721 95%-CI: (-0.65:0.49)
Mean ki^{cer} SN	rho = 0.284 p = 0.372 95%-CI: (-0.36:0.74)	rho = -0.033 p = 0.920 95%-CI: (-0.60:0.55)	rho = -0.053 p = 0.871 95%-CI: (-0.61:0.54)

Abbreviations: AST, associative striatum; CPZ, chlorpromazine; LST, limbic striatum; NM-MRI, neuromelanin-sensitive magnetic resonance imaging; SN, substantia nigra; SMST, sensorimotor striatum; WS, whole striatum.
[1]At the moment of the first scan. [2]We conducted Spearman's rank-order correlation coefficient tests. [3]N=12.
[4]Correlation analyses with mean NM-MRI signal in the SN and medication variables were corrected for age.
[5]95%-CI were calculated by use of Fisher z-transformation.

Results S13: Associations between imaging measures and clinical variables in healthy controls[1,2]

	DI scores[3]	**Age**[4]
Mean NM-MRI signal in SN	rho = -0.597 p = 0.069 95%-CI[5]: (-0.90:0.06)	rho = 0.177 p = 0.512 95%-CI: (-0.35:0.62)
Mean *ki*^{cer} WS	rho = 0.210 p = 0.536 95%-CI: (-0.45:0.72)	rho = -0.410 p = 0.114 95%-CI: (-0.76:0.13)
Mean *ki*^{cer} LST (0.9 threshold)	rho = 0.403 p = 0.219 95%-CI: (-0.29:0.82)	rho = -0.603 **p = 0.013** 95%-CI: (-0.86:-0.11)
Mean *ki*^{cer} AST (0.9 threshold)	rho = 0.227 p = 0.503 95%-CI: (-0.44:0.73)	rho = -0.443 p = 0.086 95%-CI: (-0.78:0.09)
Mean *ki*^{cer} SMST (0.9 threshold)	rho = 0.146 p = 0.669 95%-CI: (-0.50:0.69)	rho = -0.245 p = 0.360 95%-CI: (-0.67:0.29)
Mean *ki*^{cer} SN	rho = 0.036 p = 0.916 95%-CI: (-0.58:0.62)	rho = -0.377 p = 0.150 95%-CI: (-0.74:0.16)

Significant results are bold. Abbreviations: AST, associative striatum; BDI, Beck Depression Inventory; LST, limbic striatum; NM-MRI, neuromelanin-sensitive magnetic resonance imaging; SN, substantia nigra; SMST, sensorimotor striatum; WS, whole striatum.
[1]We conducted Spearman's rank-order correlation coefficient tests. [2]N=11 for the correlation with BDI and N=16 for the correlation with age. [3]Correlation analyses with mean NM-MRI signal in the SN and BDI were corrected for age.
[4]Age during PET and MRI scans. [5]95%-CI were calculated by use of Fisher z-transformation.

Supplementary figure

Figure S1: Post-injection mean standardized uptake values of [18F]FDOPA in grey matter cerebellum of patients with a schizophrenia spectrum disorder and healthy controls

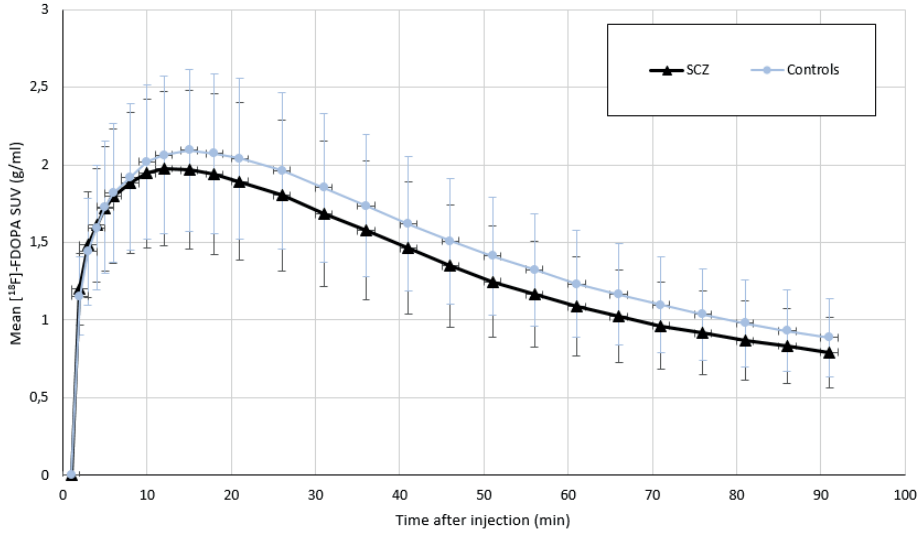

Mean standardized uptake values (SUV), corrected for body weight, in cerebellar grey matter of patients with a schizophrenia spectrum disorder (N=12) is comparable to healthy controls (N=16). Abbreviations: SCZ, patients with a schizophrenia spectrum disorder; SUV, standardized uptake values.

References

1. Leucht, S., Samara, M., Heres, S., & Davis, J. M. Dose equivalents for antipsychotic drugs: the DDD method. Schizophrenia bulletin. 2016;42,S90-S94.
2. Andreasen NC, Pressler M, Nopoulos P, Miller D, Ho B-C. Antipsychotic dose equivalents and dose-years: a standardized method for comparing exposure to different drugs. Biological psychiatry. 2010;67(3):255-62.

PART III

MARKERS FOR TREATMENT RESISTANT SCHIZOPHRENIA

Chapter | 7

Neuromelanin-sensitive MRI as candidate marker for treatment resistance in first episode schizophrenia

Marieke van der Pluijm, Kenneth Wengler, Pascalle N. Reijers, Clifford M. Cassidy, Kaithlyn Tjong Tjin Joe, Olav R. de Peuter, Guillermo Horga, Jan Booij, Lieuwe de Haan, Elsmarieke van de Giessen

Revised version under review

Abstract

Objective: Markers for treatment resistance in schizophrenia are needed to reduce delays in effective treatment. Nigrostriatal hyperdopaminergic function plays a critical role in the pathology of schizophrenia, yet antipsychotic non-responders do not show increased dopamine function. Neuromelanin-sensitive MRI (NM-MRI), which indirectly measures dopamine function in the substantia nigra (SN), has potential as a non-invasive marker for non-responders. Increased NM-MRI signal has been shown in psychosis, but has not yet been assessed in non-responders.

Methods: The current study investigates whether non-responders show lower NM-MRI signal than responders. We acquired NM-MRI scans in 79 patients with first episode psychosis and 20 matched healthy controls. Treatment response was assessed at a six-month follow-up. An a-priori voxelwise analysis within the SN tested the relation between NM-MRI signal and treatment response in patients.

Results: Fifteen patients were classified as non-responders and 47 patients as responders. Eighteen patients were excluded, primarily due to non-compliance or change in diagnosis. Voxelwise analysis revealed 297 significant voxels in the ventral tier of the SN negatively associated with treatment response. Non-responders and healthy controls had significantly lower NM-MRI signal than responders. Receiver operating characteristic curve analysis showed that NM-MRI signal separated non-responders with area-under-the-curves between 0.62-0.85. In addition, NM-MRI signal in patients did not change over six months.

Conclusion: These findings provide further evidence for dopaminergic differences between non-responders and responders, and support the potential of NM-MRI as a clinically applicable marker for treatment resistance in schizophrenia.

Introduction

Treatment resistance in schizophrenia is a major clinical problem with 20-35% of psychotic patients not responding to at least two adequate trials with first line antipsychotic treatment (1). In clinical practice, patients are often months to years on ineffective treatment before switching to potentially effective treatment (2). This delay results in prolonged experience of side effects of ineffective antipsychotics, poorer prognosis and decreased responsiveness (2,3). Hence, there is an urgent need for markers to identify non-responders in schizophrenia at an early stage and facilitate timely initiation of clozapine, the only antipsychotic with proven efficacy in non-responders (4). Ideally these markers would be non-invasive to facilitate incorporation into clinical practice.

A well-established finding in schizophrenia is increased striatal dopamine function, which is associated with positive symptoms (5,6). On average patients with schizophrenia show a moderate increase in striatal dopamine synthesis capacity compared to healthy controls as measured with [^{18}F]F-DOPA positron emission tomography (PET) (7). Crucially, non-responders do not show this elevation in striatal dopamine synthesis capacity and instead show levels comparable to healthy controls (8-10). These findings suggest a different neurobiological mechanism underlying symptoms in non-responders, which could explain why antipsychotics, predominantly acting as dopamine antagonists, are ineffective in this population (11). Moreover, they suggest the potential of dopaminergic-function markers for treatment resistance. Indeed, striatal dopamine synthesis capacity has shown to be able to identify 40%-60% of non-responders with a specificity of 100% and area-under-the-curves (AUC) of 0.78-0.88 using [^{18}F]F-DOPA PET (12). However, PET imaging is currently not feasible for routine clinical screening to identify non-responders, given its costs, invasiveness, and associated radiation exposure.

Recently, neuromelanin-sensitive magnetic resonance imaging (NM-MRI) has been developed to measure dopamine function non-invasively (13). Neuromelanin deposition depends on cytosolic dopamine excess in dopamine cells, itself increases with dopamine synthesis (14), and accumulates in dopaminergic cell bodies in the substantia nigra (SN), in particular pars compacta, and ventral tegmental area (15,16). These midbrain dopaminergic neurons are an anatomically heterogeneous group of cells most prominently located ventral, in the SN pars compacta, and project predominantly to the dorsal striatum through the nigrostriatal pathway (17).

The paramagnetic neuromelanin-iron complexes which lead to T1 reduction in combination with reduced magnetization-transfer effects results in high signal intensity in the SN using NM-MRI (18,19). NM-MRI signal correlates with regional neuromelanin concentration in post-mortem SN tissue and to PET measures of dopamine release in the dorsal striatum *in*

vivo (20). Further, NM-MRI exhibits excellent test-retest reliability, including for voxelwise analyses (20-22). SN NM-MRI is therefore a reliable proxy measure of dopamine function in the nigrostriatal pathway. In schizophrenia, NM-MRI SN signal is increased compared to healthy controls (23). In particular signal in a ventral/anterior subregion of the SN was positively associated with positive symptoms (20). These results are in line with previous PET studies on presynaptic dopamine function in striatum and SN (7,24) and support NM-MRI's ability to index hyperdopaminergic function in schizophrenia. However, NM-MRI has not yet been investigated in treatment resistant schizophrenia. The aim of the current study is to assess whether, in line with earlier [^{18}F]F-DOPA PET results, NM-MRI SN signal is elevated in treatment responders compared to non-responders, a crucial first step to evaluate NM-MRI's potential as an non-invasive marker for treatment resistance in first episode schizophrenia.

Methods

Participants

We recruited first episode psychosis patients with a primary diagnosis in the schizophrenia spectrum through specialized Early Psychosis Clinics in Amsterdam, the Netherlands. All patients were diagnosed according to DSM-5 criteria by a specialized early psychosis psychiatrist and were undergoing treatment at a specialized early psychosis clinic. Healthy volunteers were recruited through (online) advertisement as control group. All participants were between 18 and 35 years. Exclusion criteria included: use of antipsychotic medication longer than one year; past or present substance use disorder and current substance use with the exception of nicotine, alcohol and cannabis; use of dopaminergic drugs; neurological disorder or brain damage; MRI contraindications and pregnancy. We allowed for medication use up to one year and cannabis use to acquire a representative group of first episode patients with an initial referral to a specialized early psychosis clinic. Additional exclusion criteria for controls included current or past diagnosis of a psychiatric disorder, psychotropic medication use and positive family history (first and second degree) for psychotic disorders. Controls were matched based on age, gender, IQ and smoking status. This study was approved by the Medical Ethics Committee of the Amsterdam Medical Centre, University of Amsterdam (METC 2017_307) and registered at the Central Committee on Research Involving Human Subjects (NL63410.018.17). All participants provided written informed consent before entering the study, after receiving a complete description of the study.

Study design

Participants were assessed at baseline and patients were consecutively followed up at six months to determine treatment response status. Baseline measurements included a MRI scan, clinical interview and a IQ test. During the interview general information, including demographics, current and past medication use and medical history were collected. Symptom severity in patients was measured using the Positive and Negative Syndrome Scale (PANSS)

(25). The Mini-International Neuropsychiatric Interview (MINI) was conducted in the healthy controls to rule out the presence of any psychiatric disorder (26). Global functioning was measured using the Global Assessment of Functioning (GAF) scale. Alcohol and drug use were measured with the Composite International Diagnostic Interview (CIDI) (27). IQ was determined by the shortened version of the Wechsler Adult Intelligence Scale (WAIS-III) (28). Socio-economic status (SES) was determined based on parental education and occupation (29). In addition, if consent was given, antipsychotic drug serum levels were measured, and/or patients' relatives were contacted to evaluate adherence to antipsychotic medication. Patients were excluded from analysis if treatment response could not be determined due antipsychotic drug serum levels that were below the therapeutic range, as defined by ARUP laboratories (https://ltd.aruplab.com), and/or patients were non-adherent according patients' relatives. During the entire study, patients were prescribed antipsychotic treatment based on standard clinical guidelines by their treating psychiatrist.

Treatment response

Treatment response was assessed after six months, in a follow-up clinical interview. Patients were considered non-responders if they showed non-response despite at least two trials of different antipsychotics with a duration of at least 6 weeks, or after 4 weeks if there was complete absence of response or if severe side-effects occurred, at adequate antipsychotic dose for first episode psychosis as defined by the Dutch Multidisciplinary Guidelines Schizophrenia (30). Non-response was defined when at least one of the following items of the PANSS was scored as moderate or higher (score equal or higher than 4): delusions (P1), conceptual disorganization (P2), hallucinatory behaviour (P3), mannerisms and posturing (G5) and unusual thought content (G9) (31). Patients were also classified as non-responders when their medication was switched to clozapine during the follow-up period. For patients who were lost to follow up, response was determined based on medical files and contact with their clinician. Patients were classified as non-responders if they were treated with clozapine and as responders if the clinician reported a clear and sustained overall improvement in symptoms on standard antipsychotics. If treatment response could not be determined, patients were excluded. If consent was given, a follow-up blood draw was conducted to measure antipsychotic serum levels and patients' relatives were contacted again to evaluate adherence to antipsychotic medication. Additionally, a follow-up MRI scan was conducted in patients who consented.

NM-MRI Acquisition

All MRI scans were acquired using a 3 Tesla MR scanner (Phillips, Ingenia Elition X, Best, The Netherlands) with a 32-channel head coil. Participants were asked to refrain from alcohol and cannabis 24 hours in advance of the scan. Prior to the MRI scan urine drug screening was performed, as well as a pregnancy test for women. For NM-MRI slice placement and preprocessing, whole-brain structural T1-weighted volumetric images were acquired (echo time [TE]/repetition time [TR]=4.1/9.0 ms; 189 slices; field of view [FOV]=284×284×170 mm;

voxel size: 0.9×0.9×0.9 mm, flip angle [FA]=8˚). For NM-MRI images, a 2D gradient recalled echo sequence with off-resonance magnetization transfer pulses was performed (TE/TR=3.9/260 ms, 8 slices, FOV=162×199 mm, slice thickness=2.5 mm, FA=40˚, resolution=0.39×0.39 mm^2, number of signal averages=2, magnetization transfer frequency offset and duration=1200 Hz and 15.6 ms). The NM-MRI was oriented perpendicular to the fourth ventricle floor, with slices placed from the posterior commissure to halfway through the pons.

NM-MRI analysis

The NM-MRI was preprocessed using a previously validated pipeline (22). The pipeline was written in Matlab (The MathWorks, Inc., 2019) and included ANTs (32), SPM12(33), and AFNI(34) routines. In short, preprocessing steps were as follows: 1) NM images were coregistered to the T1-weighted image using ANTs Rigid registration; 2) Brain extraction was performed for the T1-weighted images using ANTs Brain Extraction; 3) T1-weigthed images were spatially normalized into MNI standard space using ANTs MNI deformable registration; 4) The coregistered NM-MRI images were spatially normalized by applying the warping parameters that were used to normalize the T1-weigthed images to MNI space; 5) The normalized NM-MRI images were spatially smoothed with a 1-mm full-width-at-half-maximum Gaussian kernel using AFNI-smoothing. After preprocessing, all images were visually inspected using standardized quality-control summary outputs (example in the online supplement).

A-priori voxelwise analysis

For the *a-priori* voxelwise analysis of the NM-MRI signal in the SN, a mask of the SN-ventral tegmental area (SN-VTA) complex was used. This mask was created in a previous study by manually tracing the hyperintense region representing the SN-VTA complex of a NM-MRI template (20). The tracing was deliberately overinclusive to facilitate inclusion of all voxels of the SN-VTA complex from all participants. The neighbouring hypointense region constituting the crus cerebri (CC) was traced as a reference region since it is known to have negligible NM content (20).

The NM-MRI signal from these regions was used to calculate the contrast ratio (CR). The CR at each voxel was calculated as percent NM-MRI signal difference between each voxel in the SN-VTA mask (I_V) and the mode of the signal intensity in the CC (I_{CC}), with the following formula: $CR_V = \left\{\frac{[I_V - \text{mode}(I_{CC})]}{\text{mode}(I_{CC})}\right\} * 100$. The mode I_{CC} was calculated for each participant from a kernel-smoothing-function fit of a histogram of all voxels in the CC mask, as this enhances robustness to outliers and edge artifacts (20).

The *a-priori* analysis tested differences between non-responders and responders using a voxelwise robust linear regression predicting CR within the SN-VTA based on treatment-response status and age as covariate (given age effects in NM concentration and NM-MRI)

(35). Missing values because of incomplete SN coverage or extreme values smaller/greater than 1st and 99th percentile (CR < -0.11 and CR > 26.67) were excluded (on average 39 voxels (SD=32) or 2.2% of the SN-VTA voxels per patient). In keeping with previous work, we chose voxelwise analyses over region-of-interest analyses to reduce statistical circularity in defining regions via signal-intensity thresholding and to account for regional heterogeneity of dopamine neurons across tiers without well-defined anatomical boundaries. Hypothesis testing was based on a permutation test (10,000 permutations) for the treatment-response status variable, which determined the chance-level distribution of the number of SN-VTA voxels exceeding a threshold of $p<0.05$ (see supplementary methods S1) . To obtain a measure of effect size unbiased by voxel selection a leave-one-subject-out analysis was performed. Here, significant voxels for each patient were identified in a voxelwise analysis including the complete patient sample except the left-out patient. The significant voxels were then used to extract the mean CR for this left-out patient.

Post-hoc analyses

Post-hoc receiver operating curve (ROC) analysis was performed to assess the ability of NM-MRI to identify non-responders without mislabeling the responders by extracting the AUC and the sensitivity at 100% specificity. Treatment response status (responder/non-responder) was used as outcome variable and CR as independent variable. For completeness we also show the results of the region-of-interest (ROI) analysis using the whole SN-VTA (see supplementary methods S2). In addition, the mean $CR_{SN\text{-}VTA}$ from the ROI analysis was compared between non-responders and responders using a one-way ANCOVA with age as covariate.

For post-hoc analyses including the control group, the mean CR from the significant voxels (thresholded at $p<0.05$ and surviving the permutation-based family-wise-error correction for the *a-priori* voxelwise analysis) was compared between non-responders, responders, and controls using a one-way ANCOVA with age as covariate.

Secondary longitudinal analyses

A secondary aim was to assess the robustness of NM-MRI over six months, by comparing the mean CR between all baseline patients and at follow-up. A linear mixed effect model was conducted with time (baseline, follow-up) as the independent variable while controlling for treatment response status and including subject as a random effect.

Exploratory symptom correlations

Exploratory correlations assessed the relationship of the mean CR of significant voxels to clinical variables. Additional exploratory post-hoc ANCOVA's were performed controlling for clinical variables and attrition (see supplementary results S2). In general, appropriate parametric tests were used (or non-parametric tests when normality assumptions were violated) and results of post-hoc analyses were considered statistically significant at $p<0.05$.

Results

An overview of the baseline demographic and clinical characteristics of the participants is shown in Table 1 (see supplementary table S1 for an overview of diagnoses and medication use). In total 79 patients and 20 controls were included in the study. After exclusions (see supplementary results S1 and table S2), 62 patients and 20 controls were retained. A subgroup of 37 patients participated in the follow-up MRI scan (Table S3/4 in the online supplement). No significant differences were found between the three groups on sex, age, IQ, nicotine use and cannabis use at baseline (Table 1). The non-responders and responders did not differ in duration of illness or antipsychotic dose (Table 1). Non-responders had a lower age of illness onset, longer duration of antipsychotic use and lower scores on the GAF and higher scores on all subscales of the PANSS (Table 1).

A-priori voxelwise analysis

Consistent with our hypothesis, the *a-priori* NM-MRI voxelwise analysis of treatment-response status revealed a subset of significant voxels (treatment-response voxels: 297 of 1807 voxels at $p<0.05$, robust linear regression controlling for age; corrected $p=0.032$, permutation test, peak voxel MNI coordinates [x, y, z]: -4, -23, -20) with increased CR in responders versus non-responders (Figure 1). Repeating the analysis without excluding extreme voxel values yielded similar results (treatment-response voxels: 307 of 1807 voxels at $p<0.05$, corrected $p=0.031$), Treatment response had a moderate unbiased effect on NM-MRI signal in the treatment-response voxels (unbiased leave-one-out Cohen's $d=0.46$, 95% CI=-0.14,1.06).

Table 1. Baseline demographics of responders, non-responders and healthy controls

	Responders N=47		**Non-responders N=15**		**Controls N=20**		**p-value**
	N	%	N	%	N	%	
Male	32	68.1	11	73.3	14	70.0	0.96
Smoker	23	48.9	6	40.0	9	45.0	0.83
Cannabis user	28	59.6	6	40.0	12	60.0	0.38
Ethnicity/race							0.20
White	27	57.4	10	66.7	18	90.0	
Black	10	21.3	3	20.0	0	0.0	
Latinx	2	4.3	0	0.0	1	5.0	
Mixed	8	17.0	2	13.3	1	5.0	
	Mean	**SD**	**Mean**	**SD**	**Mean**	**SD**	
Age (years)	24.06	4.63	21.27	3.20	22.70	4.08	0.14
IQ	92.28	14.53	91.53	11.75	92.95	10.88	0.95
Socioeconomic status	21.95	10.38	21.07	10.18	27.68	8.93	0.09
Nicotine use (cigarettes/day)	6.38	7.77	5.13	7.19	7.75	9.70	0.69
Cannabis use (weeks/year)	15.34	20.18	13.53	20.97	21.1	24.25	0.49
GAF score	58.17	11.37	50.13	7.97	79.05	6.69	**<0.001***
Age at illness onset (years)	23.36	4.55	20.33	3.37			0.03*
Illness duration (weeks)	38.85	40.79	50.90	39.78			0.12
Antipsychotic duration (weeks)	12.87	9.28	19.84	10.15			0.02*
Antipsychotic dosage (mg/day CPZ)	397.33	164.63	330.83	134.04			0.16
PANSS positive	10.59	3.46	14.13	5.29			0.03*
PANSS negative	11.32	4.32	14.80	5.48			0.02*
PANSS general	22.62	4.47	26.20	6.06			0.04*

IQ=Intelligence quotient, GAF=global functioning scale, CPZ=chlorpromazine equivalent, PANSS=positive and negative syndrome scale, * $p < 0.05$

Post-hoc analyses

The ROI analysis also showed significantly higher $CR_{SN\text{-}VTA}$ in the responders compared to the non-responders, $F(1,59)=4.82$, $p=0.032$. The ROC analysis of the treatment-response voxels yielded a good AUC of 0.85, although these effects are inflated due to circularity in voxel selection. Non-circular analyses yielded more moderate effects (unbiased leave-one-out AUC=0.62, ROI-based AUC=0.68) (Figure 2). The post-hoc ANCOVA, including controls, revealed a significant effect of group on mean CR in the treatment-response voxels after controlling for age, $F(1,78)=14.55$, $p<0.001$. Age was not a significant covariate, $F(1,78)=0.81$, $p=0.37$. Post-hoc Tukey tests showed that non-responders (N=15, mean $\pm$ SD=13.18 $\pm$ 1.34)

and controls (N=20, mean ± SD=14.06 ± 1.48) had significantly lower CR than responders (N=47, mean ± SD=15.15 ± 1.21), p<0.001 and p=0.005, respectively. No significant difference was found between non-responders and controls, p=0.10. The main effect of treatment status remained significant in control analyses either excluding patients lost to follow up or which controlled for PANSS subscale scores and antipsychotic treatment duration (see supplementary results S2).

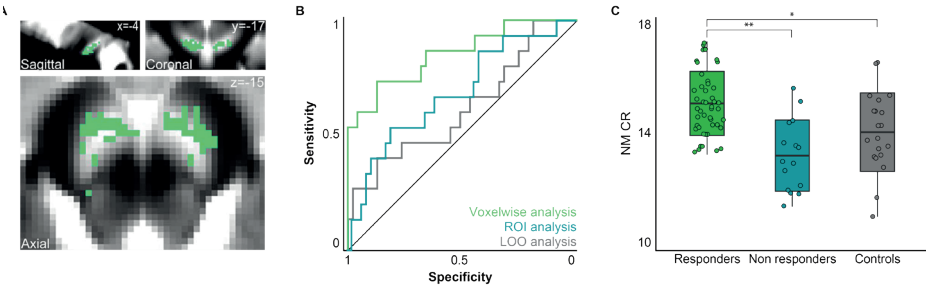

Figure 1. NM-MRI analyses of treatment-response status. A) Map of treatment-response voxels in which responders exhibited a higher neuromelanin-MRI contrast ratio (NM CR) than responders (thresholded at p<0.05, permutation corrected p-value=0.032). B) Receiver operating characteristic curves displaying the sensitivity and specificity to separate the two patient groups using the mean NM CR of the treatment-response voxels from the voxelwise analysis, the unbiased leave-one-out (LOO) analysis and the region of interest (ROI) analysis. C) Scatterplots showing the extracted NM-MRI CR from the treatment-response voxels, with the boxplot showing the group mean ± SD. * p < 0.05, ** p <0.001

Secondary longitudinal analyses

To assess differences in average CR in the treatment-response voxels between baseline and follow-up we ran a linear mixed-effects model analysis with the 62 baseline measurements and 37 follow-up measurements. There was a significant main effect of treatment-response status (beta=-1.45, t=-3.77, p<0.001). There was no significant main effect of time (beta =-0.06, t=-0.26, p=0.80), nor an interaction of time by treatment-response status (beta=0.89, t=1.66, p=0.10). At follow-up the differences in mean CR between non-responders (N=9, mean ± SD=13.47 ± 1.55) and responders (N=28, mean ± SD=15.25 ± 1.70) remained significant, after controlling for age, F(1,34)=7.66, p=0.010 (Figure 2). Age was again not a significant covariate, F(1,34)=0.47, p=0.50.

Exploratory symptom correlations

Spearman's rank correlation yielded a significant negative correlation between average CR in the treatment-response voxels and positive symptoms and general symptoms at baseline, r(60)=-0.26, p=0.041 and (r(60)=-0.25, p=0.045), respectively. This was not significant in a partial correlation controlling for group, r(59)=-0.15, p=0.26 and r(59)=-0.14, p=0.28, for positive and general symptoms respectively. Nor did this correlation reach significance

within the non-responder (r(13)=-0.36, p=0.19) or responder group (r(45)=-0.02, p=0.89) for the positive symptoms, or for the general symptoms in non-responder (r(13)=-0.22, p=0.43) or responders (r(45)=-0.09, p=0.55). No significant correlations were found between average CR in the treatment-response voxels and age (r(60)=0.03, p=0.78), illness duration (r(60)=-0.06, p=0.62), medication duration (r(60)=0.01, p=0.95) and dosage(r(60)=-0.02, p=0.87), negative symptoms (r(60)=-0.19, p=0.15).

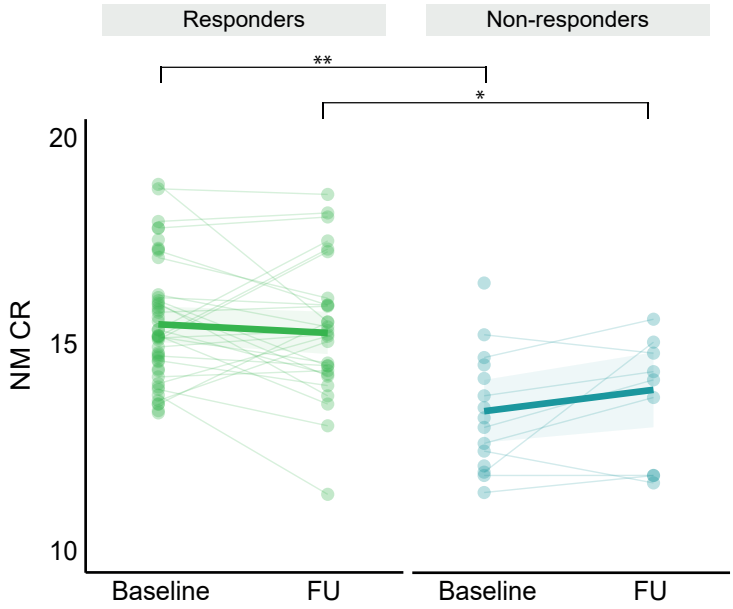

Figure 2. Secondary longitudinal analyses. Scatterplots showing the extracted neuromelanin contrast ratio (NM CR) from the treatment response voxels of all individual patients at baseline and follow-up (FU), with the thick line representing the longitudinal linear mixed effect model. At baseline and follow-up a significant difference was found between the non-responders and responders (p=0.01). No significant main effect of measurement was found. * $p < 0.05$, ** $p < 0.001$

Discussion

To our knowledge this is the first study evaluating the potential of NM-MRI as non-invasive marker for treatment resistance in first episode schizophrenia. In line with our hypothesis, non-responders showed significantly lower NM-MRI signal compared to responders, and similar NM-MRI signal compared to controls. NM-MRI is able to identify non-responders with AUCs of 0.62-0.85. The significant voxels associated with response status were predominantly localized in the ventral tier of the SN. Furthermore, NM-MRI appears to be relatively robust in that NM-MRI signal remained stable over six months follow-up and was uncorrelated with illness duration, medication duration or dosage.

Our results are consistent with the finding of lower striatal dopamine synthesis capacity using [^{18}F]F-DOPA PET in non-responders compared to responders (8-10) and provide further evidence that non-responders differ in nigrostriatal dopaminergic functioning from responders. NM-MRI is a less direct measurement of dopamine function than [^{18}F]F-DOPA PET. [^{18}F]F-DOPA PET captures state-dependent changes in dopamine functioning, whereas NM-MRI appears to be a more stable, trait-like, measure, likely due to the slow timescale of neuromelanin accumulation. In addition, other factors than only neuromelanin concentration may contribute to the NM-MRI contrast, including myelination (36), and future work is needed to elucidate the specificity of the contrast to neuromelanin concentration. However, NM-MRI has several advantages over PET imaging including reduced costs, non-invasiveness and no ionizing radiation; all of these factors are essential for a clinically applicable marker to identify treatment resistance in schizophrenia.

The subset of voxels significantly associated with response status mainly localized to ventral SN. The ventral SN provides dopaminergic innervation of the associative striatum(37). Previous studies have established that presynaptic dopamine function in schizophrenia is especially elevated in the associative striatum (38). A recent NM-MRI study found that voxels in the SN associated with psychosis severity in unmedicated patients also predominated in the ventral (and anterior) aspects of the SN (20). Together, these results support a specific involvement of the ventral SN in the pathophysiology of psychosis in schizophrenia, highlighting the functional importance of SN topography.

The current study employed a naturalistic design; the majority of patients were included from a tertiary inpatient clinic within several weeks after their admission and had a history of medication use prior to admission via general practitioner or other clinics (closed wards/ crisis services). Due to practical and ethical reasons, it was unfeasible to include patients at illness onset or during the period that symptoms were most severe. As a result, most of the included patients showed at least partial response to antipsychotics at baseline, and the patient groups differed on symptom severity and medication duration. This could have affected our results, but we observed no change in NM-MRI signal in the treatment-response voxels over a six-month period while patients were on antipsychotic medication and their positive symptoms significantly improved (see supplementary table S3). It is still possible that NM-MRI signal change may occur at longer follow-up periods given the slow temporal dynamics of neuromelanin accumulation. Longer follow-up periods might be challenging in first-episode psychosis though, as follow-up is generally difficult in this group. Indeed, we have lost 10 patients to follow-up and a considerable number was not motivated to participate in the follow-up MRI scan session. The lack of correlations with illness duration, medication duration, and antipsychotic dose, however, also suggest small or no effects of disease related aspects, or of medication, on NM-MRI signal in treatment-response voxels during early stages of first episode psychosis. We also found no significant effect of age on NM-MRI signal in

these voxels within this young age range (35), consistent with a meta-analysis of NM-MRI in schizophrenia (23). Collectively, these results further support NM-MRI as a candidate marker for treatment resistance in first episode psychosis in a naturalistic setting, where it may be unfeasible to limit markers to patients scanned at illness onset or before medication use. Circumstances may vary between countries or clinics, but it is not uncommon that patients are prescribed crisis treatment before being referred to specialized care where MRI scans can be obtained. An MRI-based marker in such settings (i.e. after start of antipsychotic medication) should still be able to aid in therapeutic decisions and have utility in reducing delays in receiving effective treatment.

It is important to mention that the majority of the non-responders, although meeting accepted criteria, are not completely treatment resistant. They experienced some effect of standard antipsychotics without reaching remission of positive symptoms. The significant negative correlation between symptom severity and NM-MRI signal did not hold when controlling for group and it is therefore likely driven by non-responders (with more severe positive symptoms) having lower NM-MRI signal. It may also hint at the notion though that approaching response as a continuum is more appropriate than a binary division, although the latter may facilitate clinical decision making (11,39). A study evaluating response dimensionally, via changes before versus after treatment initiation, would be necessary to assess this notion and could account for some of the overlap in the NM-MRI signal, assuming signal scales with response magnitude. In addition, results might differ for ultra-treatment resistant patients (non-clozapine responders). In our sample, 12 of the 15 non-responders responded to clozapine at follow up. The relatively large number of non-responding patients that received clozapine treatment is likely due to the fact the majority of our sample were treated by a specialized early psychosis group with extensive experience in clozapine treatment. Furthermore, the fact that the majority of the non-responders responded to clozapine could be a result of the early initiation of clozapine as this can increase clozapine responsiveness (3,40).

Conclusion

This study demonstrates the potential of NM-MRI as a non-invasive marker for treatment resistance in schizophrenia at an early stage and provides further evidence for heterogeneity in the neurobiology of schizophrenia. Further research is needed to determine the out-of-sample predictive value of NM-MRI for non-responders in larger samples, e.g. by applying machine learning approaches. Eventually, an adequate prediction model could lead to early identification of treatment resistance in schizophrenia and thereby substantially reduce delays in effective treatment and improve outcome.

References

1. Elkis H, Buckley PF: Treatment-Resistant Schizophrenia. Psychiatr Clin North Am. 2016; 39:239-265
2. Howes OD, Vergunst F, Gee S, McGuire P, Kapur S, Taylor D: Adherence to treatment guidelines in clinical practice: study of antipsychotic treatment prior to clozapine initiation. Br J Psychiatry. 2012; 201:481-485
3. Yoshimura B, Yada Y, So R, Takaki M, Yamada N: The critical treatment window of clozapine in treatment-resistant schizophrenia: Secondary analysis of an observational study. Psychiatry Research. 2017; 250:65-70
4. Lewis SW, Barnes TR, Davies L, Murray RM, Dunn G, Hayhurst KP, et al: Randomized controlled trial of effect of prescription of clozapine versus other second-generation antipsychotic drugs in resistant schizophrenia. Schizophr Bull. 2006; 32:715-723
5. Kapur S, Zipursky R, Jones C, Remington G, Houle S: Relationship Between Dopamine D2 Occupancy, Clinical Response, and Side Effects: A Double-Blind PET Study of First-Episode Schizophrenia. American Journal of Psychiatry. 2000; 157:514-520
6. Maia TV, Frank MJ: An Integrative Perspective on the Role of Dopamine in Schizophrenia. Biol Psychiatry. 2017; 81:52-66
7. Fusar-Poli P, Meyer-Lindenberg A: Striatal presynaptic dopamine in schizophrenia, part II: Meta-analysis of [^{18}F/^{11}C]-DOPA PET studies. Schizophrenia Bulletin. 2013; 39:33-42
8. Demjaha A, Murray RM, McGuire PK, Kapur S, Howes OD: Dopamine synthesis capacity in patients with treatment-resistant schizophrenia. American Journal of Psychiatry. 2012; 169:1203-1210
9. Kim E, Howes OD, Veronese M, Beck K, Seo S, Park JW, et al: Presynaptic Dopamine Capacity in Patients with Treatment-Resistant Schizophrenia Taking Clozapine: An [^{18}F]DOPA PET Study. Neuropsychopharmacology. 2017; 42:941-950
10. Jauhar S, Veronese M, Nour MM, Rogdaki M, Hathway P, Turkheimer FE, et al: Determinants of treatment response in first-episode psychosis: an (18)F-DOPA PET study. Mol Psychiatry. 2019; 24:1502-1512
11. Howes OD, Kapur S: A neurobiological hypothesis for the classification of schizophrenia: type A (hyperdopaminergic) and type B (normodopaminergic). Br J Psychiatry. 2014; 205:1-3
12. Veronese M, Santangelo B, Jauhar S, D'Ambrosio E, Demjaha A, Salimbeni H, et al: A potential biomarker for treatment stratification in psychosis: evaluation of an [(18)F] FDOPA PET imaging approach. Neuropsychopharmacology. 2021; 46:1122-1132
13. Shibata E, Sasaki M, Tohyama K, Otsuka K, Endoh J, Terayama Y, et al: Use of Neuromelanin-Sensitive MRI to Distinguish Schizophrenic and Depressive Patients and Healthy Individuals Based on Signal Alterations in the Substantia Nigra and Locus Ceruleus. Biological Psychiatry. 2008; 64:401-406.
14. Sulzer D, Bogulavsky J, Larsen KE, Behr G, Karatekin E, Kleinman MH, et al: Neuromelanin biosynthesis is driven by excess cytosolic catecholamines not accumulated by synaptic vesicles. Proceedings of the National Academy of Sciences. 2000; 97:11869-11874
15. Graham DG: On the origin and significance of neuromelanin. Arch Pathol Lab Med. 1979; 103:359-362
16. Zucca FA, Vanna R, Cupaioli FA, Bellei C, De Palma A, Di Silvestre D, et al: Neuromelanin organelles are specialized autolysosomes that accumulate undegraded proteins and lipids in aging human brain and are likely involved in Parkinson's disease. NPJ Parkinsons Dis. 2018; 4:17
17. Chinta SJ, Andersen JK: Dopaminergic neurons. Int J Biochem Cell Biol. 2005; 37:942-946
18. Zucca FA, Basso E, Cupaioli FA, Ferrari E, Sulzer D, Casella L, et al: Neuromelanin of the human substantia nigra: an update. Neurotox Res. 2014; 25:13-23
19. Trujillo P, Summers PE, Ferrari E, Zucca FA, Sturini M, Mainardi LT, et al: Contrast mechanisms associated with neuromelanin-MRI. Magnetic Resonance in Medicine. 2017; 78:1790-1800
20. Cassidy CM, Zucca FA, Girgis RR, Baker SC, Weinstein JJ, Sharp ME, et al: Neuromelanin-sensitive MRI as a noninvasive proxy measure of dopamine function in the human brain. Proceedings of the National Academy of Sciences of the United States of America. 2019; 116:5108-5117
21. van der Pluijm M, Cassidy C, Zandstra M,

Wallert E, de Bruin K, Booij J, et al: Reliability and Reproducibility of Neuromelanin-Sensitive Imaging of the Substantia Nigra: A Comparison of Three Different Sequences. Journal of Magnetic Resonance Imaging. 2020

22. Wengler K, He X, Abi-Dargham A, Horga G: Reproducibility Assessment of Neuromelanin-Sensitive Magnetic Resonance Imaging Protocols for Region-of-Interest and Voxelwise Analyses. NeuroImage. 2019: 1-37
23. Ueno F, Iwata Y, Nakajima S, Caravaggio F, Rubio JM, Horga G, et al: Neuromelanin accumulation in patients with schizophrenia: A systematic review and meta-analysis. Neurosci Biobehav Rev. 2022; 132:1205-1213
24. Howes OD, Williams M, Ibrahim K, Leung G, Egerton A, McGuire PK, et al: Midbrain dopamine function in schizophrenia and depression: a post-mortem and positron emission tomographic imaging study. Brain. 2013; 136:3242-3251
25. Kay SR, Fiszbein A, Opler LA: The Positive and Negative Syndrome Scale for schizophrenia. Schizophrenia Bulletin. 1987; 13(2):261-76
26. Sheehan DV, Lecrubier Y, Sheehan KH, Amorim P, Janavs J, Weiller E, et al: The Mini-International Neuropsychiatric Interview (M.I.N.I.): the development and validation of a structured diagnostic psychiatric interview for DSM-IV and ICD-10. J Clin Psychiatry. 1998; 59 (Suppl 20:22-33)
27. Andrews G, Peters L: The psychometric properties of the Composite International Diagnostic Interview. Soc Psychiatry Psychiatr Epidemiol. 1998; 33:80-88
28. Velthorst E, Levine SZ, Henquet C, de Haan L, van Os J, Myin-Germeys I, et al: To cut a short test even shorter: Reliability and validity of a brief assessment of intellectual ability in Schizophrenia-a control-case family study. Cognitive neuropsychiatry. 2012; 18:37-41
29. Hollingshead AB: Four factor index of social status. New Haven, CT; 1975
30. Van Alphen C, Ammeraal M, Blanke C, Boonstra N, Boumans, H, Bruggeman R, et al: Dutch Multidisciplinary Guidelines Schizophrenia 2012
31. Andreasen NC, Carpenter WT, Kane JM, Lasser RA, Marder SR, Weinberger DR: Remission in schizophrenia: proposed criteria and rationale for consensus. Am J Psychiatry. 2005;162(3):441-9
32. Avants B, Tustison N, Song G: Advanced normalization tools (ANTS). Insight J. 2008; 1–35
33. Penny WD, Friston KJ, Ashburner JT, Kiebel SJ, Nichols TE: Statistical parametric mapping: the analysis of functional brain images: Elsevier; 2011
34. Cox RW: AFNI: software for analysis and visualization of functional magnetic resonance neuroimages. Comput Biomed Res. 1996; 29:162-173
35. Xing Y, Sapuan A, Dineen RA, Auer DP: Life span pigmentation changes of the substantia nigra detected by neuromelanin-sensitive MRI. Mov Disord. 2018; 33:1792-1799
36. Lee H, Baek SY, Chun SY, Lee JH, Cho H: Specific visualization of neuromelanin-iron complex and ferric iron in the human post-mortem substantia nigra using MR relaxometry at 7T. Neuroimage. 2018;172:874-85.
37. Zhang Y, Larcher KM, Misic B, Dagher A: Anatomical and functional organization of the human substantia nigra and its connections. Elife. 2017; 6
38. McCutcheon R, Beck K, Jauhar S, Howes OD: Defining the Locus of Dopaminergic Dysfunction in Schizophrenia: A Meta-analysis and Test of the Mesolimbic Hypothesis. Schizophr Bull. 2018; 44:1301-1311
39. McCutcheon RA, Pillinger T, Efthimiou O, Maslej M, Mulsant BH, Young AH, et al: Reappraising the variability of effects of antipsychotic medication in schizophrenia: a meta-analysis. World Psychiatry. 2022;21(2):287-94.
40. Üçok A, Cikrikcili U, Karabulut S, Salaj A, Ozturk M, Tabak O, et al: Delayed initiation of clozapine may be related to poor response in treatment-resistant schizophrenia. Int Clin Psychopharmacol. 2015; 30:290-295

Author contributions

EvdG, JB and LdH conceived the study. EvdG and MvdP designed and planned the study. MvdP performed the data collection, with help from LdH and OdP. MvdP analyzed the data with support from KW and PR and under supervision of EvdG and GH. MP wrote the original draft of the manuscript. All authors reviewed and edited the manuscript. All authors have read and agreed to the published version of the manuscript.

Supplementary material

Table of contents:

Supplementary methods

Methods S1: Voxelwise analysis

Our a-priori analysis consisted of a voxelwsie analysis predicting CR within the SN+VTA mask based on treatment response status with age as covariate, (given age effects in NM concentration and NM-MRI). A voxelwise robust linear regression was performed using the MATLAB fit linear regression model (fitlm) with robust fitting using the 'bisquare' weight function with the default tuning constant. A robust regression was performed to minimize the impact of outliers and limits the effect of other violations of regression assumptions. This is particularly useful for voxelwise analyses since detailed inspection of the all voxelwise data is unfeasible, it has been previously shown to improve sensitivity and reduce false positives (e.g., Wager et al. Neuroimage 2005), and it is incorporated as part of some popular MRI toolboxes (e.g., Tor Wager's CANlab toolbox). Significance testing was determined by use of a permutation test in which treatment response status was randomly shuffled with respect to the CR in the SN-VTA mask. The permutation test corrects for multiple comparisons by determining whether the effect's spatial extent (number of voxels showing a certain directional effect in a one-sided test, e.g., responders>non-responders) was greater than would be expected by chance (p-corrected <0.05, 10,000 permutations). This is equivalent to a cluster-level familywise- error-corrected p-value, although in this case voxels were not required to form a cluster of adjacent voxels, and the degree of freedom could differ between voxels as a results of missing or extreme values.

Methods S2. Region of interest analysis

For the region of interest analysis the mean CR in the SN-VTA mask ($CR_{SN\text{-}VTA}$) was calculated for each participant by averaging the CR-values of all voxels in the SN-VTA mask that had a non-negative value. The mean $CR_{SN\text{-}VTA}$ was used for the receiver operating curve analysis and ANCOVA between responders and non-responders in the main manuscript. Furthermore the post-hoc and exploratory results from the main manuscript are repeated with $CR_{SN\text{-}VTA}$ in the supplementary results S3.

Supplementary results

Results S1. Reasons for exclusion

A total of 17 patients were excluded from analysis. Reasons for exclusion for the patients were: change in diagnosis (non-schizophrenia spectrum, such as bipolar disorder) during follow-up (N=5), history of drug dependence or failed drug screening (N=3), unclear treatment response, e.g. due to non-compliance (N=6), or excessive motion artifacts (N=1). Ten patients were lost to follow-up. For N=2, treatment response could not be determined and they were excluded. The excluded patients smoked significantly more cigarettes per day than the included patients, but did not differ significantly on any other demographics or disease related variables. Furthermore, they did not differ in mean CR in the response voxels or $CR_{SN\text{-}VTA}$ (Table S2).

Results S2. Exploratory post-hoc analysis

Two additional exploratory post-hoc ANCOVAs were performed to assess the robustness of the group effect. For the first additional ANCOVA we excluded the lost to follow-up participants. With the second additional ANCOVA within patients we controlled for the PANSS scores and duration of antipsychotic use, as these variables differed between our patient groups and could have an effect on the results. Both additional ANCOVAs showed a significant effect of group on CR, $F(1,74)=14.54$, $p<0.001$ and $F(1,55)=18.26$, $p<0.001$ respectively. PANSS positive ($F(1,55)=0.04$, $p=0.84$), PANSS negative ($F(1,55)=0.21$, $p=0.65$), PANSS general ($F(1,55)=0.43$, $p=0.52$) and duration of antipsychotic use ($F(1,55)=0.11$, $p=0.74$) were not significant covariates.

Results S3. Region of interest analysis

A One-way ANCOVA, controlling for age, was performed to assess the difference in groups between mean $CR_{SN\text{-}VTA}$. A significant effect of group was found, $F(1,78)=4.1$, $p=0.02$. Age was not a significant covariate, $F(1,78)=0.12$, $p=0.73$. Post-hoc Tukey test did not reach significance between group comparisons. Trend significance was found for non-responders (N=15, mean $\pm$ SD=12.99 $\pm$ 1.14) and healthy controls (N=20, mean $\pm$ SD=13.06 $\pm$ 1.06) compared to responders (N=47, mean $\pm$ SD = 13.79 $\pm$ 1.24), $p=0.07$ and $p=0.09$ respectively. No significant difference was found between non-responders and healthy controls, $p=0.99$.

To assess differences in average $CR_{SN\text{-}VTA}$ between baseline and follow-up we ran a linear mixed-effects model analysis with the 62 baseline measurements and 37 follow-up measurements. There was a significant main effect of treatment-response status (beta=-0.60, t=-2.14, $p=0.04$). There was no significant main effect of time (beta =-0.03, t=-0.19, $p=0.85$), nor an interaction of time by treatment-response status (beta=-0.15, t=-0.44, $p=0.66$). At follow-up the differences in $CR_{SN\text{-}VTA}$ between non-responders (N=9, mean $\pm$ SD=12.56 $\pm$ 1.37) and responders (N=28, mean $\pm$ SD=13.75 $\pm$ 1.43) remained significant, after controlling for age, $F(1,34)=4.71$, $p=0.04$. Age was again not a significant covariate, $F(1,34)=0.38$, $p=0.54$.

No significant correlations were found between average $CR_{SN\text{-}VTA}$ and age ($r(60)=0.008$, $p=0.95$), illness duration ($r(60)=0.03$, $p=0.83$), medication duration ($r(60)=-0.08$, $p=0.54$) and dosage ($r(60)=-0.05$, $p=0.73$), positive symptoms ($r(60)=-0.05$, $p=0.73$), negative symptoms ($r(60)=-0.06$, $p=0.64$) and general symptoms($r(60)=-0.01$, $p=0.92$).

Supplementary tables

Table S1. Diagnoses and medication use of responders and non-responders

	Responders N=47	**Non-responders N=15**
DSM-5 diagnosis		
Schizophrenia	24	13
Schizophreniform	16	2
Schizoaffective	4	0
Unspecified schizospectrum disorder	3	0
Medication use at baseline		
Antipsychotics	45	15
Sedatives	9	6
Antidepressants	3	0
Thyrax	0	1
Vitamins / Supplements	11	3
Antihistamin	1	0
Amlodipine	1	0
Macrogol	0	1
Antibiotics	1	0
Anticonceptives	1	0
Mean n. medication switches to FU	1.19	2.07
Reasons medication switch		
Inefficacy	10	7
Side effects	17	5
Own initiative	7	3
Doctor's initiative	15	7
Unknown	7	9

Note, reasons for medication switch are the answers of the patients. Doctor's initiative most often relates to inefficacy whereas own initiative could relate to side effects or inefficacy.

Table S2. Demographics and symptom severity of excluded patients

	Included Patients N=62		**Excluded Patients N=17**		**p-value**
	N	%	N	%	
Male	43	69.35	16	94.12	0.08
Smoker	29	46.77	12	70.59	0.08
Cannabis user	34	54.84	12	70.59	0.24
Ethnicity/race					0.22
White	37	59.68	14	82.35	
Black	13	20.97	3	17.65	
Latinx	2	3.23	0	0.00	
Mixed	10	16.13	0	0.00	
	Mean	**SD**	**Mean**	**SD**	
Age (years)	23.39	4.47	25.53	4.99	0.08
IQ	92.10	13.82	96.53	17.74	0.42
Socioeconomic status	21.73	10.25	26.56	11.27	0.13
Nicotine use (cigarettes/day)	6.08	7.60	11.06	8.47	**0.02***
Cannabis use (weeks/year)	14.05	19.73	23.06	22.48	0.05
GAF score	56.23	11.14	56.35	12.02	0.84
Age at illness onset (years)	22.63	4.47	24.85	4.47	0.10
Illness duration (weeks)	41.76	40.55	49.85	34.47	0.24
Antipsychotic duration (weeks)	14.56	9.88	24.06	18.86	0.14
Antipsychotic dosage (mg/day CPZ)	381.24	159.33	362.21	225.87	0.91
PANSS positive	11.44	4.22	12.06	3.90	0.45
PANSS negative	12.15	4.87	11.06	3.27	0.65
PANSS general	23.44	5.15	24.65	5.67	0.45
CR SN-VTA	13.59	1.26	13.53	1.53	0.86
CR response voxels	14.92	1.71	14.83	1.47	0.85

IQ=Intelligence quotient, GAF=global functioning scale, CPZ=chlorpromazine equivalent, PANSS=positive and negative syndrome scale, CR=contrast ratio, SN-VTA=substantia nigra – ventral tegmental area. * $p < 0.05$

Table S3. Baseline and follow-up demographics and symptom severity of patients

	Baseline N=62		**Follow-up N=37**		**p-value**
	N	%	N	%	
Male	43	69.4	24	64.9	0.81
Non-responder	15	24.1	9	24.3	1
Smoker	29	46.8	16	43.2	0.89
Cannabis user	34	54.8	12	32.4	**0.05***
	Mean	**SD**	**Mean**	**SD**	
Age (years)	23.39	4.47	23.65	4.04	0.47
Nicotine use (cigarettes/day)	6.05	7.6	5.38	6.8	0.72
Cannabis use (weeks/year)	14.05	19.73	6.06	12.63	0.05
GAF score	56.23	11.14	67.92	8.2	**<0.001***
PANSS positive	11.44	4.22	9.03	2.39	**<0.01***
PANSS negative	12.14	4.87	10.48	3.84	0.08
PANSS general	23.44	5.15	20.78	3.79	**0.01***

GAF=global functioning scale, PANSS=positive and negative syndrome scale

Table S4. Baseline and follow-up demographics and symptom severity of responders and non-responders

	Responder				**Non-responder**			
	Baseline N=47		**Follow-up N=28**		**Baseline N=15**		**Follow-up N=9**	
	N	%	N	%	N	%	N	%
Male	32	68.1	18	64.29	11	73.3	6	66.67
Smoker	23	48.9	12	42.86	6	40.00	4	44.44
Cannabis user	28	59.6	9	32.14	6	40.00	1	11.11
	Mean	**SD**	**Mean**	**SD**	**Mean**	**SD**	**Mean**	**SD**
Age (years)	24.06	4.63	24.00	4.12	21.27	3.20	22.56	3.81
Nicotine use (cigarettes/day)	6.38	7.77	5.39	6.91	7.75	9.70	5.33	6.85
Cannabis use (weeks/year)	15.34	20.18	0.68	1.09	21.10	24.25	0.25	0.71
GAF score	58.17	11.37	69.46	7.74	50.13	7.97	63.11	8.12
PANSS positive	10.59	3.46	8.89	2.23	14.13	5.29	9.44	2.92
PANSS negative	11.32	4.32	9.18	2.30	14.80	5.48	14.56	4.90
PANSS general	22.62	4.47	20.39	3.60	26.20	6.06	22.00	4.30
CR SN-VTA	13.79	1.24	13.75	1.43	12.99	1.14	12.56	1.37
CR TR voxels	15.15	1.21	15.31	1.67	13.18	1.34	13.59	1.53

CR=contrast ratio, GAF=global functioning scale, PANSS=positive and negative syndrome scale, SN-VTA=Substantia nigra – Ventral Tegmental Area, TR=treatment response.

Supplementary figure

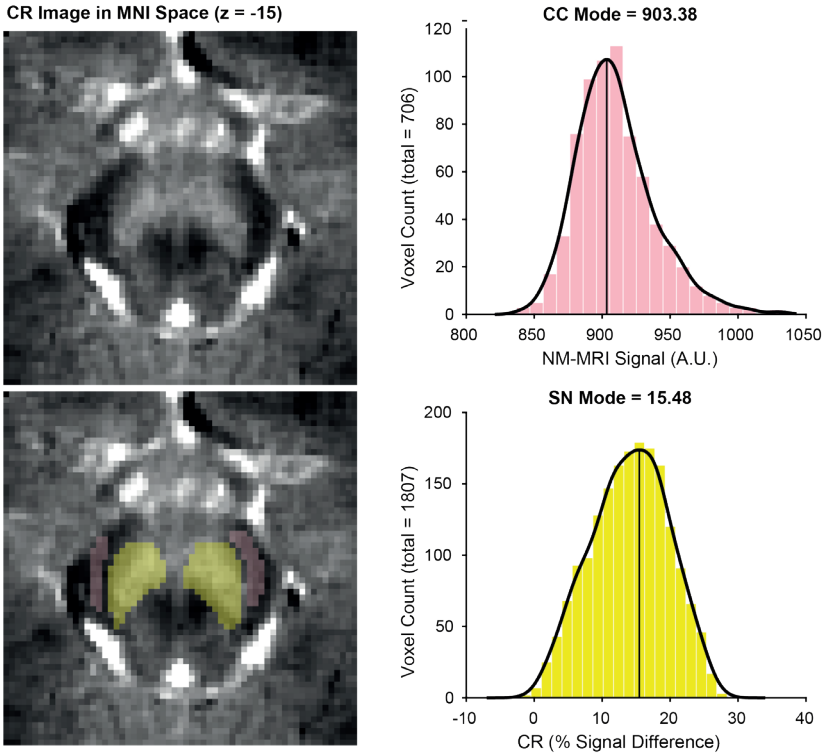

Figure S1. Example of standardized quality-control output. An example of one patient's quality control output. On the left is the contrast ratio (CR) image in MNI space with in yellow the substantia nigra-ventral tegmental area (SN-VTA) mask and in pink the crus cerebri (CC) mask. Contrast ratio (CR) is calculated at each voxel as percent neuromelanin-MRI signal change between each voxel in the SN-VTA mask and the mode of the signal intensity in the CC.

Chapter | 8

Plasma dopa decarboxylase activity in treatment-resistant recent-onset psychosis patients

Marieke van der Pluijm, Arjen L. Sutterland, André B. P. van Kuilenburg, Lida Zoetekouw, Lieuwe de Haan, Jan Booij, Elsmarieke van de Giessen

Therapeutic Advances in Psychopharmacology, 2019; 9:1-7
DOI: 10.1177/2045125319872341

Abstract

Treatment resistance (TR) in psychosis is a major clinical problem. A biomarker predicting TR against conventional antipsychotic drugs would be relevant, potentially reducing unnecessary delay to adequate treatment with clozapine. Dopa decarboxylase (DDC) activity in the striatum, measured with positron emission tomography, is elevated in responders, but not in treatment-resistant patients. Plasma DDC activity could be a surrogate marker for DDC brain activity, and thus a potential biomarker that could be used in daily clinical practice. Therefore, we determined plasma DDC activity in 40 male patients with recent-onset psychosis, of whom the majority had started treatment, whereby 21 turned out to be treatment responders and 19 treatment resistant during follow up. We observed no significant group differences. Furthermore, symptom severity was not associated with plasma DCC activity. We did observe a trend level difference in the distribution of plasma DDC activity across categories of medication, with subsequent *post hoc* analysis showing lower DDC activity in risperidone-using patients. This may suggest that risperidone could influence plasma DDC activity. Based on these results, plasma DDC activity does not appear to be a promising biomarker for TR in recent-onset psychosis patients who are already receiving antipsychotic treatment.

Introduction

Treatment resistance (TR) in psychosis is a major clinical problem, with 20–35% of psychotic patients showing nonresponse to conventional antipsychotic treatment (1). This leads to months or years of delay in effective treatment, resulting in hospitalization and the unnecessary side effects of ineffective antipsychotics. Therefore, a biomarker is needed that could be used to guide treatment decisions, for example to switch TR patients at an early stage to clozapine, the only antipsychotic with recognized superior effectiveness in TR (2). Recent findings indicate that a longer duration of TR before instalment of clozapine could diminish the potential for clozapine to still render a therapeutic response (3–5). This further underlines the necessity of pursuing a biomarker that can be used in clinical practice.

A well-established finding in psychosis is increased dopamine synthesis capacity in the striatum, which has not only been replicated in patients with schizophrenia (6,7), but also in other psychiatric disorders such as bipolar disorder (8). Increased dopamine concentrations are related to positive symptoms (i.e. hallucinations, delusions) of the illness (9). However, TR patients seem to have lower striatal dopamine synthesis capacity than the responders, actually being comparable to healthy controls (10,11). This was demonstrated with positron emission tomography (PET) imaging using [^{18}F]F-DOPA, which is processed by dopa decarboxylase (DDC), an enzyme required for dopamine synthesis. Moreover, a genome-wide association study also identified a locus next to the gene encoding DDC that was associated with TR (12). DDC activity would therefore be a good candidate biomarker for TR. However, the gold standard for assessing dopamine synthesis, [^{18}F]F-DOPA PET imaging, is not feasible for routine screening to identify TR patients, since it is costly, invasive, time-consuming, and leads to radiation exposure.

Apart from being required for the synthesis of dopamine, DDC is also the rate-limiting enzyme for the production of the neuromodulator 2-phenylethylamine. 2-Phenylethylamine concentration is demonstrated to be higher in plasma in patients with schizophrenia and also in cerebrospinal fluid (13,14). This suggests that plasma DDC activity might be an accurate reflection of DDC activity in the brain.

Therefore, the current study aims to explore plasma DDC activity as a potential biomarker by testing the hypothesis that plasma DDC activity is lower in TR patients than in responders. In addition, we will explore whether there is an effect of different antipsychotics on plasma DDC activity.

Experimental procedures

Data originate from a longitudinal study in recent-onset psychosis patients, investigating the influence of immune disturbances on the clinical profile and course of psychosis, with follow up at 1, 2, and 3 years after baseline. The research protocol of this study was reviewed and approved by the Medical Ethics Committee of the Academic Medical Center (AMC) of Amsterdam (10.141 # 11.17.0174). Patients with recent-onset psychosis, that is, within 4 years of symptom onset, were recruited during diagnostic intake at the specialized Early Psychosis Clinic of the Academic Medical Center (AMC) of Amsterdam, the Netherlands. Detailed medical and psychiatric histories, as well as baseline demographic data, symptom severity, medication status and blood samples were obtained during the diagnostic assessment at the clinic for all participants and defined as baseline measurement. Diagnosis was defined by the standardized criteria of the Comprehensive Assessment of Symptoms and History (CASH). Symptom severity was scored by the clinician at intake with the Positive and Negative Syndrome Scale for Schizophrenia (PANSS) (15). The total score of the PANSS (PANSSt) and the score of the positive subscale (PANSSp) were chosen as outcome measurements.

Plasma was quickly separated after blood withdrawal and stored at –80°C. DDC activity and the dopamine metabolites vanilglycolic acid (VGA), 3-methoxy-4-hydroxyphenylethylene glycol (MPHG), homovanillic acid (HVA), and 5-hydroxyindoleacetic acid (5-HIAA) were measured as described by Leuzzi and colleagues (16).

TR was determined based on information in the medical records during follow up, defined as showing no adequate response to a minimum of two sufficiently dosed conventional antipsychotics for a minimum of 6 weeks. Adequate response is defined as a PANSS score lower than 4 on the positive symptoms. Data were available for a minimum follow-up time of 1 year and a maximum of 3 years after baseline measurements.

Plasma DDC activity was compared between TR patients and responders, and between different categories of medication (including medication free) to assess the possible confounding effect of medication status. In addition, the relationship between plasma DDC activity and the PANSS total and positive subscale score was assessed. Appropriate parametric and nonparametric tests were used, and a probability value of 0.05 was selected as level of significance for all analyses.

Results

Plasma samples of 24 responders and 20 TR recent-onset psychosis patients were analyzed. We excluded three outliers (mean $\pm$ 2SD), two responding females and one TR male, as outliers might indicate bad data or an experimental error. In addition, we excluded the only

female (responder) that was left from the analyses, to exclude gender as a confounding factor, leaving 21 male treatment responders and 19 male TR patients. Demographics of the subjects are reported in Table 1.

Table 1. Demographics of treatment resistant and treatment responders groups.

	Responder N=21	**Resistant** N=19	**Statistics**
Age in years (mean ±SD))	24.4 ± 3.0	23.1 ± 3.0	t=1.41, p=0.17[a]
Diagnosis (SZ:SZa:SZf:P:Bi)	10:1:1:4:5	16:3:0:0:0	$\chi 2$=10.85, p=0.03[b]
Nicotine use (Yes:No)	16:5	10:9	$\chi 2$=2.43, p=0.12[b]
Cannabis use (Yes:No)	8:13	9:10	$\chi 2$=0.35, p=0.55[b]
Medication (Yes:No)	16:5	17:2	$\chi 2$=1.22, p=0.27[b]
Medication (N:R:O:Q:A:C:H:P:F:Rd)	5:3:4:1:3:0:3:1:1:0	2:3:7:2:1:2:1:0:0:1	$\chi 2$=9.36, p=0.41[b]
Medication use in weeks (Median (IQ1-IQ3))	10.0 (1.0-34.0)	16.0 (5.5-26.5)	U=225, p=0.50[c]
Symptom onset in weeks (Median (IQ1-IQ3))	34.0 (18.0-72.0)	31.0 (22.0-112.0)	U=207, p=0.85[c]

SZ= Schizophrenic disorder; SZa= Schizoaffective disorder; SZf= Schizofreniform disorder; P= Psychotic disorder not otherwise specified; Bi=Bipolair I-disorder; N=No medication; R=Risperidon; O=Olanzapine; Q=Quetiapine; A=Aripiprazole; C=Clozapine; H=Haloperidol; P=Penfluridol; F=Flupentixol; Rd=Risperidon depot; [a] Independent T-test; [b] Chi-square test [c] Mann-Whitney test

DDC activity (mean ± SD) did not differ significantly between TR patients [23.0 ± 8.7 nmol/(l/min)] and treatment responders [23.7 ± 8.2 nmol/(l/min)] (Table 2 and Figure 1; t = 0.28, p = 0.78). Adding the excluded patients in analyses increased DDC activity (mean ± SD) for TR patients [24.4 ± 10.5 nmol/(l/min)] and treatment responders [26.8 ± 12.8 nmol/(l/min)]; however, the results remained nonsignificant [t(42) = 0.68, p = 0.50]. Furthermore, excluding the bipolar and psychotic disorder not otherwise specified patients showed similar results [t(30) = 0.20, p = 0.85], with similar DDC activity (mean ± SD) for the responders [23.6 ± 7.8 nmol/(l/min)]. In addition, DDC activity (mean ± SD) between schizophrenia TR patients [23.1 ± 9.4 nmol/(l/min)] and schizophrenia treatment responding patients [23.3 ± 8.2 nmol/(l/min)], yielded no significant results [t(25) = 0.056, p = 0.96]. Explorative nonparametric analyses demonstrated that the dopamine metabolites also did not differ significantly between TR patients and treatment responders (Table 1). As expected, positive symptom severity (mean ± SD) did differ between TR (20.1 ± 7.9) patients and treatment responders (13.6 ± 6.4), whereas total symptom severity did not differ between TR (76.5 ± 23.7) and treatment responders (61.9 ± 22.0) from baseline (Table 1). Symptom severity was not related to plasma DCC activity (PANSSp r_τ = 0.00, p = 1.00; PANSSt r_τ = –0.045, p = 0.71). Controlling for nicotine and cannabis use, by adding the variables as covariate in a general linear model, yielded similar results as the original analyses.

Table 2. Group comparisons between treatment resistant patients and treatment responders.

	Responder		Resistant		Statistics
	Median (IQ1-IQ3)	**N**	**Median (IQ1-IQ3)**	**N**	
DDC activity (nmol/(L.min))	23.7 ± 8.2*	21	23.0 ± 8.8*	19	t=0.28, p=0.78[a]
VGA (nM)	40.8 (31.0-53.4)	21	39.4 (30.6-52.1)	18	U=180, p=0.81[b]
MPHG (nM)	16.6 (12.2-23.7)	21	17.1 (11.0-25.2)	18	U=180, p=0.81[b]
5-HIAA (nM)	28.9 (17.7-41.4)	21	38.0 (26.2-46.3)	18	U=143, p=0.20[b]
HVA (nM)	56.1 (45.9-66.0)	21	54.3 (41.9-80.9)	18	U=186, p=0.95[b]
PANSSt	59.5 (40.0-78.0)	18	69.0 (57.5-87.8)	16	U=101, p=0.14[b]
PANSSp	11.0 (7.3-18.8)	20	20.0 (13.5-23.8)	18	U=91.5, p=0.01[b]

* Mean ±SD; [a] Independent T-test; [b] Mann-Whitney test

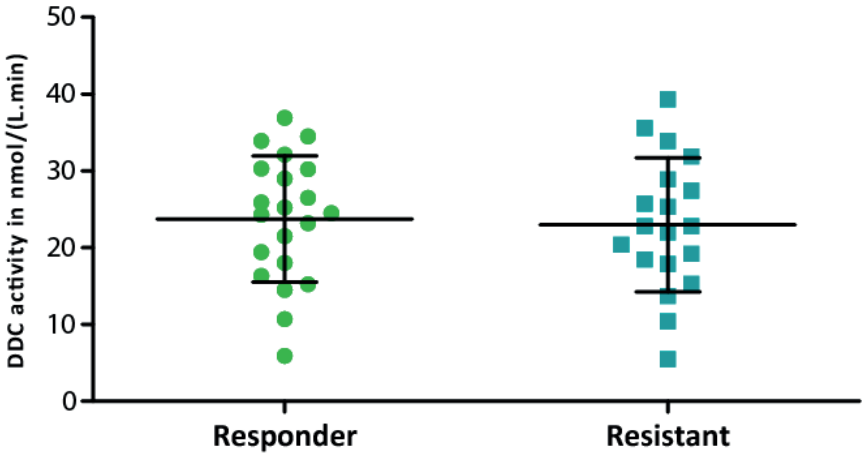

Figure 1. Plasma DDC activity in nmol/(l/min) for TR patients (Resistant) and treatment responders (Responder). Line displays mean, error bars display SD. DDC, Dopa decarboxylase; SD, standard deviation; TR, treatment resistance.

Discussion

The current study assessed plasma DDC activity as a candidate biomarker for TR in recent-onset psychosis. No significant group differences in plasma DDC activity or dopamine metabolites were observed between TR patients and responders, indicating that DDC plasma activity is an unlikely predictor of TR. We did, however, observe a trend level difference in the distribution of plasma DDC activity across categories of medication, based on lower plasma DDC activity in risperidone-using patients.

As expected, we found a greater severity of positive symptoms in the TR group compared with the responders. These results are in line with previous research (17) and can be expected by the fact that TR is defined mainly by severity of (positive) symptoms (1,18). However, although it is well known that higher striatal dopamine levels contribute to the positive symptoms in psychosis (9) we did not find an association between severity of positive symptoms and plasma DCC activity.

A possible explanation for the lack of difference in plasma DDC activity between TR patients and responders could be that peripheral plasma DDC activity insufficiently reflects the central dopamine synthesis capacity. Studies using [^{18}F]F-DOPA PET, in which the PET tracer is processed by DDC, previously showed elevated uptake in the striatum in psychosis (6–8,19), but not in TR patients as a subgroup, even while they were using antipsychotics (10,11). In line with the [^{18}F]F-DOPA PET studies, also amphetamine-induced dopamine release is elevated in the striatum in schizophrenia (20,21). In contrast, cortical dopamine release is lower in schizophrenia patients (22). This shows that, even within the brain, dopamine synthesis capacity, and, related to that, DDC activity, might be region specific. Thus, plasma DDC activity may not necessarily be related to striatal DDC activity. To verify this assumption, it would be necessary to correlate [^{18}F]F-DOPA PET with plasma DDC activity measurements in future studies.

The observed trend level effect of type of medication on the plasma DDC activity and trend level correlation between medication use in weeks and plasma DDC activity, could indicate that the use of antipsychotics might have influenced our results. This might also suggest that chronic schizophrenia patients with long-term medication use differ in plasma DDC activity compared with recent-onset patients, therefore our results are not applicable to chronic schizophrenia patients. Subsequent post hoc analysis showed lower DDC activity in risperidone-using patients. Risperidone is less lipophilic than most antipsychotics and has a lower brain-to-plasma ratio, resulting in a relatively higher peripheral concentration (23,24). Especially the active metabolite 9-hydroxy-risperidone of risperidone might influence the DDC activity. 9-Hydroxy-risperidone has strong dopamine D_2 receptor antagonistic properties, and, compared with risperidone, an even lower brain-to-plasma ratio and a longer half-life

(24). In addition, this metabolite appears to play a role in plasma prolactin elevation (25), and elevated prolactin level increases dopamine synthesis in pituitary neurons by increasing tyrosine hydroxylase activity. Although the mechanism is not exactly clear, this may suggest that risperidone could influence plasma DDC activity as well. Exclusion of these patients from the analyses yielded no relevant change of results though. Other antipsychotic medications were not significantly associated with DDC activity. Also nonuse of medication did not result in significantly different DDC activity (N = 7, mean ± SD = 23.1 ± 5.4). However, the current study included a modest sample size and there was a wide variety in antipsychotic use. Ideally, plasma DDC activity should be assessed in medication-naïve patients, or at least in patients with short period of treatment with antipsychotic medication and who are medication-free at time of plasma sampling. Evaluating plasma DDC activity in these patients may still be of interest before ruling out plasma DDC activity measure as potential biomarker.

This study has several limitations, including modest sample size, heterogeneity in diagnosis, heterogeneity in antipsychotic use, and inclusion of patients with nicotine and cannabis use (which may affect presynaptic striatal dopamine) (26). Furthermore, results are only applicable to male recent onset psychotic patients, because women were not included in the analyses. Taken together, it should be regarded as a pilot study to assess the potential of plasma DDC activity as biomarker for TR. The current findings point out that a future study that would investigate plasma DCC activity as biomarker for TR should include a larger sample size, ideally in medication-naïve schizophrenia male and female patients without substance abuse. A longitudinal study design would preferably include structured follow up with PANSS assessment and blood sampling. Plasma DDC activity measurements at follow up could provide information about changes in plasma DDC activity in TR and responders and the effect of medication use on plasma DDC activity. Furthermore, correlation of plasma DDC activity with [^{18}F]F-DOPA PET could validate the plasma measure as surrogate for striatal DDC activity. In spite of the limitations of the current study, the results show very similar plasma DDC activity between responders and TR. We cannot exclude the possibility of a false negative finding with this study, but it does suggest that a potential effect size would be too small for clinical use. Taken together, plasma DDC activity does not appear to be a promising biomarker for TR in patients currently using antipsychotic medication. Future research on biomarkers for TR could focus on other potential derivatives of dopamine synthesis in the brain or on other neurotransmitter systems (e.g. glutamate) (27,28).

References

1. Suzuki T, Remington G, Mulsant BH, et al. Defining treatment-resistant schizophrenia and response to antipsychotics: a review and recommendation. Psychiatry Res 2012; 197: 1–6.
2. Chakos M, Lieberman J, Hoffman E, et al. Effectiveness of second-generation antipsychotics in patients with treatment-resistant schizophrenia: a review and meta-analysis of randomized trials. Am J Psychiatry 2001; 158: 518–526.
3. Yada Y, Yoshimura B, Kishi Y. Correlation between delay in initiating clozapine and symptomatic improvement. Schizophr Res 2015; 168: 585–586.
4. Yoshimura B, Yada Y, So R, et al. The critical treatment window of clozapine in treatment-resistant schizophrenia: secondary analysis of an observational study. Psychiatry Res 2017; 250: 65–70.
5. Üçok A, Çikrikçili U, Karabulut S, et al. Delayed initiation of clozapine may be related to poor response in treatment-resistant schizophrenia. Int Clin Psychopharmacol 2015; 30: 290–295.
6. Fusar-Poli P, Meyer-Lindenberg A. Striatal presynaptic dopamine in schizophrenia, part II: meta-analysis of [^{18}F/^{11}C]-DOPA PET studies. Schizophr Bull 2013; 39: 33–42.
7. Weinstein JJ, Chohan MO, Slifstein M, et al. Pathway-specific dopamine abnormalities in schizophrenia. Biol Psychiatry 2017; 81: 31–42.
8. Jauhar S, Nour MM, Veronese M, et al. A test of the transdiagnostic dopamine hypothesis of psychosis using positron emission tomographic imaging in bipolar affective disorder and schizophrenia. JAMA Psychiatry 2017; 74: 1206–1213.
9. Laruelle M, Abi-Dargham A, Gil R, et al. Increased dopamine transmission in schizophrenia: relationship to illness phases. Biol Psychiatry 1999; 46: 56–72.
10. Demjaha A, Murray RM, McGuire PK, et al. Dopamine synthesis capacity in patients with treatment-resistant schizophrenia. Am J Psychiatry 2012; 169: 1203–1210.
11. Kim E, Howes OD, Veronese M, et al. Presynaptic dopamine capacity in patients with treatment-resistant schizophrenia taking clozapine: an [^{18}F] DOPA PET study. Neuropsychopharmacology 2017; 42: 941–950.
12. Li J, Meltzer HY. A genetic locus in 7p12.2 associated with treatment resistant schizophrenia. Schizophr Res 2014; 159: 333–339.
13. O'Reilly R, Davis BA, Durden DA, et al. Plasma phenylethylamine in schizophrenic patients. Biol Psychiatry 1991; 30: 145–150.
14. Davis BA, Shrikhande S, Paralikar VP, et al. Phenylacetic acid in CSF and serum in Indian schizophrenic patients. Prog Neuropsychopharmacol Biol Psychiatry 1991; 15: 41–47.
15. Kay S, Fiszbein A, Opler L. The positive and negative syndrome scale for schizophrenia. Schizophr Bull 1987; 13: 261–276.
16. Leuzzi V, Mastrangelo M, Polizzi A, et al. Report of two never treated adult sisters with aromatic l-amino Acid decarboxylase deficiency: a portrait of the natural history of the disease or an expanding phenotype? JIMD Reports 2014; 15: 39–45.
17. De Bartolomeis A, Balletta R, Giordano S, et al. Differential cognitive performances between schizophrenic responders and non-responders to antipsychotics: correlation with course of the illness, psychopathology, attitude to the treatment and antipsychotics doses. Psychiatry Res 2013; 210: 387–395.
18. Lee J, Fervaha G, Takeuchi H, et al. Positive symptoms are associated with clinicians' global impression in treatment-resistant schizophrenia. J Clin Psychopharmacol 2015; 35: 237–241.
19. McCutcheon R, Beck K, Jauhar S, et al. Defining the locus of dopaminergic dysfunction in schizophrenia: a meta-analysis and test of the mesolimbic hypothesis. Schizophr Bull 2017: 1–4.
20. Laruelle M, Abi-Dargham A, van Dyck CH, et al. Single photon emission computerized tomography imaging of amphetamine-induced dopamine release in drug-free schizophrenic subjects. Proc Natl Acad Sci USA 1996; 93: 9235–9240.
21. Breier A, Su TP, Saunders R, et al. Schizophrenia is associated with elevated amphetamine-induced synaptic dopamine concentrations: evidence from a novel positron emission tomography method. Proc Natl Acad Sci USA 1997; 94: 2569–2574.

22. Slifstein M, Van De Giessen E, Van Snellenberg J, et al. Deficits in prefrontal cortical and extrastriatal dopamine release in schizophrenia a positron emission tomographic functional magnetic resonance imaging study. JAMA Psychiatry 2015; 72: 316–324.
23. Aravagiri M, Yuwiler A, Marder SR. Distribution after repeated oral administration of different dose levels of risperidone and 9-hydroxy-risperidone in the brain and other tissues of rat. Psychopharmacology 1998; 139: 356–363.
24. Heykants J, Huang ML, Mannens G, et al. The pharmacokinetics of risperidone in humans: a summary. J Clin Psychiatry 1994; 55(Suppl): 13–7.
25. Knegtering R, Baselmans P, Castelein S, et al. Predominant role of the 9-hydroxy metabolite of risperidone in elevating blood prolactin levels. Am J Psychiatry 2005; 162: 1010–1012.
26. Thompson JL, Urban N, Slifstein M, et al. Striatal dopamine release in schizophrenia comorbid with substance dependence. Mol Psychiatry 2013; 18: 909–915.
27. Egerton A, Brugger S, Raffin M, et al. Anterior cingulate glutamate levels related to clinical status following treatment in first-episode schizophrenia. Neuropsychopharmacology 2012; 37: 2515–2521.
28. Demjaha A, Egerton A, Murray RM, et al. Antipsychotic treatment resistance in schizophrenia associated with elevated glutamate levels but normal dopamine function. Biol Psychiatry 2014; 75: e11–e13.

Author Contributions

JB, LdH and AS conceived and designed the study. AK and LZ analysed the blood samples. MvdP statistically analysed the data with the support of AS. MvdP wrote the draft of the original manuscript. All the authors critically reviewed the manuscript for intellectual content. All authors approved the final version of the manuscript for publication.

Chapter | 9

Glutamate and GABA levels in the anterior cingulate cortex in treatment resistant first episode psychosis patients

Marieke van der Pluijm, Maartje Alting, Anouk Schrantee, Richard A.E. Edden, Jan Booij, Lieuwe de Haan, Elsmarieke van de Giessen

Abstract

Around 30% of schizophrenic patients do not sufficiently respond to conventional antipsychotic treatment. The excitatory neurotransmitter glutamate and the inhibitory neurotransmitter γ-aminobutyric acid (GABA) are implicated treatment resistant (TR) patients. It is hypothesized that TR patients have more marked glutamatergic deficits than responders, but findings are inconclusive and the two neurotransmitters have only rarely been assessed in conjunction. Further research is needed to elucidate the role of glutamate and GABA in TR schizophrenia, especially in the early disease stage. We aimed to investigate the role of GABA and glutamate in first episode TR patients and explore whether GABA and/or glutamate could be potential markers for TR schizophrenia. Magnetic resonance spectroscopy (MRS) was used to assess glutamate and GABA+ in the anterior cingulate cortex (ACC) of 58 first episode psychosis patients. At 6 months follow-up treatment response was determined and in a subgroup of 33 patients a follow-up MRS was acquired. Glutamate and GABA+ levels were not significantly difference between TR patients and responders at baseline nor did we find an effect of time at follow-up. Importantly, the groups differed in voxel fractions of white matter and cerebral spinal fluid, which could have influenced our results. In sum, we did not find evidence for ACC glutamate or GABA+ as potential markers for treatment resistant antipsychotic using schizophrenia patients.

Introduction

Approximately 30% of patients with schizophrenia are treatment resistant (TR) and do not respond adequately to treatment with conventional antipsychotics (1). Patients are considered TR when they do not sufficiently respond to at least two adequate trials with first-line antipsychotics. This results in delays in effective treatment and is accompanied with unnecessary side effects of ineffective medication, lower quality of life, and longer hospitalizations (2). To date, clozapine is the only recognized treatment for TR patients. Clozapine, however, is associated with serious adverse effects and therefore underutilized (3) with delays in clozapine initiation that can mount up to years (4). This is a problem as delay in effective treatment results in a poorer prognosis (5,6). Elucidating the underlying neurobiology of treatment resistance in schizophrenia may aid in the development of new treatments and early markers for TR in schizophrenia.

Conventional antipsychotics have in common that they act as dopamine D_2-like receptor antagonists (7). Their working mechanism is thought to be based on blocking the presynaptic striatal hyperdopaminergic signal that has been associated with the positive symptoms in schizophrenia (8). However, TR patients do not show this striatal hyperdopaminergic state (9), which may explain why conventional antipsychotics are not effective in these patients. The pathophysiology of TR patients might therefore be more reliant on non-dopaminergic neurotransmitter systems. Instead, the glutamatergic system may have a more substantial role in TR schizophrenia (10). Whereas TR patients show normal striatal dopamine synthesis capacity, they have elevated glutamate levels in the anterior cingulate cortex (ACC) (9). Responders to first-line antipsychotics, on the other hand, showed relatively normal ACC glutamate levels. Indeed, data from other Magnetic Resonance Spectroscopy (MRS) studies suggest that increased ACC glutamate levels are associated with TR schizophrenia (11-14). One study showed that higher baseline ACC glutamate levels in antipsychotic-naïve first episode patients were associated with a higher likelihood of non-response (15).

The glutamate hypothesis postulates that the increased glutamate in schizophrenia is secondary to a loss of γ-aminobutyric acid (GABA) inhibition as a result of N-methyl-D-aspartate (NMDA) receptor hypofunctioning (16). As such, GABA could also be dysregulated in treatment resistance. One longitudinal MRS study found that lower ACC GABA levels in antipsychotic-naïve patients compared to controls are associated with eventual non-response (17). While the above-mentioned studies suggest elevated glutamate levels and decreased GABA levels in the ACC as markers for treatment resistance in schizophrenia, the number of studies are limited and some have found no changes or even contrary results (18-20). Only one other MRS study has investigated GABA levels in the ACC of TR patients and showed increased GABA levels in ultra-TR patients compared to TR patients that did respond to clozapine, but no differences were found in GABA levels compared to responders or healthy controls (21).

In addition, they found no significant difference in glutamate levels between all groups. In fact, a meta-analysis including four studies on ACC glutamate levels in TR patients showed no significant difference between TR patients and responders (10). This finding is uncertain since there was significant heterogeneity in group demographics, especially illness duration, across studies. Kumar and colleagues highlighted the need for research in patients that are in the early stages of schizophrenia, as clinical application of markers for TR patients are most relevant for first episode psychosis patients.

The primary objective of the current study is to further elucidate the roles of glutamate and GABA in the ACC in TR first episode psychosis. We hypothesized that TR patients show increased glutamate levels and decreased GABA levels compared to responders. Furthermore, we explored whether glutamate and GABA levels, or a combination, could have potential as marker for identifying TR in first episode schizophrenia patients.

Methods

Participants

First episode psychosis patients with a primary diagnosis in the schizophrenia spectrum were recruited through specialized early psychosis clinics in Amsterdam, the Netherlands. Healthy volunteers were recruited through (online) advertisement to serve as control group. All participants were aged between 18 and 35 years. Exclusion criteria were: use of antipsychotic medication longer than one year; current use of other dopaminergic medication or recreational drugs; use of benzodiazepines on the test day; past or present substance use disorder and current substance use with the exception of nicotine, alcohol and cannabis; neurological disorder; MRI contraindications and pregnancy. We allowed for medication use up to one year and cannabis use to be able to acquire a representative group of first episode patients with an initial referral to a specialized early psychosis clinic. In addition, controls were excluded if they had a diagnosis of a psychiatric disorder, used psychotropic medication or had a positive family history (first and second degree) for psychotic disorders. Controls were matched based on age, gender, smoking status and IQ. This study was approved by the Medical Ethics Committee of the Amsterdam Medical Centre, University of Amsterdam (METC 2017_307) and registered at the Central Committee on Research Involving Human Subjects (NL63410.018.17). All participants provided written informed consent before entering the study.

Study design

Participants were assessed at baseline and patients were consecutively followed up at six months to determine treatment response status. Baseline measurements included an MRI scan, clinical interview and an IQ test. During the interview, general information, including demographics, current and past medication use and medical history were collected. Symptom

severity in patients was measured using the Positive and Negative Syndrome Scale (PANSS) (22). The Mini-International Neuropsychiatric Interview (MINI) was conducted in the healthy controls to rule out the presence of any psychiatric disorder (23). Global functioning was measured using the Global Assessment of Functioning (GAF) scale. Alcohol and drug use were measured with the Composite International Diagnostic Interview (CIDI) (24). In addition, urine drug screening was performed, as well as a pregnancy test for women. IQ was estimated with shortened version of the Wechsler Adult Intelligence Scale (WAIS-III) (25). During the entire study, patients were prescribed antipsychotic treatment based on standard clinical guidelines by their treating psychiatrist.

Treatment response

Treatment response was assessed after six months follow-up using the PANSS. Patients were considered TR when, despite adequate treatment of minimal two trials of different antipsychotics, at least one of the following items of the PANSS was scored moderate or higher: delusions (P1), conceptual disorganization (P2), hallucinatory behaviour (P3), mannerisms and posturing (G5) and unusual thought content (G9) (26). Patients were also classified as TR when they used clozapine at follow-up. For patients who were lost to follow up, response was determined based on medical files and contact with their clinician. This subgroup of patients were classified as TR if they were treated with clozapine, and as responders if the clinician reported remission on standard antipsychotic treatment. If treatment response could not be determined, patients were not included in the analyses. If consent was given, at baseline and follow-up a blood draw was conducted in the patients to measure antipsychotic serum levels and patients' relatives were contacted at 6 months follow-up to evaluate adherence to antipsychotic medication. In addition, a follow-up MRI scan was conducted in patients who consented.

MR Acquisition

Single voxel proton MRS was obtained to assess glutamate and GABA levels in the ACC. All MR scans were acquired using a 3 Tesla Philips MR scanner (Philips, Ingenia Elition X, Best, The Netherlands) with a 32-channel head coil. For placement of the MRS voxels and brain tissue segmentation, a 3D whole brain-structural T1-weighted image was acquired (echo time [TE]/repetition time [TR]=4.1/9.0 ms; 189 slices; field of view [FOV]=284×284×170 mm; voxel size: 0.9 mm^3 isotropic, flip angle [FA]=8˚). MRS voxels were placed parallel to the corpus callosum on the sagittal midline, as shown in Figure 1 (similar to (11,15,20)).

Point Resolved Spectroscopy (PRESS) pulse sequence was used to acquire the metabolite spectra for glutamatergic measurements (TE = 35 ms; TR = 2000 ms; 128 averages; spectral width = 2000 Hz; voxel size = 20 x 20 x 20 mm, with MOIST water-suppression). GABA-edited ^{1}H J-difference spectra were acquired using a Meshcher-Garwood Point Resolved Spectroscopy (MEGA-PRESS) pulse sequence with an on-resonance editing pulse (ON) applied at 1.9 ppm

and an off-resonance editing pulse (OFF) applied at 7.5 ppm (TE = 68 ms; TR = 2000 ms; 320 averages; spectral width = 2000 Hz; voxel size = 30 x 30 x 25 mm, with VAPOR water-suppression) (27,28). See supplementary table S1 for additional parameters of the MRS sequences.

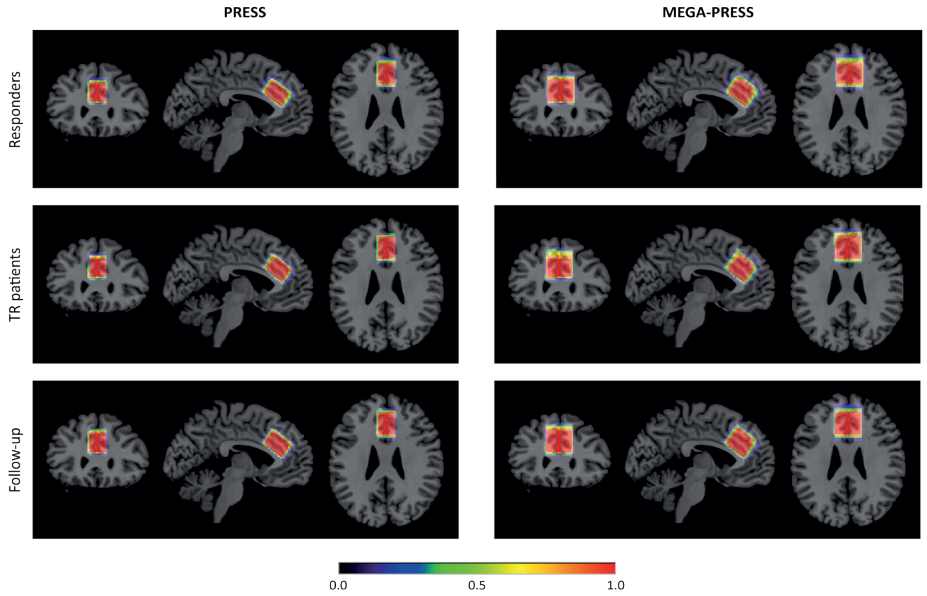

Figure 1. MRS voxel placement of A) Point resolved spectroscopy (PRESS) and B) Meshcher-Garwood Point Resolved Spectroscopy (MEGA-PRESS). The voxel was placed parallel to the anterior cingulate cortex (ACC). The color bar represents fraction of voxel overlap within groups (responders, treatment resistant patients (TR), follow-up (including responders and TR), after normalization to MNI-space, with red indicating greater overlap between participants.

Spectral quantification and quality control

Glutamate + glutamine (Glx) concentrations were determined from the PRESS spectra as proxy measure of glutamate, due to overlap in spectral assignment of glutamate and glutamine on a 3 Tesla scanner (29). The PRESS spectra were fitted using Linear Combination model (LCModel) version 6.3-1P with a standard basis set with 16 metabolites. The node spacing for the spline function (DKNTMN) was set to 0.5 ppm to stiffen the baseline (30). After eddy current correction, water scaling was applied to estimate Glx concentrations, as well as other neurometabolites (supplementary methods S1). PRESS spectra were visually checked, and spectra with a Full-Width at Half-Maximum (FWHM) >0.1ppm, Signal-to-Noise ratio (SNR) <20 or with Cramer-Rao Lower Bounds (CRLB) >15% for Glx were classified as poor-quality spectra and were excluded from further analysis (31,32).

The MEGA-PRESS sequence is optimized for GABA measurements (27,33). We quantified GABA levels including macromolecules (GABA+), as the macromolecules resonate at the same frequency as GABA in the MEGA-PRESS sequence (3.0 ppm) (34). Analysis of the MEGA-PRESS

spectra, were automatically performed using Gannet3.1 (35) in MATLAB (The MathWorks, Inc., Natick, MA, 2016). The MEGA-PRESS spectra were visually checked, and spectra with a Fit Error (FE) >20%, FWHM >29.6Hz (0.1ppm) or SNR <8 were classified as poor-quality spectra and were subsequently excluded from further analysis (36).
3D T1-weighted images were used to determine the voxel tissue fractions for the PRESS and MEGAPRESS voxels using Gannet 3.1 (35) in MATLAB (The MathWorks, Inc., Natick, MA, 2016). The voxel tissue fractions, grey matter (GM), white matter (WM) and cerebrospinal fluid (CSF), were used to perform partial volume correction on all metabolite concentrations (12, 20, 37). This equation (supplementary equation S1) takes into account the relative densities of MR-visible water in GM, WM and CSF.

Statistical Analysis

Statistical analyses were performed using RStudio 4.0.3. Our main analysis assessed group differences at baseline between TR patients and responders for Glx and GABA+ using an independent T-test, and assessed the association between Glx and GABA+ by using Pearson correlation. In addition, we explored the effects of Glx and GABA+ at baseline on treatment response using a logistic regression with treatment response status as dependent variable. As a secondary aim, changes in neurometabolite levels over six months follow-up were assessed, using a linear mixed effect model including all baseline and follow-up participants, with time (baseline, follow-up) as the independent variable while controlling for treatment response status and including subject as a random effect.

In the supplementary materials we report post-hoc analysis for Glx and GABA+ including the control group to assess the differences between responders, TR patients and controls and exploratory group comparisons for the additional metabolites from the PRESS spectra.

Appropriate parametric tests were used or non-parametric tests when normality assumptions were violated. Outliers were defined as +/- 2 SD from the group mean, in case of outliers the results were reported with and without excluding the outliers. To account for multiple testing, Bonferroni correction was applied for the analyses on Glx and GABA+, hence results were considered statistically significant at $p<0.025$. Exploratory and post-hoc analyses were performed without correction for multiple comparisons and considered statistically significant at $p<0.05$.

Results

In total, 78 patients and 20 controls were included in the study. After exclusions, 58 patients were retained (supplementary methods S1), of which 46 responders and 12 TR patients. Thirty-four patients participated in the follow-up MRI scan (27 responders and 7 TR patients). Demographic and clinical characteristics of the participants at baseline are summarized in Table 1.

No significant differences were found between the two groups in sex, age, IQ, nicotine use, and cannabis use (Table 1). The TR patients had longer duration of antipsychotic use, a lower score on the GAF and a higher score on the PANSS positive scale than responders (Table 1).

Table 1. Demographic and clinical characteristics of responders and TR patients

	Responders N = 46	**TR patients N= 12**	**p-value**
	Mean (SD)	**Mean (SD)**	
Male[1]	31 (67.4%)	9 (75.0%)	0.612
Age (years)	24.15 (4.64)	21.67 (3.42)	0.095
IQ	91.74 (14.22)	90.75 (13.06)	0.828
Smoker (N)[1]	22 (47.8%)	5 (41.1%)	0.756
Nicotine use (sig/day)	5.98 (7.34)	5.58 (7.19)	0.820
Cannabis user (N) [1]	27 (58.7%)	5 (41.7%)	0.341
Cannabis use (weeks/year)	14.17 (19.21)	14.50 (22.55)	0.828
GAF score	58.24 (11.49)	51.00 (8.68)	0.047*
Age at illness onset (years)	23.44 (4.57)	20.75 (3.67)	0.095
Illness duration (weeks)	39.51 (40.98)	53.76 (42.97)	0.189
Medication duration (weeks)	13.08 (9.27)	20.02 (10.5)	0.032*
Medication dosage (mg/day CPZ)	365.38 (186.97)	312.88 (160.13)	0.284
PANSS positive	10.52 (3.48)	14.33 (5.47)	0.028*
PANSS negative	11.37 (4.20)	14.00 (5.69)	0.134
PANSS general	22.44 (4.52)	24.83 (5.73)	0.193

CPZ, chlorpromazine equivalent; GAF, global assessment of functioning; IQ, Intelligence quotient; PANSS, positive and negative syndrome scale; TR, treatment resistant.
* $p < 0.05$ [1] Number (%) instead of Mean (SD)

MRS Data Quality

One responder was excluded from the glutamate analysis and one TR from the GABA+ analysis due to low SNR. One TR and one responder did not complete the MEGA-PRESS acquisition. This resulted in a group of 45 responders and 12 TR patients for the glutamate analysis and 45 responders and 10 TR patients for the GABA+ analysis. MRS spectral quality measurements (after quality control) are summarized in Table 2. Even though significant between-group differences were found in SNR and CRLB for the PRESS spectra, all were of good quality (CRLB <5% and SNR >21, see supplementary figure S1 for an example spectrum). Voxel fractions differed between TR patients and responders for WM and CSF but not GM (Table 2), even though voxel placement was consistent (Figure 1).

Table 2. MRS Spectral Quality Measurements for responders and TR patients

	Responders	TR patients	Statistic	P-value
PRESS	**N=45**	**N=12**		
CRLB Glu	3.62 (0.49)	4.17 (0.39)	X^2=12.7	0.002*
CRLB Glx	3.53 (0.55)	4.08 (0.52)	X^2= 8.80	0.012*
FWHM	0.036 (0.008)	0.036 (0.006)	W=273.5	0.952
SNR	27.60 (2.33)	25.75 (2.49)	*t*=2.32	0.034*
GM	0.69 (0.034)	0.67 (0.035)	*t*=1.14	0.270
WM	0.17 (0.0260)	0.15 (0.022)	*t*=2.51	0.021*
CSF	0.15 (0.036)	0.18 (0.036)	W=130	0.005*
MEGAPRESS	**N=45**	**N=10**		
FE GABA+	6.77 (1.84)	7.28 (2.69)	W=196	0.606
FWHM	18.6 (2.13)	18.1 (1.91)	W=298	0.397
SNR	15.3 (2.44)	14.1 (3.14)	t=1.16	0.271
GM	0.514 (0.0271)	0.515 (0.0271)	t=-0.05	0.959
WM	0.380 (0.0286)	0.354 (0.0337)	t=2.32	0.039*
CSF	0.105 (0.0221)	0.131 (0.0321)	t=-2.45	0.032*

CRLB, Cramer-Rao Lower Bound; CSF, cerebrospinal fluid; FE, Fit Error; FWHM, full-width at half maximum; GABA+, γ-aminobutyric acid; Glu, glutamate; Glx, glutamate + glutamine; GM, grey matter; SNR, signal-to-noise ratio; WM, white matter.
*p<0.05

Baseline glutamate and GABA+

No significant difference was found for Glx between responders (mean ± SD=17.82 ±1.38) and TR patients (mean ± SD= 17.07 ± 1.54), $t(56)=1.55$, p=0.14 (Figure 2). After exclusion of outliers, results remained similar ($t(52) = 1.49$, $p = 0.160$). In addition, no significant differences were found for GABA+ between responders (mean ± SD=2.51 ± 0.41) and TR patients (mean ± SD= 2.44 ± 0.48), $t(57)=0.46$, p=0.66 (Figure 2). Moreover, no difference were found in Glx and GABA+ between controls, responders and TR patients, $F(1,74)=1.21$, p=0.304 and $F(1,71)=0.793$, p=0.456, respectively (supplementary table S3). Pearson's correlation analysis showed that GABA+ did not correlate with Glx, $r(52)=-0.035$, p=0.80.

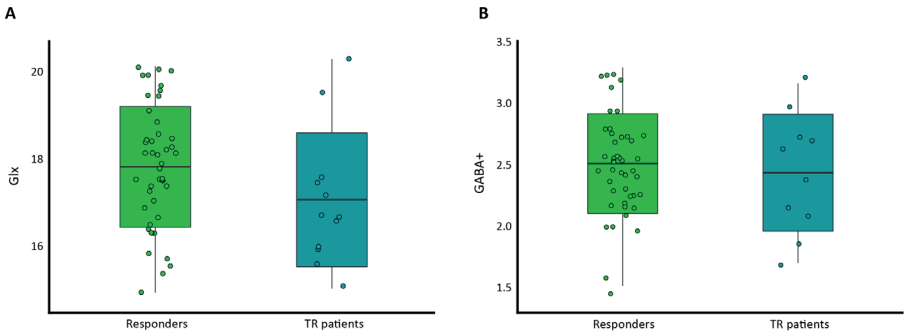

Figure 2. Scatterplots of metabolite levels for responders and treatment resistant (TR) patients at baseline with A) glutamate + glutamine (Glx) and B) γ-aminobutyric acid (GABA+). Boxplots showing the group mean ± SD.

Secondary analyses

The binary logistic regression indicated that there was no significant association of Glx and GABA+ on treatment response at baseline, $\chi2(2) = 3.521$, $p = 0.172$ (supplementary table S4). The linear mixed effects model, including all baseline and follow-up measurements, showed no significant effect of 6 months follow-up on Glx and GABA+, p=0.093 and p=0.315, respectively (supplementary table S4).

Post-hoc exploratory correlations

Spearman's correlation analyses were performed to assess the relationship between metabolite concentrations and duration of antipsychotic use, GAF-score and PANSS positive score, WM, CSF and SNR, because the TR patients and responders differed on these variables. No significant correlations were found (supplementary table S5). In addition, we explored the association between voxel fractions and quality of the MR spectrum and found a significant correlation between WM and CSF, and the FWHM and SNR for the PRESS sequence (supplementary table S6).

Discussion

The aim of this study was to elucidate the roles of glutamate and GABA in the ACC in TR first episode psychosis. No significant differences between TR patients and responders for glutamate and GABA were found. Hence, we did not find evidence that these metabolites can aid to identify TR patients. Moreover, GABA levels did not correlate with glutamate levels. Lastly, the longitudinal analysis did not reveal an effect of 6 months follow up on GABA or glutamate levels.

Contrary to our hypothesis, and to previous literature demonstrating increased glutamate metabolite levels (11,13,14,38), glutamate was not significantly different between responders and TR patients.

A possible explanation for our findings might be that 10 of the 12 TR patients in our sample responded to clozapine at follow-up. Studies that did find elevated levels of glutamatergic metabolites in TR patients, excluded (former) clozapine-users (12,14). Indeed, one study showed elevated glutamate levels in clozapine-resistant patients compared to responders, while no elevated glutamate levels were seen in clozapine-responsive patients (13). Another explanation could be the high heterogeneity in illness duration and medication use between studies. Most studies included patients that are in a later stage of the illness, with a duration of illness of five years (12), ten years (18), or even 16 years (9). Interestingly, a study with an illness duration similar to our sample also did not find any difference in glutamate levels in the ACC between TR patients and responders at baseline nor at 9 months follow-up (20). They hypothesized that their null findings might be due to the fact that their patients, similar to the patients in the current study, were not antipsychotic-naïve. Namely, a study in antipsychotic-naïve patients show reductions in glutamate after four weeks of treatment (15). Moreover, a mega-regression has shown that glutamate levels are susceptible to antipsychotic dose (39).

The number of MRS studies investigating GABA in TR schizophrenia are limited, even though especially GABA levels in the ACC are implicated in schizophrenia (40). We expected decreased GABA levels in TR patients based upon earlier GABA findings in schizophrenia, the glutamate hypothesis, and the finding that lower GABA baseline levels in the ACC were associated with non-response (17). Conversely, the only cross-sectional study that compared TR patients with responders (instead of controls) found, in line with our results, no difference between TR and responders (21). They did find decreased GABA in clozapine responding TR patients compared to ultra-TR patients. This again highlights the importance of differentiating between TR and ultra-TR. It is important to note that, contrary to our current study, this study included chronic schizophrenia patients with an illness duration around 20 years. The meta-analysis of Kumar et al. (2022) demonstrated that the decrease of GABA levels in schizophrenia compared to controls are most pronounced in first-episode schizophrenia (40). Bojesen et al. (2019), did include first episode antipsychotic-naïve patients, but did not compare TR patients with responders and only assessed the predictive value of glutamate and GABA relative to controls (17). However, in clinical practice it would be essential for a TR marker to be able to differentiate between TR patients and responders at an early illness stage.

The strength of the current study is that we compared both GABA and glutamate between responders and TR patients in first episode schizophrenia patients using a longitudinal design. However, a limitation of our study is that the patients were not antipsychotic-naïve at baseline, and TR patients had a longer duration of antipsychotic use and higher symptom severity. This could have influenced our results, however the post-hoc correlations did not reveal any significant correlations with the GABA or glutamate metabolites in the complete patient sample. Moreover, we found no significant differences between baseline and follow-up, while all patients were on antipsychotic medication during the follow-up period. In addition,

although results are inconsistent and an effect of antipsychotic dose has been found, there is no evidence of an effect of antipsychotic medication duration or symptom severity on glutamate levels in the ACC (39).

Most importantly, we found a significant difference in the voxel fractions of CSF and WM. These differences might influence the quality of the MRS spectrum and metabolite levels. For the PRESS sequence higher WM and lower CSF fractions were associated with better spectrum quality, and WM and CSF fraction were significantly correlated (supplementary table S6). These findings are not a result of a-priori analyses and therefore need to be interpreted with caution. In the CSF the metabolite concentrations are negligible, hence higher fractions of CSF in the voxel could render lower metabolite levels. We correct for CSF content using the voxel fraction correction equation, however this might not be sufficient. Glutamate and GABA concentrations also differ between GM and WM and variation in tissue composition could lead to variance in glutamate and GABA measurements (41,42). The voxel fraction differences are, however, in line with previous research. Schizophrenia is known to be associated with brain volume reductions, including in the ACC (43). Several studies have shown GM and cortical thickness associated with treatment non-response (44), however more recent papers have implicated especially WM deficits with treatment resistance (45-47). These findings stress the importance to take voxel fractions into account in MRS studies comparing TR patients and responders. The exploratory analyses, including healthy controls, showed a significant effect of group for all additional metabolites. However, again differences in voxel fractions might underlie these differences.

Conclusion

We did not find evidence that glutamate or GABA levels in the ACC could be a potential marker for treatment resistance in schizophrenia. Previous studies and our results suggest that MRS measurements of glutamate and GABA, are susceptible to multiple confounders including brain fractions, medication dose, illness duration and clozapine responsiveness. This complicates disentangling the role of glutamate and GABA in treatment resistance schizophrenia. Future research to explore the role of GABA and glutamate in treatment resistance schizophrenia should take these confounders into account, e.g., include medication naïve patients, follow up longitudinal, and distinguish between TR-clozapine responders and TR-clozapine resistant patients.

References

1. Elkis H, Buckley PF. Treatment-Resistant Schizophrenia. Psychiatr Clin North Am. 2016;39(2):239-65.
2. Kennedy JL, Altar CA, Taylor DL, Degtiar I, Hornberger JC. The social and economic burden of treatment-resistant schizophrenia: a systematic literature review. Int Clin Psychopharmacol. 2014;29(2):63-76.
3. Warnez S, Alessi-Severini S. Clozapine: a review of clinical practice guidelines and prescribing trends. BMC Psychiatry. 2014;14(1):102.
4. Howes OD, Vergunst F, Gee S, McGuire P, Kapur S, Taylor D. Adherence to treatment guidelines in clinical practice: study of antipsychotic treatment prior to clozapine initiation. Br J Psychiatry. 2012;201(6):481-5.
5. Black K, Peters L, Rui Q, Milliken H, Whitehorn D, Kopala LC. Duration of untreated psychosis predicts treatment outcome in an early psychosis program. Schizophrenia Research. 2001;47(2):215-22.
6. Yoshimura B, Yada Y, So R, Takaki M, Yamada N. The critical treatment window of clozapine in treatment-resistant schizophrenia: Secondary analysis of an observational study. Psychiatry Res. 2017;250:65-70.
7. Martel JC, Gatti McArthur S. Dopamine Receptor Subtypes, Physiology and Pharmacology: New Ligands and Concepts in Schizophrenia. Front Pharmacol. 2020;11:1003.
8. Howes OD, Kapur S. The dopamine hypothesis of schizophrenia: version III--the final common pathway. Schizophr Bull. 2009;35(3):549-62.
9. Demjaha A, Egerton A, Murray RM, Kapur S, Howes OD, Stone JM, et al. Antipsychotic treatment resistance in schizophrenia associated with elevated glutamate levels but normal dopamine function. Biol Psychiatry. 2014;75(5):e11-3.
10. Kumar V, Manchegowda S, Jacob A, Rao NP. Glutamate metabolites in treatment resistant schizophrenia: A meta-analysis and systematic review of (1)H-MRS studies. Psychiatry Res Neuroimaging. 2020;300:111080.
11. Egerton A, Brugger S, Raffin M, Barker GJ, Lythgoe DJ, McGuire PK, et al. Anterior cingulate glutamate levels related to clinical status following treatment in first-episode schizophrenia. Neuropsychopharmacology. 2012;37(11):2515-21 .
12. Egerton A, Murphy A, Donocik J, Anton A, Barker GJ, Collier T, et al. Dopamine and Glutamate in Antipsychotic-Responsive Compared With Antipsychotic-Nonresponsive Psychosis: A Multicenter Positron Emission Tomography and Magnetic Resonance Spectroscopy Study (STRATA). Schizophr Bull. 2021;47(2):505-16.
13. Iwata Y, Nakajima S, Plitman E, Caravaggio F, Kim J, Shah P, et al. Glutamatergic Neurometabolite Levels in Patients With Ultra-Treatment-Resistant Schizophrenia: A Cross-Sectional 3T Proton Magnetic Resonance Spectroscopy Study. Biol Psychiatry. 2019;85(7):596-605.
14. Mouchlianitis E, Bloomfield MAP, Law V, Beck K, Selvaraj S, Rasquinha N, et al. Treatment-Resistant Schizophrenia Patients Show Elevated Anterior Cingulate Cortex Glutamate Compared to Treatment-Responsive. Schizophrenia Bulletin. 2016;42(3):744-52.
15. Egerton A, Broberg BV, Van Haren N, Merritt K, Barker GJ, Lythgoe DJ, et al. Response to initial antipsychotic treatment in first episode psychosis is related to anterior cingulate glutamate levels: a multicentre (1)H-MRS study (OPTiMiSE). Mol Psychiatry. 2018;23(11):2145-55.
16. Moghaddam B, Javitt D. From revolution to evolution: the glutamate hypothesis of schizophrenia and its implication for treatment. Neuropsychopharmacology. 2012;37(1):4-15.
17. Bojesen KB, Ebdrup BH, Jessen K, Sigvard A, Tangmose K, Edden RAE, et al. Treatment response after 6 and 26 weeks is related to baseline glutamate and GABA levels in antipsychotic-naive patients with psychosis. Psychol Med. 2020;50(13):2182-93.
18. Goldstein ME, Anderson VM, Pillai A, Kydd RR, Russell BR. Glutamatergic neurometabolites in clozapine-responsive and -resistant schizophrenia. Int J Neuropsychopharmacol. 2015;18(6).
19. Li J, Ren H, He Y, Li Z, Ma X, Yuan L, et al. Anterior Cingulate Cortex Glutamate Levels Are Related to Response to Initial Antipsychotic Treatment in Drug-Naive First-Episode Schizophrenia Patients. Front Psychiatry. 2020;11:553269.
20. Merritt K, Perez-Iglesias R, Sendt KV, Goozee R, Jauhar S, Pepper F, et al. Remission from

antipsychotic treatment in first episode psychosis related to longitudinal changes in brain glutamate. NPJ Schizophr. 2019;5(1):12.

21. Ueno F, Nakajima S, Iwata Y, Honda S, Torres-Carmona E, Mar W, et al. Gamma-aminobutyric acid (GABA) levels in the midcingulate cortex and clozapine response in patients with treatment-resistant schizophrenia: A proton magnetic resonance spectroscopy ((1) H-MRS) study. Psychiatry Clin Neurosci. 2022;76(11):587-94.
22. Kay SR, Fiszbein A, Opler LA. The positive and negative syndrome scale (PANSS) for schizophrenia. Schizophrenia bulletin. 1987;13(2):261-76.
23. Sheehan DV, Lecrubier Y, Sheehan KH, Amorim P, Janavs J, Weiller E, et al. The Mini-International Neuropsychiatric Interview (MINI): the development and validation of a structured diagnostic psychiatric interview for DSM-IV and ICD-10. Journal of clinical psychiatry. 1998;59(20):22-33.
24. Cooper L, Peters L, Andrews G. Validity of the Composite International Diagnostic Interview (CIDI) psychosis module in a psychiatric setting. Journal of Psychiatric Research. 1998;32(6):361-8.
25. Velthorst E, Levine SZ, Henquet C, de Haan L, van Os J, Myin-Germeys I, et al. To cut a short test even shorter: reliability and validity of a brief assessment of intellectual ability in schizophrenia--a control-case family study. Cogn Neuropsychiatry. 2013;18(6):574-93.
26. Nancy C. Andreasen, M.D., Ph.D. ,, William T. Carpenter J, , M.D. ,, John M. Kane, M.D. ,, Robert A. Lasser, M.D. ,, Stephen R. Marder, M.D. , and, Daniel R. Weinberger, M.D. Remission in Schizophrenia: Proposed Criteria and Rationale for Consensus. American Journal of Psychiatry. 2005;162(3):441-9.
27. O'Gorman RL, Michels L, Edden RA, Murdoch JB, Martin E. In vivo detection of GABA and glutamate with MEGA-PRESS: reproducibility and gender effects. J Magn Reson Imaging. 2011;33(5):1262-7.
28. Mescher M, Merkle H, Kirsch J, Garwood M, Gruetter R. Simultaneousin vivo spectral editing and water suppression. NMR in Biomedicine. 1998;11(6):266-72.
29. Ramadan S, Lin A, Stanwell P. Glutamate and glutamine: a review of in vivo MRS in the human brain. NMR Biomed. 2013;26(12):1630-46.
30. Bhogal AA, Schur RR, Houtepen LC, van de Bank B, Boer VO, Marsman A, et al. (1) H-MRS processing parameters affect metabolite quantification: The urgent need for uniform and transparent standardization. NMR Biomed. 2017;30(11).
31. Duda JM, Moser AD, Zuo CS, Du F, Chen X, Perlo S, et al. Repeatability and reliability of GABA measurements with magnetic resonance spectroscopy in healthy young adults. Magn Reson Med. 2021;85(5):2359-69.
32. Smucny J, Carter CS, Maddock RJ. Medial Prefrontal Cortex Glutamate Is Reduced in Schizophrenia and Moderated by Measurement Quality: A Meta-analysis of Proton Magnetic Resonance Spectroscopy Studies. Biol Psychiatry. 2021;90(9):643-51.
33. Mullins PG, McGonigle DJ, O'Gorman RL, Puts NA, Vidyasagar R, Evans CJ, et al. Current practice in the use of MEGA-PRESS spectroscopy for the detection of GABA. Neuroimage. 2014;86:43-52.
34. Bell T, Boudes ES, Loo RS, Barker GJ, Lythgoe DJ, Edden RAE, et al. In vivo Glx and Glu measurements from GABA-edited MRS at 3 T. NMR Biomed. 2021;34(5):e4245.
35. Edden RA, Puts NA, Harris AD, Barker PB, Evans CJ. Gannet: A batch-processing tool for the quantitative analysis of gamma-aminobutyric acid-edited MR spectroscopy spectra. J Magn Reson Imaging. 2014;40(6):1445-52.
36. Wood ET, Cummings KK, Jung J, Patterson G, Okada N, Guo J, et al. Sensory over-responsivity is related to GABAergic inhibition in thalamocortical circuits. Transl Psychiatry. 2021;11(1):39.
37. Gasparovic C, Song T, Devier D, Bockholt HJ, Caprihan A, Mullins PG, et al. Use of tissue water as a concentration reference for proton spectroscopic imaging. Magn Reson Med. 2006;55(6):1219-26.
38. Egerton A, Grace AA, Stone J, Bossong MG, Sand M, McGuire P. Glutamate in schizophrenia: Neurodevelopmental perspectives and drug development. Schizophr Res. 2020;223:59-70.
39. Merritt K, McGuire PK, Egerton A, Investigators HMiS, Aleman A, Block W, et al. Association of Age, Antipsychotic Medication, and Symptom Severity in Schizophrenia With Proton Magnetic Resonance Spectroscopy Brain Glutamate Level: A Mega-analysis of Individual Participant-Level Data. JAMA Psychiatry. 2021;78(6):667-81.
40. Kumar V, Vajawat B, Rao NP. Frontal GABA in schizophrenia: A meta-analysis of (1)H-MRS studies. World J Biol Psychiatry. 2020:1-13.
41. Zhang Y, Shen J. Regional and tissue-specific differences in brain glutamate concentration measured by in vivo single voxel MRS. J Neurosci Methods. 2015;239:94-9.

42. Harris AD, Puts NA, Edden RA. Tissue correction for GABA-edited MRS: Considerations of voxel composition, tissue segmentation, and tissue relaxations. J Magn Reson Imaging. 2015;42(5):1431-40.
43. Baiano M, David A, Versace A, Churchill R, Balestrieri M, Brambilla P. Anterior cingulate volumes in schizophrenia: a systematic review and a meta-analysis of MRI studies. Schizophr Res. 2007;93(1-3):1-12.
44. Nakajima S, Takeuchi H, Plitman E, Fervaha G, Gerretsen P, Caravaggio F, et al. Neuroimaging findings in treatment-resistant schizophrenia: A systematic review: Lack of neuroimaging correlates of treatment-resistant schizophrenia. Schizophr Res. 2015;164(1-3):164-75.
45. McNabb CB, McIlwain ME, Anderson VM, Kydd RR, Sundram F, Russell BR. Aberrant white matter microstructure in treatment-resistant schizophrenia(☆). Psychiatry Res Neuroimaging. 2020;305:111198.
46. Kochunov P, Huang J, Chen S, Li Y, Tan S, Fan F, et al. White Matter in Schizophrenia Treatment Resistance. Am J Psychiatry. 2019;176(10):829-38.
47. Tong J, Zhou Y, Huang J, Zhang P, Fan F, Chen S, et al. N-methyl-D-aspartate Receptor Antibody and White Matter Deficits in Schizophrenia Treatment-Resistance. Schizophr Bull. 2021;47(5):1463-72.

Author Contributions

EvdG, JB and LdH conceived the study. EvdG and MvdP designed and planned the study. AS and RE implemented the MRI methods. MvdP performed the data collection. MvdP and MA analysed the data under supervision of AS and EvdG. MvdP wrote the draft of the original manuscript with support from MA. All the authors critically reviewed the manuscript for intellectual content. All authors approved the final version of the manuscript for publication.

Supplementary material

Table of contents:

Supplementary methods

Methods S1. Exploratory metabolites

PRESS spectra were fitted and quantified using Linear Combination Model (LCModel) version 6.3–1P, with a standard basis for PRESS a 3 Tesla and a TE of 35 ms containg 16 metabolites. We report in this supplement the additional metabolites with good spectral quality, including total creatine (tCr, creatine and phosphocreatine), myo-inisotol (mI), total NAA (tNAA, N-acetylaspartate and N-acetyl-aspartyl-glutamate), and total choline (tCho, glycerophosphocholine plus phosphocholine). A tissue fraction correction was performed on all metabolite levels to account for individual differences in CSF, WM and GM volumes and their relative water densities in the voxel, according to Equation S1.

Equation S1. Voxel fraction correction

[M]corr = [M]*(WM + 1.21*GM + 1.55*CSF) / (WM + GM)

[M]corr = Tissue fraction corrected metabolite level (mM)
[M] = Uncorrected metabolite level (mM)
WM = White matter content in voxel (%)
GM = Grey matter content in voxel (%)
CSF = Cerebrospinal fluid content in voxel (%)

Supplementary results

Results S1. Reasons for exclusion

A total of 20 patients were excluded from analysis. Reasons for exclusion were: change in diagnosis (non-schizophrenia spectrum, such as bipolar disorder) during follow-up (N=5), history of drug dependence or failed drug screening (N=3), use of benzodiazepines on the scan day (N=3), unclear treatment response, e.g. due to non-compliance (N=6) or excessive motion artifacts (N=1). Nine patients were lost to follow-up, for N=7, treatment response could be determined based on medical files and contact with clinicians and were retained in the sample.

Results S2. Exploratory analyses

As exploratory analyses we compared all metabolites, including the additional metabolites described in Methods S1, between responders, TR patients and healthy controls using an One Way ANOVA(Table S1). We found difference in GM and CSF between the three groups, with Tukey post-hoc analyses showing higher GM in controls compared to responders (PRESS p=0.002, MEGAPRESS p=0.041) and TR patients (PRESS p=0.002). Higher CSF was found for TR patients compared to responders (PRESS p=0.013, MEGAPRESS p=0.004) and controls (PRESS p<0.001, MEGAPRESS p<0.001). In addition, higher CSF was found in responders compared to controls (PRESS p=0.012). TCho, mI, tNAA yielded a significant difference, and tCR a trend significant difference, between the three groups (Table S1). Post-hoc analyses

revealed higher tCho (p<0.001), mI (p=0.002), in the TR patients than controls and trend level higher tNAA (p=0.051). In addition, responders showed higher tCho (p<0.001), mI (p=0.007) compared to controls, and trend level higher tNAA (p=0.060).

Supplementary tables and Figure

Table S1. Description of MRS data acquisition, analysis, and quality assessment.

	PRESS	**MEGA-PRESS**
1. Hardware		
a. Field Strenght	3T	3T
b. Manufacturer	Philips	Philips
c. Model	Ingenia Elition X	Ingenia Elition X
d. RF coil	32 channel coil	32 channel coil
e. Additional hardware	N/A	N/A
2. Acquisition		
a. Pulse sequence	PRESS	MEGA-PRESS
b. Volume of interest	ACC	ACC
c. Nominal VOI size	20 x 20 x 20 mm	30 x 30 x 25 mm
d. Repetition time (TR), echo time (TE)	TR/TE=2000/35 ms	TR/TE=2000/68 ms
e. Total number of acquisitions/averages	128	320
f. Additional sequence parameters	2000 Hz; 2048 data points	2000 Hz; 2048 data points
g. Water suppression method	MOIST	VAPOR
h. Shimming method	Automated	Automated
i. Triggering or motion correction method	None	None
3. Data analysis methods and outputs		
a. Analysis software	LC model 6.3-1P	GANNET 3.1
b. Processing steps deviating from quoted product	0.5 ppm DKNTMN	
c. Output measure	Water scaled, partial volume corrected	Water scaled, partial volume corrected
d. Quantification references and assumptions	Default basis set	Default fitting
4. Data quality		
a. Reported variables	SNR, FWHM	SNR, FWHM
b. Data exclusion criteria	SNR < 20, FWHM > 0.1 ppm, CRLB > 15%	SNR < 8, FWHM > 0.1 ppm, FE > 20%
c. Quality measures of postprocessing model fitting	CRLB	FE
d. Sample spectrum	Figure S1a	Figure S1b

Table S2. Demographics of responders, TR patients and controls at baseline

	Responders N = 46	**TR patients N= 12**	**Controls N = 20**	**p-value**
	Mean (SD)	Mean (SD)	Mean (SD)	
Male[1]	31 (67.4%)	9 (75.0%)	14 (70%)	0.875
Age (years)	24.15 (4.64)	21.67 (3.42)	22.7 (4.08)	0.242
IQ	91.74 (14.22)	90.75 (13.06)	92.95 (10.88)	0.867
Smoker[1]	22 (47.8%)	5 (41.1%)	9 (45%)	0.923
Nicotine use (sig/day)	5.98 (7.34)	5.58 (7.19)	7.75 (9.70)	0.433
Cannabis user[1]	27 (58.7%)	5 (41.7%)	12 (60%)	0.532
Cannabis use (weeks/year)	14.17 (19.21)	14.5 (22.55)	21.1 (24.25)	0.487
GAF score	58.24 (11.49)	51.00 (8.68)	79.05 (6.69)	<0.001*

GAF, global assessment of functioning; IQ, Intelligence quotient; TR, treatment resistant
* $p < 0.05$
[1] Number (%) instead of Mean (SD)

Table S3. MRS group comparisons between responders, TR patients and controls

	Responders	**TR patients**	**Controls**	**F-Statistic**	**p-value**
PRESS	**N=45**	**N=12**	**N=20**		
GM (SD)	0.685 (0.034)	0.673 (0.035)	0.719 (0.037)	8.76	<0.001*
WM (SD)	0.170 (0.026)	0.151 (0.022)	0.162 (0.035)	2.20	0.118
CSF (SD)	0.145 (0.036)	0.176 (0.036)	0.119 (0.023)	11.54	<0.001*
Glx (SD)	17.82 (1.38)	17.07 (1.54)	17.44 (2.02)	1.21	0.304
tCr (SD)	8.53 (0.60)	8.74 (0.57)	8.26 (0.48)	2.89	0.062
tCho (SD)	2.33 (0.25)	2.40 (0.31)	2.02 (0.19)	12.91	<0.001*
mI (SD)	6.24 (0.57)	6.53 (0.90)	5.70 (0.56)	7.61	<0.001*
tNAA (SD)	10.27 (0.79)	10.45 (0.79)	9.82(0.49)	3.66	0.030*
MEGAPRESS	**N=45**	**N=10**	**N=19**		
GM (SD)	0.514 (0.027)	0.515 (0.027)	0.535 (0.041)	3.21	0.046*
WM (SD)	0.380 (0.029)	0.354 (0.034)	0.371 (0.046)	2.53	0.087
CSF (SD)	0.105 (0.022)	0.131 (0.032)	0.093 (0.017)	9.52	<0.001*
GABA (SD)	2.51 (0.41)	2.44 (0.48)	2.63 (0.41)	0.79	0.456

CSF, cerebral spinal fluid; GABA, γ-aminobutyric acid; tCho, total choline; tCr, total creatine; Glx, glutamate + glutamine; GM, gray matter; mI, myo-inositol; tNAA, total N-acetylaspartate; WM, white matter

Table S4. Secondary analyses

Logistic regression for treatment response at baseline				
	Effect	**Estimate**	**SE**	**p-value**
	Intercept	8.463	5.703	0.138
	Glx	-0.491	0.289	0.090
	GABA+	-0.572	0.894	0.522
Longitudinal Linear Mixed models				
	Effect	**Estimate**	**SE**	**p-value**
Glx	Intercept	17.836	0.210	<0.001
	Time	0.207	0.250	0.416
	TR	-0.768	0.450	0.093
	Time x TR	0.043	0.550	0.938
GABA+	Intercept	2.513	0.059	<0.001
	Time	-0.087	0.086	0.315
	TR	-0.065	0.133	0.626
	Time x TR	0.290	0.192	0.136

GABA+, γ-aminobutyric acid; Glx, glutamate + glutamine; SE, standard error; TR, treatment response

Table S5. Post-hoc exploratory Spearman's rank correlations for metabolites in patients at baseline

	Glx		**GABA**	
	rho	**p-value**	**rho**	**p-value**
Antipsychotic duration	-0.045	0.741	-0.037	0.788
PANSS positive	-0.083	0.541	-0.216	0.112
GAF	-0.012	0.928	0.181	0.185
WM	-0.112	0.407	-0.198	0.148
CSF	0.184	0.170	0.026	0.852
SNR	-0.072	0.594	-	-

CSF, cerebrospinal fluid; GABA, γ-aminobutyric acid; GAF, global assessment of functioning; Glx, glutamate + glutamine; PANSS, positive and negative syndrome scale; SNR, signal-to-noise ratio; WM, white matter.

Table S6. Post-hoc exploratory Pearson's correlations for voxel fractions and quality of MRS spectrum in patients at baseline

	GM		WM		CSF	
	r-statistic	**p-value**	**r-statistic**	**p-value**	**r-statistic**	**p-value**
PRESS						
GM	-	-	-0.244	0.067	-0.654[1]	<.001
WM	-0.244	0.067	-	-	-0.465[1]	<.001
CSF	-0.654[1]	<.001	-0.465[1]	<.001*	-	-
FWHM	0.053[1]	0.694	-0.345[1]	0.009*	0.209[1]	0.119
SNR	0.018	0.896	0.302	0.022*	-0.287[1]	0.030*
MEGAPRESS						
GM	-	-	-0.608	<.001*	-0.307	0.023*
WM	-0.608	<0.001*	-	-	-0.569	<0.001*
CSF	-0.307	0.023*	-0.569	<.001*	-	-
FWHM	0.126	0.365	-0.045	0.709	-0.150	0.279
SNR	-0.123	0.376	0.132	0.340	-0.031	0.824

CSF, cerebrospinal fluid; FE, Fit Error; FWHM, full-width at half maximum; GM, grey matter; SNR, signal-to-noise ratio; WM, white matter.
*p<0.05
[1] Spearman's rho

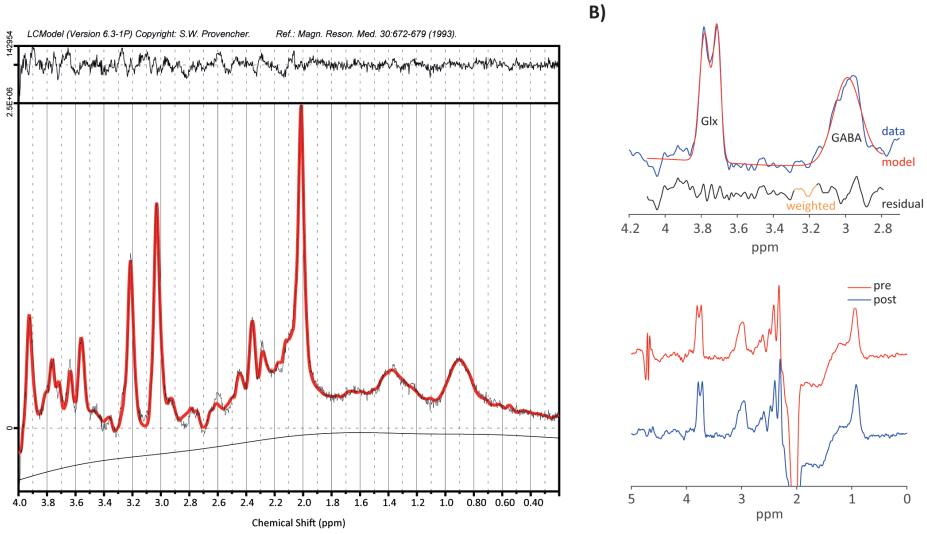

Figure S1. Example MRS spectra of one responder for A) PRESS spectrum fitted by LCModel (SNR=29, FWHM=0.027), and B) MEGA-PRESS spectrum fitted by GANNET (FE=6.57, FHWM=20.05).

Chapter | 10

Shortening duration of treatment resistance: the next step in the treatment of schizophrenia

Arjen L. Sutterland, Marieke van der Pluijm, Hiske E Becker, Elsmarieke van de Giessen, Lieuwe de Haan

Schizophrenia Bulletin Open; 1:1
DOI: 10.1093/schizbullopen/sgaa043

Abstract

The early psychosis movement was fuelled by the concept that early recognition and treatment of patients with psychosis could prevent long-term chronic impairment. Indeed, duration of untreated psychosis (DUP) predicts treatment response and early intervention services have since shown added value. However, considerable chronic impairment remains, with about 20%–30% of the patients with schizophrenia not responding to 2 different conventional antipsychotics in adequate doses and duration. In contrast to the research on DUP and early intervention in schizophrenia in general, far less research has systemically assessed the benefits of shortening the time between treatment onset and adequate treatment response. Yet timely recognition of treatment-resistant schizophrenia (TRS) could be vital since studies have indicated that a critical time window in which clozapine is most effective for TRS patients could exist. We believe that introducing the concept of Duration of Treatment Resistance (DTR) may help to investigate whether shortening of DTR by optimizing medication schedules can further prevent or mitigate long-term disability in patients with schizophrenia. In this editorial, we propose a definition of DTR and encourage the field to investigate the potential merits of this concept in future studies.

Viewpoint

The early psychosis movement was fuelled by the concept that earlier recognition and treatment of patients with schizophrenia could prevent long-term chronic impairment. Indeed, duration of untreated psychosis (DUP) predicts treatment response and early intervention services have since shown added value (1,2). However, considerable chronic impairment remains, with about 20%–30% of the patients with schizophrenia not responding to 2 different conventional antipsychotics in adequate doses during at least 6 weeks (3,4). These patients are considered to have treatment-resistant schizophrenia (TRS), although resistance to conventional antipsychotics would be more apt, as about 50% of these patients do show a beneficial response to clozapine (3,4). Unfortunately, clozapine still remains underutilized in TRS. Initiation of clozapine is often started years after treatment onset, while patients go through unsuccessful trials of 4 or more antipsychotics (2). In this period, substantial disability and damage to supporting networks of family and friends have often developed, increasing the probability that patients end up permanently institutionalized or homeless. In contrast to the research on DUP and early intervention in schizophrenia, far less research has systemically assessed benefits of shortening the time between treatment onset and adequate treatment response. Yet timely recognition of TRS could be vital, since studies have indicated that a critical time window in which clozapine is most effective for this group of patients could exist (5). Furthermore, in clozapine non-responders, electroconvulsive therapy may further improve remission rates (4).

The identified clinical and demographic factors that are associated with treatment response (DUP, age at onset, negative symptoms (3)) are insufficient to predict treatment response in individual patients. Biomarkers are pursued to help early identification of potential TRS (1,4). A promising predictor is striatal dopamine synthesis capacity, since this is increased in patients responding to conventional antipsychotics but not in TRS patients. Instead, a variety of studies recognize TRS as a subgroup, which might be characterized by more marked glutamate alterations (4). Other research points at serotonin pathway dysfunction, inflammation, and oxidative stress (4). More research is needed to determine which biomarker findings are robust and translatable to clinical practice. As biomarkers will not be available for clinical practice in the foreseeable future, we believe that introducing the concept of Duration of Treatment Resistance (DTR) may help to investigate whether shortening of DTR by optimizing medication schedules can further prevent long-term disability in patients with schizophrenia.

When defining DTR, we need to be aware of a complex and developing field concerning criteria for adequate treatment response, necessary doses of conventional antipsychotics, minimum duration of treatment, and adherence measurements before meeting the definition of TRS. Firstly, based on all available evidence, consensus criteria for TRS have been formulated (3). The authors acknowledge that defining treatment response with relative thresholds (a 20%

decrease in symptoms measured by validated scales) raises methodological problems as TRS becomes dependent on symptom levels before treatment and suggest to focus on acceptable levels of residual symptom and impairment severity (3). This is in line with Andreasen et al (6) that defines adequate treatment response as attenuation of symptom severity, below the level of inference with functioning. Therefore, we propose to define TRS as not achieving remission criteria of Andreasen et al (6). The advantage of this definition is that it is applicable in practice, measurable and unrelated to symptom levels before treatment (6).

Secondly, the dose of conventional antipsychotics needed in Recent Onset Schizophrenia (ROS) to achieve an adequate response is generally lower. While it is recognized that adequate dosing of conventional antipsychotics differ between ROS and chronic schizophrenia in most guidelines, this is not reflected in the suggested criteria of treatment resistance, where chlorpromazine equivalent doses of 600 mg are required for conventional antipsychotics in order to fulfill treatment resistance criteria (3). These proposed dosing strategies in chronic schizophrenia patients could lead to intolerable side effects in ROS, of which we know that they do not outweigh potential benefits and contribute to unnecessary prolongation of inadequate treatment.

Finally, taking 6 weeks as a minimal treatment period per antipsychotic drug has been put into question, whereby at one hand, some literature points at a negligible chance of reaching response criteria at 6 weeks when patients have not improved at all after 2 weeks, and on the other hand, some patients have a delayed response exceeding 6 weeks (3). Although a minimal treatment period of 12 weeks would currently be regarded as a very short period to determine TRS, unnecessary prolongation of an unsuccessful treatment should be regarded in the light of the guiding principle "primum non nocere."

By having more attention for DTR as the next challenge after early intervention treatment and research, the field needs to explore previously mentioned issues in order to determine if we should adjust our treatment guidelines in ROS in order to timely recognize TRS, without pursuing potentially harmful dosing strategies. Lastly, it is important to consider that different pathways to treatment resistance have been identified (2): early TRS (patients not responding to 2 consecutively conventional antipsychotics from the start of the treatment) and late TRS (patients who cease to respond to conventional antipsychotics, constituting the minority of TRS patient), also known as tachyphylaxias.

With these facts in mind, we propose to define DTR as follows:

- In case patients never adequately responded to 2 adequate conventional antipsychotic trials, DTR is calculated as time between start of antipsychotic treatment and reaching remission criteria (6) on clozapine or another therapy.

- In case patients cease to react to previously successful treatment, DTR is calculated as time between the loss of effectiveness of conventional antipsychotic treatment and reaching remission criteria (6) on clozapine or another therapy.

We encourage the field to investigate DTR, its proposed remission criteria and required dosing strategies for ROS in future studies in order to gain knowledge about different aspects of treatment response and resistance. The possibility of a critical time window to optimally respond to clozapine in the course of schizophrenia needs to be explored prospectively, as well as to what extend shortening DTR promotes favorable disease course. Finally, discovering biomarkers that identify response potential to either conventional antipsychotics, clozapine, or other treatments remain direly needed.

References

1. Lieberman JA, First MB. Psychotic Disorders. The New England journal of medicine Jul 19 2018;379(3):270-280.
2. Demjaha A, Lappin JM, Stahl D, et al. Antipsychotic treatment resistance in first-episode psychosis: prevalence, subtypes and predictors. Psychological medicine Aug 2017;47(11):1981-1989.
3. Howes OD, McCutcheon R, Agid O, et al. Treatment-Resistant Schizophrenia: Treatment Response and Resistance in Psychosis (TRRIP) Working Group Consensus Guidelines on Diagnosis and Terminology. The American journal of psychiatry Mar 1 2017;174(3):216-229.
4. Potkin SG, Kane JM, Correll CU, Lindenmayer JP, Agid O, Marder SR, Olfson M, Howes OD. The neurobiology of treatment-resistant schizophrenia: paths to antipsychotic resistance and a roadmap for future research. NPJ schizophrenia Jan 7 2020;6(1):1.
5. Jones R, MacCabe JH, Price MJ, Xiangxin L, Upthegrove R. Effect of age on the relative efficacy of clozapine in schizophrenia. Acta psychiatrica Scandinavica Jan 24 2020.
6. Andreasen NC, Carpenter WT, Jr., Kane JM, Lasser RA, Marder SR, Weinberger DR. Remission in schizophrenia: proposed criteria and rationale for consensus. The American journal of psychiatry Mar 2005;162(3):441-449.

Author Contributions

LdH and AS conceptualized the viewpoint. AS wrote the manuscript with support from MvdP. All the authors critically reviewed the manuscript for intellectual content. All authors approved the final version of the manuscript for publication.

GENERAL DISCUSSION
SUMMARY
APPENDICES

Chapter | 11

General discussion

General discussion

The overall aim of this thesis was to provide more insight into the neurobiological mechanisms underlying treatment-resistant schizophrenia and to investigate potential markers for identifying treatment-resistant patients. The main focus was on the dopaminergic system and the novel MRI sequence neuromelanin MRI (NM-MRI) that can non-invasively provide an indirect measure of nigrostriatal dopamine functioning (**chapter 2**). In part I, we established the reproducibility of NM-MRI and demonstrated that the sequence could be reliably accelerated (**chapters 3-4**), which contributes to its applicability for clinical practice. In part II, we gained more insight into how NM-MRI of the substantia nigra relates to striatal dopamine synthesis capacity (**chapter 6**) and summarized evidence that *in-vivo* imaging of the substantia nigra is important in schizophrenia (**chapter 5**). In part III, we demonstrate that NM-MRI has potential as a marker for treatment-resistant schizophrenia (**chapter 7**). Moreover, we explored differences in plasma dopa decarboxylase activity (**chapter 8**), glutamate and γ-aminobutyric acid (GABA) levels (**chapter 9**) between responders and non-responders. We did not find evidence that these measures could be used as potential markers for treatment-resistant schizophrenia, at least not in early-episode psychosis patients on antipsychotic treatment. We emphasize an urgent need for treatment-resistant markers to improve outcomes, and introduce the concept of duration of treatment resistance (DTR) to facilitate treatment optimization and research in treatment-resistant schizophrenia (**chapter 10**). In the following part, these main findings in relation to current literature, as well as the clinical implications of these findings and future directions will be discussed.

Theories of treatment-resistant schizophrenia

Dopamine

Data from [^{18}F]F-DOPA positron emission tomography (PET) studies showed lower dopamine striatal capacity in treatment-resistant patients compared to responders (1-4). This observation gave rise to the hypothesis that a subtype of schizophrenia exists that lacks striatal hyperdopaminergia, and is unresponsive to initial treatment with antipsychotic medication (5). Instead, studies suggest that this subtype has more marked glutamatergic abnormalities (6). Our NM-MRI findings from **chapter 7** are in line with this hypothesis and show for the first time that non-responders have significantly lower NM-MRI signal in the substantia nigra compared to responders, and that non-responders even show levels comparable to healthy controls. This critical finding provides further evidence that treatment-resistant patients do not show nigrostriatal hyperdopaminergia and demonstrates that NM-MRI might be a potential imaging marker for treatment-resistant schizophrenia. Moreover, NM-MRI appears to be a stable measure, and is not affected by antipsychotic use or illness duration over six months follow-up, which suggests that it might be a trait marker.

In contrast with the dopaminergic subgroup hypothesis, we did not find significant differences in plasma dopa decarboxylase activity between treatment-resistant patients and responders (**chapter 8**). Considering that the hyperdopaminergic dysfunction in schizophrenia is region-specific, it is possible that plasma dopa decarboxylase activity may not be a precise surrogate marker to discern these differences. Additionally, plasma dopa decarboxylase activity may be a less stable measure than NM-MRI, and medication use could have influenced the results.

Glutamate

The glutamate/GABA findings from **chapter 9** did not confirm the expected glutamatergic abnormalities in treatment-resistant schizophrenia (6-9). We did not find significant differences in glutamate and GABA in the anterior cingulate cortex between responders and treatment-resistant patients. This finding is consistent with other recent work in first-episode psychosis patients (10,11). MRS measurements of glutamate and GABA appear to be more susceptible to different factors, including age and medication use (12). This renders MRS a less reliable marker and challenges its applicability in clinical practice for treatment-resistant schizophrenia. However, it does not yet rule out that glutamate and GABA play a role in the underlying neurobiology of treatment-resistant schizophrenia. Previous studies did show increased glutamate levels in the anterior cingulate cortex of treatment-resistant patients, and GABA-related genes have been implicated in treatment-resistant schizophrenia (13). In addition, MRS studies in other brain regions have shown aberrant glutamate and GABA functioning in schizophrenia. However, results are mixed and the number of studies in treatment-resistant schizophrenia is limited (14). MRS studies using multiple brain voxels and ultra-high field scanners (>7T) could offer insight into the glutamate and GABA system in treatment-resistant schizophrenia. Ultra-high field scanners provide a more reliable means of exploring lower concentration metabolites like GABA, and separating glutamate and glutamine resonances (15). Moreover, a recently developed PET ligand for the N-methyl-D-aspartate (NMDA) receptor enables the examination of NMDA receptor functioning *in vivo* (16), and might further elucidate the role of the NMDA receptor in treatment-resistant schizophrenia. Further research into NMDA receptor and glutamate/GABA functioning could potentially identify new treatment targets that would be effective for patients who do not respond to current antipsychotics. Clozapine, the only recognized antipsychotic for treatment-resistant patients, affects many other neurotransmitter systems, including glutamate/GABA (17,18). In preclinical studies, clozapine administration has been shown to improve glutamatergic transmission and increase the release of L-glutamate and D-serine, both implicated in the regulation of NMDA receptors (19). One study showed lower D-serine plasma levels in treatment-resistant patients compared to healthy controls, and this difference disappeared after clozapine initiation (20). This supports that glutamate could be a treatment target for treatment-resistant schizophrenia. Nonetheless, studies regarding glutamatergic drugs and supplements have yielded mixed results (17,18,21). Further clinical trials are needed to establish the effectiveness of glutamatergic treatment strategies.

Dopamine supersensitivity

Another theory for the neurobiological underpinnings of treatment-resistant schizophrenia is the dopamine supersensitivity theory (22). This theory is mainly implicated in secondary treatment-resistant patients, patients that initially responded to first-line antipsychotic treatment and later became resistant. The dopamine supersensitivity theory proposes that continuous blockade of the D_2 receptor results in increased D_2 receptor density. This would lead to the need for increasing doses of antipsychotic medication to render the same therapeutic effect. Eventually, first-line antipsychotic medication will not be sufficient anymore, and symptoms will re-emerge.

Heterogeneity in treatment-resistant schizophrenia

In line with the different theories, there might be several pathways leading to treatment-resistant schizophrenia. Some individuals with treatment-resistant schizophrenia respond to clozapine, whereas other individuals respond better to electroconvulsive therapy or do not respond to any current treatment options at all. This heterogeneity in treatment-resistant schizophrenia requires further investigation. Moreover, combining these diverse treatment-resistant subgroups could potentially compromise findings. For instance, MRS studies yielded different glutamate and GABA findings between treatment-resistant patients who did and did not respond to clozapine treatment (11,23). Longitudinal prospective studies that include frequent and comprehensive assessments of treatment response (e.g., DTR, **chapter 10**) are essential to explore the heterogeneity observed in treatment-resistant schizophrenia. In addition, longitudinal studies should investigate whether dopaminergic differences in treatment-resistant schizophrenia are categorical, as proposed by the theories mentioned above, or a continuum, as suggested by correlations between dopamine synthesis capacity and response to antipsychotic treatment (2,24). The treatment-resistant group showing no response at all to first-line antipsychotic treatment might be small. Our sample in **chapter 7** and **chapter 9** primarily consisted of partial responders, i.e. they showed partial response to first-line antipsychotics but insufficient to be in remission. Comparable to the continuum in treatment response, the neuropathology might as well follow a continuous scale (25). This complicates research and clinical decision-making, but it is essential to recognize this heterogeneity in treatment-resistant schizophrenia and at least consider the possible subgroups, including partial responders, secondary non-responders, clozapine-responders, and clozapine non-responders.

Defining treatment-resistant schizophrenia in research

For research purposes, it is important that treatment-resistant schizophrenia is defined using standardized criteria. Currently, studies use a wide range of definitions which complicates comparing and generalizing studies. It is essential that such criteria fully capture the construct and that it is implementable in a wide range of settings and studies. The Treatment

Response and Resistance in Psychosis (TRIPP) working group developed consensus criteria and guidelines with three key elements: "1) a confirmed diagnosis of schizophrenia; 2) adequate pharmacological treatment; and 3) persistence of significant symptoms despite this treatment" (26). Criteria for adequate treatment include ≥ 2 past adequate treatments with a duration of at least 6 weeks at a therapeutic dose equivalent to ≥ 600 mg chlorpromazine per day. Most patients in our first episode psychosis sample (**chapters 7-9**) did not reach the therapeutic dose of 600 mg chlorpromazine. This is in line with the Dutch Multidisciplinary guidelines, which recommend lower doses, especially in first-episode psychosis. Antipsychotic medication (excluding clozapine) has its greatest effects within the first two weeks, and after that the improvements are more marginal (27). One wants to minimize false positives of treatment resistance, but also not delay adequate treatment. The balance of criteria being rigorous, yet practical and generalizable, is challenging. However, we agree with the TRIPP working group that standardized criteria would improve the interpretation and replication of studies. Regarding the persistence of symptoms, the TRIPP consensus recommends that response is ascertained prospectively, and it is defined as at least a 20% improvement in symptom scores (26). Certainly, prospective studies in first-episode psychosis will be required to assess the clinically relevant markers for treatment resistance. Ideally these studies start from illness onset, before medication initiation, and response to medication is monitored prospectively. However, in clinical practice, it is challenging to include the patients during illness onset, before medication initiation. It is unlikely that patients who experience a full range of severe symptoms would be able and willing to participate in a study.

The Andreasen criteria provide a more practical approach and define treatment resistance as the persistence of moderate symptom severity on at least one of the core symptoms of schizophrenia (28). These criteria are not dependent on measurements at illness onset and incorporate real-world interpretability, a moderate symptom score indicates that the remaining symptoms interfere significantly with the individual's behavior (**chapter 10**). The applicability of change scores as a primary outcome measure is constrained due to the variation in baseline symptom intensity observed across interventional trials. The adoption of threshold criteria to characterize remission enables direct comparisons across different trials and can be implemented in studies that do not include patients at illness onset. This facilitates further research, since the majority of patients have already undergone antipsychotic treatment before any study evaluations, especially MRI, can be performed. Moreover, such a patient sample highly represents the group in which a clinically relevant marker would be utilized. In clinical practice, most patients will initially receive crisis treatment before being derived to specialized care where MRI scans can be obtained.

Clinical implications and future directions

All studies described in this thesis have been carried out to increase knowledge about the neurobiology underlying treatment-resistant schizophrenia in order to contribute to the development of (bio)markers to identify treatment resistance at an earlier stage of the disease. Although we still have a long way to go before we can get "back in control" in treatment decision making for treatment-resistant schizophrenia patients, the studies described in this thesis have provided new insights which give rise to further research and might eventually aid treatment decision making.

Broader application of NM-MRI

This thesis demonstrates the potential of NM-MRI as a tool to measure dopaminergic functioning in the substantia nigra. Besides the potential as a marker for treatment-resistant schizophrenia, NM-MRI might also be promising as a marker in Parkinson's disease (**chapter 2**). Furthermore, a body of research suggests that NM-MRI may also capture dopamine dysfunction in other psychiatric disorders, including major depressive disorder (29) and cocaine addiction (30). In line with previous research (31,32), **chapter 7** further supports that NM-MRI captures dopamine dysfunction in psychosis. Continuing the development and validation of NM-MRI can further broaden the application of NM-MRI. This thesis contributes to this effort by establishing the reproducibility of NM-MRI (**chapter 3**) and demonstrating several approaches to reliably accelerate NM-MRI (**chapter 4**). Well-validated and fast NM-MRI sequences can expedite the implementation of NM-MRI in both research and clinical practice.

This thesis focussed on NM-MRI of the substantia nigra. However, neuromelanin accumulates in other catecholaminergic neurons as well, such as the noradrenergic neurons in the locus coeruleus. Noradrenergic functioning in the locus coeruleus plays a role in several psychiatric (e.g., anxiety and depression) and neurodegenerative disorders (e.g,. Parkinson's disease, Alzheimer's disease, and multiple sclerosis) (33). Hence, NM-MRI applied in the locus coeruleus might have the potential to shine a light on several other psychiatric and neurodegenerative disorders, e.g. in Alzheimer's disease (34), depression (35), and post-traumatic stress disorder (36).

NM-MRI signal

Despite its potential in neurodegenerative as well as psychiatric disorders, the contrast mechanism of NM-MRI is still debated. The paramagnetic T1 effects are thought to originate from the neuromelanin-iron complexes (37). The direct or indirect magnetization transfer effects might be influenced by the content of macromolecules in the surrounding white matter vs. the relative high-water content of catecholamine neurons (38). Indeed, in **chapter 3**, we

found that the NM-MRI sequence with MT effects had higher contrast and was associated with higher reliability. Future work should further disentangle the contrast mechanism of NM-MRI and its specificity to NM concentration vs. other factors.

Most importantly, the NM-MRI signal in the substantia nigra and locus coeruleus correlates and co-localizes with NM concentration in the catecholaminergic neurons in post-mortem histology (32,39). Moreover, neuronal loss in these regions, as observed in Parkinson's disease, is associated with a decrease of NM-MRI signal (40). How the neuromelanin concentration precisely relates to catecholaminergic functioning is a question that needs to be further addressed. In the end, neuromelanin concentration reflects a combination of processes involved in neuromelanin accumulation, including synthesis and vesicular transport (**chapter 2**). Assessing the extent of the contributions of each of these processes is critical in further understanding the variability in NM-MRI signal.

Previous studies have explored this through triangulation with PET measures and preclinical studies. NM-MRI signal in the substantia nigra positively correlated with a PET measure of dopamine release in the dorsal striatum (32). Furthermore, a preclinical study showed that dopamine synthesis induces neuromelanin accumulation, whereas VMAT2 abolished neuromelanin synthesis (41). In **chapter 6**, we showed a negative correlation between NM-MRI and a [^{18}F]F-DOPA PET measure of dopamine synthesis capacity in the striatum of controls, but not with dopamine synthesis capacity in the substantia nigra, nor did we find any correlations in schizophrenia patients. The negative association in healthy controls seems to highlight the interdependence of VMAT2, dopamine synthesis and neuromelanin. It suggests that under physiological conditions, higher dopamine synthesis is related to increased VMAT2 activity and vesicular storage, and hence lower levels of cytosolic dopamine and neuromelanin deposition. All three components are implicated in schizophrenia and seem out of balance in the disease (**chapter 5**). Further research is needed to elucidate the association of NM-MRI signal with the function of the catecholamine pathways, e.g., by exploring the relation between VMAT-2 PET and NM-MRI. After further validation, NM-MRI could be developed for various psychiatric and neurodegenerative disorders.

Application of NM-MRI in treatment-resistant schizophrenia

In this thesis, we developed and assessed NM-MRI of the substantia nigra as a potential marker for treatment-resistant schizophrenia. Although we demonstrated the potential of NM-MRI as a non-invasive marker in **chapter 7**, additional research is needed to determine its potential as an out-of-sample predictor of treatment-resistant schizophrenia. If NM-MRI is further developed as a marker, it could enable early identification of treatment-resistant patients and reduce delays in clozapine initiation. Earlier use of clozapine and fewer antipsychotic

trials prior to clozapine initiation are associated with improved efficacy and better treatment outcomes for treatment-resistant patients (42,43). In our studies, **chapters 7** and **9**, patients were prescribed clozapine relatively fast, as third or fourth treatment option. Interestingly, approximately 90% of our clozapine users responded to clozapine at six months follow-up, substantially higher than the previously reported 40% response rate (44). This increase in clozapine responsiveness might be a result of the early transition to clozapine. Early recognition of treatment-resistant patients could substantially reduce delays in remission, improve outcomes, and reduce healthcare costs through shorter inpatient admission, lower rates of relapse, and reduced rehospitalization (45,46). A previous study estimated that if 20% of the treatment-resistant patients started clozapine, this could reduce the annual health costs of $22,444 per patient treated with clozapine (47). Subsequently, an [^{18}F]-FDOPA PET study estimated that a screening test with PET could lead to healthcare savings of £3,400 per patient with schizophrenia (4). Given the lower cost of MRI compared to PET, if NM-MRI would be further developed and achieve similar performance as [^{18}F]-FDOPA PET, it could result in even greater healthcare savings.

In clinical practice, first-episode psychosis patients typically receive acute crisis treatment before they can undergo an MRI scan. If a patient responds well to this initial treatment, there is no need for an NM-MRI scan. However, a longer treatment optimization phase is required for patients who do not respond to the initial treatment within weeks (48). At this stage, NM-MRI as a marker might aid in reducing delays in effective treatment. Patients who do not respond to the first antipsychotic medication have a significantly lower likelihood of responding to a second antipsychotic drug. A study has shown that for non-responders who were switched to a second trial of antipsychotics, the response rate dropped from 75% to only 17% (49). Especially for these patients NM-MRI could aid treatment decision making, leading to earlier initiation of clozapine.

However, further research is necessary to determine the potential of NM-MRI as a marker for treatment-resistant schizophrenia. To advance the development of NM-MRI and to evaluate whether NM-MRI could be a generalizable marker for treatment-resistant schizophrenia, multi-centre collaborations are required. Regarding MRI, the critical concern is whether the method can be generalized across different equipment and locations. Fortunately, several methods for MRI data harmonization have been developed. ComBat (50) is a well-established harmonization model and has been shown to remove differences in NM-MRI signal across scanners while preserving biologically meaningful variability (51). Furthermore developing and implementing standardized data processing and analysis pipelines are essential. There is a risk of potential errors and biases in different steps of the process, such as during MRI acquisition, by differences in imaged volume selection, as well as in pre- and post-processing by using various software packages, co-registration/normalization among images (particularly for small structures like the substantia nigra), and smoothing procedures (52). It is crucial to

consider these factors when comparing results across research sites and study populations. Hence, optimizing the NM-MRI sequence, as well as acquisition and pre- and post-processing methods, are necessary to enhance data quality and reproducibility.

Multifactor prediction models

Combining NM-MRI with other MRI modalities or clinical data may enhance the predictive value and provide a more comprehensive understanding of the underlying biological mechanisms responsible for treatment-resistant schizophrenia. Leveraging the relative contributions of different neurobiological substrates by using various MRI contrast or joint models, or implementing complex computational approaches to derive new measures, may increase the sensitivity of prediction models (53,54). Multiple imaging modalities are implicated in treatment-resistant schizophrenia, including structural, functional, and neurochemical deficits (13,17). Combining these modalities with multivariate approaches could provide useful information and detect more subtle differences. Furthermore, clinical predictors, including age of onset and negative symptoms, may improve the association of NM-MRI with treatment response (55). Combining multiple predictive markers could provide better stratification compared to a singular marker (56,57).

Artificial intelligence and machine learning can combine data from heterogeneous multimodalities, including medical histories, genetic information, plasma values, brain imaging data, and behavioral data, to further capture the complexity of treatment-resistant schizophrenia and increase prediction power (56,58,59). Hence, machine learning models could turn group-level data into personalized medicine applications, by classifying a patient based on individual risk factors. Studies using machine learning have already successfully differentiated between controls and schizophrenia patients and, to some degree, predicted treatment outcomes (59-63). Prediction models for treatment-resistant schizophrenia need high specificity, as prescribing clozapine to responders should be avoided considering the risks associated with this antipsychotic (64), and should be sensitive to the heterogeneity in treatment-resistant schizophrenia. Such prediction models have not yet been applied for treatment-resistant schizophrenia.

Developing accurate predictive models for treatment-resistant schizophrenia requires high-quality, reliable, and representative data. It is essential to perform external validation of these models, which can be challenging, but is necessary for clinical implementation and generalizability. Overfitting is a potential problem with artificial intelligence methods, especially with insufficient sample sizes for training data. Developing machine learning-based tools for universal use may also pose challenges related to data harmonization and potential biases. To address these limitations, open-access datasets and open-source software are critical for the success of prediction models. To mitigate potential biases resulting from differences

in study purposes, patient recruitment, and model designs, a standardized framework for comparing models between independent projects may be useful. Such a framework could enhance both the prognostic accuracy and sensitivity for predictive factors among different samples. Hence, extensive validation through international collaboration is essential to gain a deeper understanding and develop more sophisticated prediction models for treatment-resistant schizophrenia.

References

1. Demjaha A, Egerton A, Murray RM, Kapur S, Howes OD, Stone JM, et al. Antipsychotic treatment resistance in schizophrenia associated with elevated glutamate levels but normal dopamine function. Biol Psychiatry. 2014;75(5):e11-3.
2. Jauhar S, Veronese M, Nour MM, Rogdaki M, Hathway P, Turkheimer FE, et al. Determinants of treatment response in first-episode psychosis: an (18)F-DOPA PET study. Mol Psychiatry. 2019;24(10):1502-12.
3. Kim E, Howes OD, Veronese M, Beck K, Seo S, Park JW, et al. Presynaptic Dopamine Capacity in Patients with Treatment-Resistant Schizophrenia Taking Clozapine: An [(18)F]DOPA PET Study. Neuropsychopharmacology. 2017;42(4):941-50.
4. Veronese M, Santangelo B, Jauhar S, D'Ambrosio E, Demjaha A, Salimbeni H, et al. A potential biomarker for treatment stratification in psychosis: evaluation of an [(18)F] FDOPA PET imaging approach. Neuropsychopharmacology. 2021;46(6):1122-32.
5. Howes OD, Kapur S. A neurobiological hypothesis for the classification of schizophrenia: type A (hyperdopaminergic) and type B (normodopaminergic). Br J Psychiatry. 2014;205(1):1-3.
6. Howes O, McCutcheon R, Stone J. Glutamate and dopamine in schizophrenia: an update for the 21st century. J Psychopharmacol. 2015;29(2):97-115.
7. Egerton A, Brugger S, Raffin M, Barker GJ, Lythgoe DJ, McGuire PK, et al. Anterior cingulate glutamate levels related to clinical status following treatment in first-episode schizophrenia. Neuropsychopharmacology. 2012;37(11):2515-21.
8. Egerton A, Grace AA, Stone J, Bossong MG, Sand M, McGuire P. Glutamate in schizophrenia: Neurodevelopmental perspectives and drug development. Schizophr Res. 2020;223:59-70.
9. Mouchlianitis E, Bloomfield MAP, Law V, Beck K, Selvaraj S, Rasquinha N, et al. Treatment-Resistant Schizophrenia Patients Show Elevated Anterior Cingulate Cortex Glutamate Compared to Treatment-Responsive. Schizophrenia Bulletin. 2016;42(3):744-52.
10. Merritt K, Perez-Iglesias R, Sendt KV, Goozee R, Jauhar S, Pepper F, et al. Remission from antipsychotic treatment in first episode psychosis related to longitudinal changes in brain glutamate. NPJ Schizophr. 2019;5(1):12.
11. Ueno F, Nakajima S, Iwata Y, Honda S, Torres-Carmona E, Mar W, et al. Gamma-aminobutyric acid (GABA) levels in the midcingulate cortex and clozapine response in patients with treatment-resistant schizophrenia: A proton magnetic resonance spectroscopy ((1) H-MRS) study. Psychiatry Clin Neurosci. 2022;76(11):587-94.
12. Merritt K, McGuire PK, Egerton A, Investigators HMiS, Aleman A, Block W, et al. Association of Age, Antipsychotic Medication, and Symptom Severity in Schizophrenia With Proton Magnetic Resonance Spectroscopy Brain Glutamate Level: A Mega-analysis of Individual Participant-Level Data. JAMA Psychiatry. 2021;78(6):667-81.
13. Vita A, Minelli A, Barlati S, Deste G, Giacopuzzi E, Valsecchi P, et al. Treatment-Resistant Schizophrenia: Genetic and Neuroimaging Correlates. Front Pharmacol. 2019;10:402.
14. Nakahara T, Tsugawa S, Noda Y, Ueno F, Honda S, Kinjo M, et al. Glutamatergic and GABAergic metabolite levels in schizophrenia-spectrum disorders: a meta-analysis of (1)H-magnetic resonance spectroscopy studies. Mol Psychiatry. 2022;27(1):744-57.
15. Godlewska BR, Clare S, Cowen PJ, Emir UE. Ultra-High-Field Magnetic Resonance Spectroscopy in Psychiatry. Front Psychiatry. 2017;8:123.
16. Galovic M, Al-Diwani A, Vivekananda U, Torrealdea F, Erlandsson K, Fryer TD, et al. In Vivo N-Methyl-d-Aspartate Receptor (NMDAR) Density as Assessed Using Positron Emission Tomography During Recovery From NMDAR-Antibody Encephalitis. JAMA Neurol. 2023;80(2):211–213.
17. Potkin SG, Kane JM, Correll CU, Lindenmayer JP, Agid O, Marder SR, et al. The neurobiology of treatment-resistant schizophrenia: paths to antipsychotic resistance and a roadmap for future research. NPJ Schizophr. 2020;6(1):1.
18. Veerman SR, Schulte PF, Begemann MJ, Engelsbel F, de Haan L. Clozapine augmented with glutamate modulators in refractory schizophrenia: a review and metaanalysis. Pharmacopsychiatry. 2014;47(6):185-94.
19. Tanahashi S, Yamamura S, Nakagawa M, Motomura E, Okada M. Clozapine, but not haloperidol, enhances glial D-serine and L-glutamate release in rat frontal cortex and primary cultured astrocytes. Br J Pharmacol. 2012;165(5):1543-55.

20. Yamamori H, Hashimoto R, Fujita Y, Numata S, Yasuda Y, Fujimoto M, et al. Changes in plasma D-serine, L-serine, and glycine levels in treatment-resistant schizophrenia before and after clozapine treatment. Neurosci Lett. 2014;582:93-8.
21. Nasyrova RF, Khasanova AK, Altynbekov KS, Asadullin AR, Markina EA, Gayduk AJ, et al. The Role of D-Serine and D-Aspartate in the Pathogenesis and Therapy of Treatment-Resistant Schizophrenia. Nutrients. 2022;14(23).
22. Chouinard G, Samaha AN, Chouinard VA, Peretti CS, Kanahara N, Takase M, et al. Antipsychotic-Induced Dopamine Supersensitivity Psychosis: Pharmacology, Criteria, and Therapy. Psychother Psychosom. 2017;86(4):189-219.
23. Iwata Y, Nakajima S, Plitman E, Caravaggio F, Kim J, Shah P, et al. Glutamatergic Neurometabolite Levels in Patients With Ultra-Treatment-Resistant Schizophrenia: A Cross-Sectional 3T Proton Magnetic Resonance Spectroscopy Study. Biological Psychiatry. 2019;85(7):596-605.
24. Mouchlianitis E, McCutcheon R, Howes OD. Brain-imaging studies of treatment-resistant schizophrenia: a systematic review. The Lancet Psychiatry. 2016;3(5):451-63.
25. McCutcheon RA, Pillinger T, Efthimiou O, Maslej M, Mulsant BH, Young AH, et al. Reappraising the variability of effects of antipsychotic medication in schizophrenia: a meta-analysis. World Psychiatry. 2022;21(2):287-94.
26. Howes OD, McCutcheon R, Agid O, de Bartolomeis A, van Beveren NJ, Birnbaum ML, et al. Treatment-Resistant Schizophrenia: Treatment Response and Resistance in Psychosis (TRRIP) Working Group Consensus Guidelines on Diagnosis and Terminology. Am J Psychiatry. 2017;174(3):216-29.
27. Agid O, Kapur S, Arenovich T, Zipursky RB. Delayed-Onset Hypothesis of Antipsychotic Action: A Hypothesis Tested and Rejected. Archives of General Psychiatry. 2003;60(12):1228-35.
28. Nancy C. Andreasen, M.D., Ph.D. ,, William T. Carpenter J, , M.D. ,, John M. Kane, M.D. ,, Robert A. Lasser, M.D. ,, Stephen R. Marder, M.D. , and, Daniel R. Weinberger, M.D. Remission in Schizophrenia: Proposed Criteria and Rationale for Consensus. American Journal of Psychiatry. 2005;162(3):441-9.
29. Wengler K, Ashinoff BK, Pueraro E, Cassidy CM, Horga G, Rutherford BR. Association between neuromelanin-sensitive MRI signal and psychomotor slowing in late-life depression. Neuropsychopharmacology. 2021;46(7):1233-9.
30. Cassidy CM, Carpenter KM, Konova AB, Cheung V, Grassetti A, Zecca L, et al. Evidence for Dopamine Abnormalities in the Substantia Nigra in Cocaine Addiction Revealed by Neuromelanin-Sensitive MRI. Am J Psychiatry. 2020;177(11):1038-47.
31. Ueno F, Iwata Y, Nakajima S, Caravaggio F, Rubio JM, Horga G, et al. Neuromelanin accumulation in patients with schizophrenia: A systematic review and meta-analysis. Neurosci Biobehav Rev. 2022;132:1205-13.
32. Cassidy CM, Zucca FA, Girgis RR, Baker SC, Weinstein JJ, Sharp ME, et al. Neuromelanin-sensitive MRI as a noninvasive proxy measure of dopamine function in the human brain. Proc Natl Acad Sci U S A. 2019;116(11):5108-17.
33. Schwarz LA, Luo L. Organization of the locus coeruleus-norepinephrine system. Curr Biol. 2015;25(21):R1051-R6.
34. Beardmore R, Hou R, Darekar A, Holmes C, Boche D. The Locus Coeruleus in Aging and Alzheimer's Disease: A Postmortem and Brain Imaging Review. Journal of Alzheimer's Disease. 2021;83:5-22.
35. Calarco N, Cassidy CM, Selby B, Hawco C, Voineskos AN, Diniz BS, et al. Associations between locus coeruleus integrity and diagnosis, age, and cognitive performance in older adults with and without late-life depression: An exploratory study. Neuroimage Clin. 2022;36:103182.
36. Cassidy C, Rosa-Neto P, Kaminsky Z, Robillard R. Examining the Locus Coeruleus Norepinephrine System With Neuromelanin-Sensitive MRI: Applications in Psychiatric and Neurodegenerative Illness. Biological Psychiatry. 2022;91(9).
37. Trujillo P, Summers PE, Ferrari E, Zucca FA, Sturini M, Mainardi LT, et al. Contrast mechanisms associated with neuromelanin-MRI. Magn Reson Med. 2017;78(5):1790-800.
38. Priovoulos N, van Boxel SCJ, Jacobs HIL, Poser BA, Uludag K, Verhey FRJ, et al. Unraveling the contributions to the neuromelanin-MRI contrast. Brain Struct Funct. 2020;225(9):2757-74.
39. Sulzer D, Cassidy C, Horga G, Kang UJ, Fahn S, Casella L, et al. Neuromelanin detection by magnetic resonance imaging (MRI) and its promise as a biomarker for Parkinson's disease. NPJ Parkinsons Dis. 2018;4:11.
40. Porter E, Roussakis AA, Lao-Kaim NP, Piccini P. Multimodal dopamine transporter (DAT) imaging and magnetic resonance imaging (MRI) to characterise early Parkinson's disease. Parkinsonism Relat Disord. 2020;79:26-33.

41. Sulzer D, Bogulavsky J, Larsen KE, Behr G, Karatekin E, Kleinman MH, et al. Neuromelanin biosynthesis is driven by excess cytosolic catecholamines not accumulated by synaptic vesicles. Proceedings of the National Academy of Sciences. 2000;97(22):11869-74.
42. Üçok A, Çikrikçili U, Karabulut S, Salaj A, Öztürk M, Tabak Ö, et al. Delayed initiation of clozapine may be related to poor response in treatment-resistant schizophrenia. International Clinical Psychopharmacology. 2015;30(5):290-5.
43. Okhuijsen-Pfeifer C, Huijsman EAH, Hasan A, Sommer IEC, Leucht S, Kahn RS, et al. Clozapine as a first- or second-line treatment in schizophrenia: a systematic review and meta-analysis. Acta Psychiatr Scand. 2018;138(4):281-8.
44. Siskind D, Siskind V, Kisely S. Clozapine Response Rates among People with Treatment-Resistant Schizophrenia: Data from a Systematic Review and Meta-Analysis. Can J Psychiatry. 2017;62(11):772-7.
45. Kirwan P, O'Connor L, Sharma K, McDonald C. The impact of switching to clozapine on psychiatric hospital admissions: a mirror-image study. Ir J Psychol Med. 2019;36(4):259-63.
46. Land R, Siskind D, McArdle P, Kisely S, Winckel K, Hollingworth SA. The impact of clozapine on hospital use: a systematic review and meta-analysis. Acta Psychiatr Scand. 2017;135(4):296-309.
47. Goren JL, Rose AJ, Smith EG, Ney JP. The Business Case for Expanded Clozapine Utilization. Psychiatr Serv. 2016;67(11):1197-205.
48. Howes OD, Vergunst F, Gee S, McGuire P, Kapur S, Taylor D. Adherence to treatment guidelines in clinical practice: study of antipsychotic treatment prior to clozapine initiation. Br J Psychiatry. 2012;201(6):481-5.
49. Agid O, Arenovich T, Sajeev G, Zipursky RB, Kapur S, Foussias G, et al. An algorithm-based approach to first-episode schizophrenia: response rates over 3 prospective antipsychotic trials with a retrospective data analysis. J Clin Psychiatry. 2011;72(11):1439-44.
50. Johnson WE, Li C, Rabinovic A. Adjusting batch effects in microarray expression data using empirical Bayes methods. Biostatistics. 2007;8(1):118-27.
51. Wengler K, Cassidy C, van der Pluijm M, Weinstein JJ, Abi-Dargham A, van de Giessen E, et al. Cross-Scanner Harmonization of Neuromelanin-Sensitive MRI for Multisite Studies. J Magn Reson Imaging. 2021;54(4):1189-99.
52. Wengler K, He X, Abi-Dargham A, Horga G. Reproducibility assessment of neuromelanin-sensitive magnetic resonance imaging protocols for region-of-interest and voxelwise analyses. Neuroimage. 2020;208:116457.
53. Cercignani M, Bouyagoub S. Brain microstructure by multi-modal MRI: Is the whole greater than the sum of its parts? Neuroimage. 2018;182:117-27.
54. Sui J, He H, Yu Q, Chen J, Rogers J, Pearlson GD, et al. Combination of Resting State fMRI, DTI, and sMRI Data to Discriminate Schizophrenia by N-way MCCA + jICA. Front Hum Neurosci. 2013;7:235.
55. Bozzatello P, Bellino S, Rocca P. Predictive Factors of Treatment Resistance in First Episode of Psychosis: A Systematic Review. Front Psychiatry. 2019;10:67.
56. Yang H, Liu J, Sui J, Pearlson G, Calhoun VD. A Hybrid Machine Learning Method for Fusing fMRI and Genetic Data: Combining both Improves Classification of Schizophrenia. Front Hum Neurosci. 2010;4:192.
57. Egerton A, Broberg BV, Van Haren N, Merritt K, Barker GJ, Lythgoe DJ, et al. Response to initial antipsychotic treatment in first episode psychosis is related to anterior cingulate glutamate levels: a multicentre 1 H-MRS study (OPTiMiSE). Molecular Psychiatry. 2018;23(11):2145-55.
58. Schnack HG. Improving individual predictions: Machine learning approaches for detecting and attacking heterogeneity in schizophrenia (and other psychiatric diseases). Schizophr Res. 2019;214:34-42.
59. Ambrosen KS, Skjerbaek MW, Foldager J, Axelsen MC, Bak N, Arvastson L, et al. A machine-learning framework for robust and reliable prediction of short- and long-term treatment response in initially antipsychotic-naive schizophrenia patients based on multimodal neuropsychiatric data. Transl Psychiatry. 2020;10(1):276.
60. Mourao-Miranda J, Reinders AA, Rocha-Rego V, Lappin J, Rondina J, Morgan C, et al. Individualized prediction of illness course at the first psychotic episode: a support vector machine MRI study. Psychol Med. 2012;42(5):1037-47.
61. Koutsouleris N, Meisenzahl EM, Davatzikos C, Bottlender R, Frodl T, Scheuerecker J, et al. Use of Neuroanatomical Pattern Classification to Identify Subjects in At-Risk Mental States of Psychosis and Predict Disease Transition. Archives of General Psychiatry. 2009;66(7):700-12.
62. Yassin W, Nakatani H, Zhu Y, Kojima M, Owada K, Kuwabara H, et al. Machine-learning classification

using neuroimaging data in schizophrenia, autism, ultra-high risk and first-episode psychosis. Transl Psychiatry. 2020;10(1):278.

63. Schnack HG, Nieuwenhuis M, van Haren NE, Abramovic L, Scheewe TW, Brouwer RM, et al. Can structural MRI aid in clinical classification? A machine learning study in two independent samples of patients with schizophrenia, bipolar disorder and healthy subjects. Neuroimage. 2014;84:299-306.
64. Warnez S, Alessi-Severini S. Clozapine: a review of clinical practice guidelines and prescribing trends. BMC Psychiatry. 2014;14(1):102.

Chapter | 12

Summary

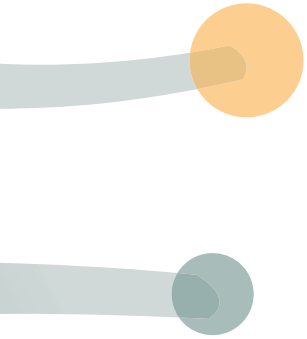

English Summary

Back in control

Towards early identification of treatment resistance in schizophrenia

Treatment resistance in schizophrenia is a major clinical problem, with 20-35% of schizophrenic patients showing no response to first-line antipsychotic treatment. Despite ongoing efforts, it remains difficult to predict who will not respond to first-line antipsychotic treatment. This leads to delays in effective treatment, which can mount up to four years, resulting in longer hospitalization and unnecessary side effects of ineffective antipsychotics. Therefore, there is an urgent need for (bio)markers that could identify treatment-resistant patients at an early disease stage to guide treatment decision to clozapine, the only antipsychotic with recognized effectiveness in treatment-resistant schizophrenia. This would reduce delays in effective treatment, improve prognosis and reduce social and functional disabilities.

A well-established finding in schizophrenia, using [^{18}F]F-DOPA positron emission tomography (PET) imaging, is increased striatal dopamine synthesis capacity. Interestingly, treatment resistant patients do not show this increased dopamine synthesis capacity and show levels comparable to controls. However, the gold standard for assessing dopamine synthesis capacity (PET imaging) is too expensive and relatively burdensome for the patient to be used for treatment resistance screening. A novel neuromelanin-sensitive MRI sequence (NM-MRI), which indirectly assesses dopamine functioning, has potential as a marker for treatment-resistant schizophrenia. NM-MRI indeed shows increased signal in schizophrenia patients, but had not yet been tested in treatment resistant schizophrenia. Another potential marker is a recently developed plasma measure of dopa decarboxylase activity, an enzyme required for dopamine synthesis. Since treatment-resistant schizophrenia has been linked to a normodopaminergic instead of a hyperdopaminergic striatal system, other neurotransmitters are hypothesized to be involved. Specifically, alterations in the neurotransmitters glutamate and gamma-aminobutyric acid (GABA) are implicated in treatment-resistant patients.

The aim of this thesis was to investigate potential (bio)markers for earlier identification of treatment-resistant schizophrenia. The development and application of the novel NM-MRI technique as a clinical marker for treatment-resistant schizophrenia was the primary

emphasis of the thesis. In addition, we explored other potential markers of treatment-resistant schizophrenia, including plasma dopa decarboxylase activity and glutamatergic or GABA alterations.

Part I: Development of NM-MRI

In chapter 2 we reviewed new developments in MR imaging that provide proxy measures of the dopamine system in the brain with a focus on pharmacological MRI (phMRI) and NM-MRI. PhMRI involves administering a pharmacological challenge and using functional MRI techniques to assess the effect of the challenge on brain hemodynamics. This way, phMRI can indirectly assess brain neurotransmitter function, including dopaminergic functioning. NM-MRI enables *in vivo* visualization of neuromelanin in the substantia nigra. Neuromelanin is a by-product of dopamine synthesis and is located in dopaminergic neurons of the nigrostriatal pathway. Visualization and semi-quantification of neuromelanin by NM-MRI can therefore be used as a proxy measure of dopamine function or visualize degeneration of dopaminergic neurons. We conclude that these techniques have promise for clinical application, since alterations of the dopaminergic system in the brain are implicated in various neurologic and psychiatric disorders. Both techniques, however, have primarily been used in research, and applications in clinical practice still seem far away. Currently, NM-MRI shows some potential for clinical application in the diagnostic process of Parkinson's disease. However, we also conclude that further development and standardization are necessary before clinical application.

In chapter 3 we assessed the test-retest reproducibility of three commonly used NM-MRI sequences for imaging the substantia nigra. Different NM-MRI sequences are used in the literature, and we wanted to investigate which had the highest reproducibility. We compared a turbo spin echo (TSE) sequence with an off-resonance magnetization transfer (MT) pulse, a TSE sequence without an MT pulse, and a gradient recalled echo (GRE) sequence with an off-resonance MT pulse. The GRE sequence achieved the lowest variability and the highest contrast. In addition, we explored three different analysis methods, 1) manual analysis, 2) threshold analysis, and 3) voxelwise analysis, for signal (contrast ratio [CR]) and volume measurements. Especially the CR showed high reproducibility. Volume measurement showed a higher variability, especially using manual analysis, hence a threshold analysis is recommended for volume measurements. Based on these results we applied the GRE sequence and CR method in our further research.

In chapter 4 we explored if we could reliably accelerate the GRE sequence from chapter 3. For a clinical protocol it is essential that an MRI sequence is fast and reliable. The original GRE sequence takes over 10 minutes, which limits its use in clinical protocols since these are usually time constricted. We aimed to accelerate the sequence using standard available MRI options, including different combinations of compressed sense (CS), repetition times and MT

pulse. Furthermore, we assessed a more recent 3D NM-MRI sequence with a scan duration of approximately 4 minutes. Our results show that there are several reliable approaches to accelerate NM-MRI. The original (2D) GRE sequences performed best, in particular when using a CS factor of 2.

Part II: Substantia nigra in schizophrenia

In chapter 5 we addressed the role of the substantia nigra in schizophrenia pathology by integrating findings from post-mortem and molecular imaging studies. Increased striatal dopamine functioning is considered to be a robust feature of schizophrenia. Despite being the region that provides the majority of the dopaminergic input to the striatum, the role of the substantia nigra in schizophrenia has been relatively understudied. Hence, this chapter reviewed the findings of nigral functioning in schizophrenia compared to controls. Evidence was found for hyperdopaminergic functioning of the nigrostriatal pathway, reduced GABAergic inhibition and excessive glutamatergic excitation of the dopaminergic neurons in the substantia nigra, and several other deficits in the substantia nigra. These results are in line with the dopamine and glutamate hypothesis, and further suggest that these abnormalities may be a target for treatments or markers in schizophrenia. Moreover, these findings verify the importance of the substantia nigra in schizophrenia pathology and highlight the need for further investigation of the substantia nigra.

In chapter 6 we compared NM-MRI with [^{18}F]F-DOPA PET in schizophrenia patients and healthy controls. The study described in this chapter aimed to elucidate the relationship between NM-MRI signal in the substantia nigra and dopamine synthesis capacity. [^{18}F]F-DOPA PET is a well-established and replicated method to investigate striatal dopamine synthesis capacity in schizophrenia. Studies using [^{18}F]F-DOPA PET have repeatedly shown elevated striatal dopamine synthesis capacity in schizophrenia patients. Similarly, NM-MRI of the substantia nigra, as a proxy for dopamine functioning, has demonstrated increased levels of NM-MRI signal in patients with schizophrenia. However, the relation between [^{18}F]F-DOPA PET and NM-MRI had yet to be assessed. Hence, this chapter aimed to explore the relation between striatal dopamine synthesis capacity and NM-MRI signal in the substantia nigra. Contrary to our hypothesis, we found a negative correlation between NM-MRI signal in the substantia nigra and dopamine synthesis capacity in the striatum in healthy controls. No significant correlation was found in schizophrenia patients. The negative correlation between NM-MRI signal and striatal dopamine synthesis capacity in the controls might be mediated by the vesicular monoamine transporter 2 (VMAT2). VMAT2 is a protein involved in the transport and storage of endogenous dopamine in dopaminergic neurons, while neuromelanin formation is dependent on the excess of cytosolic dopamine. The lack of a correlation between dopamine synthesis capacity and NM-MRI signal in schizophrenia patients might be related to an overall dysregulation in dopamine functioning and/or could be a result of disease-related variables, including symptom severity, antipsychotic medication use, and illness duration.

Part III: Markers for treatment-resistant schizophrenia

In chapter 7 we assessed the potential of NM-MRI as a marker for treatment-resistant schizophrenia. We show that specific voxels in the ventral tier of the substantia nigra are associated with treatment response. Treatment-resistant patients show lower NM-MRI signal than responders at baseline and a comparable signal to controls. At six months follow-up, the NM-MRI signal in patients did not change significantly and the difference between responders and treatment-resistant patients remained. These findings support the potential of NM-MRI as a marker for treatment-resistant schizophrenia. Moreover, these findings are in line with the hypothesis that treatment-resistant schizophrenia is not associated with striatal hyperdopaminergic function.

In chapter 8 we explored the difference in dopa decarboxylase activity between responders and treatment-resistant patients. As dopa decarboxylase activity in the striatum, measured with [^{18}F]F-DOPA PET, is elevated in responders compared to non-responders, we hypothesized that plasma dopa decarboxylase activity might show the same trend. This would prove an accessible and useful candidate marker for treatment-resistant schizophrenia. However, using a retrospective study design, we did not find differences in dopa decarboxylase activity between responders and treatment-resistant patients, and hence no evidence that plasma dopa decarboxylase could be a potential marker for treatment-resistant schizophrenia.

In chapter 9 we used proton magnetic resonance spectroscopy (MRS) to investigate the excitatory glutamate and inhibitory GABA levels between responders and treatment-resistant patients. Both neurotransmitters are implicated in treatment-resistant schizophrenia; the question remains whether these could be potential markers treatment resistance. No significant differences between treatment-resistant patients and responders were found for glutamate or GABA levels in the anterior cingulate cortex. In addition, we did not find an effect of six months follow-up on the neurotransmitters. Our results might be influenced by medication use, illness duration, or other confounders. Nevertheless, we did not find evidence that glutamate or GABA could be potential markers for treatment-resistant schizophrenia in antipsychotics using first episode psychosis patients.

In chapter 10 we introduced the concept of Duration of Treatment Resistance (DTR). We emphasize that early recognition of treatment-resistant schizophrenia could substantially improve outcomes in this subgroup. DTR may facilitate future studies investigating different aspects of treatment-resistant schizophrenia, and whether shortening of DTR by optimizing treatment can further prevent long-term disability in treatment-resistant patients.

Conclusion

The overall aim of this thesis was to further examine potential markers for treatment-resistant schizophrenia, in particular NM-MRI. We demonstrate that NM-MRI has potential as a marker for treatment resistance. Furthermore, we have established the reproducibility of NM-MRI and that the sequence could be reliably accelerated, which contributes to its applicability for clinical use. We have summarized evidence that *in-vivo* imaging of the substantia nigra is important in schizophrenia, and gained more insight into how NM-MRI of the substantia nigra relates to dopamine synthesis capacity in the striatum and substantia nigra. In addition, we explored differences in plasma dopa decarboxylase activity and glutamate/GABA levels between responders and non-responders, but did not find evidence that these measures could be potential markers for treatment-resistant schizophrenia. Finally, we introduced the concept of DTR, which could contribute to further research on treatment resistance.

Nederlandse samenvatting

Weer in controle

Op naar vroege identificatie van therapieresistentie bij schizofrenie

Therapieresistente schizofrenie is een groot klinisch probleem waarbij 20 tot 35% van de schizofrene patiënten niet reageert op eerstelijns-antipsychotische behandeling. Het is echter moeilijk te voorspellen wie wel en wie niet zal reageren op deze antipsychotische behandeling. Dit leidt tot vertragingen in effectieve behandeling oplopend tot vier jaar. Dit resulteert in langere ziekenhuisopnames en onnodige bijwerkingen van ineffectieve antipsychotica. Er is daarom een dringende behoefte aan (bio)markers die therapieresistente patiënten in een vroeg stadium van de ziekte kunnen identificeren. Dit kan ondersteuning bieden bij het maken van een behandelbeslissing omtrent het gebruik van clozapine, het enige antipsychoticum met erkende superieure effectiviteit bij therapieresistente schizofrenie. Dit zou vertragingen in effectieve behandeling verminderen, de prognose verbeteren en sociale en functionele beperkingen en onnodige lijden verminderen.

Een goed bevestigde bevinding bij schizofrenie, gebruikmakend van [^{18}F]F-DOPA-positron emissie tomografie (PET)-beeldvorming, is verhoogde dopamine-synthese capaciteit (dopamine aanmaak) in het striatum, een specifiek hersengebied. Het is interessant dat therapieresistente patiënten deze verhoogde dopamine aanmaak niet vertonen en niveaus hebben die vergelijkbaar zijn met de controles. De gouden standaard voor het beoordelen van dopamine aanmaak (PET-beeldvorming) is echter te duur en relatief belastend voor de patiënt om te worden gebruikt voor therapieresistentie screening. Een nieuwe neuromelanine-gevoelige MRI-techniek (NM-MRI), die indirect dopamine functie meet, heeft potentie als marker voor therapieresistente schizofrenie. NM-MRI signaal is inderdaad verhoogd bij schizofrenie patiënten, maar nog niet getest bij therapieresistente patiënten. Een andere potentiële marker is een recent ontwikkelde plasmameting van dopa-decarboxylase activiteit, een enzym dat nodig is voor dopamine aanmaak. Aangezien therapieresistente schizofrenie normale dopamine activiteit laat zien in plaats van een hyperactief dopamine systeem, wordt er verondersteld dat er andere neurotransmitters zijn aangedaan in therapieresistente schizofrenie. Er zijn voornamelijk aanwijzingen voor specifieke afwijkingen in de neurotransmitters glutamaat en gamma-aminoboterzuur (GABA).

Het doel van deze thesis is om potentiële (bio)markers voor therapieresistente schizofrenie verder te onderzoeken. De ontwikkeling en toepassing van de nieuwe NM-MRI-techniek als klinische marker voor therapieresistente schizofrenie was het primaire doel van deze thesis. Daarnaast hebben we andere potentiële markers voor therapieresistente schizofrenie onderzocht, waaronder plasma dopa-decarboxylase activiteit en glutamaat of GABA-veranderingen.

Deel I: Ontwikkeling van NM-MRI

In hoofdstuk 2 bespreken we nieuwe ontwikkelingen in MRI-beeldvorming, die proxy-maten bieden voor het dopaminesysteem in de hersenen, met de nadruk op farmacologische MRI (phMRI) en NM-MRI. PhMRI houdt in dat medicatie wordt toegediend en functionele MRI-technieken worden gebruikt om het effect van de medicatie op de hersenfunctie te beoordelen. Op deze manier kan phMRI de neurotransmitterfunctie in de hersenen indirect beoordelen, inclusief de dopaminerge functie. NM-MRI maakt *in vivo* visualisatie van neuromelanine in de substantia nigra mogelijk. Neuromelanine is een bijproduct van dopamine aanmaak en bevindt zich in dopaminerge neuronen van de nigrostriatale projectie. Visualisatie en semi-kwantificering van neuromelanine door NM-MRI kunnen daarom worden gebruikt als proxy-maat voor de dopaminefunctie of om degeneratie van dopaminerge neuronen te visualiseren. We concluderen dat deze technieken mogelijkheden bieden voor klinische toepassing, omdat verstoringen van het dopaminesysteem in de hersenen betrokken zijn bij verschillende neurologische en psychiatrische stoornissen. Beide technieken worden echter voornamelijk gebruikt in onderzoek en toepassingen in de klinische praktijk lijken nog ver weg. Momenteel vertoont NM-MRI al enige mogelijke potentie voor klinische toepassing in het diagnostische proces van de ziekte van Parkinson. Verdere ontwikkeling en standaardisatie zijn nodig voordat klinische toepassing mogelijk is.

In hoofdstuk 3 hebben we de reproduceerbaarheid van drie veelgebruikte NM-MRI technieken voor de substantie nigra getest. Verschillende NM-MRI-technieken worden gerapporteerd in de literatuur en we wilden onderzoeken welke de hoogste reproduceerbaarheid had. We vergeleken een turbo spin echo (TSE) sequentie met off-resonantie magnetisatieoverdracht (MT)-puls, een TSE-sequentie zonder MT-puls en een 'gradient recalled' echo (GRE) techniek met off-resonantie MT-puls. De GRE-techniek behaalde de laagste variabiliteit en het hoogste contrast. Daarnaast hebben we drie verschillende analysemethoden onderzocht: 1) handmatige analyse, 2) drempelanalyse en 3) voxelwise analyse, voor signaal (contrastratio [CR]) en volumemetingen. Vooral de CR vertoonde een hoge reproduceerbaarheid. Volumemetingen vertoonden een hogere variabiliteit, vooral bij gebruik van de handmatige analyse, dus een drempelanalyse wordt aanbevolen voor volumemetingen. We hebben besloten om de GRE-techniek en CR in verder onderzoek te gebruiken op basis van deze resultaten.

In hoofdstuk 4 hebben we onderzocht of we de GRE-techniek uit hoofdstuk 3 betrouwbaar konden versnellen. Voor een klinisch protocol is het essentieel dat een MRI-techniek snel en betrouwbaar is. De oorspronkelijke GRE-techniek duurt meer dan 10 minuten. Dat beperkt het gebruik ervan in klinische protocollen, omdat deze meestal een tijdslimiet hebben. We probeerden de techniek te versnellen met behulp van standaard beschikbare MRI-opties, waaronder verschillende combinaties van compressed sense (CS), repetitie tijden en MT-pulsen. Daarnaast hebben we een recentere 3D NM-MRI-techniek geëvalueerd met een scantijd van ongeveer 4 minuten. Onze resultaten tonen aan dat er verschillende betrouwbare mogelijkheden zijn om NM-MRI te versnellen. De oorspronkelijke (2D) GRE-technieken presteerden het beste, vooral bij het gebruik van een CS-factor van 2.

Deel II: Substantia nigra in schizofrenie

In hoofdstuk 5 hebben we de rol van de substantia nigra in de pathologie van schizofrenie onderzocht door bevindingen uit post-mortem en moleculaire beeldvorming studies van het brein te integreren. Verhoogde dopaminerge functie in het striatum wordt beschouwd als een robuust kenmerk van schizofrenie. Ondanks dat de substantia nigra de hersenregio is die het merendeel van de dopaminerge input naar het striatum levert, is de rol van de substantia nigra in schizofrenie relatief weinig bestudeerd. In dit hoofdstuk hebben we daarom de bevindingen van substantia nigra functie bij schizofrenie onderzocht in vergelijking met gezonde controles. We vonden in schizofrenie het volgende: 1) een overactieve dopamine functie in het nigrostriatale circuit (het systeem tussen het striatum en de substantia nigra); 2) een verminderde remmende werking van GABA en een overmatige glutamaat activatie op de dopaminerge neuronen in de substantia nigra; 3) verschillende andere afwijkingen. Deze resultaten zijn in lijn met de dopamine- en glutamaathypothese in schizofrenie en suggereren verder dat deze afwijkingen een doelwit kunnen zijn voor behandeling of markers voor schizofrenie. Bovendien bevestigen deze bevindingen het belang van de substantia nigra in de pathologie van schizofrenie en benadrukken de noodzaak van verder onderzoek naar de substantia nigra in schizofrenie.

In hoofdstuk 6 vergeleken we NM-MRI met [^{18}F]F-DOPA PET bij schizofreniepatiënten en gezonde controles. Het doel van deze studie was om de relatie tussen NM-MRI-signaal in de substantia nigra en dopamine-synthese capaciteit te begrijpen. [^{18}F]F-DOPA PET is een gevestigde en reproduceerbare methode om dopamine aanmaak in het striatum bij schizofrenie te onderzoeken. Studies met [^{18}F]F-DOPA PET hebben herhaaldelijk verhoogde dopamine aanmaak in het striatum bij schizofreniepatiënten aangetoond. Vergelijkbaar heeft NM-MRI van de substantia nigra, als proxy voor dopaminefunctie, verhoogde niveaus van NM-MRI-signaal bij patiënten met schizofrenie gedemonstreerd. De relatie tussen [^{18}F]F-DOPA PET en NM-MRI is nog niet bestudeerd. Daarom had dit onderzoek als doel de relatie tussen dopamine aanmaak in het striatum en NM-MRI-signaal in de substantia nigra te onderzoeken.

In tegenstelling tot onze hypothese vonden we een negatieve correlatie tussen NM-MRI-signaal in de substantia nigra en dopamine aanmaak in het striatum bij gezonde controles. Bij schizofreniepatiënten werden geen significante correlaties gevonden. De negatieve correlatie tussen NM-MRI-signaal en striatale dopamine aanmaak bij de controles kan worden veroorzaakt door verschillen in de expressie van de vesiculaire monoamine-transporter 2 (VMAT2). VMAT2 is een eiwit dat betrokken is bij het transport en de opslag van dopamine in dopaminerge neuronen, terwijl neuromelanine vorming afhankelijk is van het overschot aan dopamine. Het ontbreken van een correlatie tussen dopamine-synthese capaciteit en NM-MRI bij schizofreniepatiënten kan gerelateerd zijn aan een algemene disregulatie in de dopaminefunctie en/of het gevolg zijn van aan ziekte gerelateerde variabelen, zoals de ernst van de symptomen, het gebruik van antipsychotica en de duur van de ziekte.

Deel III: Markers voor therapieresistente schizofrenie

In hoofdstuk 7 hebben we de potentie van NM-MRI als marker voor therapieresistente schizofrenie beoordeeld. We laten zien dat specifieke voxels in de substantia nigra geassocieerd zijn met de therapieresistentie. Therapieresistente patiënten vertonen op baseline een lager NM-MRI-signaal dan responders en een vergelijkbaar signaal met gezonde controles. Na zes maanden follow-up veranderde het NM-MRI-signaal bij patiënten niet significant en bleef het verschil tussen responders en therapieresistente patiënten bestaan. Deze bevindingen ondersteunen de potentie van NM-MRI als marker voor therapieresistente schizofrenie. Bovendien zijn deze bevindingen in overeenstemming met de hypothese dat therapieresistentie niet geassocieerd is met de striatale hyperdopaminerge functie.

In hoofdstuk 8 onderzochten we het verschil in plasma dopa-decarboxylase activiteit tussen responders en therapieresistente patiënten. Aangezien dopa-decarboxylase activiteit in het striatum, gemeten met [^{18}F]F-DOPA PET, verhoogd is bij responders in vergelijking met non-responders, veronderstelden we dat plasma dopa-decarboxylase activiteit dezelfde trend zou laten zien. Dit zou een eenvoudige en nuttige kandidaatmarker voor therapieresistente schizofrenie kunnen zijn. Helaas vonden we in een retrospectieve studie geen verschil in dopa-decarboxylase activiteit tussen responders en therapieresistente patiënten en dus geen bewijs dat plasma dopa-decarboxylase activiteit een potentieel marker zou kunnen zijn voor therapieresistente schizofrenie.

In hoofdstuk 9 hebben we proton magnetische resonantie spectroscopie (MRS) gebruikt om de activerende glutamaat- en remmende GABA-niveaus tussen responders en therapieresistente patiënten te onderzoeken. Beide neurotransmitters zijn betrokken bij therapieresistente schizofrenie en de vraag is of deze potentiële markers kunnen zijn voor therapieresistente schizofrenie. Er werd geen significant verschil gevonden tussen therapieresistente patiënten en responders voor glutamaat- of GABA-niveaus in de anterior

cingulate cortex. Bovendien vonden we geen effect van 6 maanden follow-up op deze neurotransmitters. Onze resultaten kunnen zijn beïnvloed door medicatiegebruik, ziekteduur, of andere verstorende factoren. We hebben echter geen bewijs gevonden dat glutamaat of GABA potentiële markers zouden kunnen zijn voor therapieresistente eerste-episode psychosepatiënten die antipsychotica gebruiken.

In hoofdstuk 10 introduceren we het concept van de duur van de behandeling-resistentie (DTR). We benadrukken dat vroege herkenning van therapieresistente schizofrenie de uitkomst van deze subgroep aanzienlijk kan verbeteren. DTR kan toekomstige studies ondersteunen, om verschillende aspecten van therapieresistente schizofrenie te onderzoeken en te bepalen of verkorting van DTR door optimalisatie van de behandeling verdere langdurige invaliditeit in therapieresistente patiënten kan voorkomen.

Conclusie

Het doel van deze thesis was om mogelijke markers voor therapieresistente schizofrenie verder te onderzoeken, met name NM-MRI. We tonen aan dat NM-MRI potentie heeft als marker voor therapieresistentie. Bovendien hebben we de reproduceerbaarheid van NM-MRI vastgesteld en aangetoond dat de techniek betrouwbaar versneld kan worden, wat bijdraagt aan de toepasbaarheid ervan in de klinische praktijk. We hebben bewijs uiteengezet dat *in vivo* beeldvorming van de substantia nigra belangrijk is bij schizofrenie en meer inzicht verkregen in hoe NM-MRI van de substantia nigra zich verhoudt tot dopamine aanmaak in het striatum en de substantia nigra. Daarnaast hebben we verschillen in plasma dopa-decarboxylase activiteit en glutamaat/GABA-niveaus tussen responders en therapieresistente patiënten onderzocht, maar geen bewijs gevonden dat deze maten potentieel markers zouden kunnen zijn voor therapieresistente schizofrenie. Als laatste hebben we het concept DTR geïntroduceerd wat kan bijdragen aan verdere onderzoek naar therapieresistentie.

Chapter | 13

Appendices

List of Publications

Van Hooijdonk, C.F.M., **van der Pluijm, M**., Smith, C., Yaqub, M., van Velden, F.H.P., Horga, G., Wengler, K., Hoven, M., Van Holst, R.J., de Haan, L., Selten, J.P., van Amelsvoort T.A.M.J., Booij, J., van de Giessen, M. (2023) Striatal dopamine synthesis capacity and neuromelanin in the substantia nigra: a cross-sectional multimodal imaging study in schizophrenia and healthy controls. *Submitted*

Van der Pluijm, M., Wengler, K., Reijers. P.N. Cassidy, C., Tjong Tjin Joe, K., de Peuter, O.R., Horga, G., Booij, J., de Haan, L. & van de Giessen, E. (2023) Neuromelanin-sensitive MRI as candidate marker for treatment resistance in first episode schizophrenia. *Submitted*

Van Hooijdonk, C.F.M*., **van der Pluijm, M*.,** Bosch, I., van Amelsvoort, T.A.M.J., Booij, J., de Haan, L., Selten, J.P., & van de Giessen, E. (2023) The substantia nigra in the pathology of schizophrenia: a review on post-mortem and molecular imaging findings. *European Neuropsychopharmacology*, *68*, 57-77. doi:10.1016/j.euroneuro.2022.12.008

Van der Pluijm, M., Wallert, E.D., Coolen, B.F., Tjong Tjin Joe, K.J.T., de Haan, L., Booij, J., & van de Giessen, E. (2022) Acceleration of neuromelanin-sensitive MRI sequences in the substantia nigra using standard MRI options. *Neuroradiology*, *65*(2), 307-312. doi:10.1007/s00234-022-03058-w

Reneman, L., **van der Pluijm, M.**, Schrantee, A. & van de Giessen, E. (2021) Imaging of the Dopamine System with Focus on Pharmacological MRI and Neuromelanin Imaging. *Eur J Radiol*, *140*, 109752. doi:10.1016/j.ejrad.2021.109752

Wengler, K., Cassidy, C., **van der Pluijm, M.,** Weinstein, J.J., Abi-Dargham, A., van de Giessen, E. & Horga, G. (2021) Cross-Scanner Harmonization of Neuromelanin-Sensitive MRI for Multisite Studies. JMRI, 54(4), 1189-1199. *Journal of Magnetic Resonance Imaging*, 54(4), 1189-1199. doi:10.1002/jmri.27679

Van der Pluijm, M., Cassidy, C., Zandstra, M., Wallert, E., de Bruin, K., Booij, J., De Haan, L., Horga, G. & van de Giessen, E. (2020) Reliability and Reproducibility of Neuromelanin-Sensitive Imaging of the Substantia Nigra: A Comparison of Three Different Sequences. JMRI, 53(3), 712-721.

Sutterland, A.L., **van der Pluijm, M.,** Becker, H.E., van de Giessen, E. & de Haan, L. (2020) Shortening Duration of Treatment Resistance (DTR), the next step in the treatment of schizophrenia. *Schizophrenia Bulletin Open*, *1*(1). doi:10.1093/schizbullopen/sgaa030

Van der Pluijm, M., Sutterland, A.L., van Kuilenburg, A.B.P., Zoetekouw, L., de Haan, L., Booij, J. & van de Giessen, E. (2019) Plasma dopa decarboxylase activity in treatment-resistant recent-onset psychosis patients. *Therapeutic Advances in Psychopharmacology*, *9*. doi:10.1177/2045125319872341

Vingerhoets, C., Bakker, G., Schrantee, A., **van der Pluijm, M.,** Bloemen, O.J.N., Reneman, L., Caan, M., Booij, J. & van Amelsvoort, T.A.M.J. (2019) Influence of muscarinic M1 receptor antagonism on brain choline levels and functional connectivity in medication-free subjects with psychosis: A placebo controlled, cross-over study. Psychiatry Res Neuroimaging, 290:5-13. *Psychiatry Research - Neuroimaging*, *290*. doi:10.1016/j.pscychresns.2019.06.005

Lecei, A., van Hulst, B.M., de Zeeuw, P., **van der Pluijm, M.,** Rijks, Y. & Durston, S. (2019) Can we use neuroimaging data to differentiate between subgroups of children with ADHD symptoms: A proof of concept study using latent class analysis of brain activity. *NeuroImage: Clinical*, *21*. doi:10.1016/j.nicl.2018.11.011

Van der Aart, J., Golla, S.S.V., **van der Pluijm, M.,** Schwarte, L.A., Schuit, R.C., Klein, P.J., Metaxas, A., Windhorst, A.D., Boellaard, R., Lammertsma, A.A. & van Berckel, B.N.M. (2018) First in human evaluation of [^{18}F]PK-209, a PET ligand for the ion channel binding site of NMDA receptors. *EJNMMI research*, *8*(1). doi:10.1186/s13550-018-0424-2

* Joint first author

PhD portfolio

Name: Marieke van der Pluijm

Department: Department of Radiology and Nuclear Medicine, Department of Psychiatry, Amsterdam UMC, location AMC

Supervisors: prof. dr. Jan Booij, prof. dr. Lieuwe de Haan, dr. Elsmarieke van de Giessen

PhD period: January 2018 – October 2022

PhD training	Year	ECT
Courses		
3T MRI scan qualification	2018	0.5
Venous blood sampling	2018	0.5
OpenClinica training	2018	0.2
Basic Legislation in Science (BROK)	2018	1.5
MRI physics – basic principles	2018	1.0
Data-analysis in Matlab	2018	1.0
Radiation protection	2018	1.0
Practical Biostatistics	2019	1.4
Computing in R	2020	2.1
Advanced Topics in Biostatistics	2021	2.1
Seminars, workshops and master classes		
ECNP Workshop on Neuropsychopharmacology for Early Career Scientists in Europe; Nice, France	2022	1.5
(Inter)national conferences		
ISMRM=International Society for Magnetic Resonance in Medicine *ECNP=European College of Neuropsychopharmacology* *SIRS= Schizophrenia International Research Society*		
ECNP; Vienna (oral presentation)	2022	1.5
Amsterdam Neuroscience	2022	0.5
ISMRM; London (poster presentation)	2022	1.5
SIRS; Florence (poster presentation)	2022	1.5
ISMRM Benelux: Maastricht (poster presentation)	2022	1.5

Amsterdam Neuroscience (poster presentation)	2021	0.5
ISMRM; online (poster presentation)	2021	1.5
SIRS; online (poster presentation)	2021	1.5
Amsterdam Neuroscience; online (poster presentation)	2020	0.5
ECNP; online (poster presentation)	2020	1.5
ISMRM Benelux; Arnhem (poster presentation)	2020	1.5
Amsterdam Neuroscience (poster presentation)	2019	0.5
ISMRM Benelux; Leiden (poster presentation)	2019	1.5
SIRS; Florence (poster presentation)	2018	1.5

Teaching

Lecturing

Research QA for patients (every two weeks)	2018-2021	4
Guest lecture on MRI and research for Masters	2018, 2019	1
Clinical lesson for clinicians	2019	0.5

Supervising

Master research project: 11	2018-2022	22
Bachelor research project: 5	2018-2021	5
Literature Thesis: 4	2019-2021	2

Other

Journal Club Neuroimaging (every month)	2019-present	4
Journal Club Early Psychosis (every month; organizer)	2019-present	4

Awards and Prizes

ECNP; ECNP's got talent award	2022
SIRS; Early career award	2022
ISMRM; Educational Stipend	2022
ISMRM; Magna cum laude award	2021
ECNP: Excellence award	2020
Amsterdam Neuroscience; Best poster award	2019

Curriculum Vitae

Marieke van der Pluijm was born on the 23rd of September 1992, in Broek op Langedijk, the Netherlands. She obtained her high-school degree in 2010 from the Huygens College in Heerhugowaard and afterward moved to Amsterdam to study Psychobiology at the University of Amsterdam. She completed her Bachelor's Degree in 2013 with a thesis on the effect of social feedback processing on electroencephalography signals in healthy females. Subsequently, she enrolled in the Master's program Neurobiology at the University of Amsterdam, specializing in Cognitive Neurobiology & Clinical Neurophysiology. During her Master's, she completed her first internship at the NICHE lab, department of Psychiatry of the University Medical Center Utrecht. She completed her second internship at the department of Nuclear Medicine, Amsterdam University Medical Center (UMC), location VUMC. This led to a research position at the same department, in which she continued working part-time for a year on the project: "First in human NMDA PET tracer development and kinetic modeling". In 2016 she graduated with a Master's degree and at the same time, started her second Master's in Neuropsychology at Leiden. During this period, she completed a research internship at the department of Radiology and Nuclear Medicine, and a clinical internship at the department of Early Psychosis, Psychiatry, both at the Amsterdam UMC, location AMC. After her clinical internship and graduation of her Master's in Neuropsychology beginning of 2017, she stayed to work as a research coordinator at the department of Psychiatry. In January 2018, she started her PhD on predicting treatment resistance in schizophrenia under the supervision of prof. dr. Jan Booij, prof. dr. Lieuwe de Haan and dr. Elsmarieke van de Giessen at the department of Radiology and Nuclear Medicine in collaboration with the department of Psychiatry, at Amsterdam UMC, location AMC. From November 2020 until April 2021, she simultaneously worked part-time on a project about improving self-esteem in traumatized youth at the School for Mental Health & Neuroscience, Maastricht University. From October 2021 onwards she worked part-time, besides her PhD, as a research coordinator at the department of Early Psychosis, Psychiatry, Amsterdam UMC, location AMC. Marieke is currently employed as a post-doctoral researcher at the department of Early Psychosis, Psychiatry, Amsterdam UMC, location AMC.

Dankwoord

De afgelopen vijf jaar was een vrij turbulente periode, waarbij ik me niet altijd “in control” voelde. Een periode vol uitdagende en bijzondere momenten, met als resultaat dit prachtige proefschrift. Graag wil ik iedereen bedanken die op welke manier dan ook , indirect of direct, heeft bijgedragen aan dit succesvolle resultaat.

Allereest ongelofelijk veel dank aan de deelnemers van de verschillende studies in dit proefschrift. Zonder jullie inzet en deelname was dit proefschrift niet mogelijk geweest. Ik wil in het bijzonder de deelnemers van de TREVOS-studie bedanken. Jullie hebben tientallen vragen beantwoord, urenlang taken gedaan en bovendien dat eindeloze uur (en voor sommigen anderhalf uur!) stilgelegen in de scanner. Dankzij jullie toewijding hebben we de waardevolle wetenschappelijke data voor dit proefschrift kunnen verzamelen.

Graag wil ik mijn promotoren, **Jan** en **Lieuwe**, bedanken voor hun vertrouwen en begeleiding tijdens mijn promotietraject. Voordat deze PhD-positie op mijn pad kwam, had ik nog geen definitief besluit genomen over een PhD-traject. Ik was mij er zeer bewust van dat het promotieteam van cruciaal belang is voor het succes (en de onvermijdelijke stress) van een PhD-student. Ik noemde wel eens dat ik enkel zou willen promoveren onder de meest ideale omstandigheden, namelijk op het perfecte project met MRI, PET en psychose, en met prof. de Haan en prof. Booij als promotoren. Ik had jullie beiden ontmoet tijdens mijn stages en hoewel we destijds nauwelijks contact hadden, kwamen jullie op mij over als toegankelijk, oprecht en consistent. Deze eigenschappen, gepaard met een scheutje nuchterheid en humor, maken jullie de ideale promotoren om mee samen te werken. Bedankt voor het delen van jullie oneindige passie en kennis.

Elsmarieke, jij hebt dit perfecte PhD-project gecreëerd en daar ben ik je ontzettend dankbaar voor. Hoewel we elkaar in eerste instantie niet kenden, beschouw ik je retrospectief als een essentieel lid van mijn promotie dreamteam. Jouw betrokkenheid tijdens zowel de moeilijke als positieve momenten was een enorme steun. Onze samenwerking verliep altijd soepel, omdat we goed op één lijn liggen. Je hebt me wetenschappelijk en persoonlijk enorm veel geleerd. Je gedrevenheid en uitgebreide expertise waren zeer motiverend. Ik hoop nog lang door je geïnspireerd te worden, we houden zeker contact.

Leden van de leescommissie, bedankt voor jullie deskundige oordeel en aanwezigheid. Ik kijk er naar uit om van gedachten te wisselen tijdens de verdediging.

Om weer terug te gaan naar het begin. **Claudia** en **Geor**, zonder jullie had ik hier niet gestaan. Vanaf een strandbedje op Curaçao hebben jullie mij deze prachtige PhD-positie bezorgd. Ik herinner me nog precies het moment waarop jullie mij enthousiast belden dat ik direct

mijn CV moest opsturen naar Elsmarieke. Jullie waren mijn oud stagebegeleiders, en als mijn wetenschappelijke peetouders hebben jullie mij altijd gesteund en begeleid. Daarvoor ben ik jullie ontzettend dankbaar. Claudia, als mama eend, bleef jij nog wat langer om me te begeleiden en te ondersteunen tijdens mijn eerste stappen als PhD-student. En hoewel je uiteindelijk Z0 moest verlaten, ben ik blij dat je nog een vinger aan de pols houdt tijdens onze gin & tonic-avonden.

Z0-familie: Joena, Claudia, Geor, Melissa, Toni, Sophie, Koen, Zarah, Renske, Anne, Elon, Daphne B., Carmen, Liza, Bobby, Nienke, Myrte, Daphne N., Susi, Laura, Hugo, Mariah, Natalia, Wilhelm, Daan B., Daan K., Anouk, Bram, Lukas, Eva, Jitsha, Jasper, Paul dH., Oliver, Eric, Pim, Sofieke, Ot, Paul G., Sandra, Anita, Jules, Katinka, Alexandra, Gustav, Aart bedankt voor jullie steun en warmte. De gezellige lunches, koffies, borrels, congressen en feestjes, hebben niet alleen mijn werkleven, maar ook mijn sociale leven gevuld. Jullie hebben mijn PhD-tijd onvergetelijk gemaakt en ik zal deze momenten nog lang koesteren. **Joena**, als opzichter van Z0, speelde jij een grote rol bij de huiselijke sfeer. Ik kon altijd op je rekenen voor adviezen en creatieve oplossingen. Ik ben blij dat ik hier als vriendin gebruik van kan blijven maken. Jij krijgt alles voor elkaar (zoals de prachtige daglichtlampen). **Bram en Anouk**, bedankt dat ik meermaals gebruik heb mogen maken van jullie onuitputtelijke bron van MRI-kennis. **Paul G.,** bedankt voor je onmisbare hulp bij de MRI-data. **Sandra**, bedankt dat ik bij twijfel alles aan je kon vragen en je me af en toe een hart onder de riem stak.

Lieve **roomies** van Z0.174, jullie hebben mij ontzettend gesteund de afgelopen jaren. Van lachen tot huilen en klagen, alles kon ik met jullie delen. Ik zal jullie gezelligheid enorm missen, maar ik ben blij dat ik via mijn psychiatriekom verbonden mag blijven met jullie aquarium. **Koen**, ik mis jouw frequente kamerbezoekjes, hoewel je misschien meer voor de snoep kwam dan voor de gezelligheid. **Claudia, Melissa,** wat ik totaal niet mis zijn die verschrikkelijke muziek video's van C-artiesten waar jullie veel te lang met regelmaat mijn mailbox mee bevuilden. **Toni en Zarah,** bedankt dat ik altijd bij jullie terecht kon met vragen, hoe klein dan ook, als bureauburen. **Elon**, ik ben blij dat jij mijn vervanger bent op Z0.174. Met jouw humor en gezelligheid ben je een fijne afleiding voor de kamer. Probeer alleen wel wat vaker naar de borrels te gaan. **Renske**, jouw goede vragen en eindeloze interesse, zowel op persoonlijk als wetenschappelijk vlak, hebben me gemotiveerd. **Anne,** je grappige, behulpzame en lieve persoonlijkheid maken je een fijne collega (en talentvolle vlogger?).

Neurobuddies (Anouk, Carmen, Daphne B., Daphne N., Elon, Margo, Niels, Toni, Zarah), bedankt voor de ondersteuning die jullie mij als neurocollega's hebben geboden. Het was fantastisch om met jullie te kunnen brainstormen tijdens de journal clubs, congressen en gezellige borrels.

Studenten, Alaya, Anne, Asta, Charlotte, Laura, Lissa, Luca, Maartje, Manon, Melissa, Menno, Michelle, Pascalle, Ryanne, bedankt voor jullie onmisbare hulp en toewijding bij de dataverzameling. Ik heb veel geluk gehad met jullie als studenten, dankzij jullie flexibiliteit en gedrevenheid heb ik de dataverzameling succesvol kunnen afronden. **Maartje**, bedankt voor je hulp met het MRS artikel. Zonder jou had dit manuscript mijn boekje niet gehaald. **Merel**, ik ben jou enorm dankbaar voor jouw redding tijdens de eindstreep met mijn Covid/bruiloft debacle. Ik was al fan van jou, maar daardoor heb je nog meer indruk op mij en het team gemaakt. Ik ben dan ook blij dat we in de toekomst kunnen blijven samenwerken bij jouw eigen PhD-project.

Vroege Psychose, allereest ontzettend veel dank aan alle verpleegkundigen, arts-assistenten en psychiaters van VP. Jullie toewijding aan de patiënten en de studie is een belangrijk fundament van het succes van ons onderzoek. Bedankt voor jullie geduld en flexibiliteit. Ook wil ik mijn mede psychose onderzoekers bedanken (o.a. Jentien, Frederike, Arjen, Julie, Sanne, Steven, Tim en Dorien) voor jullie betrokkenheid. Ik heb veel van jullie geleerd tijdens de journal clubs en van jullie ervaring met de doelgroep. **Nicole**, bedankt alle ondersteuning en je altijd snelle reactie. **Eerste Constantijn Huygensstraat**, **Olav,** heel erg bedankt voor jullie samenwerking, enthousiasme en het creatief meedenken met de inclusie van TREVOS. **VIP,** bedankt dat jullie tijd maakte voor de TREVOS tussen de hectiek van de dag door. Met name veel dank aan Rimke en Madelon voor jullie harde werk tijdens de laatste inclusie fase.

Guillermo, **Ken**, and **Cliff,** thank you for the inspiring meetings and your valuable help with the neuromelanin MRI analyses. **Meng-Fong, Edwin** en **Ehsan**, bedankt voor jullie hulp bij het FDOPA scannen en jullie creativiteit bij de PET opzet om de scans zo goed mogelijk en met zo min mogelijk beweging te laten verlopen. **Kora,** bedankt voor je prachtige tekenvaardigheden waarmee je met bloed, zweet en tranen meerdere scans voor ons hebt ingetekend. **Maqsood**, bedankt voor je ondersteuning bij de FDOPA-analyse, je enthousiasme werkt aanstekelijk.

Carmen, bedankt voor onze geweldige samenwerking. Dankzij de gelijkenis van onze projecten en de obstakels die we moesten overwinnen, konden we altijd op elkaar rekenen. Het was een plezier om met je samen te werken op projecten. Je bent ontzettend georganiseerd en je hebt een talent voor schrijven. We vullen elkaar goed aan en dat heeft tot mooie manuscripten geleid.

Zarah, het nieuwste lid van de Jordaan crew. We ontmoetten elkaar tijdens Covid-tijd, ik in een spijkerbroek, jij in een discoglitter broek. Jouw enthousiasme viel meteen op en het was prettig (en handig) om jou als buurvrouw te hebben. De avondklok tijdens quarantaine was geen uitdaging voor ons, zodra de klok begon te slaan was ik thuis voor de laatste slag.

Melissa, bedankt voor al je waardevolle advies en steun. Ik heb me ontelbaar vaak op mijn bureaustoel omgedraaid om even mijn hart bij je te luchten. Jouw nuchterheid en "niets moet" mentaliteit zet alles in perspectief. Ook heb ik erg genoten van jouw gezelligheid, je bent op alle borrels te vinden en onze eigen gin & tonic-bijeenkomsten waren, en zijn, ontzettend gezellig.

Sophie, mijn sportbuddy en belangrijk lid van de Jordaan crew. Bedankt voor alle gezelligheid. Even een drankje doen, een wandeling of gewoon bijpraten, jij bent overal voor te porren. Je bent een ontzettend lief persoon en ik lijd met niemand liever tijdens de pilateslessen van onze zingende vriendin.

Koen, ik kan altijd bij je terecht met al mijn vragen o.a. over MRI en Matlab. Bedankt voor je geduld bij het uitleggen en voor al je geduld als je weer op me moest wachten wanneer we samen naar huis reisden. Het was altijd erg fijn en gezellig om met jou de werkdag af te sluiten. Het is dan ook iconisch dat jij nu naast me staat als paranimf om mijn PhD-avontuur af te sluiten.

Toni, je bent een geweldige collega en een fantastische vriendin. Je staat altijd voor me klaar, of het nu gaat om hulp bij statistiek, Matlab, het flyeren om mijn vermiste kat te vinden of het organiseren van mijn vrijgezellenfeest. Ik heb het echt gewaardeerd om je buurvrouw te zijn op Z0.174 en in Amsterdam. Het was geweldig om samen dit PhD-avontuur als science sisters te beleven. Ik ben ontzettend dankbaar dat je naast me staat als paranimf.

Ik wil ook graag mijn vrienden buiten werk bedanken voor hun hulp om in balans te blijven en te blijven genieten. Jullie hebben allemaal een onmisbare rol gespeeld in mijn leven en bijgedragen aan het pad dat me hier heeft gebracht. **Myrthe en Inger**, onze vriendschap gaat terug naar de basisschool en hoewel we elkaar niet altijd regelmatig zien, is het elke keer als vanouds als we afspreken. **Sapkedoodlies**, ons avontuur begon 15 jaar geleden bij ons eerste concert van Franz Ferdinand in Rotterdam, gevolgd door talloze andere concerten, festivals en gezellige wijn- en spelletjesavonden. Ik ben zo dankbaar dat we na al die jaren nog steeds zo'n geweldige "band" hebben. **Zeinab,** ik waardeer enorm dat ik altijd bij je terecht kan, er is niemand met wie ik zo vaak en lang bel. **Jorien en Birgit,** bedankt voor jullie vriendschap vanaf de middelbare school. Op 16-jarige leeftijd behaalde ik met jullie mijn eerste "publicatie", de opstap naar mijn wetenschappelijke carrière. Jorien, ik ben je heel dankbaar dat ik met jou als huisgenoot het avontuur van wonen en studeren in Amsterdam heb kunnen beleven. **Sanne en Florine,** het is altijd gezellig met jullie, of het nu Heerhugowaard, Amsterdam, Londen, Den Haag of Landsmeer is, wij hebben overal heerlijke gesprekken. **Sasja**, het was geweldig om met jou de studie psychobiologie en de stad Amsterdam te ontdekken. Bedankt voor je Twentse nuchterheid en uitgebreide samenvattingen, beiden waren een grote steun tijdens de studie. **Floriana**, onze vriendschap is ook begonnen tijdens de studie psychobiologie, het

was ontzettend leuk toen bleek dat wij vrij dicht bij elkaar waren opgegroeid en dezelfde mensen kenden. **Nikita**, onze ontmoeting tijdens mijn eerste masterstage was meteen raak. Als Bert en Ernie voelden we ons helemaal op onze plek in het NICHE lab, mede dankzij de fantastische begeleiding van Branko. Bedankt voor een geweldige stageperiode waarin mijn passie voor onderzoek is ontstaan.

Danielle, zowel tijdens de goede als slechte tijden sta je aan mijn zijde. We hebben samen zoveel avonturen beleefd en de doordeweekse avondjes samen op de bank zijn even heerlijk. Ik ben immens dankbaar voor onze vriendschap.

Schoonfamilie, Sjaak, Anneke, Lisa en Stefan, ik ben heel blij met jullie als bonus familie. Ik voel mij vanaf het begin thuis bij jullie en ben dankbaar voor alle fijne gesprekken onder het genot van heerlijke biertjes. De prachtige vakanties in Sri Lanka en Guatemala zal ik nooit vergeten, wat hebben we tijdens die reizen veel beleefd en gelachen. Bedankt voor alle goede zorgen en mooie herinneringen.

Eric en Jessica, wat bof ik met jullie als broer en schoonzus. Het is zo fijn om jullie dichtbij te hebben in Amsterdam. Samen heerlijk eten of spelletjes doen (geen escape room is tegen ons opgewassen), het is altijd gezellig met jullie. Ik waardeer jullie steun en adviezen enorm en ik ben dankbaar dat ik altijd bij jullie terecht kan.

Pap en mam, jullie hebben mij geleerd om sterk te zijn en om altijd te blijven doorzetten, zelfs in de moeilijkste tijden. Van jongs af aan hebben jullie mij de waarden en normen bijgebracht die mij hebben gevormd tot wie ik nu ben. Ik ben ontzettend dankbaar voor jullie onvoorwaardelijke liefde en steun.

Thomas, ik kan niet anders dan het dankwoord met jou afsluiten. Dit proefschrift is een team-effort en niet alleen dankzij je hulp bij de plaatjes. Jij hebt mij enorm gesteund in de afgelopen jaren, zowel privé als tijdens dit promotie traject. Kleine of grote dingen, ik mag altijd mijn hart bij je luchten. Ik ben ontzettend dankbaar dat je altijd aan mijn zijde staat tijdens de moeilijke tijden, maar ook dat we altijd de mooie momenten (van inclusie mijlpalen tot geaccepteerde artikelen) samen kunnen vieren, met sushi of cocktails. Samen vormen we het perfecte team en het maakt me dolgelukkig dat ik je mijn "man" mag noemen.